



Yeast as a platform for identification of chemo- protectors of Alzheimer's disease

A thesis submitted in fulfilment of the requirements for the degree of Doctor of Philosophy

Afsaneh Porzoor

BSc (Hons), GDip Biotech

School of Applied Sciences

College of Science Engineering and Health

RMIT University

January 2015

Declaration

I certify that except where due acknowledgement has been made, the work is that of the author alone; the work has not been submitted previously, in whole or in part, to qualify for any other academic award; the content of the thesis/project is the result of work which has been carried out since the official commencement date of the approved research program; any editorial work, paid or unpaid, carried out by a third party is acknowledged; and, ethics procedures and guidelines have been followed.

Afsaneh Porzoor

28/01/2015

ORIGINALITY STATEMENT

I hereby declare that this submission is my own work and to the best of my knowledge it contains no materials written by another person, or substantial proportion of materials which have been accepted for the award of any other qualifications at RMIT or any other educational institution, except where due acknowledgement is made in the thesis. Any contribution made to the research by others, with whom I have worked at CSIRO and RMIT or elsewhere, is explicitly acknowledged in the thesis.

I also, declare that the intellectual content of this thesis is the product of my own work, except to the extent that assistance from others in the project's design and conception or in style, presentation and linguistic expression acknowledged.

Signed

Afsaneh Porzoor

Date 28/01/2015

COPYRIGHT STATEMENT

I hereby grant the Royal Melbourne Institute of Technology University or its agents the right to archive and to make available my thesis in whole or part in the University libraries in all forms of media, now or here after known, subject to the provisions of the Copyright Act 1968. I retain all proprietary rights, such as patent right. I also retain the right to use in future works (such as articles or books) all or part of this thesis or dissertation.

I also authorise University Microfilms to use the 350 word abstract of my thesis in Dissertation Abstract International. I have either used no substantial portions of copyright materials in my thesis or I have obtained permission to use copyright materials; where permission has not been granted I have applied/ will apply for a partial restriction of the digital copy of my thesis or dissertation.

Signed

Afsaneh Porzoor

Date28/01/2015.....

AUTHENTICITY STATEMENT

I certify that the Library deposit digital copy is a direct equivalent of the final officially approved version of my thesis. No emendation of content has occurred and if there are any variations in formatting, they are the result of the conversion to digital format.

Signed

Afsaneh Porzoor

Date 28/01/2015

ABSTRACT

The complexity of cellular pathways in neurodegenerative disease has limited the understanding of the molecular mechanisms underlying Alzheimer's disease (AD). Therefore, to gain insight into AD and to devise potential therapeutic approaches, simple models are employed. *Saccharomyces cerevisiae* is currently utilised for analysing cellular toxicity and protein aggregation in neurodegenerative diseases including AD. This study has therefore focused on improvements and validation of the yeast screening model and assays to generate a more suitable disease model that can be used successfully for designing therapeutic strategies and interventions which correlate with *in vitro* and mammalian testing systems.

This thesis investigates and shows for the first time that the pretreatment method of synthetic A β ₄₂ peptide determines its activity and ultimately how it interacts with yeast cells. The effects of A β ₄₂ appear to be limited to the yeast cell wall and interactions with the amyloidogenic cell wall proteins. *S. cerevisiae* was found to be more resistant than *Candida glabrata* to the effect of A β ₄₂ peptide. It was identified that conformational changes in the peptide due to preparation methods, determine its fate on toxicity and proliferation. Hexafluoroisopropanol pretreated A β ₄₂ had a greater tendency to aggregate on yeast cells as determined by thioflavin T staining followed by flow cytometry and microscopy. Quiescent cells were found to be more resistant to the toxicity of A β ₄₂ peptide than non-quiescent cells. Also, a preparation which results in toxicity to PC12 neuronal cells caused proliferation of *S. cerevisiae*

and *C. glabrata* cells. This further indicated that extracellular toxicity assay in yeast using chemically-synthesised A β ₄₂ peptide results in a different outcome.

My study shows for the first time that exogenous folate (folic acid or folinic acid) causes *C. glabrata* cells suspended in water to undergo two cycles of cell division and to form multiple buds. This effect was limited to cells in stationary phase and was more profound in quiescent cells. This study further exploited the cellular uptake of folate by utilising a putative folate transporter (YJL163C) and examined its role. Folate uptake appeared normal in YJL163C overexpressed yeast cells and a deletant mutant strain. Furthermore, the YJL163C deletion did not abolish folate-stimulated cell division. However, YJL163C overexpression in a diploid resulted in meiotic cell divisions. The A β ₄₂ was toxic to the YJL163C deletion strain suggesting that the YJL163C putative transporter was not a unique receptor for A β ₄₂.

Another novel outcome of this study was the identification of the most suitable isomers of bio-inspired compounds with anti-amyloidogenic properties using both *in vivo* assays and *in vitro* assays. The positions of the hydroxyl moieties on the aromatic rings were found to be the major determinant of their potency rather than number of hydroxyl groups. This data implied that any yeast screening assays should be complemented with conventional *in vitro* assays to ensure their validity prior to high-throughput analyses. Another major development was the identification that the GFP-A β ₄₂ fusion system, which was utilised as a screening platform for identification of anti-oligomerisation of compounds, could only be used when expressed in *AHPI* deletant mutant strain while no effect was observed in the wild-

type strain. The data from this study highlights the pitfalls that exist in current yeast model systems and how they should be improved for future investigations.

PUBLICATIONS AND CONFERENCE PROCEEDINGS

Porzoor, A., Alford, B., Hügel, H., Grando, D., Caine, J., and Macreadie, I. 2015. Anti-amyloidogenic properties of some phenolic compounds. *Biomolec*, 5, 505-27.

Porzoor, A., and Macreadie, I. 2015 (In press). Yeast as a model for aggregation toxicity in Alzheimer's disease, autophagic responses and drug screening. *System biology of Alzheimer's disease: Methods and protocols*. Castrillo, J. I. & Oliver, S. G. (eds.) *Systems biology of Alzheimer's disease: Methods and protocols*. MIMB series Humana, Springer. New York, USA

Porzoor, A., Caine, J., and Macreadie, I. 2014. Pretreatment of chemically-synthesized A β ₄₂ affects its biological activity in yeast. *Prion*, 8, 404-10.

Porzoor, A., and Macreadie, I. G. 2013. Application of yeast to study the Tau and Amyloid- β abnormalities of Alzheimer's disease. *J Alzheimers Dis*, 35, 217-25.

Manuscript in preparation

Porzoor, A., and Macreadie, I. Effects of exogenous folates, amyloid beta peptide and a putative folate transporter on yeast. *J Microbial Cell*. (Short review)

Conference proceedings and scientific meetings:

Porzoor, A., Macreadie, I., and Caine, J. From toxicity to proliferation; effect of chemically synthesized A β ₄₂ on yeast. Combio 2014, National Convention Centre, Canberra, ACT. ASBMB.

Porzoor, A., Waddington, L., Hügel, H. M., Grando, D., Macreadie, I., and Caine, J. Anti amyloidogenic potential of danshen derived chemicals and their analogs analysed by *in vitro* and *in vivo* yeast assay. Yeast Genetics Meeting, 2014 University of Washington, Seattle, USA. GSA.

Porzoor, A., and Macreadie, I. Folate, amyloid beta and cell growth in relation to Alzheimer's disease. Alzheimer's Association International Conference, 2014 Copenhagen, Denmark. AAIC.

Macreadie, I., **Porzoor, A.,** Bharadwaj, P., Verdile, G., Caine, J., Martins, R. N., and Macaulay, S. L. Utilising yeast screens to find chemo preventatives for A β , the toxic agent of Alzheimer's disease. 12th International Symposium on the Genetics of Industrial Microorganisms 2013 Cancun, Mexico.

ACKNOWLEDGMENTS

I would like to begin by thanking my three supervisors: Associate Professor Ian Macreadie, Assoc Prof Danilla Grando and Dr Joanne Caine. I thank my senior supervisor, Ian Macreadie for giving me the opportunity to undertake this PhD research. Thanks Ian for introducing me to the powerful world of yeast and letting me find my own path.

I would like to express my sincere gratitude towards my co-supervisor Dr Joanne Caine, for being such a great mentor and friend during my candidature. Thanks Jo, without your continuous guidance, care and brainstorming discussions even when you were unwell, I would have been lost. Your generosity has been tremendous and I am indebted to you for allowing me to do part of my experiments at CSIRO.

Special thanks to Assoc Prof Danilla Grando for never-ending support, advice and guidance. I am indebted to you Danilla for the time you took in making sure that I was on the right track, providing constant feedback on the thesis writing and going above and beyond to read every line of the thesis in detail. You are a true teacher who always seeks to do the best for the students. I am forever grateful to you for your constant support.

I thank CSIRO, Parkville staff for their generosity, and welcoming attitude. I would like to particularly acknowledge, Dr Julie Nigro for her help with tissue culture work and Ms Lynne Waddington for her continues support with the TEM imaging. I am blessed to know you all and I am very proud and appreciative for the opportunity of working with you.

To the Biotech lab and my close groups of friends thank you for your friendship and support during this journey. Thanks to Prof Peter Smooker for his support and help at the start of my candidature.

I thank Assoc Prof Helmut Hugel and Dr Sylvia Urban for supplying the compounds. I am grateful to Helmut for his guidance and feedback about the structures of the compounds and chapter 5.

Everyday financial support for the Ph.D. was provided by the Australian Postgraduate Award (APA) and RMIT University supplementary scholarship.

To my dear husband, *Jelil* and my lovely children *Emma* and *Keanu*, thanks for your patience. Your love and support has been incredible and kept me going. I am so lucky and eternally blessed to have you as my family. I owe you everything and I dedicate my research to you.

“When you want something, all the universe conspires in helping you to achieve it.”

Paulo Coelho, *The Alchemist*

TABLE OF CONTENTS
ORIGINALITY STATEMENT**COPYRIGHT STATEMENT****AUTHENTICITY STATEMENT**

ABSTRACT	ii
ACKNOWLEDGMENTS	vi
LIST OF FIGURES	xiii
LIST OF TABLES	xvii
LIST OF ABBREVIATIONS	xviii

CHAPTER 1: INTRODUCTION

1.1 ALZHEIMER'S DISEASE.....	1
1.1.1 Epidemiology and incidence.....	1
1.2 POSSIBLE CAUSE AND CLINICAL FEATURES OF AD.....	2
1.2.1 Amyloid cascade hypothesis.....	3
1.2.2 Biofloculant hypothesis.....	4
1.2.3 Cell cycle hypothesis.....	5
1.3 RISK FACTORS IN THE ETIOLOGY OF AD.....	6
1.3.1 Lifestyle.....	6
1.3.2 Associated medical conditions.....	7
1.3.3 Genetics.....	7
1.4 YEAST AS A MODEL ORGANISM.....	8
1.5 HIGH-THROUGHPUT SCREENING FOR AD CHEMO-PREVENTATIVES.....	17
1.6 GENERAL AIMS AND SUMMARY OF THIS STUDY.....	24

CHAPTER 2: MATERIALS AND METHODS

2.1 INTRODUCTION.....	26
2.2 YEAST AND <i>E. COLI</i> STRAINS AND MEDIA.....	26
2.2.1 Yeast strains and media.....	26
2.2.2 Bacterial strains and media.....	27
2.3 GENERAL YEAST GROWTH CONDITIONS AND CELL FRACTIONATION.....	28
2.3.1 Stationary and exponential phase growth of yeast and storage conditions.....	28
2.3.2 Fractionation of stationary phase <i>C. glabrata</i> and <i>S. cerevisiae</i>	29
2.3.3 Viability assay using colony counts.....	30
2.3.4 Spot assay.....	30
2.3.5 Minimum inhibitory concentration of compounds.....	31
2.3.6 Folic acid and folinic acid treatment of stationary phase <i>C. glabrata</i>	31
2.3.7 MTX and folinic acid treatment of <i>S. cerevisiae</i>	32
2.3.8 Study of YJL163C on folic acid and A β_{42} entry.....	32
2.4 GENERAL MOLECULAR BIOLOGY METHODS.....	33
2.4.1 Plasmids.....	33
2.4.2 Primers.....	34
2.4.3 DNA extraction and purification.....	34
2.4.4 Polymerase chain reaction.....	36

2.4.5 Agarose gel electrophoresis.....	36
2.4.6 DNA and plasmid sequencing.....	37
2.4.7 Digestion and ligation of the genes into p416.GPD.....	37
2.4.8 Bacterial competent cells (CaCl ₂ method).....	38
2.4.9 Plasmid extraction.....	39
2.5 TRANSFORMATION METHODS.....	39
2.5.1 Transformation of <i>E. coli</i> competent cells with plasmids.....	39
2.5.2 Transformation of <i>S. cerevisiae</i> with plasmids.....	40
2.6 FLOW CYTOMETRY.....	42
2.6.1 Calcofluor white M ₂ R bud scar assay.....	43
2.6.2 Screening of compounds using GFP-A β ₄₂ transformants.....	43
2.6.3 Thioflavin T associated with aggregation of pretreated A β ₄₂ with the cell wall proteins of <i>S. cerevisiae</i>	46
2.7 SYNTHETIC A β ₄₂ PEPTIDE PREPARATION AND ANALYSIS.....	46
2.7.1 General peptide preparation and concentration determination.....	46
2.7.2 HFIP pretreatment method of A β ₄₂ peptide preparation.....	47
2.7.3 Stimulation of cell cycle in yeast by NH ₄ OH pre-treated peptide.....	48
2.7.4 Yeast treatment by the A β ₄₂ peptide pretreated by NH ₄ OH and HFIP methods.....	48
2.7.5 Cytotoxicity analysis of HFIP and NH ₄ OH pretreated A β ₄₂ on wild-type, mutant and overexpressed <i>AHP1</i>	49
2.7.6 Cytotoxicity analysis of DMSO and NaOH on exponential and stationary phase yeast cells.....	49
2.7.7 Cytotoxicity analysis of aged A β ₄₂ peptide pretreated by HFIP and NH ₄ OH.....	50
2.7.8 Cytotoxicity assay of NH ₄ OH pretreated A β ₄₂ peptide solutions in PC12 cell culture.....	50
2.8 THIOFLAVIN T ASSAY.....	51
2.9 CYTOTOXICITY SCREENING OF THE A β ₄₂ SPECIES FORMED AS A RESULT OF CO-INCUBATION WITH POTENTIAL INHIBITORS.....	52
2.10 PROTEOMIC METHODS.....	53
2.10.1 Sample preparation of compounds co-incubated with A β ₄₂ peptide for gel electrophoresis.....	53
2.10.2 SDS PAGE silver staining for detection of A β ₄₂ oligomers in the presence of compounds.....	53
2.10.3 Immunoblotting for detection of potential A β ₄₂ fibril inhibitors.....	54
2.10.4 Sample preparation for immunoblotting to identify the effect of solvent and pretreatment methods on the extent of A β ₄₂ oligomeric formation.....	55
2.11 CONFOCAL, EPIFLUORESCENCE AND BRIGHT FIELD MICROSCOPIC METHODS.....	55
2.11.1 Slide preparation.....	55
2.11.2 Microscopy.....	56
2.11.3 Meiosis event in yeast cells.....	57
2.11.4 Nuclear DNA staining.....	57
2.11.5 Calcofluor white M ₂ R staining.....	57
2.11.6 Thioflavin T staining of yeast cells.....	58
2.12 TEM.....	58
2.12.1 Sample preparation for analysis of A β ₄₂ co-incubated with the compounds.....	58
2.12.2 Sample preparation for TEM imaging of NH ₄ OH and HFIP pretreated A β ₄₂ peptide.....	59
2.13 DATABASES USED.....	59
2.14 STATISTICAL ANALYSIS.....	60

CHAPTER 3: CELL DIVISION AND PROLIFERATION ANALYSIS IN *C. GLABRATA* AND *S. CEREVISIAE* AND CHARACTERISATION OF THE FOLATE TRANSPORTER GENE

3.1 INTRODUCTION.....	61
3.2 AIMS.....	65
3.3 MATERIALS AND METHODS.....	66
3.4 RESULTS.....	68
3.4.1 Effect of folic acid and folinic acid on the morphology of stationary phase <i>C. glabrata</i>	68
3.4.2 Effect of folic acid and folinic acid on the viability of stationary phase <i>C. glabrata</i>	69
3.4.3 Calcofluor fluorescence intensity of bud scars increases in the presence of folic acid and folinic acid.....	71
3.4.4 Viability curve of stationary phase <i>C. glabrata</i> cells in the presence of folic acid after prolonged incubation and effect of introducing nutrients.....	74
3.4.5 Survival of wild-type <i>S. cerevisiae</i> and deletant <i>EHY1</i> in the presence of folic acid and folinic acid with or without addition of MTX.....	76
3.4.6 Viability assessment of the wild-type <i>S. cerevisiae</i> in the presence of folinic acid and MTX.....	78
3.4.7 Homology assessment of CAGL0M08426g and YJL163C gene and its similarity to the human folate transporter gene.....	80
3.4.8 Induction of cell division by methotrexate in the presence, absence and overexpressed folate transporter gene in <i>S. cerevisiae</i>	83
3.4.9 Folate uptake in <i>S. cerevisiae</i> in the presence and absence of folate transporter gene.....	84
3.4.10 Effect of extracellular added synthetic A β ₄₂ on wild-type, mutants (<i>YJL163CΔ</i>) and over expressed FOLT in <i>S. cerevisiae</i>	88
3.5 DISCUSSION.....	90
3.5.1 Aberrant proliferation induced by folates in <i>C. glabrata</i>	91
3.5.2 Folate causes aberrant sporulation in <i>S. cerevisiae</i> particularly in the presence of FOLT overexpression.....	96
3.6 CONCLUSION.....	100

CHAPTER 4: EFFECT OF SYNTHETIC A β ₄₂ ON YEAST AND THE ROLE OF *AHP1* IN PROTECTION

4.1 INTRODUCTION.....	101
4.2 AIMS.....	104
4.3 MATERIALS AND METHODS.....	105
4.4 RESULTS.....	107
4.4.1 Effect of solvents on the survival of yeast.....	107
4.4.2 Effect of NH ₄ OH pretreated A β ₄₂ dissolved in 60 mM NaOH on exponential phase yeast cells suspended in H ₂ O.....	109
4.4.3 Effect of NH ₄ OH pretreated A β ₄₂ dissolved in 60 mM NaOH on quiescent and non-quiescent <i>C. glabrata</i> cells.....	112
4.4.4 Effect of NH ₄ OH pretreated synthetic A β ₄₂ on <i>C. glabrata</i> cells suspended in PBS.....	114
4.4.5 Effect of NH ₄ OH pretreated A β ₄₂ on PC12 neuronal cells.....	115

4.4.6 Effect of HFIP pretreated A β ₄₂ dissolved in H ₂ O on exponentially phase growing <i>S. cerevisiae</i>	118
4.4.7 Survival of quiescent and non-quiescent <i>C. glabrata</i> in the presence of HFIP pretreated A β ₄₂ dissolved in H ₂ O.....	119
4.4.8 Effect of synthetic A β ₄₂ preparation using the HFIP and NH ₄ OH methods dissolved in H ₂ O on exponential phase yeast cells.....	121
4.4.9 Flow cytometry analysis of effect of A β ₄₂ peptide pretreated with HFIP or NH ₄ OH on <i>S. cerevisiae</i>	123
4.4.10 Microscopic analysis of amyloidogenic proteins on the surface of <i>S. cerevisiae</i> and their aggregation propensity in the presence of HFIP and NH ₄ OH pretreated A β ₄₂	125
4.4.11 TEM analysis of A β ₄₂ peptide conformers generated by pretreatment.....	127
4.4.12 Effect of prolonged incubation of A β ₄₂ peptide on <i>S. cerevisiae</i> cells.....	130
4.4.13 Western blot analysis of NH ₄ OH and HFIP pretreated A β ₄₂ peptide at 0 h and after prolonged incubation.....	131
4.4.14 Role of <i>AHP1</i> overexpression in the protection against cellular toxicity induced by HFIP pre-treated A β ₄₂	134
4.5 DISCUSSION.....	136
4.5.1 Pretreatment determines the activity of A β ₄₂ peptide.....	137
4.5.2 Older cells are more susceptible to the effect of A β ₄₂ than younger cells.....	139
4.5.3 Effect of chemically-synthesised A β ₄₂ is limited to the extracellular compartment of yeast.....	140
4.5.4 <i>Ahp1p</i> overexpression cannot rescue cells from the toxicity effect of A β ₄₂	143
4.6 CONCLUSION.....	145
CHAPTER 5: VALIDATING THE YEAST MODEL OF ALZHEIMER'S DISEASE FOR COMPOUND LIBRARY SCREENING	
5.1 INTRODUCTION.....	146
5.1.1 Danshen compounds.....	150
5.1.2 MATNAP proprietary compounds.....	151
5.1.3 Biscoumarins.....	152
5.2 AIMS.....	153
5.3 MATERIALS AND METHODS.....	154
5.4 RESULTS.....	156
5.4.1 DANSHEN COMPOUNDS ANALYSIS.....	156
5.4.1.1 Screening of danshen compounds in an <i>ahp1</i> mutant expressing green fluorescent protein fused to A β ₄₂ (GFP-A β ₄₂).....	156
5.4.1.2 Screening of danshen compounds in the BY4743 wild-type <i>S. cerevisiae</i> expressing green fluorescent protein associated with GFP and GFP-A β ₄₂	161
5.4.1.3 Anti-oligomerisation screening of danshen derivatives and analogues using thioflavin T analysis.....	165
5.4.1.4 Immunoblotting analysis of chemically-synthesised A β ₄₂ co-incubated with selected danshen compounds.....	168
5.4.1.5 TEM analysis of A β ₄₂ species formed in the presence of selected potent danshen compounds.....	171
5.4.1.6 Effect of selected danshen compounds on the toxicity of A β ₄₂	176
5.4.1.7 Cytotoxicity of the A β ₄₂ species generated in the presence of the selected five danshen compounds.....	178
5.4.2 MATNAP PROPRIETARY COMPOUNDS ANALYSIS- Minimum inhibitory concentration determination.....	179

5.4.2.1 Fluorescence produced associated with an <i>AHP1</i> deletant mutant expressing green fluorescent protein fused to A β ₄₂ (GFP-A β ₄₂) in the presence of MATNAP compounds.....	181
5.4.2.2 Fluorescence based screening of the wild-type <i>S. cerevisiae</i> (BY4743) transformed with GFP-A β ₄₂ plasmid in the presence of MATNAP compounds.....	183
5.4.2.3 Anti-oligomerisation analysis of structurally designed, MATNAP molecules by thioflavin T assay.....	186
5.4.2.4 TEM analysis of A β ₄₂ species formed in the presence of selected MATNAP compounds.....	188
5.4.2.5 Silver staining and western blot analysis of the anti-amyloidogenic candidates.....	192
5.4.2.6 Cytotoxicity of the A β ₄₂ species formed as a result of co-incubation with selected compounds on yeast.....	194
5.4.3 ANTI-OLIGOMERISATION ACTIVITIES OF BISCOUMARIN ANALOGS.....	196
5.4.3.1 Anti-oligomerisation activity of biscoumarins measured by ThT assay.....	197
5.4.3.2 Cytotoxicity effect of A β ₄₂ co-incubated with biscoumarin on <i>C. glabrata</i>	200
5.4.3.3 TEM analysis of A β ₄₂ co-incubated with bis-benzoquinone.....	201
5.5 DISCUSSION.....	202
5.5.1 The position rather than the number of -OH groups are more important determinants of anti-oligomerisation activity.....	205
5.5.2 Conformational changes and toxicity associated with co-incubation of A β ₄₂ with compounds.....	206
5.5.3 Fluorescence associated with GFP-A β ₄₂ for screening of anti-oligomers is not identical to the ThT assay.....	209
5.6 CONCLUSION.....	214
CHAPTER 6: FINAL CONCLUSIONS AND FUTURE DIRECTIONS.....	215
REFERENCES.....	223
APPENDIX.....	268

LIST OF FIGURES

FIGURE 1-1 AMINO ACID CHANGES LEADING TO THE EARLY-ONSET OF ALZHEIMER'S DISEASE.....	11
FIGURE 1-2 THERAPEUTIC STRATEGIES TO BLOCK AMYLOIDOSIS.....	19
FIGURE 2-1 SCHEMATIC ILLUSTRATION OF FOLT PLASMID CONSTRUCTS DEVELOPED AND USED IN THIS STUDY.....	41
FIGURE 2-2 SCHEMATIC ILLUSTRATION OF <i>AHP1</i> PLASMID CONSTRUCTS DEVELOPED AND USED IN THIS STUDY FOR OVEREXPRESSION OF AHP1P...	42
FIGURE 2-3 SCHEMATIC ILLUSTRATION OF FLOW CYTOMETRY USING GFP AND GFP-AB ₄₂ (GA) TRANSFORMANTS.....	45
FIGURE 3-1 SCHEMATIC ILLUSTRATION OF FOLIC ACID, FOLINIC ACID AND METHOTREXATE UPTAKE BY CELLS IN HUMANS.....	63
FIGURE 3-2 MICROSCOPIC IMAGES OF <i>C. GLABRATA</i> IN THE PRESENCE OF FOLIC ACID AND FOLINIC ACID.....	69
FIGURE 3-3 SURVIVAL OF <i>C. GLABRATA</i> IN THE PRESENCE OF FOLIC ACID AND FOLINIC ACID.....	71
FIGURE 3-4 CALCOFLUOR STAINING OF THE BUD SCARS IN STATIONARY PHASE <i>C. GLABRATA</i>	73
FIGURE 3-5 GROWTH OF STATIONARY PHASE <i>C. GLABRATA</i> IN THE PRESENCE AND ABSENCE OF FOLIC ACID.....	75
FIGURE 3-6 SURVIVAL OF THE BY4743 AND EHY1 IN THE PRESENCE OF FOLIC ACID AND FOLINIC ACID WITH OR WITHOUT ADDITION OF MTX.....	77
FIGURE 3-7 GROWTH AND VIABILITY OF BY4743 IN THE PRESENCE OF MTX AND FOLINIC ACID.....	80
FIGURE 3-8 HOMOLOGY ASSESSMENT OF PUTATIVE FOLATE TRANSPORTER.....	82
FIGURE 3-9 SPOT ASSAY ANALYSIS OF <i>S. CEREVISIAE</i> EHY1 MUTANT TRANSFORMED WITH EMPTY VECTOR (p416.GPD) AND FOLT GENE INSERT, COMPARED WITH THE <i>YJL163CA</i>	84
FIGURE 3-10 MICROSCOPIC IMAGES OF FOLIC ACID UPTAKE BY BY4743, <i>YJL163CA</i> AND FOLTP OVEREXPRESSED YEAST CELLS.....	85
FIGURE 3-11 MICROSCOPIC IMAGING OF THE <i>S. CEREVISIAE</i> OVEREXPRESSING THE FOLTP GENE REVEALED AN INDUCTION OF SPORULATION IN THE PRESENCE OF FOLATE.....	87
FIGURE 3-12 ROLE OF PUTATIVE FOLATE TRANSPORTER GENE (YJL163C) IN THE CELLULAR UPTAKE OF AB ₄₂ PEPTIDE.....	89

FIGURE 3-13 TYPE OF INSULT THAT CAN LEAD TO DNA REPLICATION AND ULTIMATELY NEURONAL DEATH.....	92
FIGURE 4-1 EFFECT OF SOLVENTS ON SURVIVAL OF <i>S. CEREVISIAE</i> AND <i>C. GLABRATA</i>	108
FIGURE 4-2 EFFECT OF NH ₄ OH PRETREATED AB ₄₂ DISSOLVED IN 60 mM NAOH ON EXPONENTIAL PHASE YEAST.....	111
FIGURE 4-3 EFFECT OF NH ₄ OH PRETREATED AB ₄₂ DISSOLVED IN 60 mM NAOH ON SURVIVAL OF STATIONARY PHASE <i>C. GLABRATA</i>	113
FIGURE 4-4 EFFECT OF SYNTHETIC AB ₄₂ PREPARATION USING THE NH ₄ OH METHOD ON <i>C. GLABRATA</i> CELLS SUSPENDED IN BUFFER (PBS).....	115
FIGURE 4-5 COMPARISON EFFECT OF NH ₄ OH PRETREATED AB ₄₂ PEPTIDES STOCKS FROM TWO LABORATORIES ON THE SURVIVAL OF PC12 CELLS.....	117
FIGURE 4-6 VIABILITY STUDIES OF <i>S. CEREVISIAE</i> IN THE PRESENCE OF HFIP PRETREATED AB ₄₂ DISSOLVED IN H ₂ O.....	119
FIGURE 4-7 CYTOTOXICITY OF HFIP PRETREATED AB ₄₂ ON THE QUIESCENT AND NON-QUIESCENT <i>C. GLABRATA</i> CELLS.....	120
FIGURE 4-8 EFFECT OF TWO PREPARATION METHODS OF SYNTHETIC AB ₄₂ DISSOLVED IN H ₂ O ON YEAST CELLS.....	122
FIGURE 4-9 FLOW CYTOMETRY ANALYSIS OF <i>S. CEREVISIAE</i> TREATED WITH HFIP AND NH ₄ OH PREPARED AB ₄₂	124
FIGURE 4-10 MICROSCOPIC ANALYSIS OF THIOFLAVIN T TREATED <i>S. CEREVISIAE</i>	126
FIGURE 4-11 TEM MICROGRAPH OF CONFORMATIONAL CHANGES IN SYNTHETIC AB ₄₂ PREPARED BY HFIP AND NH ₄ OH METHODS.....	129
FIGURE 4-12 EFFECT OF AGED PEPTIDE ON YEAST CELLS.....	131
FIGURE 4-13 WESTERN BLOT ANALYSIS OF EFFECT OF PRETREATMENT ON THE SIZE OF AB ₄₂	133
FIGURE 4-14 ROLE OF <i>AHP1</i> IN THE CYTOTOXICITY INDUCED BY AB ₄₂	135
FIGURE 5-1 OVERVIEW OF THE DIVERSE THERAPEUTIC APPLICATIONS OF DANSHEN CONSTITUENTS.....	151
FIGURE 5-2 FLUORESCENT AND LIGHT IMAGES OF <i>S. CEREVISIAE</i> TRANSFORMED WITH GFP AND GFP-AB ₄₂ PLASMIDS.....	158
FIGURE 5-3 GFP AND GFP-AB ₄₂ TRANSFORMANTS OF <i>AHP1</i> KNOCK-OUT MUTANT.....	159
FIGURE 5-4 QUANTITATIVE ANALYSIS OF DANSHEN COMPOUNDS ON WILD-TYPE BY4743 <i>S. CEREVISIAE</i> EXPRESSING GFP-AB ₄₂ MEASURED BY FLOW CYTOMETRY.....	162

FIGURE 5-5 FLOW CYTOMETRY ANALYSIS OF THE APOPTOSIS AND GREEN FLUORESCENCE EXPRESSION INDUCED BY TEN SELECTED DANSHEN COMPOUNDS ON WILD-TYPE <i>S. CEREVISIAE</i> EXPRESSING GFP-AB ₄₂	164
FIGURE 5-6 AMYLOID FORMATION ASSAYED BY THIOFLAVIN T FLUORESCENCE	167
FIGURE 5-7 SDS-PAGE ANALYSES OF AB ₄₂ CONFORMERS IN THE PRESENCE AND ABSENCE OF COMPOUNDS.....	171
FIGURE 5-8 TEM MICROGRAPHS OF AB ₄₂ CO-INCUBATED WITH SELECTED COMPOUNDS.....	173
FIGURE 5-9 CYTOTOXICITY EFFECT OF FRESHLY PREPARED AB ₄₂ ON <i>C. GLABRATA</i> CELLS.....	177
FIGURE 5-10 EFFECT OF CONFORMATIONAL CHANGES OF SYNTHETIC AB ₄₂ PRODUCED IN THE PRESENCE OF DANSHEN COMPOUNDS ON THE SURVIVAL OF YEAST CELLS.....	179
FIGURE 5-11 AN EXAMPLE OF MIC90 DETERMINATION FOR RB9_6.3 ON <i>C. ALBICANS</i> WM1172.....	180
FIGURE 5-12 INTENSITY OF FLUORESCENCE EXPRESSION IN <i>AHP1</i> TRANSFORMED WITH GFP AND GFP-AB ₄₂ (GA), AS MEASURED BY FLOW CYTOMETRY.....	182
FIGURE 5-13 ANTI AGGREGATION PROPENSITY OF MATNAP COMPOUNDS (50 μM) USING GFP-AB ₄₂ WILD-TYPE <i>S. CEREVISIAE</i> TRANSFORMANTS.....	184
FIGURE 5-14 AMYLOID FORMATION ASSAYED BY THIOFLAVIN T FLUORESCENCE AFTER INCUBATION WITH MATNAP COMPOUNDS.....	187
FIGURE 5-15 TEM MICROGRAPHS OF AB ₄₂ CO-INCUBATED WITH SELECTED THT NEGATIVE COMPOUNDS.....	190
FIGURE 5-16 SDS-PAGE ANALYSIS OF AGGREGATION STATES OF AB ₄₂ PEPTIDES.....	193
FIGURE 5-17 TOXICITY EFFECT OF SYNTHETIC AB ₄₂ SPECIES PRODUCED IN THE PRESENCE OF SELECTED THT NEGATIVE COMPOUNDS ON THE SURVIVAL OF YEAST CELLS.....	194
FIGURE 5-18 STRUCTURE OF SIX BISCOUMARIN ANALOGS INVESTIGATED IN THIS STUDY.....	197
FIGURE 5-19 AMYLOID FORMATION ASSAYED BY THIOFLAVIN T FLUORESCENCE AFTER INCUBATION WITH BISCOUMARIN ANALOGS.....	198
FIGURE 5-20 CELLULAR PROTECTIONS FROM AB ₄₂ TOXICITY MEDIATED BY BISCOUMARIN SAMPLES.....	200

FIGURE 5-21 TRANSMISSION EM MICROGRAPH OF AB₄₂ CO-INCUBATED WITH 2, 3-BIS-BENZOQUINONE.....201

FIGURE 5-22 CHEMICAL STRUCTURE OF DIHYDROXYBENZOIC ACID ISOMERS.....206

FIGURE 5-23 SCHEMATIC OVERVIEW OF COMPOUNDS IDENTIFIED THAT ENHANCED OR DECREASED FLUORESCENCE ASSOCIATED WITH GFP-AB₄₂ OR THIOFLAVIN T OR BOTH.....212

LIST OF TABLES

TABLE 1-1 MAJOR ADVANCES IN YEAST STUDIES THAT HAD A VALUABLE IMPACT ON HUMAN HEALTH AND DISEASE.....	9
TABLE 1-2 ROLE OF YEAST IN REVEALING SOME OF THE FACTORS BELIEVED TO CONTRIBUTE TO THE DEVELOPMENT OF ALZHEIMER'S DISEASE.....	14
TABLE 1-3 SELECTED CHEMICALS/COMPOUNDS TESTED IN <i>S. CEREVISIAE</i> THAT MAY HAVE BENEFITS FOR TREATMENT AND PREVENTION OF AD AND OTHER AGE-RELATED DISEASES.....	21
TABLE 2-1 YEAST STRAINS USED IN THIS STUDY.....	27
TABLE 2-2 MEDIA USED FOR GROWTH OF YEAST STRAINS IN THIS STUDY.....	28
TABLE 2-3 PLASMIDS USED IN THIS STUDY.....	33
TABLE 2-4 MOLECULAR WEIGHTS, COEFFICIENT OF EXCITATION AND ABSORBANCE OF AB ₄₂	47
TABLE A-1 CHEMICAL STRUCTURE OF DANSHEN DERIVED AND SYNTHESISED ANALOGS WITH THEIR MOLECULAR WEIGHT AND PHYSICAL PROPERTIES..	260
TABLE A-2 LIST OF PROPRIETARY MATNAP COMPOUNDS ALONG WITH THEIR COLOUR AND CALCULATED MINIMUM INHIBITORY CONCENTRATION (MIC).....	264

LIST OF ABBREVIATIONS

A ₂₁₄	absorbance measured at 214nm
A β	amyloid-beta
A β ₄₂	amyloid-beta (42-amino acid peptide)
AD	Alzheimer's disease
APP	amyloid precursor protein
APP β	amyloid precursor protein- β secretase cleavage
BACE	beta site of APP cleaving enzyme
BBB	blood brain barrier
bp	base pairs
°C	degree Celsius
CaCl ₂	calcium chloride
CFU	colony forming unit
<i>C. glabrata</i>	<i>Candida glabrata</i>
CGD	<i>Candida</i> genome database
CNS	central nervous system
CWI	cell wall integrity
d	days
DAPI	4,6-diaminido-2-phenylindole dihydrochloride
DIC	differential interference contrast
DMF	dimethyl formamide
DMSO	dimethyl sulfoxide

DNA	deoxyribonucleic acid
ddH ₂ O	double-distilled water
<i>E. coli</i>	<i>Escherichia coli</i>
ECL	enhanced chemiluminescence
EGCG	epigallocatechin gallate
EUROSCARF	European <i>Saccharomyces cerevisiae</i> Archive for Functional Analysis
FAD	familial Alzheimer's disease
FI	fluorescent intensity
F	phenylalanine
GFP	green fluorescent protein
GFP- A β ₄₂	green fluorescent protein fused to amyloid-beta (42-amino acid peptide)
h	hour(s)
H ₂ O	water
HFIP	hexafluoroisopropanol
HMW	high molecular weight
H ₂ O ₂	hydrogen peroxide
HSR	heat shock protein
kb	kilobase
kDa	kilodaltons
L	leucine
L	litre

LB	Luria-Bertani broth/media
LiOAC	lithium acetate
LMW	low molecular weight
mg	milligram
min	minute(s)
ml	milliliter
mM	millimolar
M	Molar
MFS	major facilitator superfamily
MIC	minimum inhibitory concentration
MP	mitotic plaque
MT	microtubule
MTX	methotrexate
MW	molecular weight
NaCl	sodium chloride
Na ₂ CO ₃	sodium carbonate
NEB	New England Biolabs, <i>Inc.</i>
NH ₄ OH	ammonium hydroxide
NaOH	sodium hydroxide
nm	nanometre
OD _{600nm}	optical density at 600 nm wavelength
PAGE	polyacrylamide gel electrophoresis
PBS	phosphate buffered saline

PCR	polymerase chain reaction
PI	propidium iodide
ROS	reactive oxygen species
rpm	rotation per minute
RT	room temperature
SDS	sodium dodecyl sulphate
SDS-PAGE	sodium dodecyl sulphate polyacrylamide gel electrophoresis
<i>S. cerevisiae</i>	<i>Saccharomyces cerevisiae</i>
SGD	<i>Saccharomyces cerevisiae</i> genome database
TAE	Tris-acetate-EDTA buffer
TEM	transmission electron microscopy
ThT	thioflavin T
T _m	melting temperature
TPx	thiol peroxidase
TOR	target of rapamycin
Ura	uracil
UV	ultraviolet
V	valine
V	Volts
v/v	volume per volume ratio
WT	wild-type
w/v	weight per volume ratio
x g	acceleration

YNB	yeast nitrogen base
YEPD	media containing yeast extract, peptone, and D-glucose
YEPE	media containing yeast extract, peptone, and ethanol
α	alpha
β	beta
γ	gamma
ε	epsilon
μg	microgram
μl	microliter
μM	micromolar
π	pi
τ	tau

Open reading frames (ORFs) of *Saccharomyces cerevisiae* are designated with three letters followed by a three digit numerical code and ending with either “C” or “W”. This nomenclature indicates the chromosomal position of the open reading frame (e.g. YJL163C). The *AHP1* deletant mutant strain has been referred to as *ahp1* (italicised three letters) in this study. The deletion of gene has been shown italicised and with the addition of suffix “ Δ ” (e.g. *YJL163C Δ*). Proteins have been designated by addition of suffix “p” to the standard name of the gene encoding them (e.g. Ahp1p). The putative folate transporter gene (YLR109W) has been referred to as FOLT in this study and its protein is named Foltp.

1 CHAPTER 1: INTRODUCTION

1.1 ALZHEIMER'S DISEASE

1.1.1 Epidemiology and incidence

Alzheimer's disease (AD) currently is an irreversible and progressive neurodegenerative disorder characterized by a decline in memory, intellect, comprehension and learning capacity. AD was first identified in 1906 and reported in 1907 by the German neurologist Alois Alzheimer, although in the same year Oskar Fischer reported the presence of neuritic plaques in sufferers of senile dementia (Alzheimer, 1906, 1907; Goedert, 2009). The clinical features of AD were first described by Redlich in 1898 (Redlich, 1898). It is an epidemic disease that most often occurs as an age-related disease. Among people of 80 years of age, AD affects 25% (World Health Organisation, 2012). Currently over 35.6 million individuals worldwide live with this disease and it has been estimated that approximately 106 million people will suffer from AD by 2050 due to increasing longevity (WHO, 2012). These attributes make it one of the biggest social burdens in the world.

The early-onset or familial forms of AD (FAD) are caused by genetic mutations that directly influence the overproduction of amyloid beta ($A\beta$) peptide (Schellenberg et al., 1989; Armstrong et al., 1996; Woo et al., 2011). The sporadic (late-onset) form of AD however, is caused by genetics and/or environmental factors which enhances the level of $A\beta$ production as well as reduction in its clearance rate (reviewed by Braak and Del Tredici, 2012).

1.2 POSSIBLE CAUSE AND CLINICAL FEATURES OF AD

The possible causes of AD have not been definitively established yet but invaluable insights into the disease have suggested the involvement of A β peptide (Esler et al., 1997; Kane et al., 2000; Rochet and Lansbury, 2000). The classic hallmarks of AD are the presence of senile plaques and neurofibrillary tangles in the hippocampal and cerebral cortex regions of the brain causing impairment in memory and cognition (Hardy and Allsop, 1991; Yankner and Mesulam, 1991). Death of neuronal cells and loss of synapses are typified by extracellular plaques of A β and intracellular neurofibrillary tangles (NFTs) of tau protein (Kamenetz et al., 2003; Irie et al., 2005). The strong association of A β and tau levels, combined with their toxicity implicates them as causative agents in the development of AD (reviewed in Ballard et al., 2011). A β peptide consists of 39-42 amino acids and is produced as a result of cleavage of a large trans-membrane protein called the amyloid precursor protein (APP) (Kamenetz et al., 2003). It is known that A β is produced throughout life and is present in the blood and brains of healthy individuals. The overall production and clearance rate of A β from the brain however, is still poorly understood. Studies by Motter et al. (1995) and Ida et al. (1996) have shown that the concentration of A β_{42} in cerebrospinal fluid (CSF) of non-AD individuals (0.501 ng/ml), to be reportedly ~1.7 times higher than AD patients (0.277 ng/ml). Other studies however have shown that the clearance rate of A β_{42} is impaired in AD (Shibata et al., 2000; Mawuenyega et al., 2010). The physiological roles of A β have been reviewed by Pearson and Peers (2006). Over the years many hypotheses regarding the pathogenesis of AD have been proposed. Some of these hypotheses have been described below.

1.2.1 Amyloid cascade hypothesis

The amyloid cascade hypothesis was proposed in 1992 by Hardy and Higgins. This hypothesis postulates that deposition and aggregation of A β peptide into toxic deposits within the extracellular space of the brain plays a key role in the pathogenesis of AD. This hypothesis has since been modified as plaques have been found to be a source of toxic A β rather than being toxic themselves and only the A β ₄₂ isoform has been identified as the most toxic moiety rather than the total A β (Hardy, 2006). Most of the investigations towards finding a cure for AD have focused on A β and the amyloid cascade hypothesis.

A β ₄₂ fragments are generated by the action of γ -secretase cleavage of APP (Findeis, 2007; Bignante et al., 2013; Tay et al., 2013). A β ₄₂ peptide has a negative impact on neuronal cells by disrupting mitochondrial function (Eckert et al., 2008; Pagani and Eckert, 2011), impairing calcium homeostasis (Du and Yan, 2010; Anekonda and Quinn, 2011) and promoting apoptotic signalling (Deshpande et al., 2006; Chenal et al., 2012). Therefore, γ -secretase has been an attractive target for inhibiting A β ₄₂ production (Evin et al., 2006; Wolfe, 2008; Woo et al., 2011).

The amyloid cascade hypothesis with A β peptide as having a central role in AD pathogenesis is supported by extensive studies. Although this hypothesis can explain the FAD but it cannot be extrapolated to sporadic forms of the disease (reviewed in Moreno-Trevino et al., 2015). This hypothesis remains contentious due to the important role of A β in the normal physiology of the CNS (Luo et al., 1996; Luo et al., 1997; Plant et al., 2003; Esteban, 2004; Plant et al., 2006). Other factors could

contribute to the pathology of the disease such as dysfunction of transport mechanisms to degrade excess A β (Miners et al., 2009; Haque and Nazir, 2014), overexpression of receptors that normally transport A β into the brain (Yan et al., 1996; Srikanth et al., 2011) or dysfunction of receptors that transport A β out of the brain (Harris-White and Frautschy, 2005; Deane et al., 2009).

1.2.2 Biofloculant hypothesis

The “biofloculant hypothesis” of A β was introduced by Robinson and Bishop (2002). This hypothesis posits that A β is produced naturally to bind to neurotoxic agents (e.g. metal ions, proteins, pathogens) and its precipitation into plaques may be an efficient means of neutralising and presenting these toxins to phagocytes. In this view, the precipitated A β plaques cause neurodegeneration via direct injury of adjacent neurons or by impairing cellular trafficking (Bishop and Robinson, 2002; Terry, 2002).

Interestingly, many previous investigations have implicated the presence of metal ions such as iron, copper, zinc and aluminium ions in the pathogenesis of AD (Campbell, 2006; Choo et al., 2013; Mitra et al., 2014). This has led to the development of the metal theory of AD (Bush, 2013). As the production of A β cannot be prevented due to its critical role in neuroprotection and the normal physiology of brain, the biofloculant hypothesis could provide a useful alternative hypothesis.

1.2.3 Cell cycle hypothesis

The cell cycle hypothesis was introduced in 1998 by investigators after identifying a significant increase in the expression of cell cycle proteins in the brain of AD sufferers (Busser et al., 1998; Nagy et al., 1998). This aberrant expression of cell cycle proteins and DNA replication in neurons was identified earlier in mouse model experiments (Herrup and Busser, 1995). Therefore, the focus of research has been to design compounds that could act as a ligand which could end the cell cycle at the G0/G1 interface and arrest aberrant proliferation, thereby providing neuroprotection (Woods et al., 2007; Copani et al., 2008).

Studies have shown that aneuploidy of differentiated neurons along with reactivation of the cell cycle in neuronal progenitor cells contribute to cell death in AD (Smith et al., 1999; McShea et al., 2007). These studies have shown an elevated level of DNA in the neurons of the entorhinal cortex which is associated with cell cycle dysregulation and reactivation in individuals affected by AD. Further to this, Mosch and colleagues (2007), after examining the brains of 13 patients with AD in comparison to 13 postmortem healthy control subjects using *chromogenic in situ hybridization* and PCR, found that hyperploid neurons are higher in those affected by AD and the level of these type of neurons (DNA >2n) increased as disease progressed.

There have been many proposed hypotheses for AD but none have generated consistent data and all have failed to demonstrate what exactly causes AD and more

importantly cell death. Mechanisms by which each of these factors contribute to the development or progression remains to be elucidated.

1.3 RISK FACTORS IN THE ETIOLOGY OF AD

Over the years many factors have been attributed to and proposed to contribute to the development of AD. Some of these risk factors are attributed to the lifestyle, environmental factors and the health status of affected individuals whilst others are considered as hereditary and genetic.

1.3.1 Lifestyle

Many modifiable lifestyle factors such as diet, physical activity, caloric intake, smoking and cognitive stimulation might play a role in AD (Flicker, 2010; Farioli-Vecchioli et al., 2014). Studies have found that higher caloric intake is positively associated with the incidence of AD (Luchsinger et al., 2002; Pasinetti et al., 2007). Folic acid and vitamin B₁₂ deficiency has also been proposed as a risk factor for AD (Quadri et al., 2004; Ravaglia et al., 2005). As a result of this, a diet that may decrease epigenetic changes has been proposed as an anti-aging intervention (Bacalini et al., 2014). Further measures proposed for decelerating the aging process include, caloric restriction, a diet containing bioactive nutrients (e.g. resveratrol and curcumin), and a diet supplement comprising nutrients that are involved in one-carbon metabolism (e.g. folate) (Cacabelos and Torrellas, 2014; Sezgin and Dincer, 2014).

1.3.2 Associated medical conditions

Many medical conditions are associated with an increased risk of AD including high cholesterol (Puglielli et al., 2003), high blood pressure (Thorin, 2014), inflammatory responses (Avila-Muñoz and Arias, 2014) or bacterial infection (Malaguarnera et al., 2004; Honjo et al., 2009). However, there has not been agreement in defining the actual connection of the underlying medical condition with the development of AD. For instance, the benefit of cholesterol synthesis inhibitors (statins) in lowering A β production has been suggested (reviewed by Harris and Milton, 2010) whilst long term use of simvastatin (a cholesterol-lowering medication) in female mice was found to cause neurodegeneration (Ledesma and Dotti, 2005). It has been reported that the level of cholesterol in the brain is tightly regulated (Ledesma and Dotti, 2006). Therefore, such medical conditions still remain as a risk factor contributing to the progression of the disease but their direct connections to AD are not yet known.

1.3.3 Genetics

Genomic characterisation of AD has identified more than 180 genes involved in the pathology of the disease (Cacabelos, 2004). Genetic risk factors for development of AD are more relevant to the early-onset FAD and to date, mutations in three genes that are inherited in an autosomal dominant fashion have been identified as risk factors (reviewed by Tilley et al., 1998). These are APP, presenilin 1 (PS-1) and PS-2 genes. Apolipoprotein E (apoE) ϵ 4 allele is well established as a risk factor in late-onset sporadic AD (Saunders et al., 1993; Kamboh, 2004; Bird, 2008) but has also been reported in the FAD (Chartier-Harlin et al., 1994).

Recently, a single-nucleotide polymorphism in the phosphatidylinositol binding clathrin assembly protein (PICALM) gene, which encodes a protein implicated in the clathrin-mediated endocytosis, was identified as a genetic protective factor for AD (Kanatsu et al., 2014). PICALM leads to the selective decrease in the production ratio of the pathogenic species, A β ₄₂ (Jones et al., 2013).

1.4 YEAST AS A MODEL ORGANISM

Yeast have a long history of utility in biotechnology and they currently provide a mechanism to produce valuable new biopharmaceuticals, including insulin and vaccines. Cyclin dependant kinases were also first identified and characterised in *Saccharomyces cerevisiae* by Hartwell (1970, 1971), in *Schizosaccharomyces pombe* by Nurse et al. (1976) and in the sea urchin by Hunt (as reported in Evans et al., 1983). These discoveries led to the awarding of a joint Nobel prize in 2001 for Hunt, Hartwell and Nurse. Yeast are amongst the simplest eukaryotes and share many cellular mechanisms with all eukaryotic cells including humans. This is particularly true about the budding yeast *S. cerevisiae*. As yeast are a simple eukaryotic organism, they may provide insights into the study of aberrant proliferation and un-scheduled cell division. Yeast have also provided basic insights into the broad field of biological science, including primary screening for the effect of compounds, and expression of recombinant proteins. Although outcomes of any drug tests conducted in yeast should be validated with more physiologically relevant models, they can still serve as a first line system to study many diseases. Some of these developments and how they have contributed to our knowledge of human health and disease are briefly outlined in Table 1-1.

Table 1-1 Major advances in yeast studies that had a valuable impact on human health and disease.

Yeast advance	Impact on human biology
The yeast genome was the first eukaryotic genome to be sequenced (Churcher et al., 1997)	Human genes can be presumptively identified by similarity to yeast counterparts.
The yeast gene deletion collection is complete (Tong et al., 2001; Vidan and Snyder, 2001; Bach et al., 2003; Pimentel et al., 2012)	Complementation studies with human genes can be performed.
Yeast two hybrid is developed (Fields and Song, 1989)	Human protein interactions can be studied in yeast. Human gene libraries are available for screening of human protein interactions.
Yeast three hybrid is developed (SenGupta et al., 1996)	RNA-protein interactions related to many human diseases (in particular viral infections) can be studied. Receptors for small ligands can be identified.
Studies on yeast cell cycle (Culotti and Hartwell, 1971; Hartwell, 1971; Hartwell, 1992; Paulovich et al., 1997; Emili et al., 2001; Simon and Bedalov, 2004; Müller and Grossniklaus, 2010)	<i>Schizosaccharomyces pombe</i> studies recognized as applicable to cancer research, leading to 2001 Nobel Prize.
Secretory pathway, vesicle trafficking and transport system discovered in yeast (Schekman, 2010)	Revealing the machinery that regulates the transport and secretion of proteins in our cells leading to 2013 Nobel Prize.

Yeast have long been used as a model organism for studying neurodegeneration (reviewed in Vishnevskaja et al., 2007; Khurana and Lindquist, 2010; Pereira et al., 2012). Yeast are also an established model organism for analysing conserved cell death pathways such as apoptosis and necrosis (Braun et al., 2010). Most processes involved in neurodegenerative disorders such as mitochondrial damage, oxidative stress, protein aggregation and degradation can be analysed within yeast and often these can be coupled to high-throughput screens (Mager and Winderickx, 2005).

Yeast have been used as a model organism since the early 1950s, with the earliest studies providing an understanding of the mechanism of cell cycle and division (reviewed in Wittenberg and Reed, 2005). The yeast *S. cerevisiae* was the first eukaryotic organism to have its entire genome sequenced in 1996 (Goffeau et al., 1996). Knowledge of that sequence combined with the knowledge of functions of many genes allowed a comparison with the sequences of other genomes, including the human genome, where counterparts could be identified. It is recognized that around 30% of currently known genes involved in human disease have yeast orthologs (Foury, 1997).

Studies on AD mainly involve cell culture and transgenic mouse models, however, yeast studies are playing an increasing role in understanding AD and in designing chemo-preventatives. Yeast are widely used for the heterologous expression of proteins associated with human disease and for expression of orthologues of proteins involved with human disease. The genes encoding the two main proteins/peptides implicated in AD, tau and A β , do not have orthologues in yeast but they can be expressed and studied in yeast. A β has received considerable attention because of a wealth of data that implicates A β in the development of AD. In particular, early-onset FAD can occur as result of various amino acid changes in A β (shown in Figure 1-1).

A β is generated through cleavage of A β protein precursor (APP β) by β -secretase (BACE1) and γ -secretase. The cleavage products are extremely hydrophobic

peptides that include A β ₄₀, A β ₄₂, and A β ₄₃, with the last two being more prone to aggregation and more neurotoxic while the former is found in greater concentration in FAD compared to the latter (McGowan et al., 2005; Saito et al., 2011).

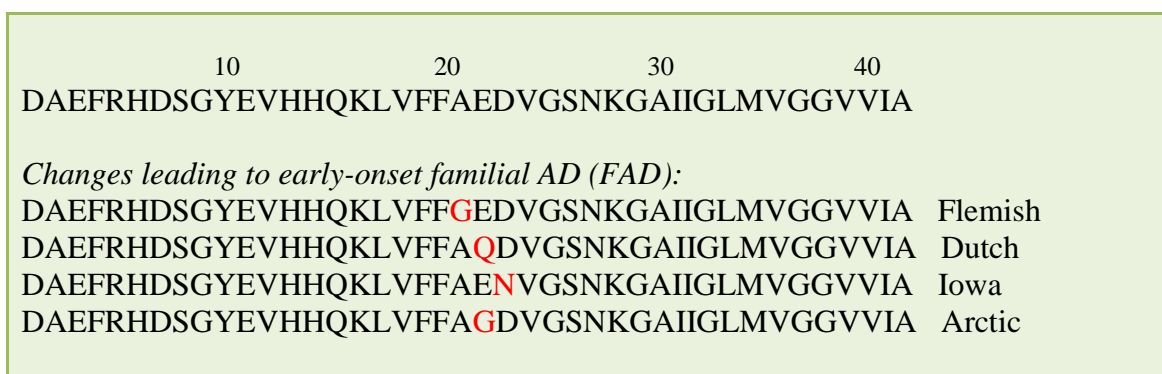


Figure 1-1 Amino acid changes leading to the early-onset of Alzheimer's disease. The amino acid sequence of A β ₄₂ is given at the top. Amino acid changes in FAD have been highlighted in: **Flemish mutation**, causing angiopathy and intracerebral haemorrhage and strokes (Hendriks et al., 1992); **Dutch mutation**, causing cerebral hemorrhage with amyloidosis and premature death (Levy et al., 1990); **Iowa mutation**, causing cerebral amyloid angiopathy and occipital calcifications (Grabowski et al., 2001); **Arctic mutation**, formation of plaques and tangle without any hemorrhage or stroke (Nilsberth et al., 2001).

In order to study A β , a few forms of these molecules are employed including chemically-synthesized A β , intracellular fused A β and intracellular recombinant forms. Studies with chemically-synthesized A β on *Candida glabrata* show an oligomerisation-dependent cytotoxicity (Bharadwaj et al., 2008). This phenomenon is now driving new approaches to block A β toxicity through inhibition of this process. The *in vivo* oligomerisation was observed when A β was fused to yeast

translational release factor, called MRF (Bagriantsev and Liebman, 2006). A β caused oligomerisation of MRF leading to loss of MRF function and growth, whereas compounds that blocked peptide aggregation led to growth. Similarly, Caine et al. (2007a) made fusions of green fluorescent protein (GFP) to A β to examine oligomerisation in the context of the fusion protein. The purpose of this was to measure the amount of correctly folded fusion protein *in vivo* through its green fluorescence, while aggregation, oligomerisation and degradation of the fusion protein would lead to loss of fluorescence. It was found that relatively small fractions of cells exhibited fluorescence but the proportion of fluorescent cells was increased by treatment with a folate (Macreadie et al., 2008), a vitamin associated with AD chemo prevention. Also, intracellular expression of A β fused to GFP was shown to be associated with reduction of yeast cell growth and an increase in the heat shock response (HSR) (Caine et al., 2007b). Increased HSR can provide protection of yeast cells from oxidative stress (Dubey et al., 2009). Yeast assays employing A β fused to MRF and GFP appear very useful for monitoring effects of compounds that influence the oligomerisation or half-life of A β (Park et al., 2011).

Yeast offer particular advantages for looking at inhibitors of A β oligomerisation. Subunits of human secretase complex such as APP β can be expressed and monitored individually in this model system. Yeast studies are inexpensive and convenient in comparison to *in vitro* studies of oligomerisation with extremely expensive and variable batches of chemically-synthesized A β that require denaturation immediately prior to use. Frequently A β is abandoned and a surrogate peptide is used in its place. A second advantage of *in vivo* studies of inhibitors of A β oligomerisation is that

compounds have to pass into the cell. The ability to pass through membranes is a definite requirement of any chemo preventative of AD, since they are required to cross the blood-brain barrier and inhibit formation of toxic oligomers within the brain. Thirdly, cytotoxic compounds fail the primary screening because they inhibit yeast growth and production of new A β . Hence, toxic molecules can be eliminated immediately. Fourthly, it is possible that compounds that act indirectly may be identified. Such compounds could include those that stimulate chaperones, or proteins that bind to A β . A summary of the contribution of yeast models to our understanding of AD is shown in Table 1-2.

It is known that intracellular A β can be stabilized and is less toxic when fused to another protein, whereas extracellular A β is highly toxic to yeast cells. While A β fusions have advantages as outlined earlier, it is expected that fusions alter the properties of A β , so it would be useful to have a yeast model producing native A β . In a recent study by D'Angelo et al. (2013), intracellular trafficking pathways were found to be essential and a major determinant for the generation of toxic species of A β in *S. cerevisiae* regardless of whether A β was used alone or fused to GFP. In transgenic mouse models for AD, A β is produced by overproduction of human APP β and secretases (Goate et al., 1991; Games et al., 1995). However, in *S. cerevisiae* the A β production is a complication that does not occur due to a lack of APP β and the two secretases (β - and γ -secretase), whereas all three endoproteases (α -, β -, and γ -secretase) has been detected in *Pichia pastoris* (Le Brocque et al., 1998).

Table 1-2 Role of yeast in revealing some of the factors believed to contribute to the development of Alzheimer's disease.

Factors that may lead to development of AD	Yeast contribution
A β oligomerisation	Two hybrid system; A β linked to LexA DNA binding domain and B42 transactivation domain (Hughes et al., 1996) Expression of A β /Sup35p fusion protein (Bagriantsev and Liebman, 2006; Von der Haar et al., 2007) Expression of A β /GFP fusion protein (Caine et al., 2007a)
Cellular toxicity with external A β	External A β is toxic to <i>C. glabrata</i> cells (Dubey et al., 2009)
Cellular toxicity with intracellular A β	Yeast models expressing intracellular A β (LaFerla et al., 2007)
Reduction of α -secretase cleavage of APP β	Expression of human APP β in yeast (Zhang et al., 1997) Identification of two aspartyl proteases, Yap3 and Mkc7 (Zhang et al., 1997) Yeast GAL reporter system (Gunyuzlu et al., 2000) APP β fused to invertase (Lüthi et al., 2003)
β -secretase cleavage of APP β	Novel growth selection allowed human β -secretase to be detected (Lüthi et al., 2003)
γ -secretase cleavage of APP β	Presenilin, nicastrin, APH-1 and PEN2 were identified as necessary components for γ -secretase activity (Edbauer et al., 2003)
Tau hyperphosphorylation	Human tau 3-R and 4-R isoforms expressed in yeast (Vandebroek et al., 2005a, Vandebroek et al., 2005b, 2006)

Chemically-synthesized A β has been shown to be toxic to *C. glabrata* (Bharadwaj et al., 2008). This has been an exciting development that further supports that yeast can model findings in neuronal cells as neuronal cells are similarly affected. Neuronal cells are terminally differentiated cells and A β stimulates cell division, which is a lethal event for them (Ding et al., 2000; Mosch et al., 2007). It is yet to be

determined how A β kills *C. glabrata* and whether this effect can also be viewed in *S. cerevisiae*. In yeast, the toxicity assay is performed in water: A β is added to cells in water and after 16 hours of incubation (Bharadwaj et al., 2008), cells are plated out to determine the viable colony count. In the absence of A β , cells in water remain quiescent for many days with no loss of viability. However, when a freshly prepared solution of A β is added, it binds the surface of the cells and kills them within hours. If the A β is allowed to form fibrils, it is no longer toxic. A study using the molecular dynamics simulations has shown that water can actually accelerate protein aggregation and fibril formation in the A β peptide similar to any hydrophobic sequence whereas this process occurs more slowly for hydrophilic sequences (Thirumalai et al., 2012). Likewise, changes within A β itself that prevent oligomerisation also block the toxic effect. Although A β is generally regarded as a toxic molecule, the opposite effect has occasionally also been shown in both yeast and human cells. In *S. cerevisiae*, A β can result in proliferation (Chacińska et al., 2002), and with adult neuronal stem cells A β can stimulate division (Heo et al., 2007).

In 1975, Weingarten and colleagues identified a protein factor named tau essential for microtubule assembly (Weingarten et al., 1975). However, when tau is hyperphosphorylated it caused formation of neurofibrillary tangles (NFTs) which are aggregates of tau formed in the intracellular region. Although controversies and questions still surround the toxicity of tau species (Le Corre et al., 2006), its presence has been identified as essential for A β -induced neurotoxicity (Rapoport et al., 2002). Like A β , NFTs are also associated with development of AD (Zabrocki et al., 2005)

as their presence impairs nutrient transport and perhaps cell signalling in neuronal cells (Vega et al., 2008). In fact, an interrelated relationship between A β and tau has been reported whereby A β accumulation triggers upstream events such as inflammation and oxidative stress leading to tau tangle formation and development of neurodegenerative disease (Oddo et al., 2004).

Tau clearance and processing is normally mediated by both caspases and the proteasome (David et al., 2002; Goldbaum et al., 2003) but in the hyperphosphorylated form, tau becomes resistant to proteasome-mediated clearance (Oddo et al., 2004; Poppek et al., 2006). Previous studies have shown however, that oxidative stress by addition of millimolar concentrations of hydrogen peroxide (H₂O₂) in primary oligodendrocyte culture of rat brain can result in dephosphorylation of tau (LoPresti and Konat, 2001) through activation of protein phosphatase 2A (Galas et al., 2006) and an increase in the activity of protein phosphatase 1 (Zambrano et al., 2004).

The tau-expressing yeast model for studying AD has been reviewed in depth previously (De Vos et al., 2011). *S. cerevisiae* has no known ortholog for human tau; however, human tau can be expressed in *S. cerevisiae*. Expression of various isoforms and mutant forms of tau in yeast has resulted in similar features to those of neuronal cells in AD (Vandebroek et al., 2006; Vanhelmont et al., 2010). De Vos and colleagues (2011) have reported that tau aggregation in those yeast expressing human tau do not display a major tau-related growth phenotype. Tau-related growth

phenotypes, however, have not been reported in stationary phase yeast cells as the majority of previous studies have been conducted on exponentially growing cells (Bretteville and Planel, 2008). Also, in a tau-GFP fusion assay, Timmers et al. (2002) found that yeast lack the microtubule binding site for tau whereas a common binding site for animals and plants was identified.

Many important yeast orthologs of tau phosphatases and kinases have been identified and are currently under investigation (Vandebroek et al., 2005b, 2006; Vanhelmont et al., 2010). Expression of human tau in yeast has further shown the presence of kinases which generate many phosphorylated and aggregated tau residues (Vandebroek et al., 2005b). The phosphorylation of tau by yeast is due to the presence of Mds1 and Pho85 kinases which are orthologous of mammalian kinases Gsk-3 β and Cdk5 respectively. Additionally, it appears that Pho85/Cdk5 has an inhibitory effect on Mds1/Gsk-3 β activity in both mammalian (Wen et al., 2008) and yeast models (Vanhelmont et al., 2010). Vanhelmont et al. (2010) also showed that induction of reactive oxygen species (ROS) in yeast, through addition of Fe²⁺, caused an increase in formation of oligomers and aggregates of tau in the absence of phosphorylation.

1.5 HIGH-THROUGHPUT SCREENING FOR AD CHEMO-PREVENTATIVES

Impediments to research for a cure for AD have been due to a number of reasons. This is probably due to the reliance on animal models which have provided fewer leads on chemo preventatives than epidemiological studies. Another difficulty is recognition of the early markers in the disease pathway.

There have been many approaches to try to cure or prevent AD. Some approaches are highly directed such as immunotherapy using both passive and active immunisation (Qu et al., 2006; Solomon and Frenkel, 2010), while others involve dietary modification such as use of polyphenol and flavonoids found in plant extracts (Misiti et al., 2006; Berhanu and Masunov, 2010; Nakdook et al., 2010; Wang et al., 2010). Many of the previous approaches for treatment have been withdrawn due to their side effects and lack of efficacy (Selkoe and Schenk, 2003; Zhu et al., 2010; Cai et al., 2012; Zhang, 2012).

Therapeutic strategies and approaches that have been developed to date include those with anti-inflammatory, anti-amyloid formation or stability, and antioxidant properties. Important key steps in the formation of amyloidosis and current therapeutic approaches have been illustrated in Figure 1-2. Many compounds and chemicals have provided promising results in cell culture and animal models of AD. Table 1-3 lists some of these modulating compounds that have shown potential benefit in yeast models.

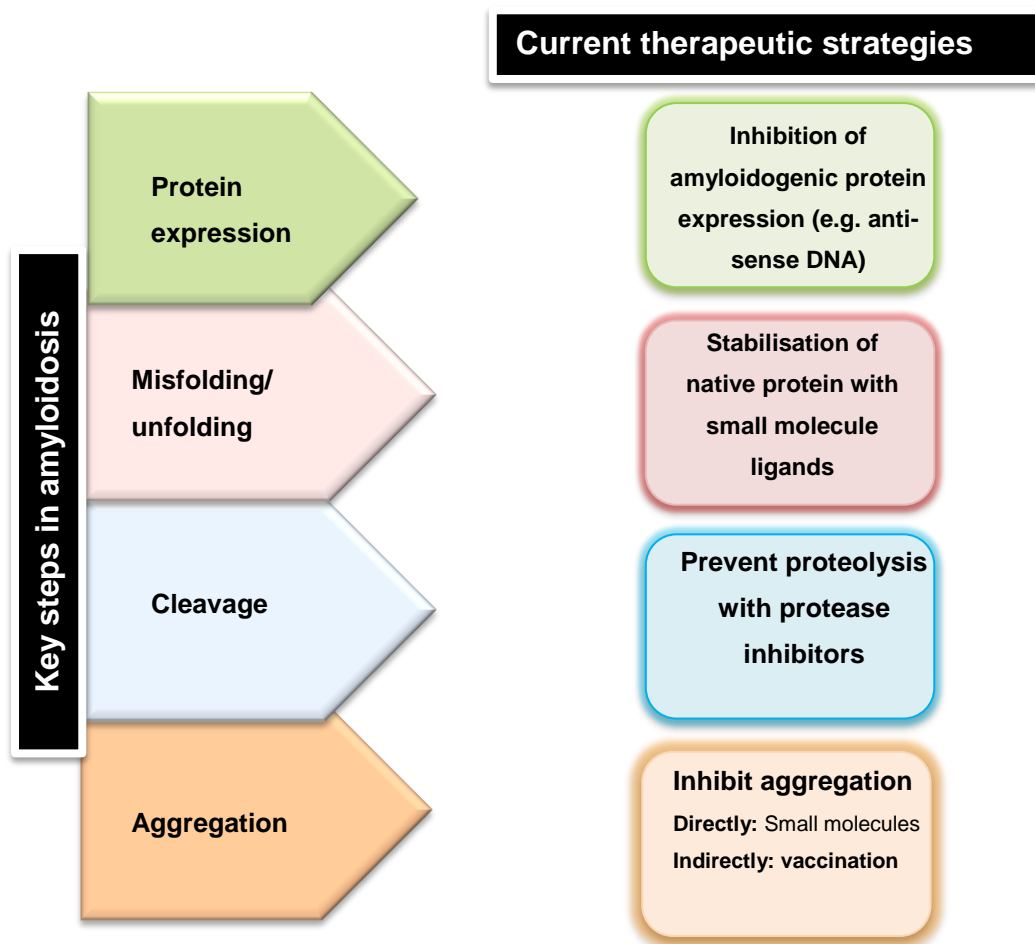


Figure 1-2 Therapeutic strategies to block amyloidosis. Adapted from Mason et al. (2003).

Microbial models are useful in the screening of AD drugs since they offer an ability to screen large numbers of compounds in short time periods (Nemavarkar et al., 2004a, 2004b; Park et al., 2011). They can interrogate compounds that affect A β oligomer formation as well as killing and toxicity. Wurth and colleagues (2002), have developed an *Escherichia coli* model that produces A β fused to GFP and have used it to identify candidates for AD chemo-preventatives. Although, it has some

useful attributes like the yeast model regarding its maintenance and cost, *E. coli* lacks many of the human orthologous proteins that may be identified in yeast screening. *S. cerevisiae*, collections of gene deletant strains are readily available and deletions in other species can also be made to study the gene-specific neurotoxic effects. Additionally, *S. cerevisiae* strains producing tau or A β can be analysed by gene arrays to determine effects on expression. Proteomic analyses may also help to identify host proteins that modulate the toxic effect and cell death.

Yeast are far simpler than humans but this simplicity allows for better understanding of the cellular mechanism and pathways to be studied in depth. For instance, Treusch et al. (2011) have taken advantage of this simplicity and have conducted genome-wide overexpression in order to screen for toxicity modulators in yeast models which resulted in identification of several toxicity suppressors including the yeast homolog of PICALM and other endocytic factors that have a role in AD. The authors also show that after screening 5,000 genes with the aim of finding A β toxicity modifiers, they have identified 12 with human homologs, further implicating the benefit of yeast models in genome-wide association studies. In a similar way, López and colleagues (2012), after screening two commercial chemical libraries, have identified four compounds capable of inhibiting A β aggregation in *S. cerevisiae* and *Podospora anserine*.

Table 1-3 Selected compounds tested in *S. cerevisiae* that may have benefits for treatment and prevention of AD and other age-related diseases.

Compound	Findings	References
Resveratrol	Increased cell survival through stimulation of Sir-2 and increased DNA stability.	(Howitz et al., 2003)
Quercetin	Increased cell protection due to reduction in ROS production, glutathione oxidation, protein carbonylation, and lipid peroxidation.	(Belinha et al., 2007)
Clioquinol	Affected metal (e.g. copper, iron, zinc) homeostasis.	(Li et al., 2010)
Curcumin	Chelated metal ions such as copper and iron, possibly preventing metal-mediated toxicity of neuronal cells.	(Minear et al., 2011)
Latrepirdine (Dimebon™)	Increased autophagy and degradation of A β .	(Bharadwaj et al., 2012)

Many human genes and proteins have counterparts in yeast, and the “housekeeping” functions, including defence mechanisms are highly similar. Therefore compounds that interact with yeast cellular processes are likely to act in the same way on human cellular processes. Some of these cellular processes include responses to ROS, protein misfolding, and apoptosis. In cases where there are substantial differences between the two, re-engineered yeast that can produce both APP β and γ -secretase can be used. Indeed yeast can also be used for screening of inhibitors of β -secretases (Middendorp et al., 2004a, 2004b).

Therapeutic approaches to prevent AD have focused on lowering A β by targeting BACE1 (Luo et al., 2003; Lüthi et al., 2003; Echeverria et al., 2005; Hu et al., 2006) and γ -secretase (Wolfe, 2008; Woo et al., 2011; Kanatsu et al., 2014). Efforts have also been made to identify the BACE1 inhibitors (Vassar et al., 2009). This notion is supported by studying BACE1-regulating proteins and by generating BACE1 knock-out animal models (Luo et al., 2001; Luo et al., 2003). Recently May et al. (2011) generated LY2811376, a non-peptidic BACE1 inhibitor which showed profound A β lowering effects in animals. The clinical trial using this inhibitor however was halted due to the adverse effects outside of the brain and toxicology findings in pre-clinical studies (May et al., 2011). It is now known that BACE1 also modulates myelination in the CNS (Hu et al., 2006; Willem et al., 2006) and plays a critical role in retinal homeostasis (Cai et al., 2012). These findings also suggest that extreme caution should be exercised in the design, use, and safety-evaluation of BACE1 inhibitors or any other chemo-protectors.

Aging has been known as one of most important factors for development of AD and that A β can induce cell cycle events in the post-mitotic neuronal cells which have been terminally differentiated. According to previous studies, age-dependent diseases can be investigated in both *S. cerevisiae* and *Schizosaccharomyces pombe* by altering the growth conditions and analysing chronological lifespan or post-diauxic phase (Fabrizio and Longo, 2008). This was achieved by growing cells into either stationary or exponential phase, with the stationary phase being more representative of the aged cells similar to the post mitotic neuronal cells (McMurray and Gottschling, 2004; Buttner et al., 2008). Although such studies have generated

invaluable data on chronological aging and regulatory pathways (Fabrizio et al., 2001; Fabrizio and Longo, 2003, 2008), it is important to distinguish differences between senescence and quiescence. Senescence occurs in terminally differentiated neuronal cells and age-related diseases and refers to permanent proliferative cell cycle arrest (reviewed in Sikora et al., 2011), whereas quiescence is a reversible event that occurs in those cells temporarily arrested in the cell cycle due to trauma or stress induced by environment. Another limitation of yeast models is the simplicity of the surrounding environment and the absence of inflammation, differentiation and migration which is triggered by A β in neuronal cells.

Neuronal cells are also highly specific, complex, differentiated cells with a unique morphology of dendrites, axons and synapses that changes with the progression of AD, as well as through the effects of their surrounding environment. Yeast cells on the other hand are not differentiated in the same way, and they can be quite adaptive and survive altered conditions. However, it should be noted that less complexity in this situation can be viewed as an advantage since cDNA libraries of yeast genes are readily available which can make molecular analyses easier. Furthermore, despite the fact *S. cerevisiae* does not carry any homologous neurotoxic protein, conserved molecular interactions mimic similar pathways of function and transport.

1.6 GENERAL AIMS AND SUMMARY OF THIS STUDY

There are three main aims addressed in this thesis based on aspects of the main two hypotheses for developing AD, namely the amyloid cascade hypothesis and the cell cycle hypothesis. The first aim was to understand and study the cell cycle in yeast and identify whether unscheduled entry into the cell cycle can be triggered in

chronologically aged yeast cells. An investigation into the effect of aging on the survival and proliferation capacity of the cells was made. The analyses were done in both *C. glabrata* and *S. cerevisiae* as previous studies have utilised both species (Chapter 3). It is well known that folic acid is crucial for proper growth and function of CNS. Therefore, folates (folic and folinic acid) and an antifolate (methotrexate) effect on yeast cells were studied. Analyses were done for both folic acid and folinic acid because their mode of cellular uptakes in humans is different. Folinic acid, a reduced form of folic acid which is metabolically active was included in the experiments to identify differences in the mechanism of cellular entry in yeast.

Chapter 4 aimed to clarify the role of synthetic A β ₄₂ on the yeast cells as there seemed to be inconsistencies in published reports. In an earlier study it was found that chemically-synthesised A β ₄₂ can induce proliferation in *S. cerevisiae* (Chacińska et al., 2002). Studies by Bharadwaj et al. (2008, 2012) however, indicated cytotoxicity associated with A β ₄₂ peptide in *C. glabrata* in particular when the peptide is in an oligomeric form, while fibrillar structures were found to be nontoxic. Therefore, in order to exclude the effect of the solvents and vehicle buffers on the final outcome and to develop a consistent protocol that can be reproducible, two main methods of peptide pretreatments were used. The effect of this pretreatment of peptides was then tested on stationary and exponential phase *S. cerevisiae* and *C. glabrata*. *AHP1* gene overexpression and mutation was examined to determine the effect of high and low levels of peroxiredoxin on the survival of yeast.

The final aim of this study was to screen a library of compounds and identify those with anti-amyloidogenic properties. Therefore, in Chapter 5, a set of 42 compounds and isomers were analysed using both *in vitro* conventional methods and the yeast model.

2 CHAPTER 2: MATERIALS AND METHODS

2.1 INTRODUCTION

This chapter describes the materials, experimental procedure and methods that were used in the following chapters. Chemicals, solvents and reagents that were used in this study have been purchased from Sigma-Aldrich[®] (Australia), Thermo-Fisher Scientific[®] (Australia) and Promega[®] (Australia). Sterilised ultrapure water (ddH₂O) was used in all experiments produced with a Millipore Direct-Q system (Millipore, Billerica, Massachusetts, USA).

2.2 YEAST AND *E. coli* STRAINS AND MEDIA

2.2.1 Yeast strains and media

Both *Saccharomyces cerevisiae* and *Candida glabrata* were used in this study. The genotypes of *S. cerevisiae* have been provided in Table 2-1 and the media in Table 2-2. All of the yeast strains were grown at 30°C unless otherwise stated on agar plates prepared by the addition of 1.5% of Bacteriological agar (Oxoid[™], Cat LP0011) to broth culture media.

Table 2-1 Yeast strains used in this study.

Strain Name	Genotype	Source
<i>Saccharomyces cerevisiae</i> (BY4743)	<i>MATa/α his3Δ1/his3Δ1 leu2Δ0/leu2Δ0 LYS2/lys2Δ0 met15Δ0/MET15 ura3Δ0/ura3Δ0</i>	Dr. J Caine CSIRO, Parkville
<i>Candida glabrata</i>	ATCC 90030	A. Prof I Macreadie
<i>Saccharomyces cerevisiae</i> (YLR109WΔ: <i>ahp1</i>)	(<i>AHP1::URA3</i>) Derived from BY4743 (<i>MATa/α his3Δ1/his3Δ1 leu2Δ0/leu2Δ0 LYS2/lys2Δ0 met15Δ0/MET15 ura3Δ0/ura3Δ0</i>)	Dr. J Caine CSIRO, Parkville
<i>Saccharomyces cerevisiae</i> (FOLT: <i>YJL163CΔ</i>)	(<i>FOLT::URA3</i>) Derived from BY4743 (<i>MATa/α his3Δ1/his3Δ1 leu2Δ0/leu2Δ0 LYS2/lys2Δ0 met15Δ0/MET15 ura3Δ0/ura3Δ0</i>)	EUROSCARF
<i>Saccharomyces cerevisiae</i> (EHY1) dihydropteroate synthase (DHPS) mutant	(<i>MATa leu2-3, 112trp1 tup1 ura3-52 DHPS::LEU2</i>) DHPS deficient strain derived from YH1 (<i>MATa leu2-3, 112 trp1 tup1 ura3-52</i>)	Dr. J Caine CSIRO, Parkville

2.2.2 Bacterial strains and media

Escherichia coli DH5αTM (*fhuA2 Δ (argF-lacZ) U169 phoA glnV44 Φ80 Δ(lacZ)M15 gyrA96 recA1 relA1 endA1 thi- lhdR17*) was used for routine plasmid amplification. Recombinant clones were grown at 37°C in Luria-Bertani medium (1% [w/v] Difco tryptone, 0.5% Difco yeast extract, 1% NaCl) containing 50-100 µg/ml ampicillin to maintain selection for recombinant plasmids.

Table 2-2 Media used for growth of yeast strains in this study.

Medium Name	Formulation
Minimal media; Yeast nitrogen base (YNB)	0.67% (w/v) Bacto-yeast nitrogen base with amino acid and ammonium sulfate, 2% (w/v) glucose
Selective media (YNB-Uracil)	0.67% (w/v) Yeast nitrogen base without amino acids, 0.19% (w/v) of synthetic drop-out medium (Sigma, Cat Y1501), 2% (w/v) glucose
Rich media/ YEPD (YPD)	1% (w/v) Bacto-yeast extract, 2% (w/v) Bacto-peptone, 2% (w/v) glucose
Selective media/ YNB plus 2% glucose, selective amino acid	Synthetic complete media minus the selected amino acid to promote selective growth for phenotypic screening
Synthetic media/ YNB complete	Minimal media (YNB & 2% glucose) supplemented with 20 mg/L of each, uracil, tryptophan, adenine, histidine and 30mg/L of leucine

2.3 GENERAL YEAST GROWTH CONDITIONS AND CELL FRACTIONATION

2.3.1 Stationary and exponential phase growth of yeast and storage conditions

In order to prepare yeast for stationary phase analysis, cells were grown in YEPD broth with aeration at 30°C for 7 d with shaking (200 rpm) (Aragon et al., 2008). Cells were then pelleted and washed twice and resuspended in filter sterilised H₂O at a density of 10⁵ cells/ ml for further treatment.

For the exponential phase of growth, yeast cells were grown overnight in YEPD broth and were harvested by centrifugation the next day and resuspended in 20 ml of fresh broth. Then 1 ml was inoculated into 80 ml of fresh broth and incubated at 30°C with shaking (200 rpm) for another 2-3 h to reach an optical density (OD) at 600 nm of 1.0. For short-term storage (<3 weeks), yeast cells were maintained on solidified YEPD media at 4°C. For long-term storage, yeast cells were stored at -80°C in YEPD or suitable selective broth with 15% w/v glycerol.

2.3.2 Fractionation of stationary phase *C. glabrata* and *S. cerevisiae*

Percoll[®] density gradients (Sigma, Cat P1644) were prepared according to the manufacturer's instruction for preformed gradient and method described by Allen et al. (2006) with some modification. Briefly, Percoll was diluted 9:1 (v/v) with 1.5 M NaCl. To form a gradient, 10 ml of the Percoll solution was added to 15 ml Corex[®] tubes (Corning Inc.[™], NY, USA) and centrifuged at 19,000 x g for 15 min at 20°C in a Beckman Coulter centrifuge with a SW41Ti rotor (Beckman Coulter Life Sciences, Avanti[®] J25-01, Indiana, USA).

Stationary phase yeast cells were pelleted by centrifugation (yielding $\sim 2 \times 10^9$ cells) and then resuspended in one ml of Tris buffer (50 mM, pH 7.5). Around 2 ml of cell suspension was overlaid onto a preformed gradient, and centrifuged at 400 x g for 60 min in a Beckman Coulter centrifuge (Avanti[®] J25-01). Fractions of quiescent (lower fraction) and non-quiescent cells (upper fraction) were collected and washed three times in 40 ml Tris buffer to remove Percoll residue and stored at -80°C for further analysis. Prior to analysis the cell fractions were washed and resuspended in ddH₂O.

2.3.3 Viability assay using colony count

Overnight cultures were re-suspended in fresh YEPD to an initial cell density of 0.2 (OD_{600nm}). Cultures were then incubated at 30°C with shaking and grown to exponential phase (OD_{600nm} 1.5-2). These cultures were washed and diluted in sterile, distilled water to a concentration of approximately 5×10^3 cells per ml. Depending on the experiment, various compounds, folic, or folinic acids were added to these cell suspensions and incubated for specific periods of time along with untreated control samples. Aliquots of 100 μ l cell suspension were plated onto YEPD agar for measurement of the colony forming units (CFU) after two days incubation at 30°C.

2.3.4 Spot assay

The spotting assays were performed under similar conditions and according to the methods described by Mitrica et al. (2012) and D'Angelo et al. (2013). Briefly, exponential phase cells of *S. cerevisiae* were obtained from overnight culture on YEPD as described in Section 2.3.1. In the case of EHY1, folinic acid was added to the growth media at a final concentration of 100 μ M. Cells were then washed and resuspended in ddH₂O. Tenfold serial dilutions were performed in sterile water starting with an equal number of cells ($OD_{600nm} = 0.1$). Spotting assays were derived from a pool of three independent fresh transformants or treated wild-type (WT) yeast strain with appropriate compounds. Drops of 10 μ l using a multipronged inoculator were then plated onto the appropriate solid selective, YNB complete or YEPD medium. In some instances various concentrations of experimental treatments such as H₂O₂, MTX, folic acid and folinic acid were added to the selective media.

2.3.5 Minimum inhibitory concentration of compounds

In order to investigate the effect of certain compounds or folates on the growth of yeast, cells were grown in 50 ml of YEPD media at 30°C to exponential phase (Barchiesi et al., 1999; Wiegand et al., 2008). Cells were then pelleted and resuspended in fresh YNB complete media to an initial OD_{600nm} at 0.03. The OD_{600nm} values of cultures were monitored using a UV/visible spectrophotometer (Bio RAD, iMark™ microplate reader). Optical density was measured at various time points to determine the minimum inhibitory concentration of the compounds.

2.3.6 Folic acid and folinic acid treatment of stationary phase *C. glabrata*

Stock solutions (10 mM) of folic acid and folinic acid were made in water. Folic acid was dissolved with addition of NaOH and the pH was then adjusted to 7.0 prior to use. All solutions including the folate stocks were filter sterilized using a 0.22 µm syringe filter (Sarstedt®, Australia). For folic acid and folinic acid treatments, the yeast cells were transferred into 96-well culture plates and 10-fold dilution series of the folates were made to achieve concentrations of 1 mM and lower. Aliquots were taken from both experimental and control samples for microscopy, flow cytometry and CFU analyses. Cells in stationary phase were incubated with either folic acid or folinic acid and were monitored for 10 d to investigate the effect of starvation in the presence and absence of the folates.

2.3.7 MTX and folic acid treatment of *S. cerevisiae*

A 5 mM stock solution of methotrexate (MTX; Sigma, Cat M8407) was prepared according to the manufacturer's instructions using 250 mM of Na₂CO₃ (pH 9.5). Approximately 2 x 10⁵ cells/ml of exponentially growing *S. cerevisiae* were washed and incubated in sterile ddH₂O in a 96 well tissue culture plate. Folic acid (10 mM stock) and MTX were added to samples to a final concentration of 10 to 1000 μM. Control samples of *S. cerevisiae* cell suspension in water and treatment with only folic acid or MTX were also prepared for comparison. Samples were incubated overnight 30°C with shaking. 100 μl samples were plated on YEPD to monitor viability. The effects of treatments versus controls were monitored by CFU determination.

2.3.8 Study of YJL163C on folic acid and Aβ₄₂ entry

In order to determine the role of putative folate transporter gene on the entry of folic acid into the yeast cells, *S. cerevisiae* WT (BY4743), knock-out mutant (YJL163Δ) and BY4743 cells overexpressing this gene (FOLT) were compared. Cells were washed and resuspended in ddH₂O and treated with folic acid to a final concentration of 100 μM and incubated for 48 h at 30°C. Samples were taken periodically for analysis.

2.4 GENERAL MOLECULAR BIOLOGY METHODS

2.4.1 Plasmids

The p416.GPD plasmid (5778 bp) backbone (Mumberg et al., 1995) was used to generate the expression of Ahp1p and folate transporter proteins (FOLT) (Table 2-3). The p416.GPD vector is a centromeric plasmid maintained at one or two copies per cell. It has an ampicillin resistance selectable marker (*AmpR*) and uracil synthesis selection marker (*URA3*) gene. It has a strong constitutive *GPD* promoter to direct heterologous gene expression throughout the yeast life cycle and a *CYC1* transcription termination sequence flanking the coding region. Plasmids were amplified in *E. coli* DH5 α strain. The GFP-A β ₄₂ fusion and GFP plasmids (Caine et al., 2007b) have also been used for microscopy and flow cytometry analysis.

Table 2-3 Plasmids used in this study.

Plasmid	Description	Source
GFP	GFP expression vector with GPD promoter and <i>URA3</i> selection marker	Dr. J Caine CSIRO
GFP-A β ₄₂	As in p416.GPD-GFP but encoding human A β ₄₂ with a C-terminal fusion to GFP	Dr. J Caine CSIRO
p416.GPD-FOLT (Figure 2-1)	Vector encoding folate transporter gene (YJL163C) of <i>S. cerevisiae</i> (S288C)	This study
p416.GPD- <i>AHP1</i> (Figure 2-2)	Vector encoding thiol-specific peroxiredoxin gene (YLR109W) of <i>S. cerevisiae</i> (S288C)	This study

2.4.2 Primers

Oligonucleotide primers were purchased from GeneWorks^{Pty Ltd.} (SA, Australia). The putative folate transporter gene of *S. cerevisiae* (YJL163C) consisting of 1668 bp was amplified and constructed in a p416.GPD backbone using the following primer set (5'-3') GCGCGCGAAAGCTTATGTCAAACGAGGATGAAACA and (5'-3') GCTGGACGGGCCTTAACTCGAGCG by creating unique *Hind*III and *Xho*I restriction sites (underlined) in the PCR product.

Thiol-specific peroxiredoxin (YLR109W) consisting of 531 bp was similarly amplified and constructed in the p416.GPD plasmid using the oligonucleotide primers (5'-3') GCGCGAATTCATGTCTGACTTAGTTAACAA and (5'-3') GTCTTGGCTCATTTGTAGAAGCTTGCG creating *Eco*RI and *Hind*III restriction sites for the PCR product. The PCR products were digested with restriction enzymes and were cloned in the centromeric plasmid p416.GPD, and introduced into *S. cerevisiae* by transformation for uracil prototrophy.

2.4.3 DNA extraction and purification

DNA extraction for the purpose of cloning was derived from the WT *S. cerevisiae* BY4743 strain (Winzeler et al., 1999). Isolation of genomic DNA (gDNA) was done according to method of Looke et al. (2011) with some modification. Eight single colonies from freshly grown *S. cerevisiae* on YEPD plate were selected and suspended in 100 µl of 200 mM LiOAc / 1% (w/v) SDS solution in eppendorf tubes and then incubated at 70°C for 5 min. Then 10 µl of 10 mg/ml Ribonuclease A

(RNase; Cat R6513) was added and the sample was incubated for 60 min at 37°C. After addition of 10 µl (20 mg/ml) Proteinase K (Cat P2308), incubation continued for 3 h at 50°C.

For purification and extraction of DNA (Sambrook and Russell, 2001) around 500 µl of phenol/ chloroform/ iso-amyl alcohol (1:1:1; v/v) was added to the DNA solution and mixed vigorously for 10 sec at RT. The aqueous layer containing the DNA was removed and transferred into a new eppendorf tube. For every 90 µl of sample around 10 µl of sodium acetate (3 M, pH 5.2) was added to the DNA solution and mixed briefly with gentle agitation.

After incubation, 500 µl of 100% ethanol (absolute) was added to the samples in order to precipitate the DNA. The samples were then mixed by brief vortexing and placed in a -80°C freezer for 20 min. DNA was subsequently collected by centrifugation at 15,000 x g for 5 min. Then 1 ml of RT 70% ethanol was added and mixed, then centrifuged for 5 min (15,000 x g). The supernatant was removed and the pellet was air dried. Precipitated DNA was then dissolved in 25 µl of TE buffer. The DNA concentration (A₂₆₀/ 280) was quantified with a NanoDrop spectrometer (NanoDrop Lite™, Thermo Fisher Scientific).

2.4.4 Polymerase chain reaction

S. cerevisiae (YJL163C) putative folate transporter gene consisting of 1668 bp was amplified using a bench top thermocycler (Applied Biosystems- GeneAmp[®]Pcr 2400). The annealing temperature for PCR with the primer set mentioned in 2.2.4 section was 63°C and GoTaq[®] Hot Start DNA polymerase master mix (Promega; Cat 5132) was used to amplify the gene. The absence of YJL163C gene in the knockout mutant *YJL163CA* strain was also confirmed by the same PCR protocol.

The annealing temperature for *S. cerevisiae* (*AHP1*/ YLR109W) consisting of 531 bp was 59°C (Section 2.2.4). The absence of the *AHP1* gene in the *ahp1* mutant strain was confirmed using the same PCR protocol.

Putative transformants of both genes were also screened by colony PCR to confirm the presence of the gene. The size of PCR products of both controls and samples were checked on 1% agarose gel (w/v).

2.4.5 Agarose gel electrophoresis

PCR products were analysed by agarose gel electrophoresis and observed under UV transillumination (Gel Doc[™] XR⁺ system, Bio-Rad). Agarose (1%, w/v) was prepared in 1 x TAE buffer (0.04M Tris- acetate, 0.001 EDTA, pH 8.3) by boiling in a microwave. Dissolved agarose was cooled to 50°C prior to adding GelRed[™] nucleic acid gel stain (Biotium, Australia; Cat 41003) and mixed. Gels were then poured into a gel tray with a comb positioned to produce wells for loading samples.

Set gels were placed in a Bio Rad gel tank filled with 1 x TAE buffer. Loading dye (Cat 31022, Biotium) was added to each sample prior to loading to the wells. Gels were electrophoresed at 90 Volts for 70 min, then visualised under UV light in a Bio-Rad Gel Doc™ UV transilluminator system. Images were processed using Quantity One 1-D analysis software (Bio-Rad, Australia; version 4.6.8)

2.4.6 DNA and plasmid sequencing

DNA was sequenced by the Micromon sequencing centre (Monash University, Clayton, Australia) using the primers that were used for amplification of the PCR product. Multiple samples of plasmids with the gene of interest were also sequenced using *CYC* and *GPD* primers. The p416.GPD vector contains the yeast *GPD* promoter sequence and a *CYC* transcription termination sequence flanking the coding region. Sequences were obtained using the *CYC* terminator primer GCGTGAATCTAAGCGTGAC and the *GPD* promoter primer CGGTAGGTATTGATTGTAATTCTG. The obtained sequences were analysed using the software *Sequence Scanner v.1.0* (Applied Biosystems® Software).

2.4.7 Digestion and ligation of the genes into p416.GPD

Digestion of the *AHP1* gene and p416.GPD plasmid was done using *HindIII* and *EcoRI* restriction enzymes in NEBuffer 3.1 (NEW ENGLAND BioLabs® Inc.) and the reaction was incubated for 90 min at 37°C. The enzymes were subsequently heat inactivated by heating the samples at 65°C for 20 min.

For digestion of the YJL163C gene and p416.GPD plasmid, *Hind*III and *Xho*I restriction enzymes in NEBuffer 2.1 (NEW ENGLAND BioLabs[®] Inc.) was used and the reaction mix was incubated at 37°C for 90 min followed by heat inactivation of enzymes as above. The folate transporter gene was then cloned into the backbone of the vector using T4 DNA ligase (New England Biolabs[®] Inc.).

A series of ligation reactions with varying ratios of insert to vector was set up to maximise the efficiency of ligation. This was performed using T4 DNA ligase (NEW ENGLAND BioLabs[®] Inc.) containing ATP overnight at 16°C.

2.4.8 Bacterial competent cells (CaCl₂ method)

For routine transformation of cloned plasmids the CaCl₂ method was adopted (Aich et al., 2012) which has a high efficiency rate of 2×10^7 colony forming units (CFU) per µg of plasmid DNA (Hanahan et al., 1991, Sahanawaz Alam and Panigrahi, 2012). A single bacterial colony was inoculated into 50 ml LB broth and grown at 37°C at 250 rpm overnight. The next day 1 ml of sample was used to inoculate 100 ml fresh LB in a 250 ml flask and grown for 3 h or until the OD_{600nm} reached approximately 0.03. The cells were then incubated on ice for 10 min and then transferred into 50 ml falcon tubes and centrifuged (3 min; 6,000 rpm). The supernatant was then discarded and the cells resuspended in 10 ml of ice cold calcium chloride (0.1 M) and incubated on ice for 20 min. After incubation, the cells were pelleted as described previously and the supernatant discarded. Cells were then resuspended in 5 ml of ice cold 0.1 M CaCl₂ containing 15% (w/v) glycerol. Around

300 µl aliquots of cell suspension were dispensed into eppendorf tubes and stored at –80°C for up to one year.

2.4.9 Plasmid extraction

For plasmid purification *E. coli* DH5α™ cultures harbouring the plasmids of interest were grown overnight in 50 ml LB media (Section 2.2.2) supplemented with ampicillin. Plasmid DNA was purified using QIAprep® (QIAGEN™) according to the protocol supplied by the manufacturer. This culture was then centrifuged to collect the pellet and subsequently was lysed in alkaline conditions. The DNA was then absorbed onto silica spin columns in the presence of high salt concentrations. Finally plasmid DNA was eluted in 10 mM Tris-HCl (pH 8.5) and stored at -20°C for subsequent procedures.

2.5 TRANSFORMATION METHODS

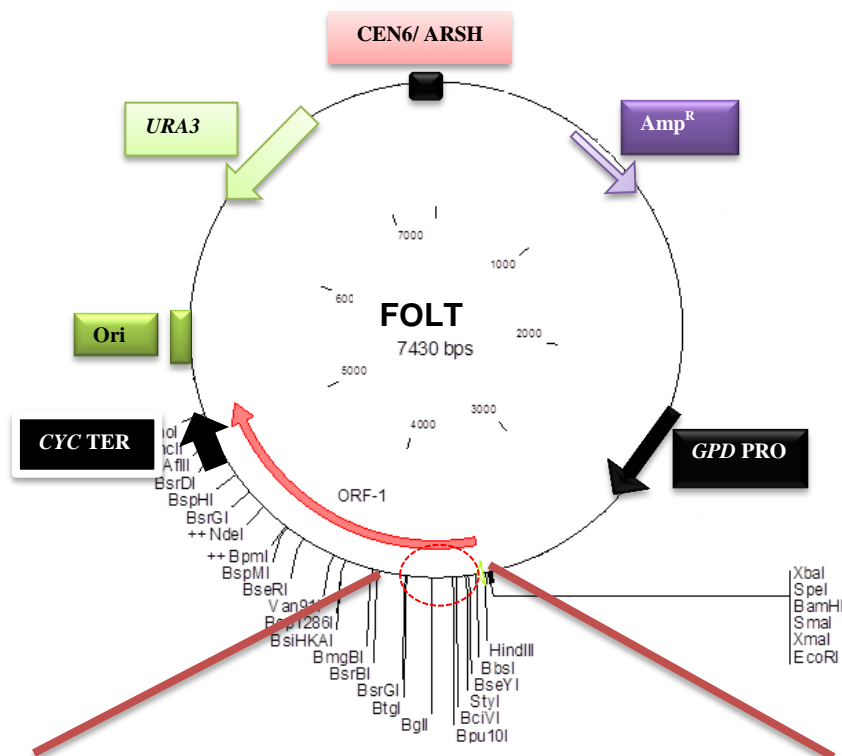
2.5.1 Transformation of *E. coli* competent cells with plasmids

Escherichia coli DH5α™ calcium chloride competent cells were prepared for plasmid amplification (Section 2.4.7). Transformation was conducted according to the method described by Cohen et al. (1972). Around 1 µl (~10 ng) of the plasmid DNA was transferred into an eppendorf tube and 100 µl of CaCl₂ (0.1 M) competent cells were gently added. The sample was then incubated for 30 min on ice. After a quick 2 min heat shock at 42°C, the samples were incubated for a further 2 min on ice. In order to revive cells, approximately 900 µl of LB was added to the samples and incubated at 37°C with shaking at 100 rpm. Cells were then briefly centrifuged at 5,000 rpm (2 min) and most of the supernatant was discarded. The cells were then gently

resuspended in the remaining supernatant. 100 µl of the cells were plated on LB plates containing 50-100 µg/ml ampicillin (Amp) to maintain selection of the plasmids. Recombinant clones were grown at 37°C in LB broth.

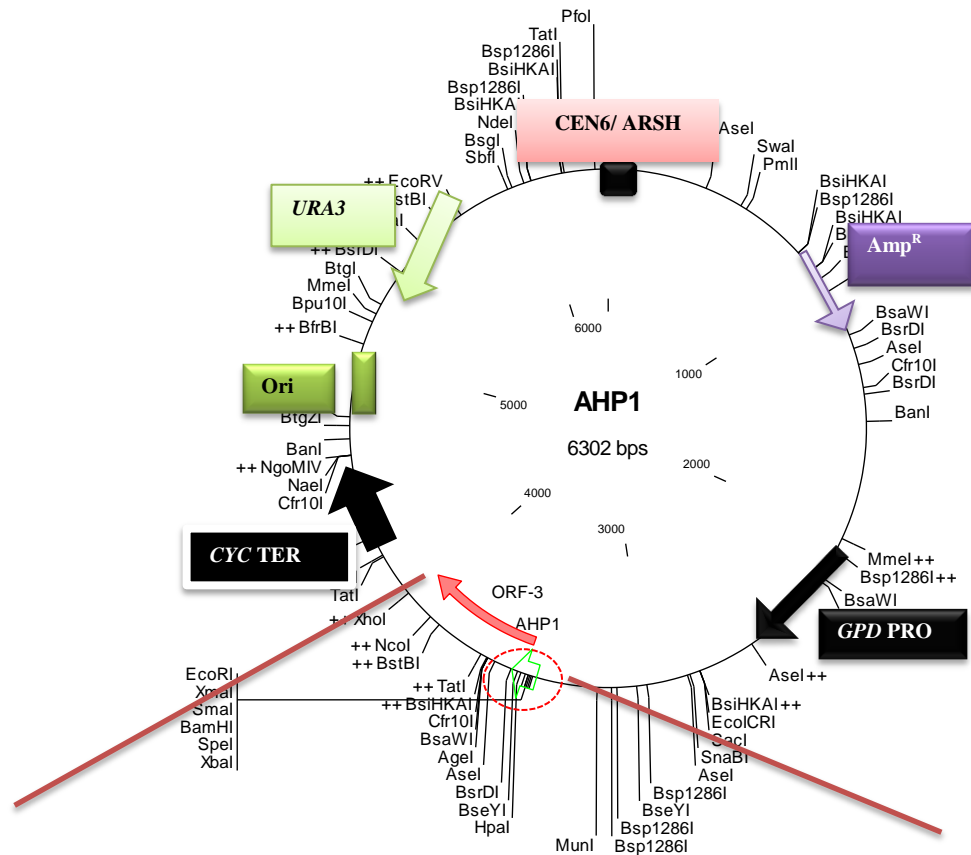
2.5.2 Transformation of *S. cerevisiae* with plasmids

Wild-type BY4743, EHY1, and *ahp1* strains of *S. cerevisiae* were transformed with plasmids of interest using a kit (EZ- Yeast™ transformation Kit- MP, Biomedicals). Cells were then plated on YNB without uracil for selection of transformants. Transformation of all the *S. cerevisiae* with various plasmids were carried out in the same manner.



MSSDEM DY LLETAGINALEEHSQNDSTGINLDTNETAQDSSYSIRRSPSILSVAKSVEGEHGRRK
 LLCLYGLVMIICIAESISMTATIPLVMDKVAEGISDENGHYDSVAVQTIVSSISSSTMMIAGAISIM
 AGKWGELSDRIGRVRVFKYMSGIRVIGLLTHVFTLSSKMKYHKWAIVLTACIVPSFGGLFALVA
 NGNSYVSDIVKTEHRMVTIGIMMSCIYATMGVGPMPFGSFLVKWTHGNGFIPIYTSIAFVILALIIC
 ETIMVEPRHETQMAHSQSTYTKRREKLRSQSGSDDARNYQSVTYGKFQIMRLMDLLAPVKKLW
 LKPDSAGSLVPRHTVILLIVLDILFVCGTTSMPALILFSTYEYKWHAVELGYFISILGIGRGVVLL
 VVSPTLLYTLKRIYQHLNHSIDKIDIFCIQFSMIVITLSLFVMIRFGKPTPTSMIIFALLQALS AFCSP
 TLQSGIHKYTSKKHTGEMFGAMALVRSCVMLVIPILLKLYGSTVSVNPSLFMYIPFSTSIVAILLT
 FFLRIYKNP

Figure 2-1 Schematic illustration of FOLT plasmid constructs developed and used in this study. Using the p416.GPD plasmid backbone to cater for expression of the folate transporter gene (YJL163C) in *S. cerevisiae*. Graphic map was prepared using Clone Manager Professional software (ver. 8.0, Scientific & Educational Software for the molecular Biologist, Morrisville, USA)



M SDLVNKKFPAGDYKFQYIAISQSDADSECKMPQTVEWSKLISENKKVIIT
 GAPAAFSPCTVSHIPGYINYLDLVEKEVDQVIVVTVDNPFANQAWAKSL
 GVKDTTHIKFASDPGCAFTKSIGFELAVGDGVYWSGRWAMVVENGIVTYAA
 KETNPGTDVTVSSVESVLAH

Figure 2-2 Schematic illustration of *AHP1* plasmid constructs developed and used in this study for overexpression of Ahp1p. The p416.GPD plasmid caters for constitutive expression of *AHP1* (YLR109W) gene in *S. cerevisiae*. Graphic map was prepared using Clone Manager Professional software (ver. 8.0, Scientific & Educational Software for the molecular Biologist, Morrisville, USA)

2.6 FLOW CYTOMETRY

Fluorescence associated with cell viability, number of bud scars on the cells and cell wall proteins in yeast was measured and quantified by flow cytometry experiments. Cells for all of the following experiments were analysed using a FACScan flow cytometer (BD FACS Canto™ II, Becton-Dickinson, Franklin Lakes, NJ, USA) and

the captured files were saved as FCS3 and processed using the free trial version of WEASEL™ software (WEHI, Parkville, VIC, Australia).

2.6.1 Calcofluor white M₂R bud scar assay

In order to quantify replicative age, Calcofluor white M₂R (Sigma) was used for the staining of bud scars. 5 mM stock solution Calcofluor white M₂R was diluted in ddH₂O to 25 μM concentration of working solution. Folic acid and folinic acid treated stationary phase *C. glabrata* cells (2×10^5) were stained with this working solution and incubated for 90 min in the dark at room temperature. Around 30,000 cells per sample were analysed with a flow cytometer (BD FACS Canto™ II) using 351 nm excitation and collecting fluorescent emission with filters at 450/65. Samples were also analysed microscopically with a pacific blue filter.

2.6.2 Screening of compounds using GFP-Aβ₄₂ transformants

Wild-type *S. cerevisiae* (BY4743) and an *ahp1* mutant strain were transformed with plasmids encoding green fluorescent protein (GFP) and GFP fused to the C-terminus of Aβ₄₂ (GA) (Section 2.4.1). Both constructs are under constitutive expression and have a *URA3* selectable marker. Prior to treatment with the compounds, transformed yeasts were grown in selective media to exponential phase with agitation (30°C; 200 rpm) (Figure 2-3). When the density of the culture reached OD_{600nm} of 0.8, around 150 μl of culture was transferred into a 96 well microtiter plate. All of the test compounds were dissolved in dimethyl sulfoxide (DMSO; Cat D2650) solvent and were pre-screened for inherent fluorescence using the GFP transformants. Compounds were then added to the GA transformants at a final concentration of 50

μM . Control samples of pure DMSO were included as the negative control and growth was continued for an additional 6 h at 30°C with shaking (200 rpm). Around 300 μl of the suspension was transferred into a flow cytometry tube. For measuring cell death, 3 μl of propidium iodide (PI) solution (100 $\mu\text{g}/\text{ml}$ stock) was added to the flow tube to achieve the final concentration of 1 $\mu\text{g}/\text{ml}$. After addition of PI to the cells, the samples were incubated in the dark for 30 min at room temperature or for 20 min at 37°C. Around 20,000 cells were counted in each sample and the percentage of cells exhibiting red and green fluorescence were recorded on BD FACS Canto™ II flow cytometer. The GFP green fluorescence level was measured using a FITC 530/30 filter (494/519-nm excitation /emission). Red fluorescence due to PI staining was measured with a PerCP 670LP filter (488 /617-nm excitation /emission). Data were recorded and saved as FCS3 files and were analysed by WEASEL™ (WEHI, Parkville, VIC, Australia). All compounds were analysed in triplicate.

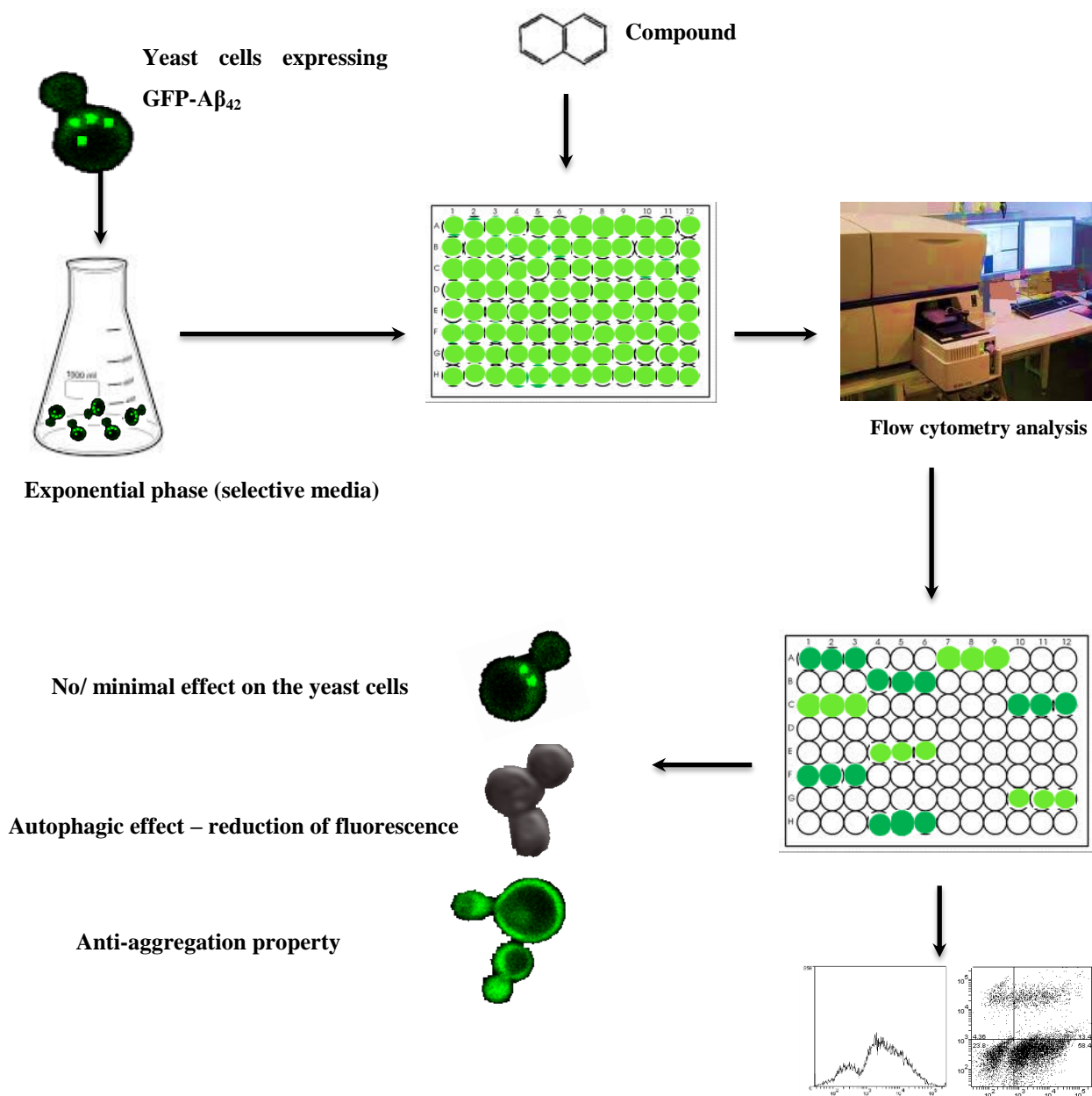


Figure 2-3 Schematic illustration of flow cytometry using GFP and GFP-A β_{42} (GA) transformants. All compounds were analysed using *S. cerevisiae* wild-type (BY4743) and knockout mutant *ahp1* transformants with GFP and GA encoding plasmids.

2.6.3 Thioflavin T associated with aggregation of pretreated A β ₄₂ with the cell wall proteins of *S. cerevisiae*

Exponentially growing *S. cerevisiae* were washed and incubated in H₂O in the presence and absence of HFIP and NH₄OH pretreated A β ₄₂ peptide. After 16 h of incubation, Thioflavin T (ThT) was added to each sample to a final concentration of 20 μ M and incubated for 10 min (LeVine, 1993). Around 10,000 cells per sample were analysed by flow cytometry (FACS, Canto II- BD™) using a pacific blue filter with 351 nm excitation and collecting fluorescent emission at 450/65. Data were recorded and saved as FCS3 files. ThT fluorescence intensity of multiple experimental samples was calculated as a percentage of unstained (untreated) yeast cells.

2.7 SYNTHETIC A β ₄₂ PEPTIDE PREPARATION AND ANALYSIS

The synthetic A β ₄₂ peptide was purchased from Keck laboratories (Yale University, New Haven, CT) in the form of lyophilized powder which was stored at -20°C. According to Keck laboratories the peptide was synthesised and purified using tBOC chemistry with DCC and HOBT coupling reagents. All solvents used for the preparation of A β ₄₂ solutions were pre-filtered and centrifuged to minimise the presence of any debris that could induce aggregation of the peptide.

2.7.1 General peptide preparation and concentration determination

Peptide preparation was done according to the protocol of Ryan et al. (2013). Briefly, 20 mg of peptide was dissolved in 40 ml of 10% NH₄OH to a final concentration of

0.5 mg/ml solution (w/v). The solution was then left at room temperature for 10 min and then sonicated for 5 min. This solution was then freeze dried and the peptide film (peptide pellet) was stored at -80°C until use.

Peptide for assay was prepared immediately prior to use. Each 0.5 mg aliquot of A β pellet was dissolved in 60 μ l of 60 mM NaOH and then vortexed to ensure dissolution of peptide. The solution was then sonicated for 5 min and centrifuged at 14,000 x g to pellet any undissolved peptide. The supernatant was removed carefully from the pellet to a new tube on ice. The peptide concentration was determined using a quartz cuvette at A_{214nm} reading (Thermo 3S BioMate™ spectrophotometer). The concentration of peptide was then estimated according to Table 2-4.

Table 2-4 Molecular weight, coefficient of excitation and absorbance of A β ₄₂.

Type	MW	A _{214nm} ϵ (M ⁻¹ cm ⁻¹)	A _{214nm} 1mg/ml
A β wt 1-42	4514	76848	17.04

2.7.2 HFIP pretreatment method of A β ₄₂ peptide preparation

For toxicity assays, oligomeric A β ₄₂ was dissolved in 1,1,1,3,3,3-hexafluoro-2 propanol (HFIP; Cat 52512) according to the method described by (Crescenzi et al., 2002) with some modification. Briefly the peptide film was dissolved in 100% HFIP to a concentration of 1 mg/ml, sonicated for 5 min on ice and dried overnight to form a clear film. The film was subsequently dissolved in 60 μ l of ddH₂O, sonicated for 5

min and centrifuged to remove any seeded oligomer. The peptide concentration was determined as described in Section 2.7.1.

2.7.3 Stimulation of cell cycle in yeast by NH₄OH pre-treated peptide

Stationary or exponentially growing yeast cells were washed twice and resuspended in ddH₂O. After estimation of cell numbers by a haemocytometer, cells were transferred into a 96-well culture plate at concentration of 10³ cells/ml, 2 μM of Aβ₄₂ peptide pretreated by NH₄OH method was added and incubated overnight at 30°C with shaking. The next day, 100 μl aliquots of cell suspension were plated onto YEPD plates and incubated for two days at 30°C. Colonies were counted for each treatment and the viability was calculated as a percentage of untreated cells.

2.7.4 Yeast treatment by the Aβ₄₂ peptide pretreated by NH₄OH and HFIP methods

Exponentially growing yeast cells were washed twice and resuspended in ddH₂O. After estimation of cell numbers by a haemocytometer, cells were transferred into a 96-well culture plate at a concentration of 10³ cells/ml. Three replicate samples were treated with 2-5 μM of Aβ₄₂ peptide prepared by NH₄OH and HFIP methods, to a final volume of 200 μl in a microtiter plate and incubated overnight at 30°C with shaking. The next day 100 μl aliquots of cell suspension were plated onto YEPD plates and incubated for two days at 30°C. Colonies were counted for each treatment and the viability was calculated as a percentage of untreated cells.

2.7.5 Cytotoxicity analysis of HFIP and NH₄OH pretreated A β ₄₂ on wild-type, mutant and overexpressed *AHP1*

Wild-type *S. cerevisiae* (BY4743) transformed with p416.GPD, and Ahp1p (plasmids encoding YLR109W) along with the *AHP1* deleted strain were grown to exponential phase. Cells (10³ cells/ ml) were then treated with 2 μ M of HFIP and NH₄OH pretreated A β ₄₂ in a 96 well microtiter plate. Triplicate samples of each cell population were further incubated for 24 h at 30°C. Cell survival was determined by transferring 100 μ l of each sample onto YEPD solid media. Viability of treated samples with the peptide was determined as a percentage of untreated cells.

2.7.6 Cytotoxicity analysis of DMSO and NaOH on exponential and stationary phase yeast cells

Wild-type *S. cerevisiae* (BY4743) and *C. glabrata* (ATCC90030) cells were grown to exponential phase and then washed and resuspended in ddH₂O. Cells were counted using a haemocytometer and resuspended at a concentration of 10³ cells/ ml. Cells were then treated with either 2 - 20 μ l of 20 mM NaOH or DMSO to the final volume of 200 μ l in 96 well microtiter plates. Analysis was done in triplicate and samples were incubated overnight at 30°C. Viability was determined by growing 100 μ l of each sample on YEPD solid media for 48 h and was expressed as a percentage of untreated control.

2.7.7 Cytotoxicity analysis of aged A β ₄₂ peptide pretreated by HFIP and NH₄OH

In order to explore the effect of prolonged incubation and hence the fibrillar structures formed by the pretreatment methods on the survival of yeast cells, the A β ₄₂ samples from each pretreatment method were incubated at 35°C for 7 d. Exponentially growing *S. cerevisiae* were washed and suspended in H₂O and then were treated with 5 μ M of HFIP and NH₄OH pretreated peptide and incubated overnight. Viability was determined as a percentage of untreated control on YEPD media.

2.7.8 Cytotoxicity assay of NH₄OH pretreated A β ₄₂ peptide solutions in PC12 cell culture

The following protocol was performed by Dr. Julie Nigro at CSIRO, Parkville according to Ryan et al (2013). Rat pheochromocytoma (PC12) cells were maintained and passaged every 3-4 days in F12K media containing 15% (v/v) horse serum, 2.5% (v/v) fetal bovine serum, 100 u/ml penicillin G sodium, 100 μ g/ml streptomycin sulphate and 0.25 μ g/ml amphotericin B. Briefly, PC12 cells were treated with A β ₄₂ for 72 h (Huang et al., 2012; Ryan et al., 2013). The culture media cell supernatants were then harvested for analysis of cytotoxicity using a lactate dehydrogenase (LDH) assay. Lactate dehydrogenase (LDH) is released into the media as a result of A β ₄₂ toxicity. The cytotoxicity was normalised to the cells treated with 0.1% (v/v) Triton™ X-100 (maximum LDH release).

In order to determine cell viability the attached cells were then treated with media containing Alamar blue[®] (Life technologies[™]) reagent according to the manufacturer's instructions. The reduction of the Alamar blue reagent after 4 h of incubation at 37°C was quantitated by a change in absorbance at 570 nm by a multi-detection microplate reader (FLUOstar OPTIMA, BMG Labtech, Ortenberg, Germany). The data were then normalised to the untreated cells.

2.8 THIOFLAVIN T ASSAY

Thioflavin T (ThT) is a benzothiazole dye which is used to monitor the formation and inhibition of A β ₄₂ fibrils in the presence of anti-amyloidogenic compounds and quantify the extent of amyloid fibrils formation (De Ferrari et al., 2001; Maezawa et al., 2008; Airoidi et al., 2011; Ryan et al., 2012). Whenever this dye binds to amyloids with fibrillar morphology and β -rich structure, an enhanced level of fluorescence is exhibited (Ban and Goto, 2006; Sabate and Saupe, 2007; Freire et al., 2014). Therefore, ThT dye can be used for both quantification and visualisation of amyloid fibrils as the fluorescence emission of the dye is shifted when it bound to β -aggregate structures.

2 mM stock solutions of all compounds were made in DMSO and stored at 4°C or on ice until needed. The reactions were set up in 96 well microtiter culture plates and dispensed in triplicate. The final volume of each well was 200 μ l containing 20 μ M A β ₄₂ and 20 μ M of the compounds. Control wells for A β ₄₂ and compounds alone and their corresponding solvents (ThT blank) were also included in the experiment to

exclude any background fluorescence or aggregation related to compounds or solvents alone (Hudson et al., 2009). The plates were incubated at 37°C and samples were taken at 0, 16 and 24 h for analysis after incubation.

ThT measurements were performed by removing 20 µl from wells and adding them to 180 µl of 2 µM ThT in 50 mM phosphate buffer (pH 7.4). The resulting 200 µl was transferred into the wells of 96-well black culture plates with flat bottoms (Corning) and incubated for 15 min in the dark at RT prior to measurement. Absorption at 440/480 nm was measured by a multi-detection microplate reader (FLUOstar OPTIMA, BMG Labtech, Ortenberg, Germany). To avoid bias, the mean of three measurements of each compound was determined by subtracting the fluorescence of a ThT blank.

2.9 CYTOTOXICITY SCREENING OF THE A β ₄₂ SPECIES FORMED AS A RESULT OF CO-INCUBATION WITH POTENTIAL INHIBITORS

The A β ₄₂ oligomers were prepared fresh for the cytotoxicity assay according to Section 2.8.1. Peptide samples (20 µM) were then co-incubated with 20 µM of selected potential inhibitors for 7 d at 30°C. Exponentially growing *S. cerevisiae* and *C. glabrata* were washed and resuspended in H₂O and then were treated with 5 µM of this co-incubated peptide/compound mix. Cells were incubated overnight and after 24 h the survival was estimated. Viability was determined by counting colonies formed on YEPD solid media and calculated as a percentage of untreated control.

2.10 PROTEOMIC METHODS

2.10.1 Sample preparation of compounds co-incubated with A β ₄₂ peptide for gel electrophoresis

A β ₄₂ peptide (20 μ M) samples were co-incubated with the compounds (potential inhibitors) for 7 d and analysed by gel electrophoresis. Freshly prepared A β ₄₂ was also included (Section 2.7.1) to indicate the effect of inhibitors and incubation time on fibril formation. All of the samples were diluted into sample buffer and boiled for 3 min and electrophoretically resolved on 4-12% Bis-Tris pre-cast polyacrylamide gels (NuPAGE[®] Novex[®] LDS, Invitrogen[™]) in MES running buffer (Cat NP0002, Invitrogen[™]) at 150V for 1 h. Pre stained protein markers (SeeBlue[®] Plus2, Cat LC5925, Invitrogen[™]) were run in parallel for MW comparison.

2.10.2 SDS PAGE silver staining for detection of A β ₄₂ oligomers in the presence of compounds

For protein detection, a gel was stained using previously described silver staining methods (Blum et al., 1987; Rabilloud et al., 2009). Briefly, a gel was incubated for 30 min in 50 ml of 40% ethanol (v/v) and 10% acetic acid (w/v) and subsequently the solution was discarded and the process repeated three times. Then the gel was washed for 10 min in ddH₂O. In order to sensitise, the gel was soaked for 1 min in 0.02% Na₂S₂O₅.5H₂O and then rinsed twice with water (1 min). The gel was subsequently impregnated with silver for 20 min using silver solution (0.2% AgNO₃ and 0.075% HCHO). After three rinses of 20 sec in water the image was developed in developing solution (0.5% HCHO, 0.0004% Na₂S₂O₅.5H₂O, 6% Na₂CO₃) for 10 min. Image development was stopped by adding 40% ethanol and 10% acetic acid to the gel and

incubating for 10 min. Images of these gels were obtained using the VersaDoc™ imaging system (Bio-Rad *Inc.*).

2.10.3 Immunoblotting for detection of potential A β ₄₂ fibril inhibitors

Aliquots of A β ₄₂ conformers (25 μ M) were taken from samples of the *in situ* TEM assays after the incubation period. Fresh A β ₄₂ samples were also prepared and loaded along with 5 μ l of Novex® Sharp unstained protein standard (Invitrogen™). The proteins (0.5 μ g) were transferred from the polyacrylamide gel to a nitrocellulose membranes using an iBlot® dry system. The membrane was then blocked for one hour in 5% non-fat dry skim milk in PBS solution and washed 3 times with PBS. Primary antibody, WO2 (Miles et al., 2008) (University of Melbourne, VIC, Australia) which bound to the N-terminal of A β , was used for detection. This antibody was diluted in PBS/ Casein solution (1/200; 0.5% skim milk in PBS) prior to use. Incubation of the blot in primary antibody for 2 h continued and was followed by three washes with PBS. Secondary antibody (anti-mouse) was diluted to 1/1000 and incubated on the membrane for 1 h. After washing with PBS, the blot membrane was exposed to ECL chemiluminescent western blotting substrate (ThermoFisher Scientific) for 2 min and allowed to develop. Images were captured using the VersaDoc™ imaging system (Bio-Rad *Inc.*). The immunoreactive bands were later quantified using Quantity One 1-D analysis software (Bio Rad, Australia; version 4.6.8).

2.10.4 Sample preparation for immunoblotting to identify the effect of solvent and pretreatment methods on the extent of A β ₄₂ oligomeric formation

HFIP and NH₄OH pretreated A β ₄₂ peptide samples were dissolved in either H₂O or 60 mM NaOH. After determining the concentration of peptide (Section 2.7.1), samples were incubated for 7 d at 37°C to induce fibril formation and analyse the effect of solvent on the aggregation process. Samples were also prepared using a similar protocol to compare the effect of prolonged incubation on the self-aggregation of A β ₄₂ compared with a freshly prepared sample. Around 0.5 μ g of each sample was then loaded onto a protein gel for electrophoresis (Section 2.10.1). Immunoblotting was then carried out as stated in section 2.10.3.

2.11 CONFOCAL, EPIFLUORESCENCE AND BRIGHT FIELD MICROSCOPIC METHODS

2.11.1 Slide preparation

Microscopic slides were washed with ethanol and treated with 10 μ l of 2 mg/ml Concanavalin A and 0.1% Poly L-lysine in a 1:1 ratio and air dried. This ensures that yeast cells are immobilised to the surface of the slide during microscopic examination without affecting their viability. 10 μ l of yeast cell suspension was then applied to ConA/ poly L-lysine coated slides and a cover slip was applied. The cover slip was secured by applying nail polish to the edges.

2.11.2 Microscopy

Confocal fluorescence and differential interference contrast (DIC) microscopy was performed using a Nikon[®] A1 confocal laser-scanning microscope equipped with a Plan Apo VC X60 water-immersion objective, an argon laser (488 nm) and a solid state laser (561 nm). GFP and DAPI fluorescence was observed using 488 nm and 405 nm excitation lasers respectively. Images were acquired using a camera (Nikon, Ti-E₁, Japan) and NIS Element software.

Fluorescence and DIC microscopy was also performed for visualisation of the DNA and folate uptake using a Leica DM5500B epi-fluorescence microscope with a 100X/1.3 oil objective lens (Leica Microsystems, Germany). Images were captured electronically using a Leica camera (DFC310 FX) and processed using the Leica Application Suite (LAS, V4.3, Switzerland). DAPI was observed using the I3 FLUO- Filter cube (Leica; 450-490 nm bandpass excitation filter).

Bright field microscopy was performed using an Olympus CX31 light microscope at 100X magnification. Around 10 µl of each sample was examined using a wet mount method, loaded on a microscopic slide for imaging using oil immersion on an Olympus CX31 light microscope at 1000X magnification. Images were captured using an Olympus digital camera (E330- Japan).

2.11.3 Meiosis event in yeast cells

Samples were prepared according to Section 2.3.8 with folic acid. Cells were also treated with DAPI (Section 2.11.4) and Calcofluor white (Section 2.11.5). Time-lapse photomicroscopy was utilised to detect and capture the meiosis event.

2.11.4 Nuclear DNA staining

In order to visualize nuclear and mitochondrial DNA, 4',6'-diamidino-2-phenylindole (DAPI) staining was used (Chazotte, 2011). Cells were grown into exponential phase and exposed to treatment conditions depending on the type of analysis. Cells were subsequently pelleted (8000 x *g*, for 5 min) and resuspended in 100 µl of minimal media. DAPI was added to a final concentration of 3 µg/ml. Cells were grown for a further 30 min in the presence of DAPI (at 30°C) in the dark and then pelleted and washed twice with PBS. 10 µl of sample was applied to a slide and a coverslip applied and examined immediately under confocal microscope with 488 laser (excitation: 360/40 nm) suitable for DAPI visualisation.

2.11.5 Calcofluor white M₂R staining

For visualisation of bud scars, Calcofluor white M₂R (Sigma) was used. A 5 mM stock solution of Calcofluor white M₂R was diluted in ddH₂O to 25 µM concentration to make a working solution. After staining yeast with this working solution, cells were incubated for 90 min in the dark at room temperature prior to visualisation under a confocal microscope with 488 laser (excitation: 360/40 nm) suitable for DAPI visualisation.

2.11.6 Thioflavin T staining of yeast cells

Confocal fluorescence and differential interference contrast (DIC) microscopy was performed using a Nikon[®] Eclipse Ti confocal laser-scanning microscope. Treated and untreated yeast cells with A β ₄₂ peptide in H₂O in a 96 well microtiter plate were treated with ThT to final concentration of 20 μ M. ThT fluorescence was observed using a DAPI filter following excitation of the sample with light of 405 nm wavelength. Images were acquired using a Nikon camera (Ti-E, Japan) and NIS-Elements imaging software.

2.12 TEM

Carbon-coated 300-mesh copper grids were glow discharged in nitrogen to render the carbon film hydrophilic. Samples were gently agitated before transferring a 4 μ l aliquot onto the grids. After 30 sec adsorption time, the excess sample was drawn off using a Whatman[®] 541 filter paper. The grids were then subsequently stained with 2% w/v potassium phosphotungstate (pH 7.2) for 10 sec. The grids were then air dried before examination. The samples were examined using a Tecnai[™] 12 Transmission Electron Microscope (FEI, Eindhoven, The Netherlands) at an operating voltage of 120 KV. Images were recorded using a Megaview III CCD camera and AnalySIS camera control software (Olympus Australia).

2.12.1 Sample preparation for analysis of A β ₄₂ co-incubated with the compounds

A freshly prepared aliquot of A β ₄₂ peptide was used for the co-incubation with compounds. The samples were prepared in screw cap eppendorf tubes containing 20

μM $\text{A}\beta_{42}$ peptide, 20 μM of the compounds, and 20 μl of 10x PBS (pH 7.4). The samples were made up to a final volume of 200 μl by adding H_2O . Control samples contained equal amount of peptide and compound solvents. All of the samples were incubated at 37°C for 7 d for TEM analysis.

2.12.2 Sample preparation for TEM imaging of NH_4OH and HFIP pretreated $\text{A}\beta_{42}$ peptide

Amyloid peptide was prepared freshly and was either treated with HFIP (Section 2.7.2) or NH_4OH (Section 2.7.3) prior to dissolution in H_2O . Pretreated lyophilised $\text{A}\beta_{42}$ samples were dissolved in dd H_2O . TEM was performed at 0 h and the samples were then incubated at 37°C with no shaking for 24 h. TEM micrographs of both pretreatment methods were also captured at 24 h. The samples were further incubated for 6 d to assay cytotoxicity.

2.13 DATABASES USED

The *Candida* genome database (CGD) was accessed for identification of gene ontology (GO) term finder, open reading frame (ORF) retrieval and analysis. Gene lists were queried using GO term finder and a phylogeny tree was created using this database for homology analysis of the putative folate transporter in *C. glabrata* CBS 138 (CAGL0M08426g), *C. albicans* SC5314 (orf19.6976).

The *S. cerevisiae* genome database (SGD, ver. 1.8.1) was accessed to gather information on the biological characteristics related to genes of interests using GO

term finder, identification and sequence retrieval (Cherry et al., 2012). The National Centre for Biotechnology Information (NCBI) website was used to access the Protein database and Nucleotide database. Genes and proteins were retrieved using BLAST (basic local alignment search tool) tool and ClustalW was performed for multiple sequence alignment of the putative folate transporter genes in human (*Homo sapiens*) and yeast (*Candida* and *S. cerevisiae*) (Altschul et al., 1990).

2.14 STATISTICAL ANALYSIS

All samples were analysed in triplicate and experiments were repeated to ensure their reproducibility. Graphs were made using Microsoft Office Excel 2010 software and data was analysed using PRISM 5 version 5.04 (GraphPad Software, Inc., La Jolla, CA, USA). All data have been presented as mean \pm SEM. Significant differences were compared using unpaired Student's *t*-test and one-way ANOVA with either *Bonferroni's* or *Tukey's post hoc* analysis. Significant differences are indicated by asterisk (*) and the corresponding *p*-values for the data are given in the text. A *p*-value of <0.05 was deemed as significant.

3 CHAPTER 3: CELL DIVISION AND PROLIFERATION ANALYSIS IN *C. GLABRATA* AND *S. CEREVISIAE* AND CHARACTERISATION OF THE FOLATE TRANSPORTER GENE

3.1 INTRODUCTION

Folic acid (vitamin B9) is an essential water soluble vitamin that is critical for the growth of all cells. It is a cofactor in one-carbon metabolism for DNA, RNA and amino acid synthesis as well as promoting the re-methylation of homocysteine (Bailey and Gregory, 1999; Crider et al., 2012). Folate deficiency has also been proposed as a risk factor for development of Alzheimer's disease (AD) (Kim, 2003; Quadri et al., 2004; Ravaglia et al., 2005; Kim et al., 2008; Wang et al., 2011). Humans are not able to produce their daily folate requirements and rely on exogenous sources of folate.

The effect of this water soluble vitamin on cell division has been well established (Bailey and Gregory, 1999; Kruman et al., 2002; Frits, 2005; Mason and Kim, 2010; Crider et al., 2012). Folate receptors and carrier-mediated transporters enable cellular import of folate and antifolates such as methotrexate (MTX) as well as cellular export (reviewed by Antony, 1992, 1996; Muller and Schibli, 2013). Adequate amounts of folate intake ensure normal development of the nervous system, regulating programmed cell death and neurogenesis (Mattson and Shea, 2003; Morris, 2003; Sezgin and Dincer, 2014). Folate supplementation has been shown to be chemo-protective in AD (Faux et al., 2011), however the mechanism of folate protection in AD remains unclear. It has been reported however that folate supplementation leads

to greater retention of grey matter and a reduction in the levels of the toxic amyloid beta (A β) peptide (Erickson et al., 2008; Douaud et al., 2013).

Folic acid is a natural substrate for dihydrofolate reductase (DHFR) which initiates the synthesis of dihydrofolate (DHF) and then is further reduced to tetrahydrofolate (THF) (Yao et al., 1996; Fowler, 2001; Whitehead, 2006). THF itself is essential for the synthesis of deoxythymidine monophosphate (dTMP). Folinic acid (Leucovorin) shares similar molecular structure with folic acid but unlike folic acid it does not require the reduction by the enzymes within the cells (Halsted, 1991). Folic acid enters the cells mainly through transmembrane folate receptors (FR) while folinic acid uptake occurs through active transport mediated by the reduced folate carriers (RFC) (Prasad et al., 1994; Antony, 1996). This is illustrated in figure 3-1 which shows differences in folic acid and folinic acid cellular uptake. MTX on the other hand is an antineoplastic antimetabolite and structurally very similar to folic acid but is a potent inhibitor of DHFR and thymidine synthesis. MTX activates 5-methyltetrahydrofolate (5-CH₃-THF) related enzymes such as thymidylate synthetase (TYMS) which ultimately leads to homocysteine elevation (Figure 3-1) (Owen et al., 2013). MTX enters cells primarily via the RFC similar to folinic acid, whereas the efflux of MTX across the cell membrane is mediated by various ABC transporters. Within the cell, MTX undergo polyglutamation, similar to folic acid by folypolyglutamate synthetase (FPGS) enzyme (Figure 3-1) (Vickers et al., 1985; Rots et al., 1999; Yanagimachi et al., 2011). MTX is an effective antifolate due to its capacity to inhibit cell growth.

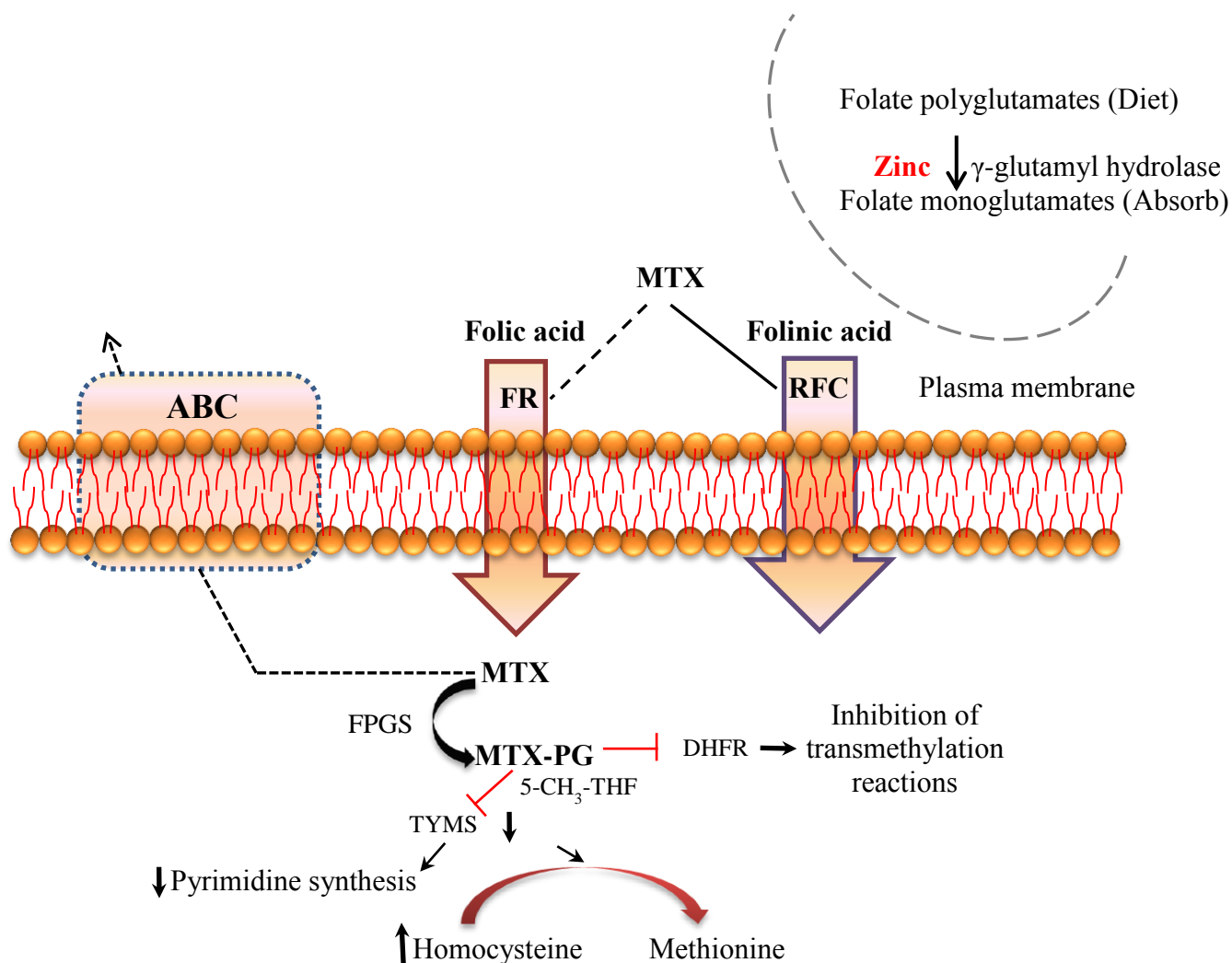


Figure 3-1 Schematic illustration of folic acid, folinic acid and methotrexate uptake by cells in humans.

Mammalian cells do not synthesize folate and must obtain it through diet, utilising receptors and transporters to deliver folates (folic acid and folinic acid) into cells (Wright et al., 2007). Plants and microbes synthesise folates *de novo* and therefore have no need for folate uptake and for folate transporters and receptors (Swarbrick et al., 2008). In *Saccharomyces cerevisiae* disruption of genes involved in folate

synthesis is lethal, unless folates, or methionine, adenine, histidine and thymidine monophosphate are provided (Bayly and Macreadie, 2002). Microbial models have been important in providing fundamental information about human health and disease, yet insights into folate uptake have not occurred in microbial models due to a perception that they are irrelevant, since they do not rely on exogenous folates.

Many yeast cells in the absence of mitotic stimulating environmental signals leave the cell cycle and exist in a state of quiescence. They remain in this state, until a time when nutrients reach their environment. These nutrients then supply the needs for cell division. In the case of higher eukaryotes, the cells cycle arrest results in senescence which is triggered by a multitude of stresses (Sikora et al., 2011). Some of the molecular events that impact chronological life span in budding yeast likely mimic events in post-mitotic cells in higher eukaryotes (McMurray and Gottschling, 2004). In the case of AD, senescence and unscheduled entry into the cell cycle (Yang et al., 2001; Yang et al., 2006; Sikora et al., 2011) leads to neuronal cell death and is a likely cause of AD (Herrup et al., 2004). Therefore, targeting cell cycle re-entry may provide opportunities for future therapeutic interventions.

In this chapter the effects of exogenous folates (folic acid and folinic acid) and antifolate (MTX) on yeast are investigated as yeast can be extensively manipulated in terms of their environment and their genes. For example, yeast can be maintained for long periods in a quiescent state simply by holding them in an aqueous suspension. Analyses are done in both *S. cerevisiae* and *Candida glabrata* to identify any differences in the effect of folate uptake between the two species. Both folic acid and

folinic acid were investigated to determine whether similar to humans or if different modes of transport are used across the cell membrane in yeast. Analysis of MTX was done on WT *S. cerevisiae* and an auxotrophic mutant strain (EHY1) in which the *FOLI* gene has been disrupted (responsible for encoding dihydropteroate synthetase). In the absence of folate synthesis, strain EHY1 requires the pathway end products methionine, adenine, histidine, and dTMP (MAHT) (Meneau et al., 2004). Additionally, the role of the putative folate transporter gene (YJL163C) (Cherry et al., 2012), which I have named FOLT in the cellular entry and mechanism of proliferation is studied. The folate transporter gene is a part of a major facilitator superfamily (MFS) which is one of the two largest membrane transporters in eukaryotes and some prokaryotes (Gaur et al., 2008). The entry of folic acid, folinic acid, MTX and A β ₄₂ in a wild-type, deletant strain (*YJL163CΔ*), and a strain overexpressing Foltp are compared. All *S. cerevisiae* (EHY1, *YJL163CΔ* and BY4743) that are used in this chapter are derived from the S288C reference stain.

3.2 AIMS

- 1) Investigate the effect of folate as a stimulator of cell division in a yeast model
- 2) Identify differences in the effect of folate on *C. glabrata* and *S. cerevisiae*
- 3) Examine the role of the putative folate transporter and its function in the extracellular folate and folinic acid uptake
- 4) Determine the effect of the age of cells on cell division and susceptibility to toxicity of extracellular A β ₄₂ peptide

3.3 MATERIALS AND METHODS

Candida glabrata (ATCC9003) and *Saccharomyces cerevisiae* (BY4743) (Section 2.2.1) were grown to exponential and stationary phase according to Section 2.3.1. In order to investigate the effect of age of cells on their survival with any treatment, stationary phase cells were fractionated into quiescent and non-quiescent populations as described in Section 2.3.2. Stationary phase *C. glabrata* cells were incubated with folic acid and folinic acid as described in Section 2.3.6. Morphological changes were studied using bright field microscopy (Section 2.11.2) and viability was estimated by obtaining colony forming units as described in Section 2.3.3.

Yeast cells are capable of producing folate naturally but the *FOLI* deficient strain (EHY1) relies on an exogenous source of folate. Therefore, in some experiments the EHY1 strain which relies on an exogenous source of folate has been utilised. The effects of folic acid, folinic acid and, MTX treatment on the WT *S. cerevisiae* (Section 2.3.7) were compared with the EHY1 strain qualitatively using spot assays as described in Section 2.3.4. Bud scars were stained with Calcofluor White dye according to Section 2.11.5. The fluorescent intensity associated with calcofluor was quantified using flow cytometry as described in Section 2.6.1. The generated flow cytometry data were analysed by Weasel[®] (WEHI) software.

The role of the putative folate transporter gene (YJL163C) in *S. cerevisiae* was studied by cloning and overexpression of the gene and comparisons with the null-mutant and WT strain in folate uptake. This transporter gene consisting of 1668 bp was amplified by PCR from the genomic DNA sequence of *S. cerevisiae* S288C. This

was done using the oligonucleotide primer set (5'-3') GCGCGCGAAGCTTATGTCAAACGAGGATGAAACA and (5'-3') GCTGGACGGGCCTTAACTCGAGCG by creating unique *Hind*III and *Xho*I restriction sites (underlined) for the PCR product (Section 2.4.3 and Section 2.4.4). The PCR product was then cloned into the p416.GPD plasmid with a *URA3* selectable marker as described in Section 2.4.7. The homozygous deletant mutant strain (*YJL163CΔ*) was obtained from the EUROSCARF collection for study of the putative folate transporter. The WT *S. cerevisiae* BY4743 strain, *YJL163CΔ* and a BY4743 strain overexpressing *Foltp* were screened in order to determine the effect of folic acid uptake in the presence and absence of the transporter gene as described in section 2.3.8. Cells incubated in the presence of folic acid were stained with DAPI to reveal DNA (Section 2.11.4). Imaging of nuclease and sporulation were captured by an epifluorescent microscope as described in Section 2.11.3.

The effect of the folate transporter gene in the cellular uptake and sensitivity to the effect of A β ₄₂ peptide was also investigated. Ammonium hydroxide (NH₄OH) and HFIP pretreated A β ₄₂ were used for this assay and were prepared as described in Section 2.7.1 and Section 2.7.2 respectively. *S. cerevisiae* cells overexpressing *Foltp* were compared with WT and *YJL163CΔ* for their susceptibility with these pretreated A β ₄₂ peptides as described in Section 2.7.4.

3.4 RESULTS

3.4.1 Effect of folic acid and folinic acid on the morphology of stationary phase *C. glabrata*

Stationary phase *C. glabrata* cultures were examined by microscopy periodically during 10 days after treatment with 100 μM of folic acid and folinic acid. Before treatment the population consisted of over 90% unbudded cells and approximately 10% budded cells (Figure 3-2). After 24 h incubation in water, most cells grew at least one bud, while folic acid and folinic acid treated cells showed an ability to form multiple buds (Figure 3-2). Some treated cells grew three or four buds, while without folate the budding did not increase. Interestingly, both axial and bipolar forms of budding were viewed in the presence of treatments. Although some cells in the control samples had more than one bud the number of budding cells was much lower than those of the treated samples. After prolonged incubation (192 h) in water these yeast cells became larger and more transparent. Cells also seemed to adhere (240 h) and became larger and more elongated as the incubation continued (Figure 3-2).

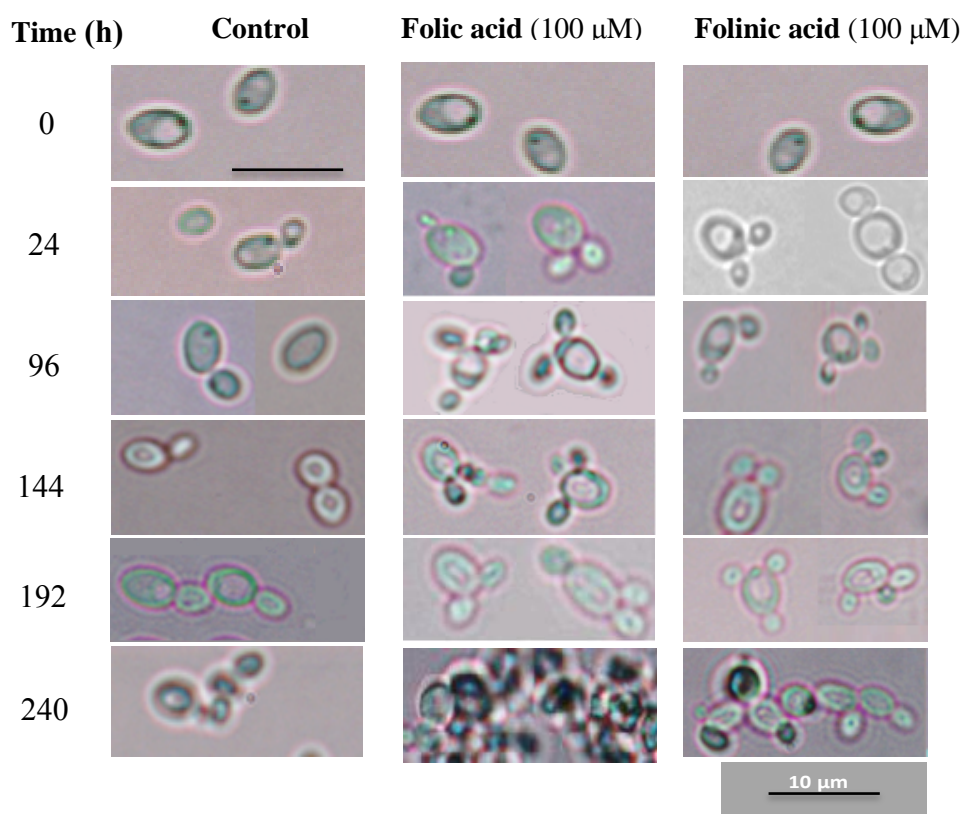


Figure 3-2 Microscopic images of *C. glabrata* in the presence of folic acid and folinic acid. *C. glabrata* cells treated with 100 μ M of folic acid or folinic acid were compared to the control periodically over 10 d. (Scale bar = 10 μ m).

3.4.2 Effect of folic acid and folinic acid on the viability of stationary phase *C. glabrata*

When *C. glabrata* cells (10^3 cells/ml) were grown to stationary phase and then suspended in water for one to ten days their numbers, judged by plating out to determine colony forming units, remained relatively constant over the entire period. Addition of folic acid and folinic acid solutions however caused a significant increase in the number of CFUs in the first 24 h (Figure 3-3A, B). Treatments with 10 μ M ($p < 0.05$) and 100 μ M folic acid ($p < 0.005$) (Figure 3-3A) or 100 μ M ($p < 0.005$) and 1000 μ M ($p < 0.01$) concentrations of folinic acid (Figure 3-2B) led to significant

increases in CFUs. The effect on cell proliferation by folates was limited to stationary phase cells and no effect was detected on cells growing in exponential phase (data not shown).

After separating the two distinct populations of quiescent and non-quiescent stationary phase cells by density gradient centrifugation, each population was treated with folic acid or folinic acid. The effect of folates to induce cell proliferation was limited to quiescent cells with significant increase in the number of cells in the presence of 100 μ M of folic acid ($p < 0.01$) and folinic acid ($p < 0.05$) (Figure 3-3C). A non-quiescent sub-fraction of cells did not behave similarly. In fact, in the presence of treatments their viability seemed to be reduced in particular with 100 μ M of either folic acid ($p < 0.005$) or folinic acid ($p < 0.01$) (Figure 3-3D).

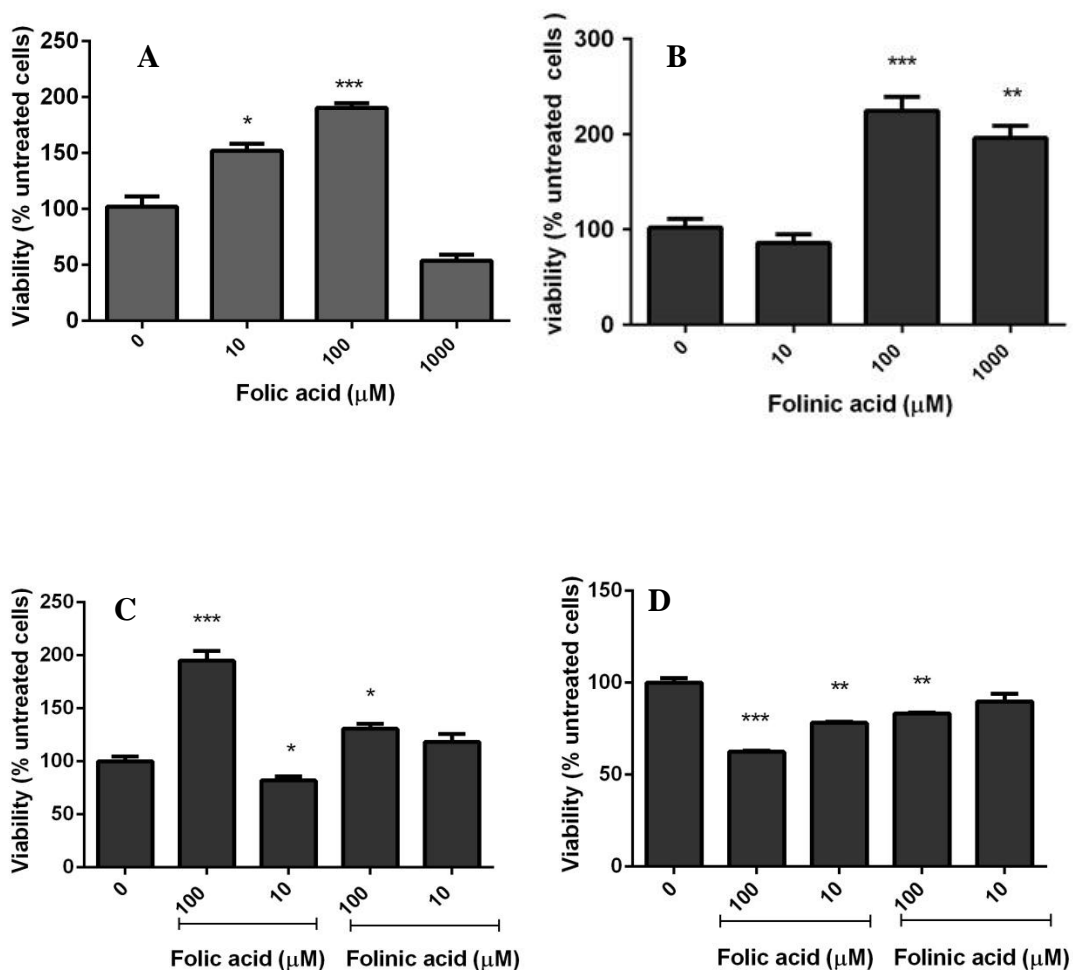


Figure 3-3 Survival of *C. glabrata* in the presence of folic acid and folinic acid. *C. glabrata* (10^3 cells/ml) were incubated in the presence of folic acid (A) and folinic acid (B) overnight at 30°C. Viability was estimated by determination of CFUs. The viability of quiescent (C) and non-quiescent (D) fractions of *C. glabrata* in the presence of 10 μM and 100 μM of folic acid and folinic acid are shown. (* $p < 0.05$, ** $p < 0.01$, *** $p < 0.005$). All data are expressed as mean \pm SEM.

3.4.3 Calcofluor fluorescence intensity of bud scars increases in the presence of folic acid and folinic acid

Calcofluor white staining of bud scars in the stationary phase *C. glabrata* (Figure 3-4A) revealed an increase in the fluorescence intensity in the presence of folic acid and folinic acid in a dose response manner compared with the control (Figure 3-4A). These results further support observations from both microscopy (Section 3.4.1) and

plate counts (Section 3.4.2) which showed an increase in the number of cells and particularly the multi-budded cells. The fluorescence intensity increased by 41.4% ($p < 0.005$), 24.8% ($p < 0.01$) and 19.0% ($p < 0.05$) in samples (10^5 cells/ml) treated with 1000, 100 and 10 μM of folic acid respectively compared with control (15.6%) (Figure 3-4A). Folinic acid also increased the fluorescent intensity of the cells but to a lesser level compared with the folic acid (26.8%, 21.0% and 19.0%) respectively, further indicating the existence of multiple bud formation and the presence of high level of chitin on the surface of the yeast cells.

Three distinct populations were observed in the untreated stationary phase *C. glabrata* cells (Figure 3-4B). The least stained cells are newly budded cells, and the more highly stained cells have one or more bud scars. It can be seen that treatment with folic or folinic acid led to an increased proportion of the populations with one or more bud scars. Yeast that naturally exhaust the glucose from their environment have been found previously to differentiate into three distinct cell types distinguished by flow cytometry (Li et al., 2013). In the presence of folic acid and folinic acid, however, there was a shift in the level of these populations. In the presence of 1000 μM folinic acid the *C. glabrata* cells formed a very distinct population whereas folic acid caused a merge in the population (Figure 3-4B).

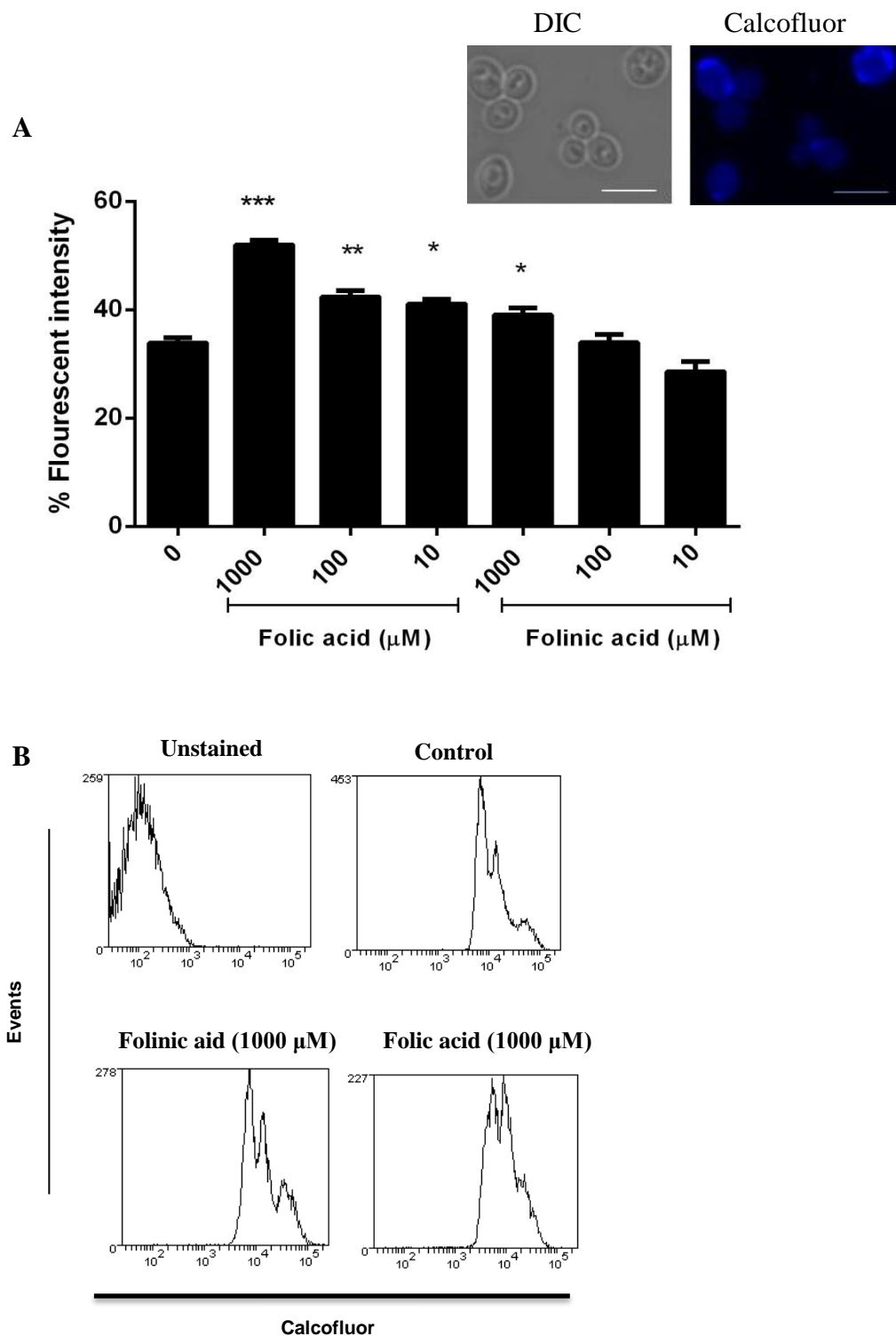


Figure 3-4 Calcofluor staining of the bud scars in stationary phase *C. glabrata*. Cells were incubated in the presence of 1000 μM, 100 μM, and 10 μM folic acid and folinic acid, analysed by flow cytometry (A). Intensity of the fluorescence in each sample was analysed by averaging the results from three independent experiments. Population analysis of *C. glabrata* cells treated with 1000 μM of folic acid and folinic acid, compared with control and unstained sample (B) (Scale bar = 10 μm). (***) $p < 0.005$, (**) $p < 0.01$, (*) $p < 0.05$).

3.4.4 Viability curve of stationary phase *C. glabrata* cells in the presence of folic acid after prolonged incubation and effect of introducing nutrients

Growth and viability of stationary phase samples suspended in water in the presence or absence of 100 μ M folic acid were measured and compared with untreated control samples (Figure 3-4A). The doubling effect of folic acid treatment mainly occurred in the first 48 h (Figure 3-4A). Interestingly there was fluctuation in the growth and viability of both treated and control samples indicating that perhaps at any time only a certain phenotype population is capable of forming colonies. A significantly higher number of viable cells were detected in the folic acid samples ($p < 0.01$) compared with control after 10 d of incubation in water (Figure 3-5A).

When the 10 d starved stationary phase cultures of untreated and folic acid treated cells were introduced into fresh YEPD broth, the cells started budding synchronously and re-entered mitosis after 2 h (Figure 3-5B) similar to previous observations (Allen et al., 2006; Li et al., 2009). No differences in the viability between the folic acid treated cells and control were found. This viability however was reduced after overnight incubation and the number of cells became very similar to those at the 0 h (Figure 3-5B).

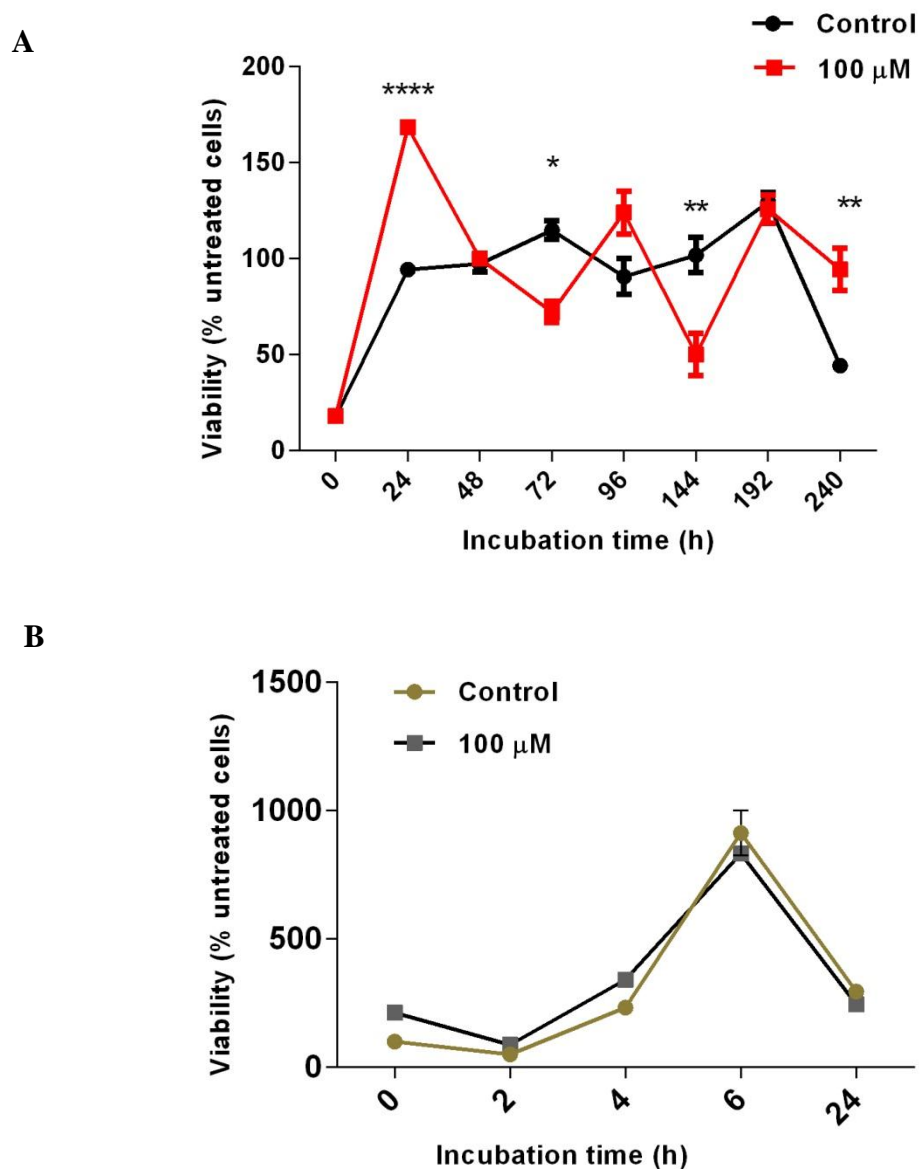


Figure 3-5 Growth of stationary phase *C. glabrata* in the presence and absence of folic acid. Growth and viability of stationary phase sample suspended in water in the presence or absence of 100 μ M folic acid compared with untreated control sample over a period of 10 days (A). Effect of introducing YEPD media to 10 d old starved *C. glabrata* culture treated with 100 μ M folic acid compared with untreated sample measured by CFUs determination after 2, 4, 6 and 24 h incubation in the media (B). Viability was measured by the ability of the cells to form colonies on YEPD solid media. (* $p < 0.05$, ** $p < 0.01$, *** $p < 0.005$, **** $p < 0.001$). All data are expressed as mean \pm SEM.

3.4.5 Survival of wild-type *S. cerevisiae* and EHY1 strain in the presence of folic acid and folinic acid with or without addition of MTX

In order to study the effect of folic acid and folinic acid on the survival of *S. cerevisiae*, the EHY1 strain was used which relies on an exogenous source of folate for survival and compared with the WT strain. The folic acid and folinic acid were added to the YEPD solid media to a final concentration of 50 μM , and 100 μM . 10-fold serial dilutions of cell suspensions were transferred using a multipronged inoculator onto the YEPD agar plates and examined qualitatively. Comparison of the colonies spotted on the media revealed that folinic acid caused a small increase in colony size in BY4743 compared with the folic acid treated samples (Figure 3-6). Addition of MTX to a final concentration of 1 $\mu\text{g}/\text{ml}$ (equivalent of 2 μM) and 2 $\mu\text{g}/\text{ml}$ (4 μM) into the solid media also resulted in more growth into the fifth row. Simultaneous treatment with MTX, folic acid and folinic acid resulted in larger colonies (Figure 3-6). The EHY1 strain was only able to grow in the presence of folic acid and folinic acid, while MTX was inhibitory. EHY1 showed more profound growth in the presence of folinic acid and the growth increased in a dose dependent manner (Figure 3-6). Absence of *FOL1* gene has been shown previously to confer susceptibility to MTX in the mutant strain (Cherry et al., 2012; Hoepfner et al., 2014). Interestingly, MTX inhibited the survival of EHY1 cells even in the presence of the highest concentration of folic acid as no growth was detected on the agar (Figure 3-6). Addition of folinic acid however, restored the inhibitory effect with both concentrations of MTX (Figure 3-6).

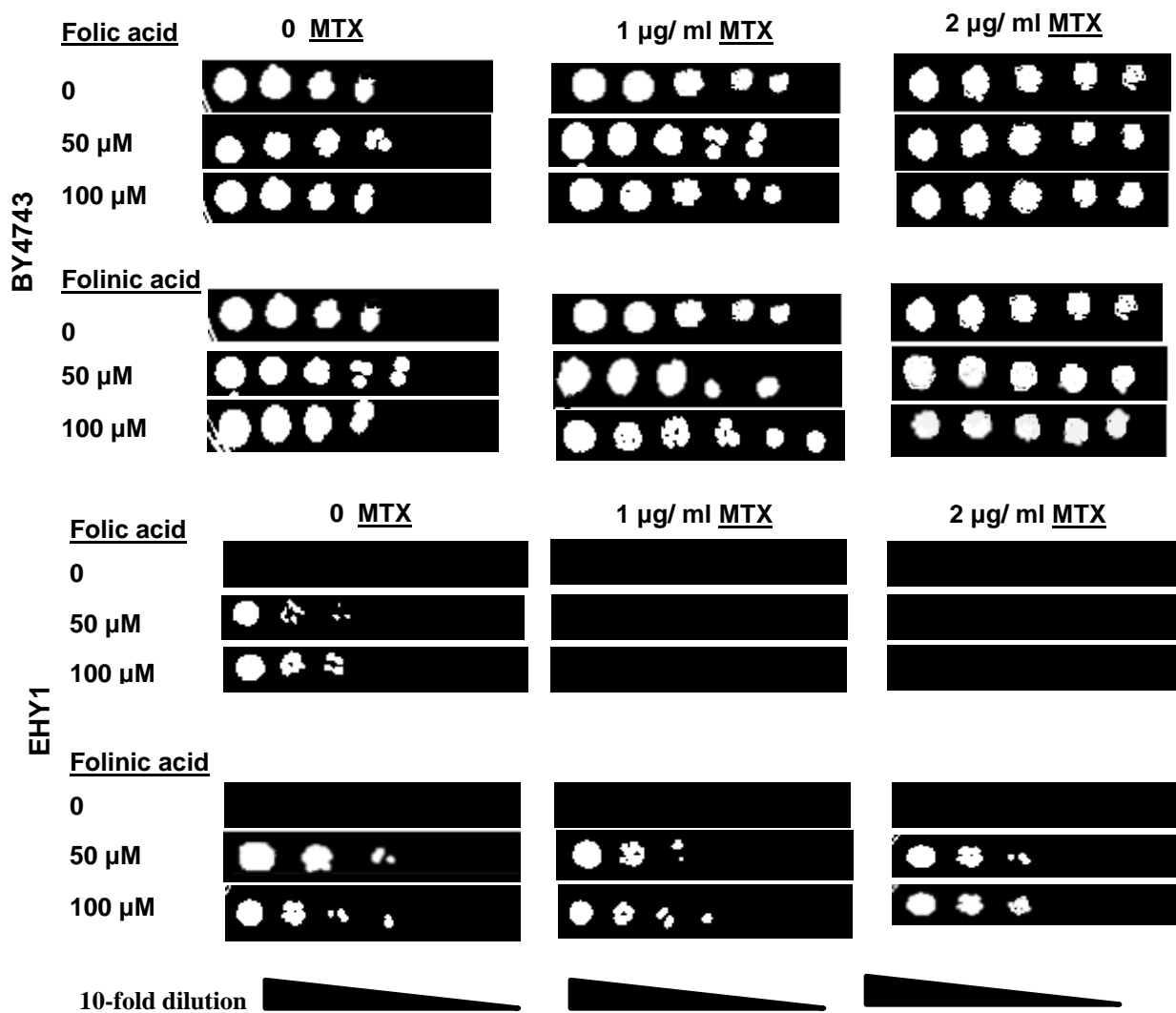
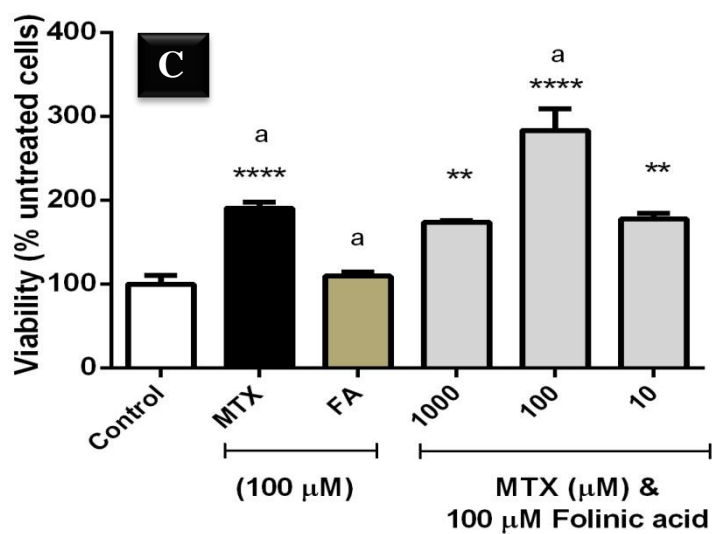
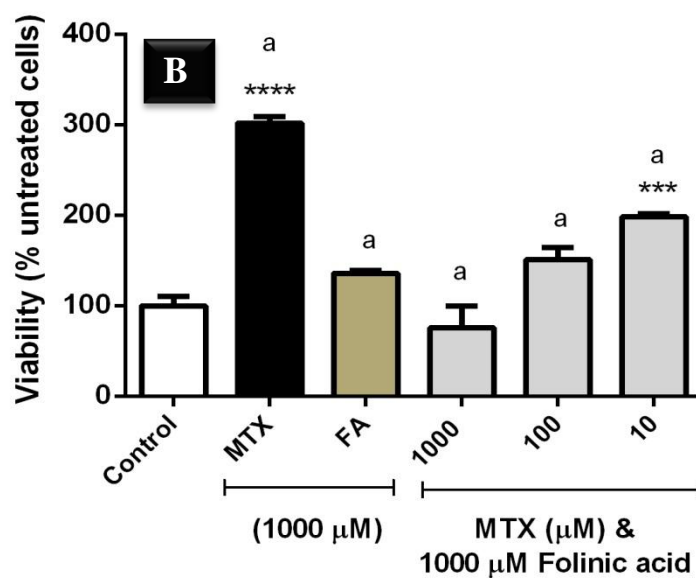
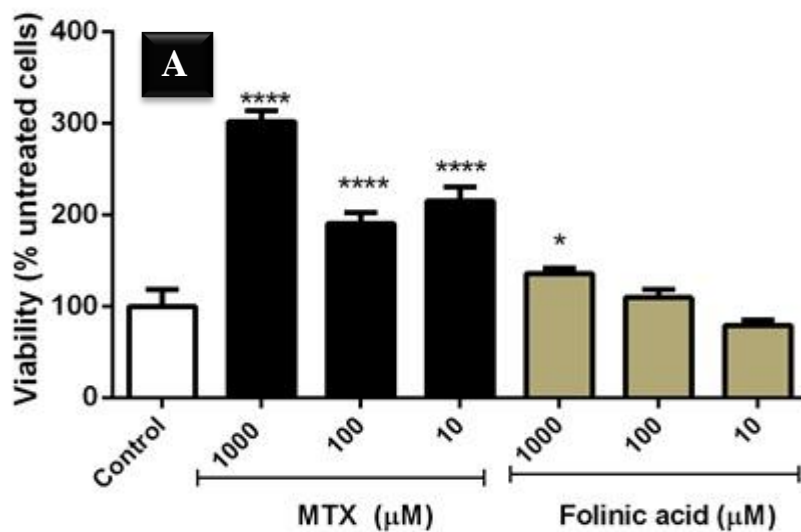


Figure 3-6 Survival of the BY4743 and EHY1 in the presence of folic acid and folinic acid with or without addition of MTX. In order to determine the effect of folic acid and folinic acid on the survival of stationary phase *S. cerevisiae*, cells were grown into stationary phase and resuspended in dilution series in H₂O. The folate treatments were added into the YEPD solid media to final concentration of 50 µM and 100 µM with or without 1 or 2 µg per ml of MTX.

3.4.6 Viability assessment of the wild-type *S. cerevisiae* in the presence of folic acid and MTX

Analysis of results from Section 3.4.4, implied that the cellular uptake mechanism of folic acid and MTX might be different to that of folic acid. Therefore, the effect of folic acid and MTX individually or in combination on the growth of stationary phase BY4743 cells was investigated after incubation of cells with 10 μM , 100 μM , and 1000 μM of either folic acid or MTX or in combination for 24 h. Analysis of the data showed that MTX significantly increased the viability with every concentration ($p < 0.001$) (Figure 3-7 A). Folic acid was more effective at the highest concentration of 1000 μM which significantly increased the survival of the cells ($p < 0.05$) (Figure 3-7A).

The effect of MTX on the BY4743 cells when combined with folic acid was very different. At a concentration of 1000 μM of MTX combined with 100 μM ($p < 0.001$) and 10 μM ($p < 0.005$) folic acid, there was a significant reduction in the survival compared with 1000 μM of MTX treatment alone (Figure 3-7B). A combination of 100 μM MTX with 10 μM ($p < 0.01$), 100 μM ($p < 0.001$) and 1000 μM ($p < 0.01$) of folic acid however resulted in higher viability of the cells compared with the control (Figure 3-7C). MTX at the lowest concentration of 10 μM in combination with 1000 μM ($p < 0.001$), 100 μM ($p < 0.001$) and 10 μM ($p < 0.05$) of folic acid resulted in the highest percentage of viability compared with the control and MTX treatment alone ($p < 0.01$) (Figure 3-7D).



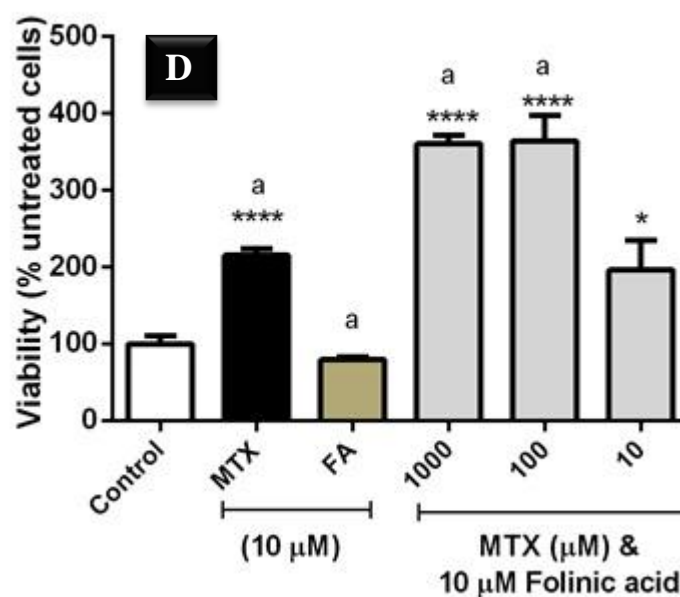


Figure 3-7 Growth and viability of BY4743 in the presence of MTX and folic acid. Stationary phase yeast cells were resuspended in water and then were treated with 10 μ M, 100 μ M, and 1000 μ M of either folic acid or MTX (A). Combinations of 1000 μ M folic acid with 10-1000 μ M of MTX (B), 100 μ M folic acid with 10-1000 μ M of MTX (C), and 10 μ M folic acid with 10-1000 μ M of MTX (D) were compared with control samples. (* $p < 0.05$, ** $p < 0.01$, *** $p < 0.005$, **** $p < 0.001$). **a**: indicates significant differences between MTX and other treatments. All data are expressed as mean \pm SEM.

3.4.7 Homology assessment of CAGL0M08426g and YJL163C gene and its similarity to the human folate transporter gene

The putative folate transporter is a predicted major facilitator superfamily (MFS) membrane transporter. Since exogenous folic acid and folic acid induce cell proliferation, this suggests an effect of folates on the cell cycle, possibly through a cell surface receptor and thus allows signalling which enables cell division processes to commence. The effects of folate on yeast then may indicate the presence of a specific transporter for folate. A search for analogs of human folate transporters was

performed using BLASTP analyses (Altschul et al., 1990). A strong lead was obtained using a transporter that was initially thought to be a heme transporter but more recently was identified to play a role in folate transport (Zhao et al., 2009; Shin et al., 2012). The comparison of its sequence compared with counterparts in *C. glabrata* and *S. cerevisiae* is shown in Figure 3-8A. It is apparent that this protein has counterparts in all yeasts, however, the null mutants have no remarkable phenotype and until now the function of the protein has remained unknown. Although, the YJL163C only shares 22% sequence similarity with the human proton coupled folate transporter isoform 1 (SLC46A1) (Zhao et al., 2009), it was hypothesised that folic acid and MTX might be targeting this transporter for entry into the EHY1 cells. The phylogeny tree for identification of the homology of putative folate transporter in *C. glabrata* CBS 138 (CAGL0M08426g), *C. albicans* SC5314 (orf19.6976) and *S. cerevisiae* S288C (YJL163C) species indicated that *S. cerevisiae* and *C. glabrata* to be closely rooted (Figure 3-8B).

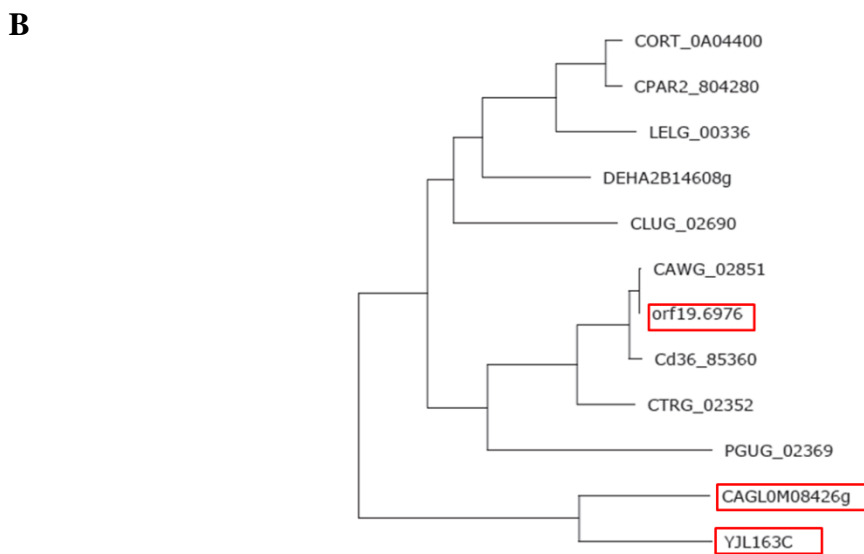
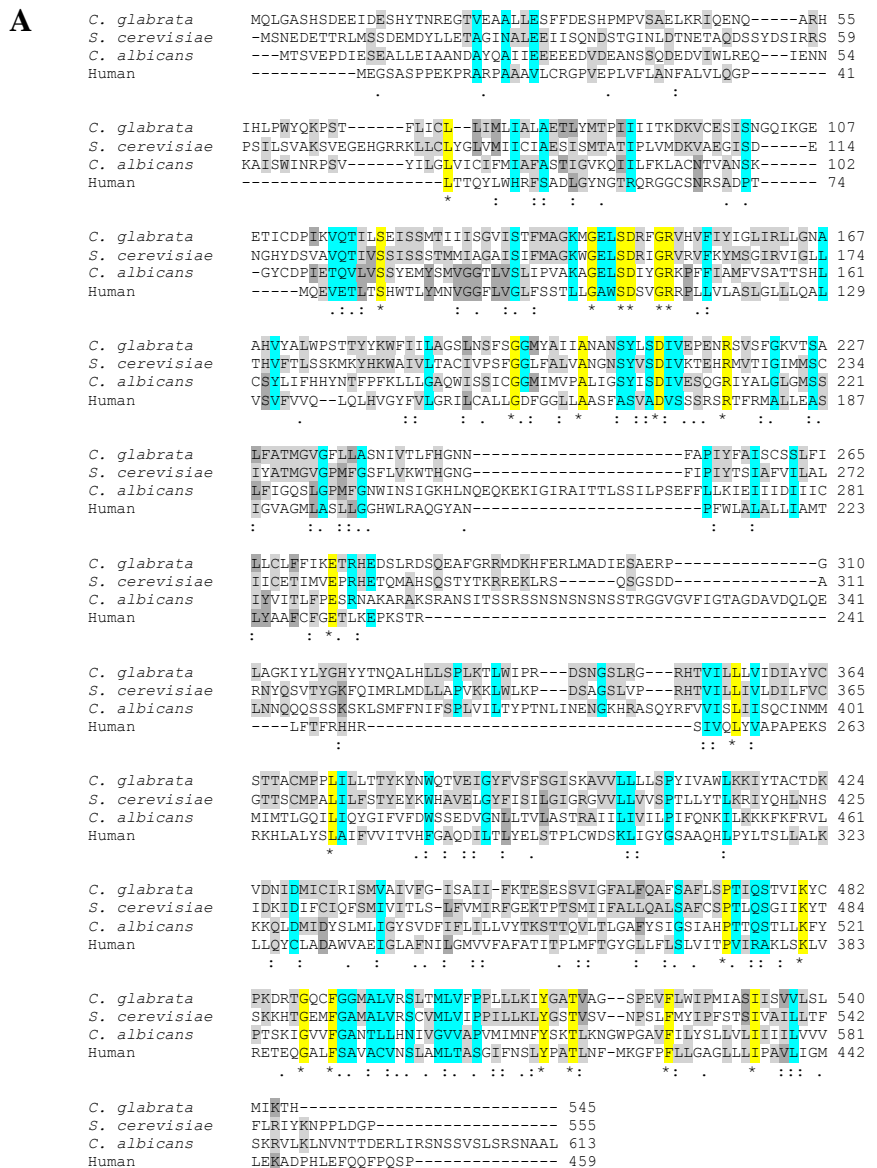


Figure 3-8 Homology assessment of putative folate transporter. (A) Multiple sequence alignment of yeast putative folate transporter and *Homo sapiens* proton

coupled folate transporter/ heme carrier protein 1 (PCFT/HCP1). The human proton coupled folate transporter isoform 1 (SLC46A1) is aligned with *C. glabrata* (CAGL0M08426g), *S. cerevisiae* (YJL163C), *C. albicans* (orf19.6976) putative folate transporter using ClustalW multiple sequence alignment. The identical residues are highlighted in yellow, conservation of strong groups is shown in blue and other conservations are coloured in grey. Asterisk (*) and period (.) indicate perfectly conserved and well conserved positions, respectively. (B) Phylogeny tree for homology analysis of putative folate transporter in *C. glabrata* CBS 138 (CAGL0M08426g), *C. albicans* SC5314 (orf19.6976) and *S. cerevisiae* S288C (YJL163C) species. *C. albicans* sequence was used as a reference sequence.

3.4.8 Induction of cell division by methotrexate in the presence, absence and overexpressed folate transporter gene in *S. cerevisiae*

The folate transporter gene was cloned into a p416.GPD plasmid and was used to over express the Foltp in the EHY1 strain. Analysis of the effect of folic acid and folinic acid in the presence and absence of 1 µg/ ml (2 µM) of MTX were done in the EHY1 strain transformed with the overexpressed gene (p416.GPD and FOLT) and empty vector (p416.GPD). Analysis of plates after 48 h incubation showed MTX to be inhibitory while 25 µM of folinic acid contributed to survival (Figure 3-9). Transformation of the EHY1 strain (which relies on the exogenous source of folate for survival) with the FOLT gene increased its viability slightly in the presence of 25 µM folinic acid compared with the EHY1 and empty vector (Figure 3-9). Addition of 1 µg/ ml MTX inhibited the growth of EHY1 transformed with the FOLT gene, further indicating that it does not play a role in folinic acid uptake (Figure 3-9). The survival of *YJL163CA* mutant strain which was expected to be affected by MTX and folinic acid was not found to play a role in sensitivity to MTX (Figure 3-9)

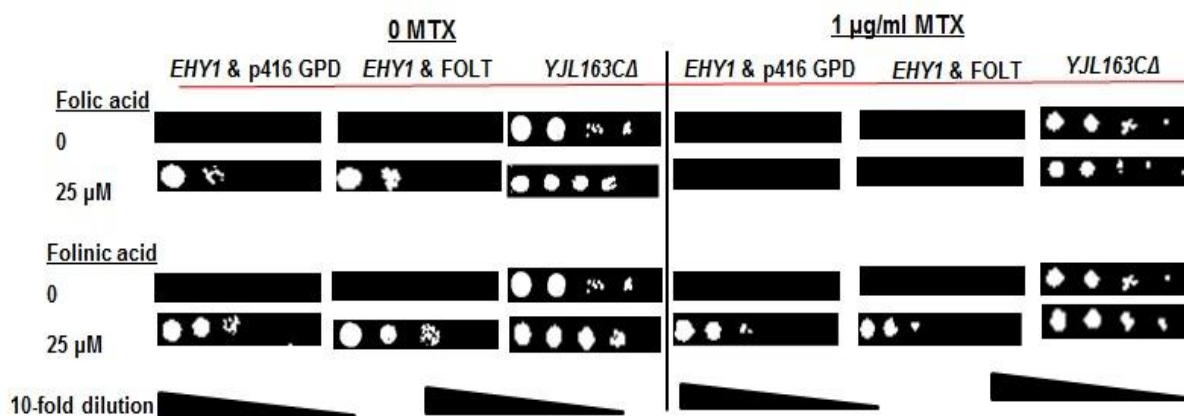


Figure 3-9 Spot assay analysis of *S. cerevisiae* EHY1 strain transformed with empty vector (p416.GPD) and FOLT gene insert, compared with the *YJL163CA*. Chemicals were added to YNB plates and exponentially growing yeast cells were spotted on each plate (A). 1 µg/ ml MTX and 100 µM folic acid were added alone or in combination.

3.4.9 Folate uptake in *S. cerevisiae* in the presence and absence of the folate transporter gene

The uptake of folic acid, which has an intense yellow colour, was examined using fluorescent microscopy in various *S. cerevisiae* transformants. Microscopic analysis of the WT *S. cerevisiae*, a putative folate transporter mutant (*YJL163CA*) and BY4743 overexpressing the Foltp treated with folic acid revealed the uptake of folic acid into the cells (Figure 3-10A). After 24 h incubation of the wild-type, *YJL163CA* deletant and Foltp overexpression strain with 100 µM folate, intense yellow fluorescence was observed indicative of folic acid localised within various organelles of the yeast cells (Figure 3-10B). Folic acid has been taken up by all of the cells regardless of presence or absence of the folate transporter gene, indicating that another mechanism is probably involved in the folate uptake and entry.

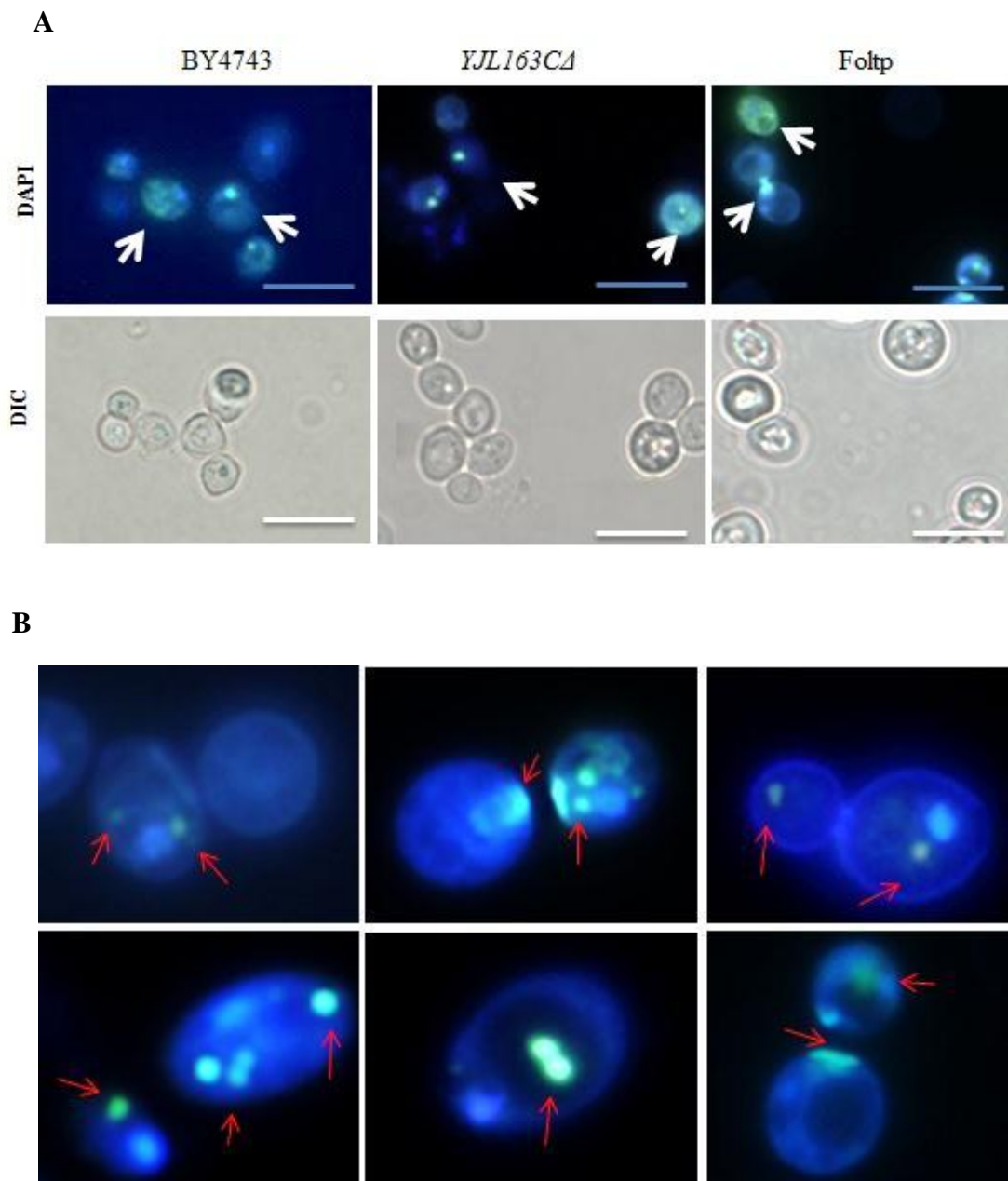


Figure 3-10 Microscopic images of folic acid uptake by BY4743, *YJL163CΔ* and Foltp overexpressed yeast cells. Comparison between the strains for folic acid uptake is shown (A). DAPI has been added to cells for visualisation of the DNA and Calcofluor for bud scar labelling. Top panel shows DAPI whereas the lower panel is bright field images (DIC), (Scale bar = 10 μ m). Folic acid has a yellow colour which can be visualised under fluorescent microscope as yellow-green pigments inside the cells (B). Arrows indicate the location of the folic acid within the cells.

Transformants of *S. cerevisiae* (BY4743) with the plasmid encoding the folate transporter gene were incubated in the presence of 100 μ M folic acid for 48 h. After 24 h incubation, meiosis events in the mutant strain, FOLT overexpression and the WT were observed and captured by time-lapse photomicroscopy. The first meiotic division and telomere clustering is shown by time lapse images in Figure 3-11A. The microscopy imaging also revealed the presence of spores in the suspension and after further incubation the number of spores increased (Figure 3-11B). Although the sporulation was viewed in all strains, an aberrant sporulation was detected in the presence of folate transporter overexpression (Foltp) (Figure 3-11B). This aberrant sporulation in the Foltp strain also increased over the time with numbers increasing after 48 h incubation (Figure 3-11B). Observation of asci indicated presence of three visible spores with triad arrangement within the ascus (Figure 3-11B).

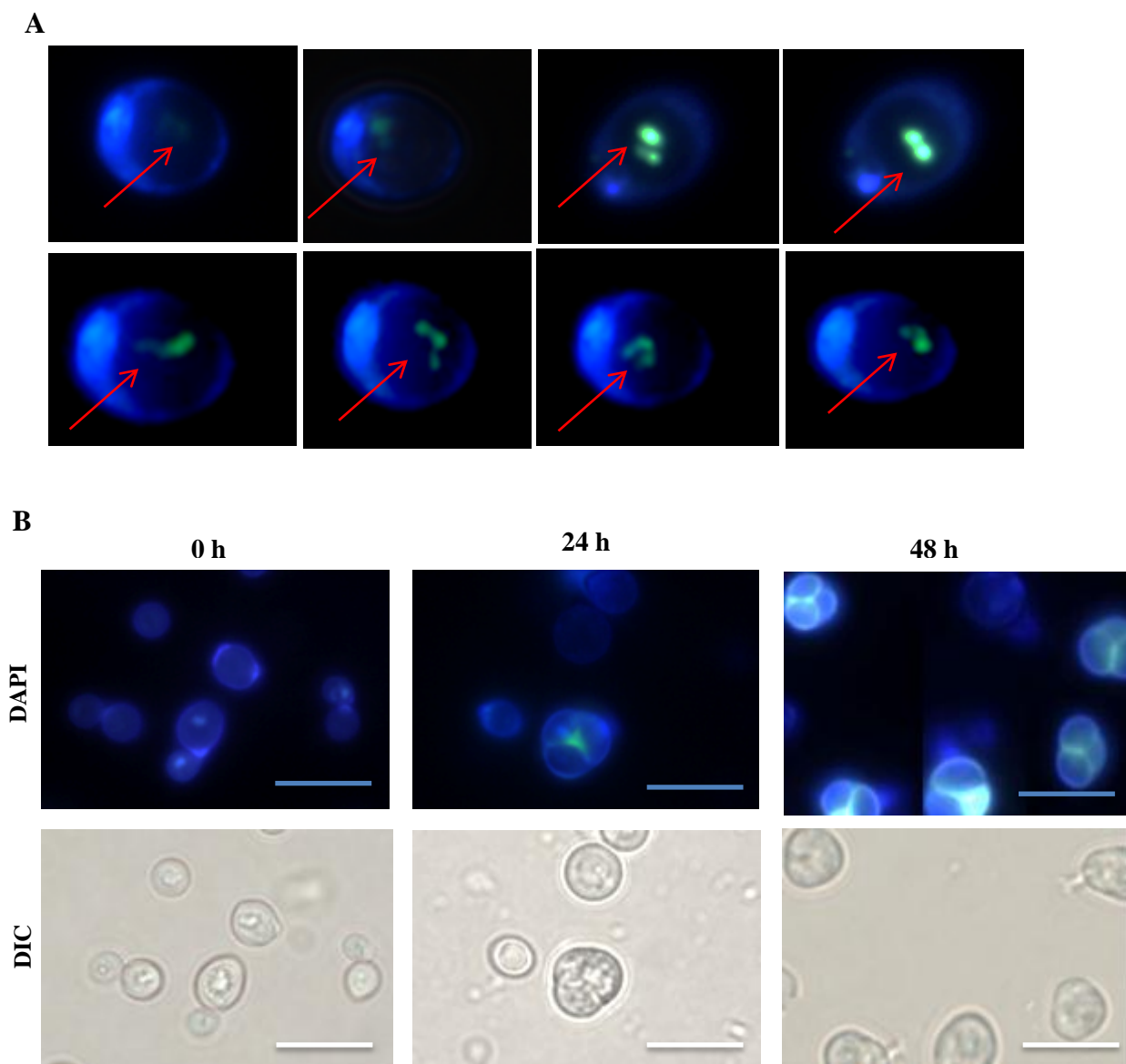


Figure 3-11 Microscopic imaging of the *S. cerevisiae* overexpressing the *Foltp* gene revealed an induction of sporulation in the presence of folate. Time lapse images of telomere clustering and movement during first meiotic division viewed in all tested strains (A). The number of spores increased over time (B). Cells have been treated with DAPI and Calcofluor white and samples were visualised under the fluorescent microscope UV filter at 0, 24 and 48 h after incubation in water and 100 μ M of folic acid. (Scale bar= 10 μ m)

3.4.10 Effect of extracellular added synthetic A β ₄₂ on wild-type, mutant (*YJL163CA*) and over expressed FOLT in *S. cerevisiae*

Chemically-synthesised A β ₄₂ was pretreated with either HFIP or NH₄OH prior to dissolution in H₂O (pretreatment of A β ₄₂ peptide is explained in Chapter 4). Exponentially growing cells of BY4743, deletant strain of *YJL163CA* and overexpression Foltp were resuspended in H₂O and treated with 2 μ M of chemically-synthesised A β ₄₂. Analysis of the results showed that NH₄OH pretreated A β ₄₂ significantly increased the proliferation after 24 h in all three strains ($p < 0.005$) (Figure 3-12A). The HFIP pretreated A β ₄₂ on the other hand was toxic to all tested strains and significantly contributed to the loss of viability compared with the control samples ($p < 0.001$) (Figure 3-12B). This analysis does not support a role for the transporter gene in the entry of the A β ₄₂ peptide as all three strains resulted in similar outcome in the presence of HFIP or NH₄OH pretreated A β ₄₂ peptide.

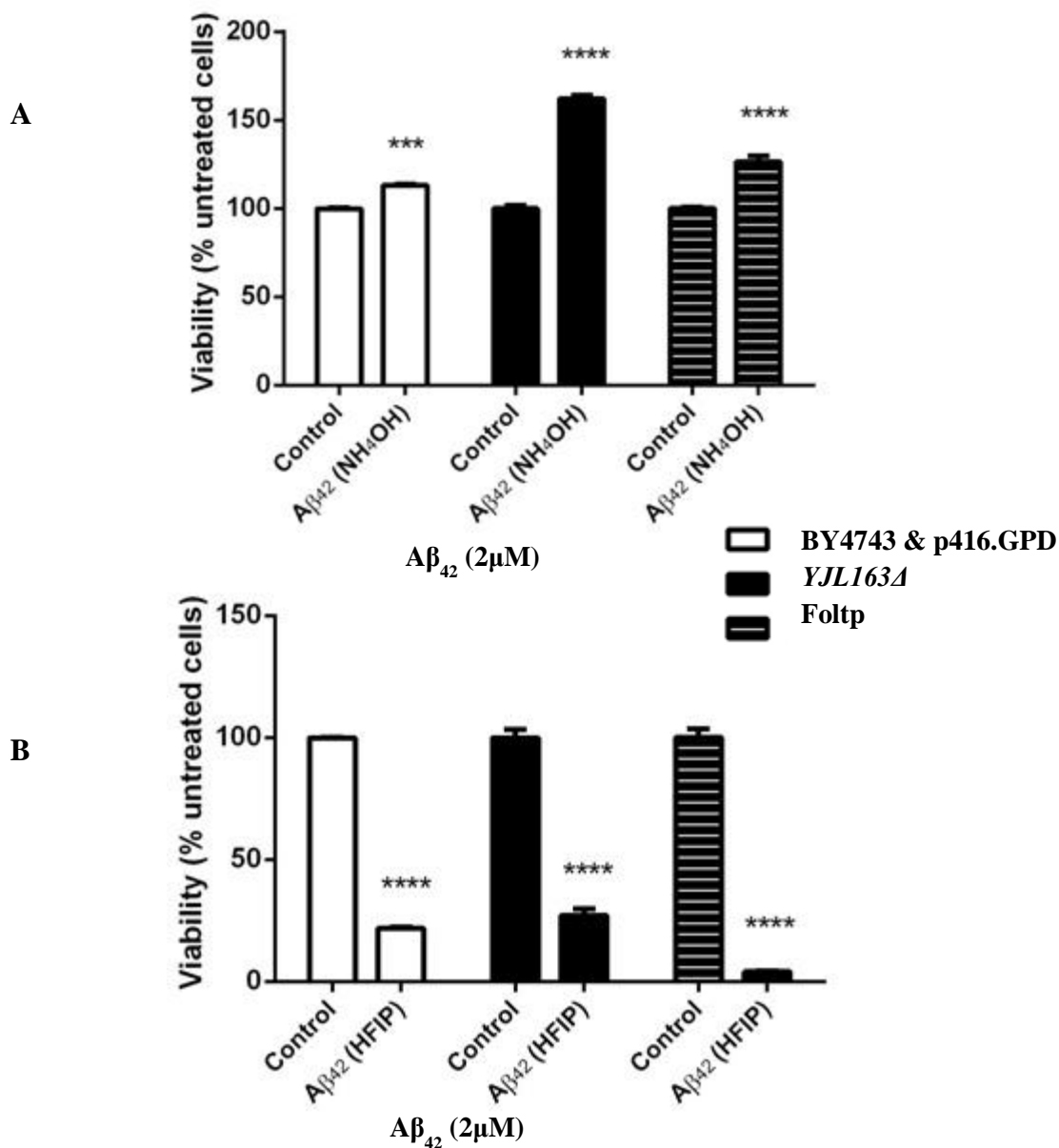


Figure 3-12 Role of putative folate transporter gene (YJL163C) in the cellular uptake of $A\beta_{42}$ peptide. Exponentially growing WT (BY4743) transformed with p416.GPD vector, *YJL163C Δ* and BY4743 overexpressing Foltp yeast were used to compare effect of exogenous peptide on the cell proliferation level. The $A\beta_{42}$ peptide was pretreated using two distinct methods of HFIP and NH_4OH ($2\mu M$). Viability of the cells was estimated by the ability of the cells to grow on YEPD media and was estimated as a percentage of the control samples. (***) $p < 0.005$, (****) $p < 0.001$. All data are expressed as mean \pm SEM.

3.5 DISCUSSION

Alzheimer's disease (AD) is an aging disease which can be studied in yeast, a simple eukaryote that enables the study of the cell chronological lifespan. In the nutrient-depleted and non-dividing state, budding yeast cells reflect similar features to post-mitotic differentiated cells in aging of higher eukaryotes (Fabrizio and Longo, 2003; Buttner et al., 2008; Braun et al., 2010). Many studies of DNA replication and checkpoints have also used budding yeast as a model organism. This is not however surprising as cyclin dependant kinases (CDKs) were first identified in *Saccharomyces cerevisiae* (Hartwell et al., 1970). It has been reported that unscheduled cell division due to atypical mitotic activation in neurons undergoing degeneration in AD leads to nerve cell death in the central nervous system (CNS) (Ding et al., 2000; Herrup et al., 2004; McShea et al., 2007). Further, Cdc25A tyrosine phosphatase which plays a key role in cell-cycle progression, is absent from terminally differentiated healthy adult neurons, yet activated in the brain of AD sufferers (Ding et al., 2000). The cell cycle events in non-dividing cells in AD reportedly can be activated by amyloid precursor protein (APP) signalling, A β peptide and oxidative damage due to accumulation of reactive oxygen species (ROS) (Herrup et al., 2004; Yang et al., 2006; Nagy, 2007).

The critical role of folic acid in the CNS is illustrated by its importance in preventing maternal neural tube defects (Boot et al., 2003; Mayanil et al., 2011; Yu et al., 2014b). Folic acid intake is well known to induce proliferation and differentiation of the neural crest stem cells (Mayanil et al., 2011). Folic acid deficiency in APP mutant mice resulted in impaired DNA repair in hippocampal neurons which ultimately sensitised them to the toxicity of A β ₄₂ (Kruman et al., 2002). Therefore, it is hypothesised that intake of methotrexate (MTX) antifolate drug for prevention of

other diseases can have a detrimental effect on neural cells and exacerbate the effect of AD.

3.5.1 Aberrant proliferation induced by folates in *C. glabrata*

Both folic acid and folinic acid were shown in this chapter to result in increased cell numbers and DNA synthesis in *C. glabrata* apparent by the presence of multiple buds on cells. Increased bud formation in *C. glabrata* resistant to fluconazole has been reported previously (Samaranayake et al., 2013). One explanation for this observation of multiple bud formation in *C. glabrata* cells is that cells are responding to stress in a way that signals survival. Moreover, this aberrant proliferation would allow biofilm formation which ultimately contributes to the survival of cells. In neuronal cells, aberrant cell proliferation leads to neurodegeneration (reviewed by Bonda et al., 2010) (Figure 3-13). The aberrant proliferation in *C. glabrata* was limited to stationary phase cells. Similar to previous findings reported by Paz and Choder (2001), the outcome of the current study suggests that regulation of gene expression in yeast varies during stationary phase of the growth cycle compared to that of the exponential phase.

Accumulation of oxidative stress has been found to cause cell cycle misregulation, with ROS inducing DNA damage in a dose dependent manner (Burdon, 1995; Day and Suzuki, 2005). Further, high dosage of oxidants such as H₂O₂ and other peroxidases were found to be toxic and cause cell cycle arrest, but in low doses they have been associated with proliferation and survival (D'Souza et al., 1993; Burdon et al., 1996). This suggests that below toxic levels, chemicals that induce ROS can serve

as a signalling molecule (Figure 3-13) (Day and Suzuki, 2005). Therefore, the aberrant proliferation shown by stationary phase cells in this chapter is similar to that reportedly seen in neuronal cells that are susceptible to moderate insults. Further, cell death eventuates as a result of ROS accumulation (Herrup et al., 2004). Wirth et al. (2004) have shown that loss of the anaphase promoting complex (APC) in quiescent cells is also a major contributor to unscheduled cell division, even in the absence of proliferative stimuli. Although the lack of APC has not been investigated in the current study, it could be an explanation for the aberrant proliferation that was observed in quiescent cells.

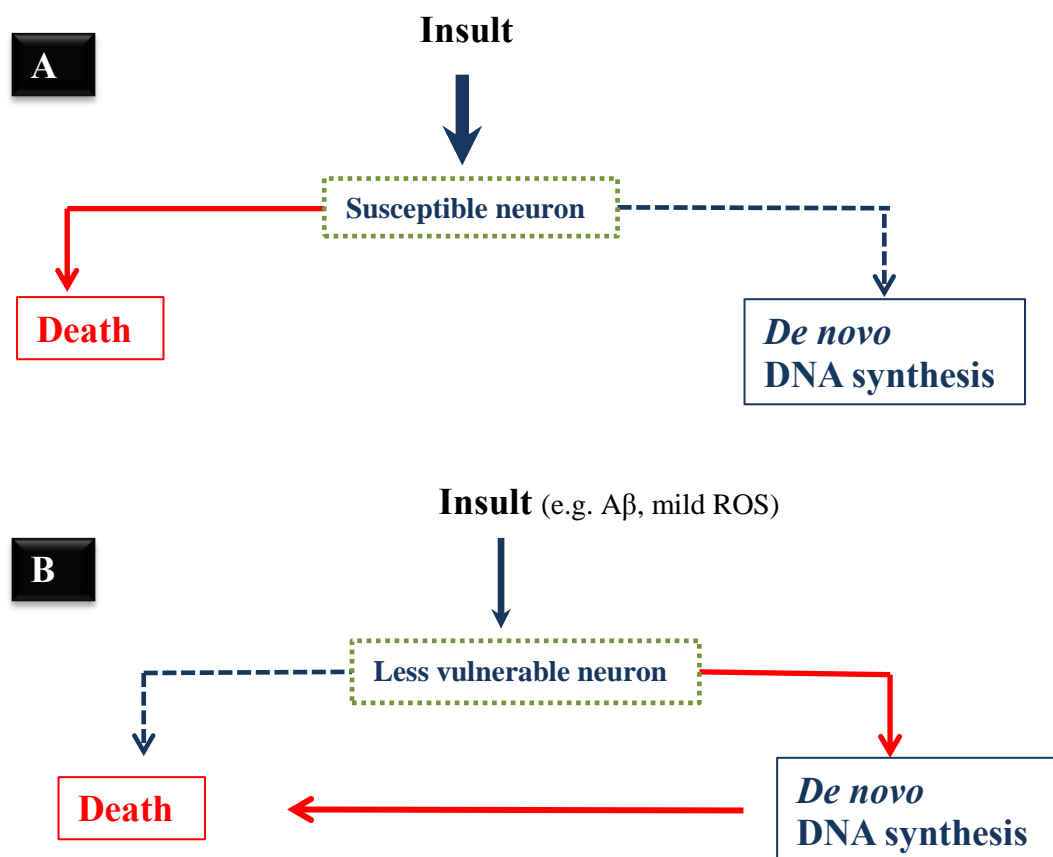


Figure 3-13 Type of insult that can lead to DNA replication and ultimately neuronal death. Susceptible neurons (A) in the presence of severe insults suffer from extensive DNA damage and die without any *de novo* DNA synthesis. In less vulnerable neurons (B) exposed to other types of insults such as A β and mild ROS, *de*

*nov*o DNA synthesis becomes essential for neuronal death. Adapted from Herrup et al. (2004).

Based on evolutionary biology a population can optimise its fitness in fluctuating environments. This was shown by the results of the current study when the number of cells fluctuated over the 10 d incubation in the absence of nutrients. This fluctuation might be due to stochastic switching which is indicated by the data that shows at any time point, only one particular phenotype is able to survive and re-generate (Minois et al., 2009). Cells in stationary phase are found to be well equipped for survival and have some reserves for growth which enables them to survive prolonged periods in the absence of nutrients (Werner-Washburne et al., 1993; De Virgilio, 2012). This was demonstrated by observations in the current study that such cells can double without need for additional exogenous nutrients. Previous studies on *S. cerevisiae* have also shown that the level of intracellular carbohydrate increases during stationary phase but this increase in intracellular storage does not correlate with long term viability of the cells (Slaughter and Nomura, 1992; Werner-Washburne et al., 1993). As the effect of folate appears to be limited to stationary phase cultures this further confirms that regulation of gene expression in yeast is different during the stationary phase of the growth cycle compared to that of the early exponential phase (Paz and Choder, 2001). An experiment by Hjortmo et al. (2008) reported high folate content in yeast during the exponential phase which seems to be related to requirements for DNA replication, mRNA and protein synthesis that is highest in exponential phase compared to stationary. Also, consistent with previous observations on the plasticity of death rate in stationary phase, data from the current study showed that at any time point only a certain number of cells are able to exit

stationary phase and form a colony (Granot and Snyder, 1993). This was evidenced when the 10 d treated cells were introduced to nutrient rich media; the cell viability was similar to the untreated control after 24 h incubation. Granot and Snyder (1993) similarly found that glucose was capable of inducing the cell cycle in *S. cerevisiae* suspended in water, however, this was associated with a loss of viability. The data presented in this chapter also indicated that proliferation was more prevalent in quiescent cells whereas the non-quiescent cells, which consisted of older mother cells, lost their viability in the presence of folate. This result can be explained when the findings by Gray et al. (2004) are considered as they showed the presence of premature spindle pole bodies (SPB) and accumulation of higher levels of ROS in non-quiescent cells which consequently increases their susceptibility to any change.

Folate treated stationary phase cells were analysed by flow cytometry. Flow cytometry data showed the presence of three distinct cell types similar to the previous findings of Li et al. (2009). These populations were the small daughter cells that are arrested in G1 phase, mother cells that failed G1 arrest and larger daughter cells. Daughter cells have been found to predominate in quiescent cell populations and arise through asymmetric cell division when nutrients become exhausted (Castelli et al., 2011; McFaline-Figueroa et al., 2011). Quiescent cells are also associated with more resistance to change due to modified cell walls and the presence of specific mRNA-binding proteins (e.g. Mpt5) which deliver mRNAs to P-bodies and accumulatively contribute to cell longevity (Bregues et al., 2005; Bregues and Parker, 2007; Li et al., 2009; Klosinska et al., 2011). Similarly, the folate treated samples resulted in higher levels of daughter cells which could explain the increase in the viability of folate treated samples compared to the untreated control.

Bud formation is an event of the yeast cell division cycle. A distinguishable budding pattern in stationary *C. glabrata* induced by folic acid and folinic acid was also noted in the microscopic analysis in the current study. *C. glabrata* normally exhibits only an axial budding pattern but both folic acid and folinic acid induced both axial and bipolar forms of budding (Sinnott et al., 1987; Fidel et al., 1999). It is known that the yeast actin cytoskeleton is responsible for polarized budding growth during the cell cycle (Pruyne and Bretscher, 2000). In haploid cells however the absence of sugar has been reported to cause bud switching from axial to a unipolar-distal budding pattern (Paz and Choder, 2001; Cullen and Sprague, 2002). A search of the literature failed to find any reports that have shown the appearance of three to four buds on cells deprived of nutrients whilst in stationary phase. Early studies of bud selection have revealed that when starved cells are fed again, their next bud forms in a novel site (Cullen and Sprague, 2002). Aberrant mitosis however, has been reported in fission yeast *Schizosaccharomyces pombe* temperature sensitive mutants (*cut6* and *Isd1*) defective of fatty acid synthetase and acetyl CoA carboxylase (Saitoh et al., 1996). Therefore, an adequate amount of fatty acid has been proposed to be required for the successful separation of mother and daughter cells and may suggest why multiple buds were observed in the *C. glabrata* cells in the absence of nutrients.

3.5.2 Folate causes aberrant sporulation in *S. cerevisiae* particularly in the presence of FOLT overexpression

In the current study, BY4743 *S. cerevisiae* was found to be resistant to the toxic effect of MTX similar to that found in previous investigations by Delitheos et al. (1995). This has been explained by the presence of the *FLRI* gene which confers resistance to the effect of MTX in *S. cerevisiae* (Broco et al., 1999; Hoepfner et al., 2014). The *FLRI* gene (YBR008C) encodes a transmembrane transporter belonging to the major facilitator superfamily (MFS) which is involved in efflux of many drugs including MTX (Alarco et al., 1997; Tenreiro et al., 2001; Cherry et al., 2012). This could explain why cell growth became limited when MTX was combined with folic acid. In yeast, MTX and folic acid may use a similar transporter while folinic acid entry is initiated via another transporter or carrier. It can be speculated therefore that MTX might compete with folic acid for cellular entry whereas the entry of folinic acid is not affected. This could also suggest that activation of *FLRI* in the BY4743 strain may result in an increased efflux of MTX whilst the presence of folinic acid confers viability to the cells as its mode of entry occurs independently.

Analysis of data from the current study also revealed a growth inhibition effect of MTX on the *FOLI* disrupted strain of EHY1 which was found to be very sensitive to the MTX treatments. This sensitivity however was only restored in the presence of folinic acid whilst folic acid was ineffective. Mapping of cellular response using a chemogenomic fitness signature of the effect of MTX, has revealed that almost 15 genes are essential for the survival of the yeast cells (Lee et al., 2014). Among those, *FOLI* (YNL256W) has been listed as one of the essential genes required for MTX resistance and is disrupted in the EHY1 strain. Other folate related genes such as

DFR1 (YOR236W) and *CDC21* (YFR051C) have also been listed as essential (Lee et al., 2014).

Results from this chapter have also indicated that addition of MTX to the stationary phase WT *S. cerevisiae* can result in aberrant cell proliferation. This may indicate the presence of *de novo* DNA synthesis which ultimately leads to cell death or proliferation. Mitotic events in *S. cerevisiae* are regulated by Cdc28 (reviewed by Mendenhall, 1998). In a study by Nickerson and Webb (1956) using exogenous folic acid analogues, it was found that the effect was species specific. No inhibitory effect was observed on the growth of *S. cerevisiae*, whilst visible growth inhibition along with change in morphology was reported in *Candida tropicalis* (Nickerson and Webb, 1956). Moreover, in a subsequent study by Webb and Nickerson (1955) folic acid was found to reverse the inhibitory effect of folic acid analogous in *C. tropicalis*.

Susceptibility to opportunistic fungal infection in cancer patients receiving antineoplastic drugs have been well documented (Ghannoum et al., 1989; Samonis and Bafaloukos, 1992; Ueta et al., 2001). Studies have shown that a combination of antineoplastic with antifungal drugs can provide effective treatment while, the autoplasic drugs such as MTX administered alone is not sufficient (Ghannoum et al., 1989, 1990). Ghannoum et al. (1990) further reported that both the ratios and the absolute concentrations of the tested antineoplastic and antifungal drugs in the mixture are important factors for their inhibitory effect and potency.

Additionally, Laque-Ruperez and colleagues (2003) were able to show that addition of iron (III) chloride to MTX could significantly enhance its potency in MCF-7 breast cancer cells whereas the same treatment did not modulate the MTX potency in *S. cerevisiae* cells (Ruiz-Gomez and Martinez-Morillo, 2006). This further indicates that the MTX mode of action is very different in yeast cells compared with mammalian cells which limited its investigations in the WT strain.

The results presented in this chapter indicate that overexpression of the FOLT gene (YJL163C) in *S. cerevisiae* in the presence of folate only, induces meiosis and sporulation which increased as incubation continued. Sporulation in budding yeast occurs as result of nitrogen starvation and in the current study, due to the suspension of the cells in H₂O, the cells are starved for nutrients. Enyenihi and Saunders (2003) performed a large-scale functional genome analysis and revealed that around 334 genes are essential for sporulation. It should be pointed out that YJL163C has not been listed as one of those identified genes. Therefore, the data of the current study indicates that this aberrant sporulation is not due to the YJL163C gene alone but rather the presence of folic acid may contribute to this process and signals meiosis. Another explanation maybe that the overexpression of YJL163C gene may result in increased ROS accumulation. As mentioned in Section 3.5.1, moderate ROS accumulation may contribute to *de novo* DNA synthesis and in the case of *S. cerevisiae* it might act as sporulation signal. However, the null mutant of *YJL163C* Δ has been shown to have reduced hyperosmotic and competitive fitness (Miller et al., 2005; Costanzo et al., 2010; Cherry et al., 2012; Sharifpoor et al., 2012).

Sporulation and meiosis in diploid *S. cerevisiae* cells are known to occur as a result of carbon or nitrogen source depletion (reviewed by Neiman, 2011). The target of rapamycin (TOR) in yeast consists of two protein kinases namely Tor1p and Tor2p. These regulate cell growth and metabolism in response to environmental signalling (Wullschleger et al., 2006; Blagosklonny, 2007). Almost all of the asci generated by folic acid treatment in this chapter had triad arrangement with only three spores easily visible. Previous finding by Davidow et al. (1980) and Taxis et al. (2005) have indicated that adverse and limiting conditions can contribute to the formation of less spores within the ascus due to the involvement of only one SPB in meiosis II. Meiotic plaque (MP) assembly which appears in meiosis II have been shown to play a critical role in spore number control (Taxis et al., 2005). Formation of less MP as a result of composition of the cell culture leads to formation of fewer spores which may explain the observations that were made in this current study. Further, folic acid has induced formation of only three MPs which resulted in formation of three spores in meiosis II.

3.6 CONCLUSION

Aberrant proliferation of stationary phase *C. glabrata* in the presence of folate was identified. Formation of multiple buds in the presence of folate was a novel finding. Folate led to the formation of both axial and distal budding patterns on the cells.

This study further exploited the cellular uptake of folate by utilising a putative folate transporter (YJL163C) of *S. cerevisiae* and examining its role. Aberrant sporulation of *S. cerevisiae* in the presence of this gene was detected with formation of triad spores within asci. This gene was found to be ineffective against cytotoxicity induced by A β ₄₂ peptide.

Methotrexate, an antifolate was not found to be inhibitory to the growth of WT *S. cerevisiae* strain while it inhibited the growth of EHY1 strain. The EHY1 strain was rescued only by addition of folinic acid whilst folic acid was ineffective.

4 CHAPTER 4: EFFECT OF SYNTHETIC A β ₄₂ ON YEAST AND THE ROLE OF *AHP1* IN PROTECTION

4.1 INTRODUCTION

Complex mechanisms contribute to the development of Alzheimer's disease (AD). Synaptic loss due to plaque formation (Selkoe, 2002) and neuronal death due to soluble oligomeric forms of A β ₄₂ are all hallmarks of the disease (Yoshiike et al., 2008). Soluble oligomeric aggregate structures of amyloid beta (A β ₄₂) peptide have been found to be highly neurotoxic and important in the etiology of AD in comparison to fibril forms (Rochet and Lansbury, 2000; Hardy and Selkoe, 2002; Cohen and Kelly, 2003; Klein et al., 2004; Morgan et al., 2004). However, it is still unknown which form of the aggregates are more dangerous; oligomers and protofibrils or fibrils and filaments (Zagorski et al., 1999; Stefani and Dobson, 2003; Steckmann et al., 2012). Despite these uncertainties aggregation studies used in the search for chemo-preventatives that block A β ₄₂ oligomer and fibril formation using synthetic forms of A β ₄₂ have become common practice (Chen et al., 2010; Matlack et al., 2014).

The toxicity studies using chemically-synthesised A β ₄₂ require preparation of peptide stocks where it displays biological activities. The preparation of A β ₄₂ peptide can affect its amyloidogenicity (Zagorski et al., 1999). Pretreatment of synthetic A β ₄₂ peptide is usually required in order to induce alpha helical conformations in the peptide, produce monomers and mimic the aggregation pathway in kinetic

investigations (Walsh et al., 1997; Roccatano et al., 2005; Teplow, 2006). The suspension of lyophilised peptide in a desirable buffer has been difficult due to the hydrophobic nature of the peptide, creating a hurdle for initial dissolution. Pretreatment is usually done in polar-non polar interfaces such as 1,1,1,3,3,3-hexafluoro-propan-2-ol (HFIP) or ammonium hydroxide (NH₄OH) (Nichols et al., 2005a, 2005b; Ryan et al., 2013). Additionally, Lioudyno et al. (2012) reported that pretreatment with HFIP enhanced the amyloidogenicity of the A β ₄₂ peptide as well as its interaction with biological membranes.

It has been found that different conformation of A β ₄₂ peptide induces toxicity by distinct mechanisms in human cortical neurons (Kumar and Walter, 2011; Ladiwala et al., 2012). The longer variants have higher propensity to aggregation than the shorter form (Kumar and Walter, 2011). The mechanism of A β ₄₂ toxicity is still unknown, although it is suggested that amyloidogenic protein aggregates on neural cells cause permeabilisation of lipid membranes, (Gella and Durany, 2009; Evangelisti et al., 2013; Poojari et al., 2013), increase oxidative stress, (Mattson and Goodman, 1995; Nakamura et al., 2007) mitochondrial dysfunction, (Cali et al., 2011; Ferreiro et al., 2012; Selfridge et al., 2013) and endoplasmic reticulum stress (Huang et al., 2007; Umeda et al., 2011) which ultimately leads to apoptosis.

Previous publications have reported that yeast exhibit some responses to A β ₄₂ peptide suggesting it is a relevant model for kinetic studies (reviewed in Porzoor and Macreadie, 2013). However, there is discrepancy in the outcome of results generated

from studies on the effect of exogenous A β ₄₂ on yeast cells. Further, Chacińska and colleagues (Chacińska et al., 2002) showed an induction of proliferation in the presence of synthetic A β ₄₂ in exponentially growing *Saccharomyces cerevisiae*, while findings by Bharadwaj and colleagues (2008), showed toxicity of synthetic A β ₄₂ peptide using a different preparation method on *Candida glabrata* cells. Methodological differences in peptide preparations may explain these differing results, but there is still a lack of explanation and questions remain on the suitability of yeast as a model for extracellular toxicity studies of A β ₄₂.

Chacińska and colleagues (2002) used *S. cerevisiae* and dissolved the peptide in DMSO whereas Bharadwaj and colleagues (2008) used *C. glabrata* and dissolved the peptide in 20 mM of sodium hydroxide (NaOH). In order to demonstrate whether the solvent or the yeast species affects the outcomes such as those seen in previous publications, this chapter examines these variables and suitability of toxicity studies using chemically-synthesised A β ₄₂. Two main methods of A β ₄₂ pretreatment are analysed and the results compared with mice neuronal tissue culture. The effect of exogenous A β ₄₂ peptide in both exponential and stationary phase yeast cells and *C. glabrata* (ATCC90030) and *S. cerevisiae* (BY4743) are explored.

Alkyl hydroperoxide reductase 1 (*AHPI*) is a thiol peroxidase (TPx) and a member of peroxiredoxin (type II) family expressed in *S. cerevisiae* as a 19 kDa protein (Jeong et al., 1999; Lee et al., 1999; Wong et al., 2004). The *AHPI* protein (Ahp1p) has been identified as a defence mechanism against osmotic stress and oxidative damage

induced by lipid peroxidase (Iwai et al., 2010) and metal ion toxicity (Nguyen-nhu and Knoop, 2002). The primary site of catalysis in Ahp1 was identified as one conserved cysteine within TPx (Park et al., 2000). Accumulation of intracellular reactive oxygen species (ROS) which induces stress signals has implications in aging diseases (Lian et al., 2012). This chapter therefore examines the effect of Ahp1p in the cellular protection against A β ₄₂ induced cytotoxicity.

4.2 AIMS

- 1) Determine whether different pretreatment methods of synthetic A β ₄₂ peptide affect the survival of yeast cells
- 2) Determine the mechanism of the extracellular toxicity induced by A β ₄₂ in both *S. cerevisiae* and *C. glabrata*
- 3) Analyse the role of the *AHP1* protein (Ahp1p) in resistance to A β ₄₂ induced cytotoxicity

4.3 MATERIALS AND METHODS

S. cerevisiae and *C. glabrata* cells were grown to exponential and stationary phase according to Section 2.3.1. Stationary phase yeast cells were fractionated into quiescent and non-quiescent populations as described in Section 2.3.2. Viability of the yeast cells after treatments were determined as described in Section 2.3.3. Preparation of chemically-synthesised A β ₄₂ peptide solutions pretreated with NH₄OH and HFIP was done as described respectively in Section 2.7.2 and Section 2.7.3. Yeast cell survival in the presence of A β ₄₂ peptide pretreated with NH₄OH and HFIP was determined as described in Section 2.7.5. Survival of yeast cells was also estimated in the presence of DMSO and NaOH according to Section 2.7.6. Analysis of the effect of prolonged incubation of NH₄OH and HFIP pretreated A β ₄₂ peptide compared with the freshly prepared samples were performed using yeast cytotoxicity assays and transmission electron microscopy as described in Section 2.7.7 and Section 2.12.2 respectively.

Fluorescence associated with the thioflavin T binding to the cell walls, as well as A β ₄₂ aggregation propensity was quantified by flow cytometry and microscopy as described respectively in Section 2.6.3 and Section 2.11.6. The extent of self-aggregation and fibril formation of A β ₄₂ lyophilised with NH₄OH or HFIP and dissolved in either 60 mM NaOH or H₂O at 0 h (baseline) and after prolonged incubation (7 d) was characterised by SDS-PAGE (Section 2.10.1) followed by western blotting (with WO2 anti-A β antibody) as described in Section 2.10.4. The thiol-specific peroxiredoxin gene (*AHPI*) consisting of 531 bp was amplified by PCR from the genomic DNA sequence of *S. cerevisiae* S288C. This was done using the oligonucleotide primers (5'- 3') GCGCGAATTCATGTCTGACTTAGTTAACAA

and (5' - 3') GTCTTGGCTCATTGTAGAAGCTTGCG creating *EcoRI* and *HindIII* restriction sites for the PCR product (Section 2.4.2). The PCR product was cloned into the p416.GPD plasmid as described in Section 2.4. Yeast cells were transformed with the plasmids according to Section 2.5.2. Cytotoxicity of HFIP pretreated A β ₄₂ peptide on WT *S. cerevisiae*, *ahp1* strain and a transformant overexpressing the *AHP1* gene was determined as described in Section 2.7.5. The potency of NH₄OH pretreated A β ₄₂ peptide batch was tested on murine primary mixed neuronal culture (PC12) by analysis of lactate dehydrogenase (LDH) to determine cytotoxicity and MTT assays described in Section 2.7.8. All of the experiments were conducted in triplicate as described in Section 2.14.

4.4 RESULTS

4.4.1 Effect of solvents on the survival of yeast

In order to examine the effect of solvents that were used for dissolving lyophilised A β ₄₂ in previous studies (Chacińska et al., 2002; Bharadwaj et al., 2010) on the survival of yeast, both DMSO and 20 mM NaOH were examined on exponentially growing *S. cerevisiae* (BY4743) and *C. glabrata*. The amount of added solvent was equivalent to the level that is required to conduct the toxicity assays using chemically-synthesised A β ₄₂. Analyses of data indicated that BY4743 was not significantly affected by NaOH, even at 2 mM final concentration (Figure 4-1A). In fact, BY4743 proved to be resistant to the effect of DMSO even at the concentration of 10% (Figure 4-1B). The level of DMSO for the treatment of the yeast is usually kept to less than 1%.

The influence of solvents on the survival of *C. glabrata* was different to that of *S. cerevisiae*. The data analyses revealed that *C. glabrata* was more susceptible to the effect of both solvents with cytotoxicity exhibited with 400 μ M NaOH ($p < 0.01$; Figure 4-1C). The toxicity increased as 6 to 20 μ l of NaOH was added to the cell suspension (equivalent to final concentration of 600 μ M – 2 mM NaOH), ($p < 0.001$). The effect of DMSO on the survival of the *C. glabrata* was more profound as toxicity started at a concentration of 1% (2 μ l) (Figure 4-1D). As the DMSO level increased the percentage survival of *C. glabrata* declined, with 6 μ l causing 50% cell death (Figure 4-1D; $p < 0.001$).

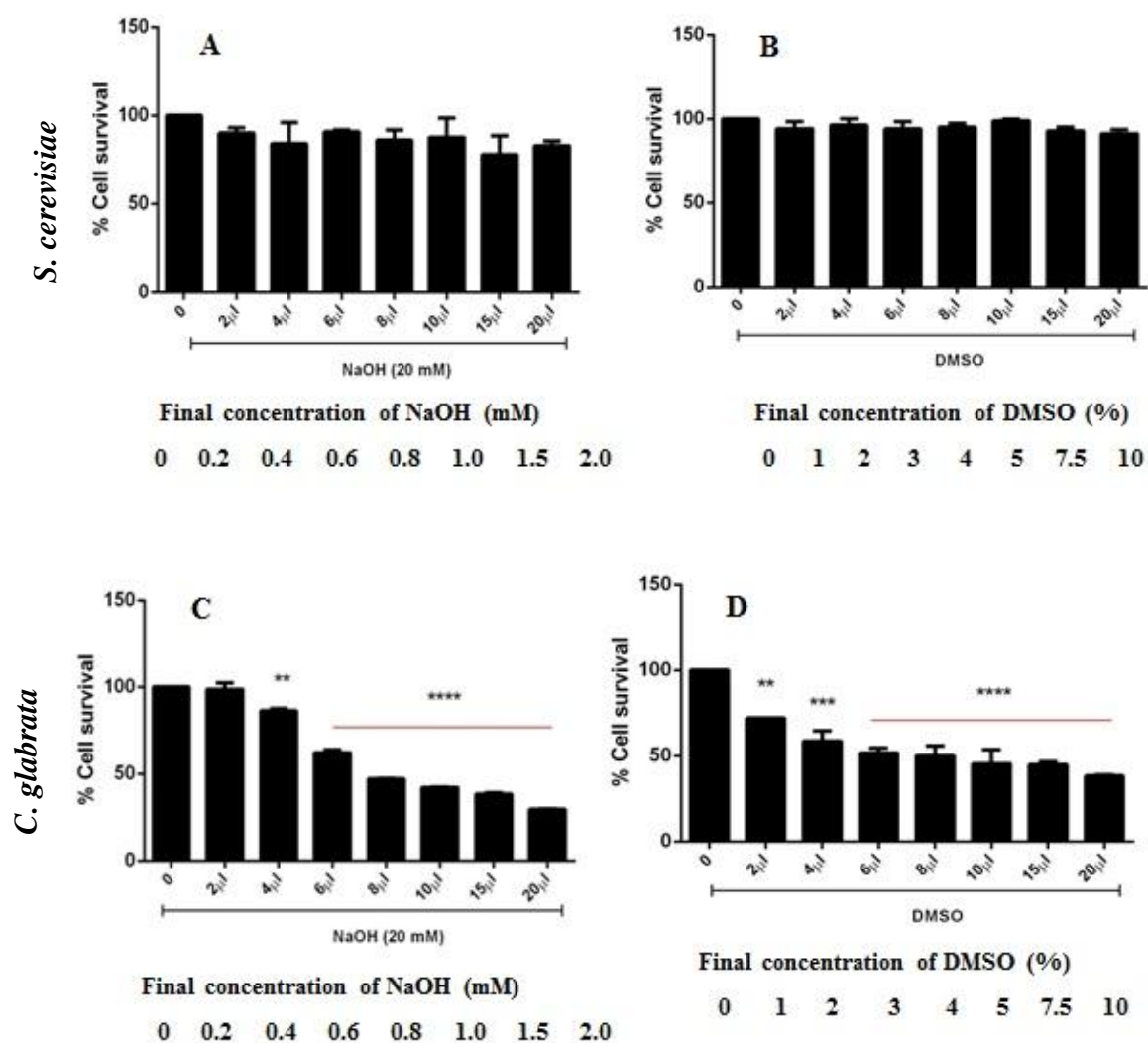


Figure 4-1 Effect of solvents on survival of *S. cerevisiae* and *C. glabrata*. Wild-type *S. cerevisiae* BY4743 and *C. glabrata* (ATCC90030) were grown to exponential phase and then washed and resuspended in H₂O (Section 2.7.7). BY4743 cells then were treated with 20 mM NaOH (A) or DMSO (B) to the final volume of 200 μ l. *C. glabrata* cells were treated with either 20 mM NaOH (C) or DMSO (D). Viability was determined by CFUs. (** $p < 0.01$, *** $p < 0.005$, **** $p < 0.001$). All data are expressed as mean \pm SEM.

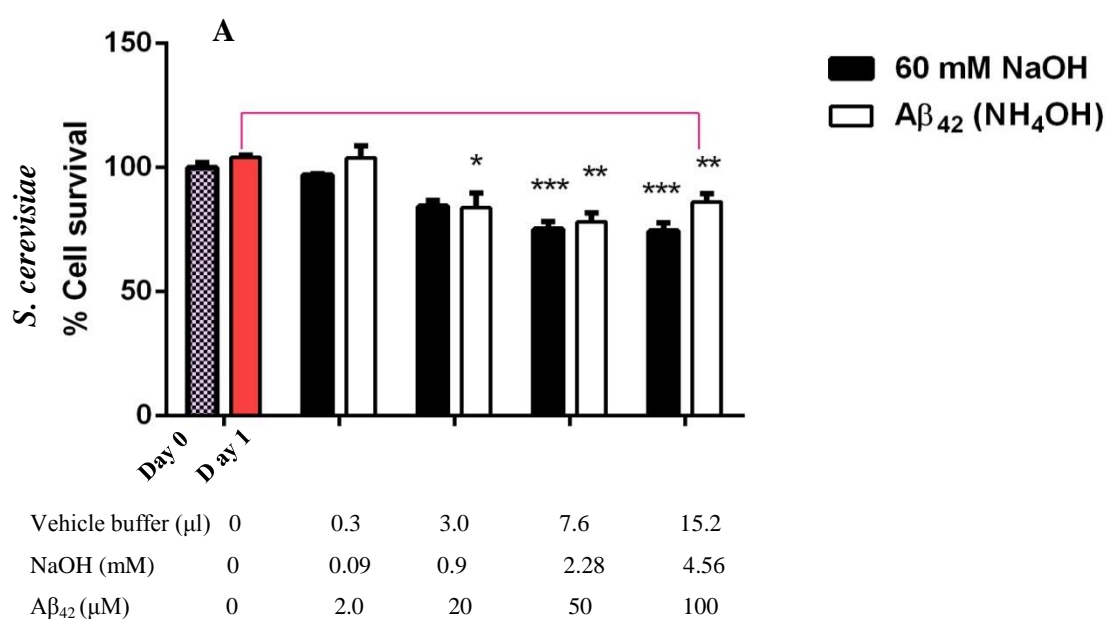
4.4.2 Effect of NH₄OH pretreated A β ₄₂ dissolved in 60 mM NaOH on exponential phase yeast cells suspended in H₂O

A study by Ryan et al. (2013) demonstrated that ammonium hydroxide (NH₄OH) treatment of A β ₄₂ results in aggregate free solutions that are more suitable for cell culture and biophysical investigations. The pretreated lyophilised peptide was then suspended in 60 mM NaOH for cytotoxicity investigations. In this experiment a similar peptide preparation (Section 2.7.3) was employed for analysis for its toxic effect on yeast.

Exponentially growing homozygous diploid BY4743 strain, the *AHP1* null mutant strain (*ahp1*), and *C. glabrata* were treated with NH₄OH pretreated A β ₄₂ dissolved in 60 mM NaOH and incubated overnight. Analyses of data indicated that the vehicle buffer itself contributes to toxicity in BY4743 with less killing observed in the presence of 50 and 100 μ M A β ₄₂ (Figure 4-2A). The peptide was ineffective at 2 μ M (Figure 4-2A) but it caused cell killing at > 20 μ M ($p < 0.05$). The cell killing in general was due to the vehicle buffer and not the A β ₄₂ peptide. The peptide provided some protection as seen by Dubey et al. (2009).

The *ahp1* mutant strain was sensitive to water with survival measured to ~32% in untreated control samples after overnight incubation in the absence of nutrients (Figure 4-2B). Although both vehicle buffer and peptide at high concentration proved to be lethal ($p < 0.005$) when compared to untreated control cells the next day, a greater cell survival was detected with lower concentration of 2 μ M A β ₄₂ and vehicle buffer (Figure 4-2B).

The A β ₄₂ treatment in *C. glabrata* resulted in proliferation (Figure 4-2C). The vehicle buffer caused killing which was significant in the presence of 15.2 μ l corresponding to 100 μ M of A β ₄₂ ($p < 0.005$). The treatment of peptide at 2, 20, and 50 μ M significantly increased percentage cell viability compared with untreated control samples ($p < 0.001$; Figure 4-2C). Interestingly these data implied that NH₄OH pretreated A β ₄₂ resulted in a peptide conformation that is not toxic to yeast cells, in particular *C. glabrata*.



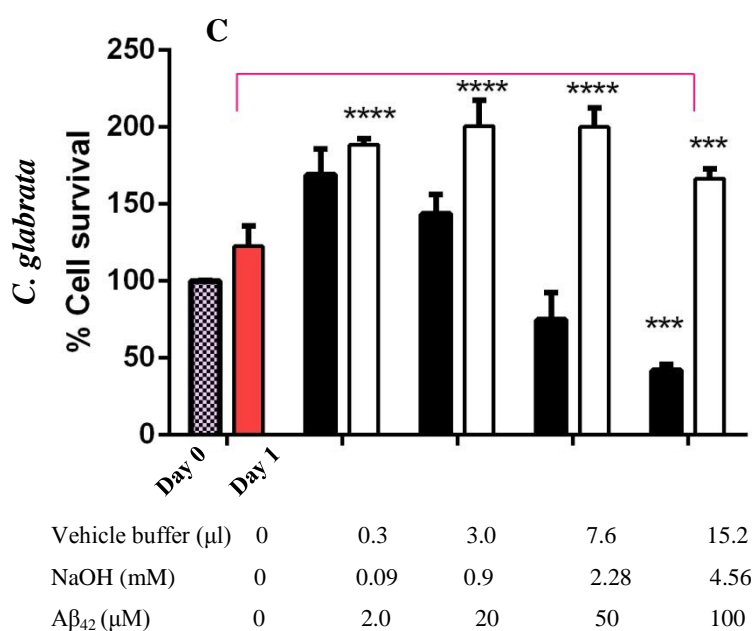
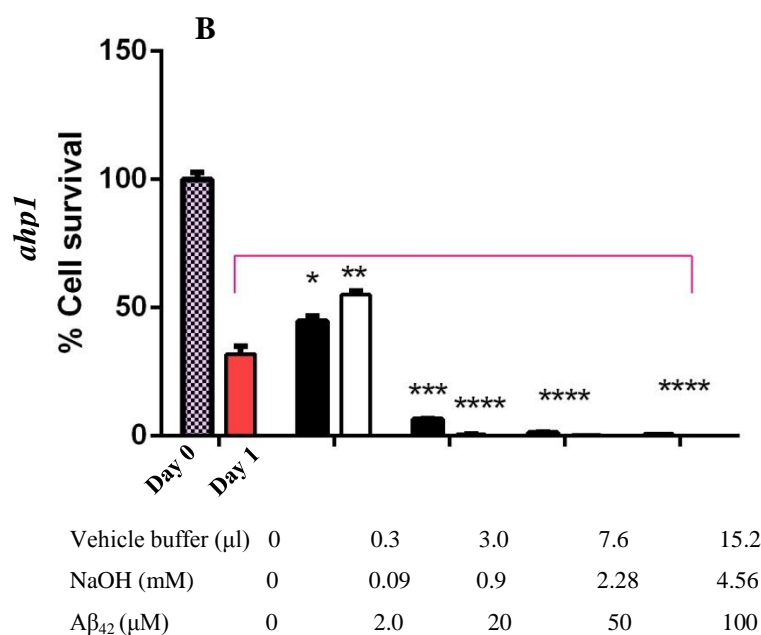


Figure 4-2 Effect of NH_4OH pretreated A β_{42} dissolved in 60 mM NaOH on exponential phase yeast. *S. cerevisiae* (A) *ahp1* (B) *C. glabrata* (C) were grown to exponential phase, then washed and resuspended in H_2O . Cells were counted using a haemocytometer and resuspended at a concentration of 10^2 cells per $100 \mu\text{l}$. NH_4OH pretreated A β_{42} dissolved in 60 mM was used for treatment of yeast cells to a final concentration of 2, 20, 50 and $100 \mu\text{M}$ of peptide in $200 \mu\text{l}$ cell suspension in a 96 well microtiter plate. Vehicle control samples (60 mM NaOH) corresponding to the amount used in treatments were also included. Samples were incubated overnight at 30°C . Viability was calculated by counting the number of colonies formed and expressed as a percentage of untreated control samples. (**** $p < 0.001$, *** $p < 0.005$, ** $p < 0.01$, * $p < 0.05$). All data are expressed as mean \pm SEM.

4.4.3 Effect of NH₄OH pretreated A β ₄₂ dissolved in 60 mM NaOH on quiescent and non-quiescent *C. glabrata* cells

Analysis of data in Section 4.4.1 indicated that NH₄OH pretreatment of A β ₄₂ dissolved in 60 mM NaOH might generate conformational changes in the peptide which induced proliferation in exponential phase *C. glabrata*. In order to determine whether this proliferation effect is unique to exponential phase cells, the stationary phase *C. glabrata* cells were also examined. Stationary *C. glabrata* cells were fractionated into quiescent and non-quiescent populations according to the method described in Section 2.3.2. The peptide treatment resulted in cell proliferation in both cell fractions (Figure 4-3). Although, there was no significant differences between the A β ₄₂ treated samples compared to untreated control in the quiescent cells (Figure 4-3A), the survival rate was significant when compared with the corresponding vehicle buffer controls. Further, the vehicle buffer was toxic to quiescent cells at the levels corresponding to 20 μ M ($p < 0.005$), 50 μ M and 100 μ M ($p < 0.001$) of peptide (Figure 4-3A).

The non-quiescent cells seemed to be more sensitive as the percentage survival decreased overnight ($p < 0.01$) in the absence of nutrients in untreated control samples (Figure 4-3B). These cells were also more susceptible to the toxic effect of NaOH, with the vehicle buffer proving to be lethal at the lowest concentration and causing significant cell killing. Compared with the vehicle control buffer, although the percentage viability significantly declined in the A β ₄₂ treated samples, these effects were not significant when compared with the vehicle control buffer samples (Figure 4-3B). These data suggest that the conformational changes produced by pretreatment of A β ₄₂ with NH₄OH results in proliferation in the stationary phase *C.*

glabrata. Also, non-quiescent cells are more prone to any environmental changes compared with quiescent cells as a decline in the survival of the untreated samples was observed.

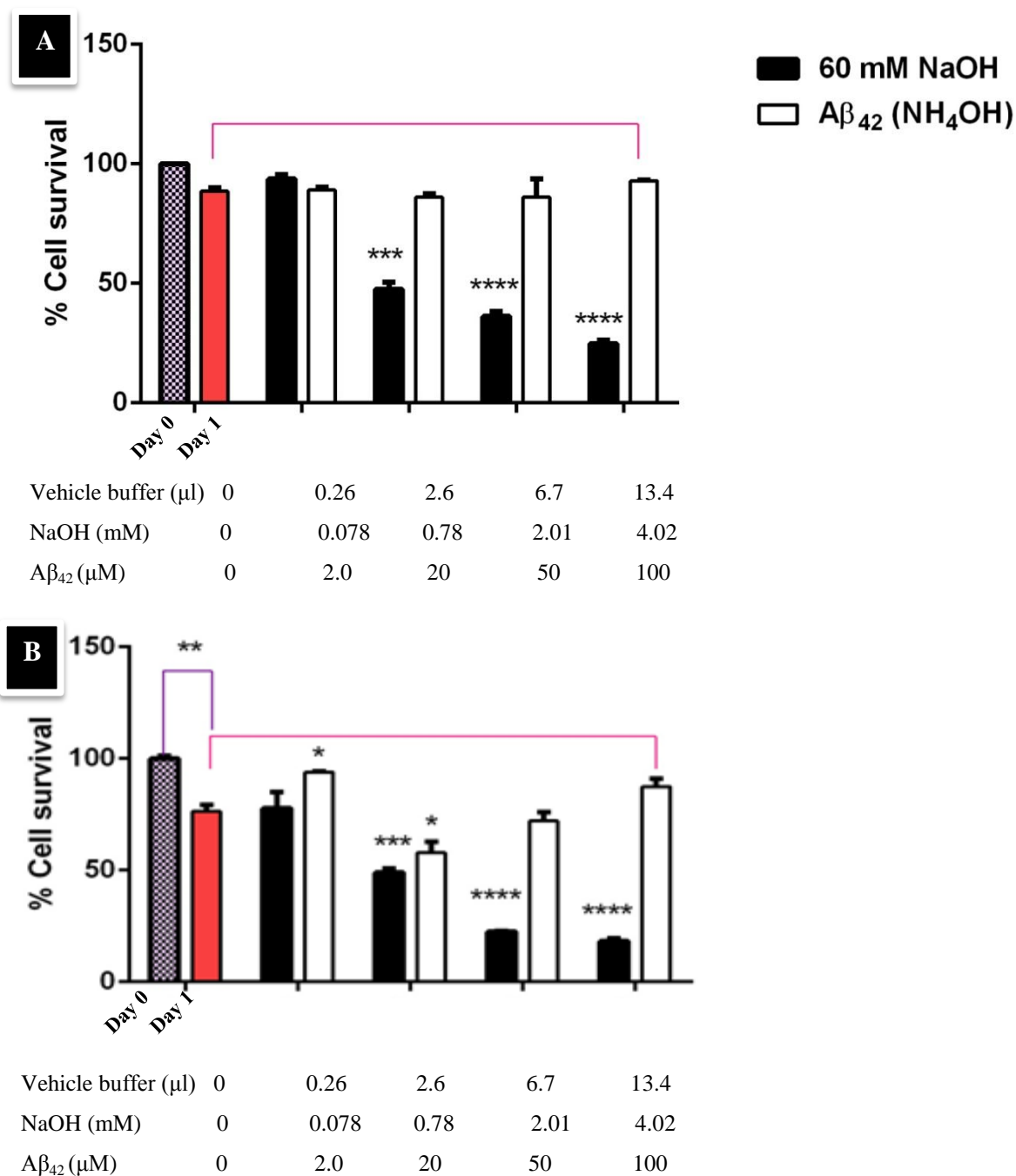


Figure 4-3 Effect of NH₄OH pretreated Aβ₄₂ dissolved in 60 mM NaOH on the survival of stationary phase *C. glabrata*. Cell fractions of quiescent (A) and non-

quiescent (B) were suspended in H₂O and treated with 2, 20, 50 and 100 μM of Aβ₄₂ peptide to a final volume of 200 μl in a 96 well microtiter plate. Vehicle control samples (60 mM NaOH) corresponding to the amount used in treatments were also included. (**** $p < 0.001$, *** $p < 0.005$, ** $p < 0.01$, * $p < 0.05$). All data are expressed as mean \pm SEM.

4.4.4 Effect of NH₄OH pretreated synthetic Aβ₄₂ on *C. glabrata* cells suspended in PBS

To determine the effect of NH₄OH pretreated synthetic Aβ₄₂ on *C. glabrata* cells without the interference of the solvent (Section 4.4.2), it was hypothesised that using a biological buffer such as PBS to suspend the cells might create more suitable conditions. In addition, NaOH at a concentration greater than 600 μM proved to be toxic to *C. glabrata* cells as shown previously (Figure 4-1C). Therefore, exponential phase cells were suspended in phosphate buffered saline (PBS) instead of H₂O to overcome the toxicity induced by sodium hydroxide related with Aβ₄₂ peptide. Control samples for vehicle buffer (20 mM NaOH) were also included. Interestingly, the buffer caused > 6 fold increase in the number of viable cells after 24 h incubation (Figure 4-4). However, the NaOH proved to be inhibitory to cells even in the presence of buffer. Addition of 8.3 μl ($p < 0.01$) and 16.6 μl ($p < 0.001$) NaOH resulted in significant decline in viability. Addition of the peptide on the other hand induced proliferation from 2-100 μM ($p < 0.001$) with a > 10-fold increase in cell viability (Figure 4-4).

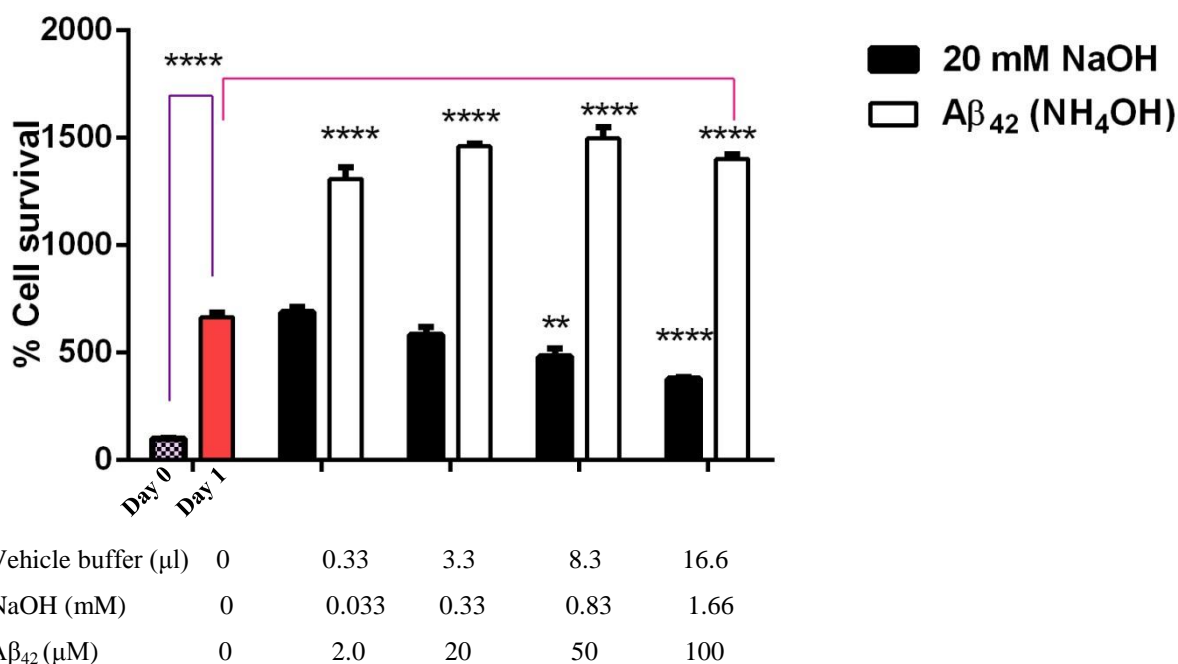


Figure 4-4 Effect of synthetic Aβ₄₂ preparation using the NH₄OH method on *C. glabrata* cells suspended in buffer (PBS). *C. glabrata* cells were grown to exponential phase, then pelleted and washed with H₂O. A haemocytometer was used to resuspend cells at a concentration of 10² cells per 100 μl in PBS buffer. NH₄OH pretreated Aβ₄₂ dissolved in 20 mM NaOH and was used at concentrations of 2, 20, 50, and 100 μM for treatment of the cells suspended in buffer. Control samples for vehicle buffer were also included. Suspension of cells in buffer induced proliferation after 24 h incubation. Although, there was a significant decrease in the rate of proliferation in the presence of higher concentrations of NaOH, the peptide treatment resulted in greater cell proliferation when compared with the vehicle control buffer. (**** $p < 0.001$, ** $p < 0.01$). All data are expressed as mean ± SEM.

4.4.5 Effect of NH₄OH pretreated Aβ₄₂ on PC12 neuronal cells

In order to demonstrate that the proliferation effect of NH₄OH pretreated Aβ₄₂ dissolved in 60 mM NaOH on yeast cells (Section 4.4.1 and Section 4.4.2) is not due to the preparation method or defect in the existing peptide batch itself, samples were tested for their potency on rat pheochromocytoma cell culture. The effectiveness of pretreated peptide samples used in these studies was also compared with those prepared in another laboratory (CSIRO). The synthetic Aβ₄₂ peptide was purchased from Keck laboratories (Yale University, New Haven, CT) in the form of lyophilized

powder. The tissue culture experiment was performed by Dr. Julie Nigro at CSIRO (Parkville, Vic, Australia).

All A β ₄₂ preparations significantly reduced ($p < 0.01$) the viability of neuronal cells to ~70% compared with the untreated and vehicle control samples (Figure 4-5A). 0.1% Triton™ X-100 detergent was used as a positive cytotoxicity control. The viability results of the peptide preparations at 10 μ M and 20 μ M concentrations were similar for both laboratories with no significant difference in the potency level. Four to 6 % increase in cytotoxicity was detected in the presence of A β ₄₂ peptide measured by the LDH level (Figure 4-5B). This cytotoxicity was significant in the presence of the A β ₄₂ peptide aliquots prepared in both laboratories ($p < 0.001$) compared with the untreated control samples (Figure 4-5B). Interestingly, at 20 μ M the peptide preparation from RMIT resulted in higher toxicity compared to CSIRO respectively 6.0% and 3.7% (Figure 4-5B). This further confirms the suitability of the peptide batch in the effect of the NH₄OH pretreated peptide on yeast cells compared with neuronal cells.

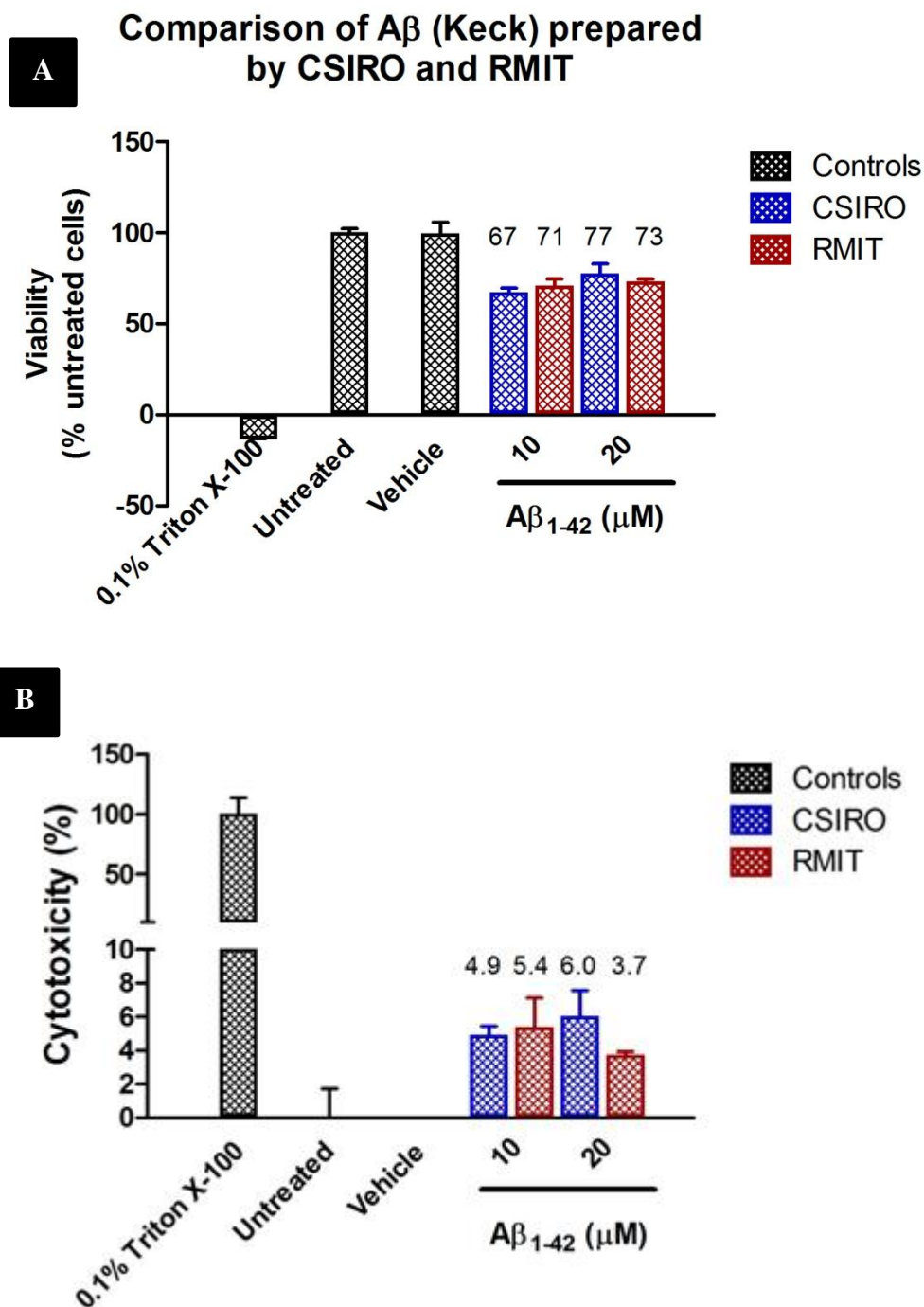


Figure 4-5 Comparison effect of NH₄OH pretreated A β ₄₂ peptides stocks from two laboratories on the survival of PC12 cells. Viability of PC12 cells was assessed by MTT assay (A). The cytotoxicity level was measured by LDH method (B). 0.1% (v/v) Triton™ X-100 was used as positive toxin control (maximum LDH release). Cell viability decreased in the presence of both peptide stock provided by RMIT and CSIRO. The assays indicate that the A β ₄₂ preparations reduce the cell viability to ~70% and increase cytotoxicity by ~4-6% (Dr. Julie Nigro).

4.4.6 Effect of HFIP pretreated A β ₄₂ dissolved in H₂O on exponentially phase growing *S. cerevisiae*

A study by Bharadwaj and colleagues (2008) reported that HFIP pretreated A β ₄₂ can induce toxicity in exponential phase *C. glabrata*. The effect of this pretreatment method however has not yet been investigated in *S. cerevisiae*. In view of further investigating the mechanism underlying the toxicity initiated by A β ₄₂, exponentially growing cells were suspended in H₂O and treated with HFIP pretreated A β ₄₂ peptide dissolved in H₂O. By dissolving both peptide and yeast cells in water any influence of the vehicle buffer was eliminated and the pH for these treatments were found to be neutral (pH = ~7).

Unlike the NH₄OH pretreated A β ₄₂ peptide, the HFIP pretreated A β ₄₂ caused a significant decline in viability ($p < 0.001$) with concentrations as low as one μ M (Figure 4-6). The cell survival rate declined to ~90% in the presence of 4 μ M A β ₄₂ peptide and at 10 μ M there was 99% cell death. These findings show that peptide preparation can determine yeast survival fate.

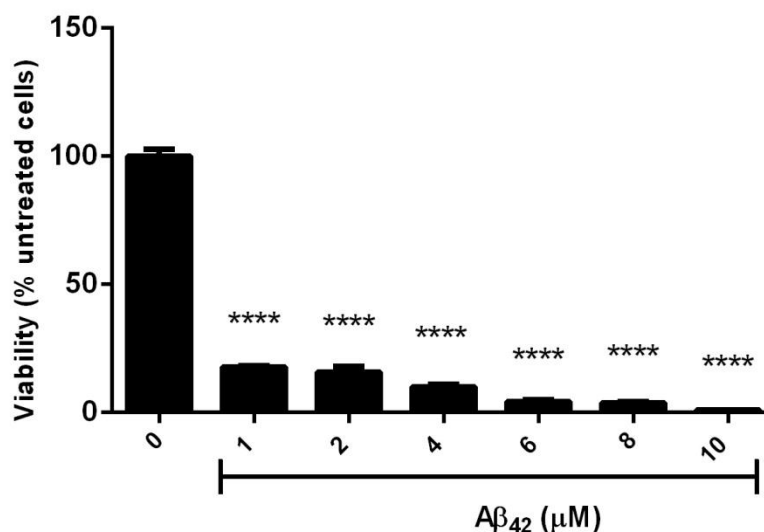


Figure 4-6 Viability studies of *S. cerevisiae* in the presence of HFIP pretreated Aβ₄₂ dissolved in H₂O. Effect of synthetic Aβ₄₂ peptide prepared by the HFIP method and dissolved in H₂O was investigated on exponentially growing BY4743. Cells were treated with the peptide and incubated for 24 h at 30°C. (**** $p < 0.001$). All data are expressed as mean \pm SEM.

4.4.7 Survival of quiescent and non-quiescent *C. glabrata* in the presence of HFIP pretreated Aβ₄₂ dissolved in H₂O

As mentioned in the previous section (Section 4.4.5), the effect of HFIP pretreated Aβ₄₂ peptide has been studied in exponential phase *C. glabrata* cells while the effect on stationary cells remained unknown. In order to further explore the cytotoxicity of Aβ₄₂ and confirm growth phase dependence, stationary phase *C. glabrata* were examined here. Quiescent and non-quiescent fractions of *C. glabrata* were tested for their susceptibility to 2 μM Aβ₄₂ peptide generated by HFIP pretreatment dissolved in H₂O. Cell fractions of quiescent and non-quiescent cells were then suspended in H₂O and treated with the peptide to a final concentration of 2 μM. Samples were incubated overnight at 30°C. Viability was determined based on survival of cells on YEPD solid media after 48 h incubation. Results indicated that quiescent cells (Figure 4-7A)

were more resistant to the toxic effect of $A\beta_{42}$ than older non-quiescent cells (Figure 4-7B). The older cells lost their viability within the first 24 h ($p < 0.005$). This significant decline continued at 48 h ($p < 0.005$) in the presence of amyloid peptide. The quiescent cells however, were only affected by the toxicity after 48 h of incubation with HFIP pretreated $A\beta_{42}$ ($p < 0.005$). These outcomes demonstrated that quiescent cells are more resistant to $A\beta_{42}$ than non-quiescent cells.

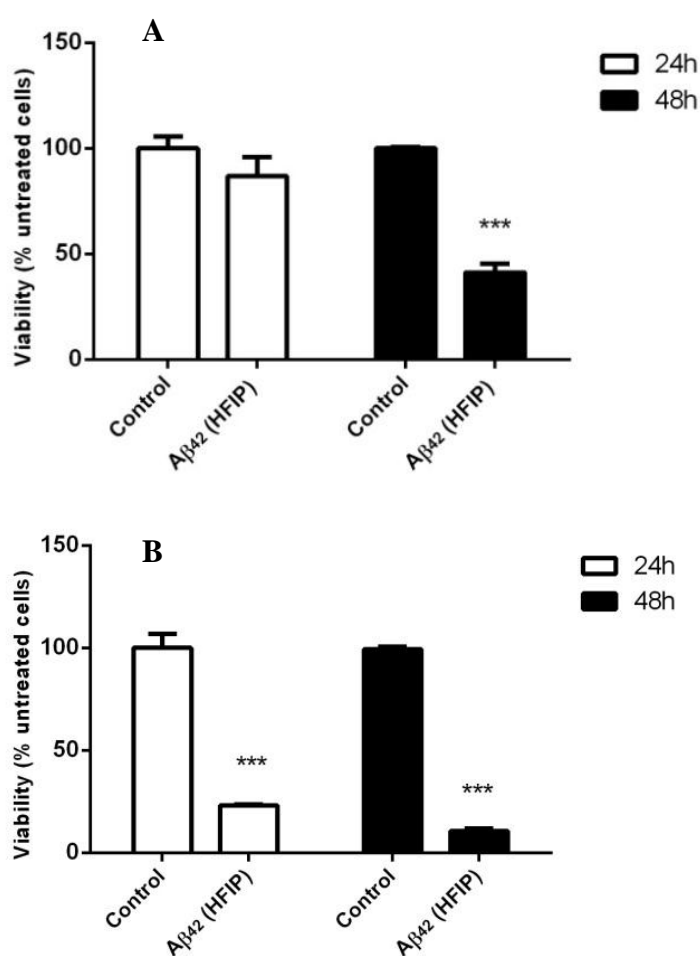


Figure 4-7 Cytotoxicity of HFIP pretreated $A\beta_{42}$ on the quiescent and non-quiescent *C. glabrata* cells. The quiescent daughter cells (A) and non-quiescent mother cells (B) were treated with 2 μ M of HFIP pretreated $A\beta_{42}$ and incubated for 48 h at 30°C. After 24 h incubation the viability was determined by plating 100 μ l of each sample on YEPD plates. Results indicated that quiescent cells were more resistant to the toxic effect of amyloid peptide prepared with the HFIP method than in the first 24 h of incubation. After 48 h of incubation both cell fractions were

susceptible to the toxicity effect of A β ₄₂ (***) $p < 0.005$). All data are expressed as mean \pm SEM.

4.4.8 Effect of synthetic A β ₄₂ preparation using the HFIP and NH₄OH methods dissolved in H₂O on exponential phase yeast cells

HFIP pretreatment of A β ₄₂ was previously shown to cause toxicity to *C. glabrata* cells (Bharadwaj et al., 2008). In this study the HFIP and NH₄OH pretreatment were compared to determine the effect on viability of the same yeast cultures over 48 h incubation periods. Also, in order to eliminate any effect as a result of solvent, all of the peptides were dissolved in water (pH = ~7). In addition, the effect of stress induced by the peptide was investigated by testing an *ahp1* mutant strain which is extremely sensitive to ROS elevation.

Exponentially growing wild-type BY4743, *AHP1* mutant strain (*ahp1*) and *C. glabrata* cells were harvested and suspended in H₂O. Cells were then treated with 2 μ M of HFIP or NH₄OH pretreated A β ₄₂ peptide and incubated at 30°C for 48 h. This study confirms significant toxicity of HFIP pretreated A β ₄₂ ($p < 0.001$) to *S. cerevisiae* (Figure 4-8 A, B) and *C. glabrata* (Figure 4-8C) after 24 h incubation. There was even more cell killing after 48 h of incubation. Conversely, NH₄OH pretreatment resulted in a significant increase in the number of cells in BY4743 ($p < 0.05$), *ahp1* ($p < 0.05$) and *C. glabrata* ($p < 0.01$) in the first 24 h (Figure 4-8). After 48 h incubation the *C. glabrata* cells more than doubled in number ($p < 0.001$; Figure 4-8C), and BY4743 (Figure 4-8A) numbers significantly increased over this time (p

<0.005). However, the *ahp1* mutant strain proved to be very sensitive, with the numbers declining in control samples after 48 h incubation in the absence of nutrients (Figure 4-8B). Comparing the viability of NH₄OH pretreated A β ₄₂ samples with those of controls, the cell number was higher in the presence of the peptide compared with the control sample (Figure 4-8B). The data provided thus far, strongly suggest that the effect of the A β ₄₂ peptide on yeast cells is not due to the peptide itself, rather the conformational changes generated through the pretreatment method. Also, the cytotoxicity or proliferation effect of the A β ₄₂ pretreatment method is not limited to the growth phase of cells.

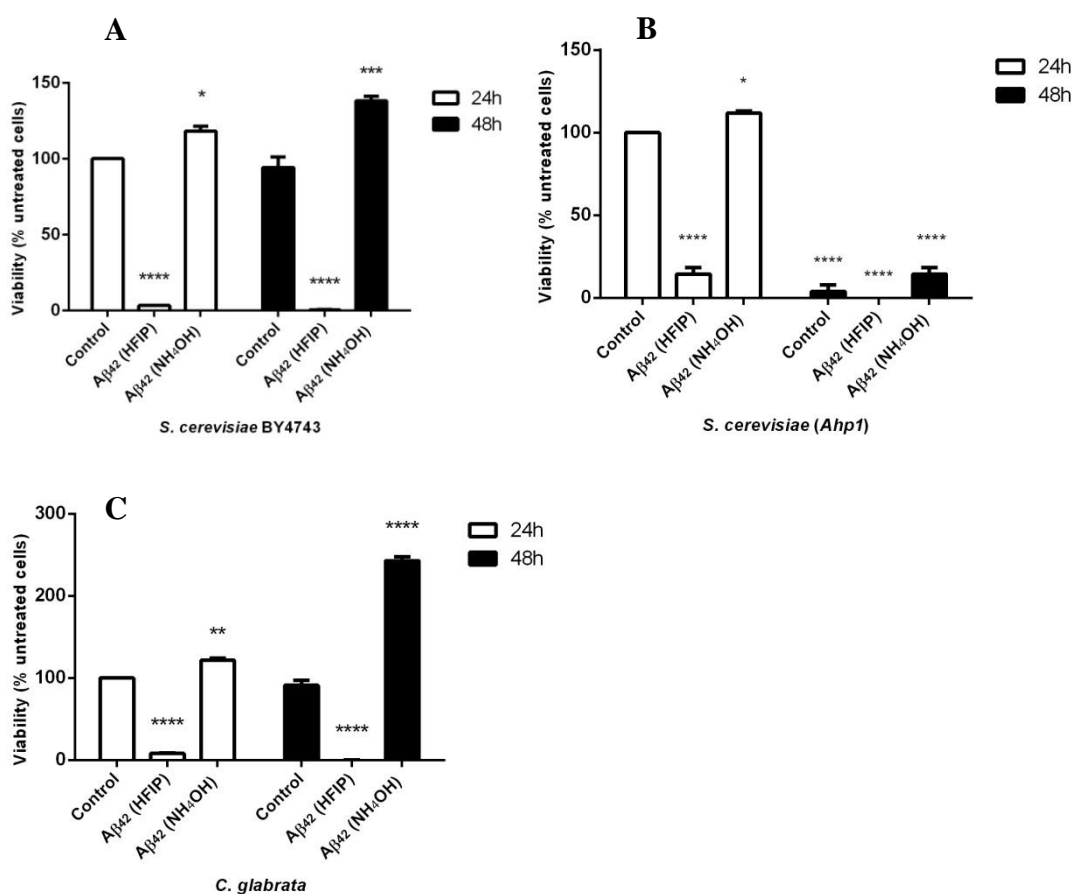


Figure 4-8 Effect of two preparation methods of synthetic A β ₄₂ dissolved in H₂O on yeast cells. 2 μ M A β ₄₂ peptide was added to exponential phase (A) *S. cerevisiae* WT (BY4743), (B) *ahp1* mutant and (C) *C. glabrata* (ATCC90030) suspended in water. Cell survival was determined after 24 and 48 h of incubation by transferring

100 μ l of samples onto YEPD solid media incubated at 30°C for 48 h. Viability was determined as a percentage of untreated cells (control). (* $p < 0.05$, ** $p < 0.01$, *** $p < 0.005$, and **** $p < 0.001$). Data are shown as mean \pm SEM.

4.4.9 Flow cytometry analysis of effect of A β ₄₂ peptide pretreated with HFIP or NH₄OH on *S. cerevisiae*

In section 4.2.7, it was identified that HFIP pretreated A β ₄₂ results in toxicity whereas NH₄OH pretreatment of the same peptide caused proliferation in *S. cerevisiae*. Also, according to previous findings yeast cells exhibit amyloidogenic proteins on their cell walls with capability to bind to Thioflavin T dye (ThT) (Kalebina et al., 2008; Ramsook et al., 2010; Bezsonov et al., 2013). Therefore, in this experiment exponentially growing BY4743 cells incubated in the presence and absence of 5 μ M of A β ₄₂ pretreated with HFIP and NH₄OH were stained with 20 μ M ThT and analysed by flow cytometry. ThT binding has been associated with peptide that has aggregation and amyloidogenic propensity and is routinely used for identification of A β ₄₂ aggregates and fibrils. Therefore, by comparing the fluorescent intensity (FI) of each sample it is possible to predict the amyloidogenic capacity of each pretreatment.

The FI associated with ThT level on the surface of the yeast cells treated with HFIP and NH₄OH amyloid peptide was calculated. These results showed an increase in FI in the presence of HFIP pretreated peptide (Figure 4-9C) compared with the NH₄OH method (Figure 4-9D), and untreated controls (Figure 4-9A) with values of 8.4%, 5.4% and 3.7% respectively. Interestingly these results suggest that the peptide conformation generated as a result of HFIP pretreatment has more propensity to induce aggregation and causes amyloid deposition on the surface of yeast cell walls.

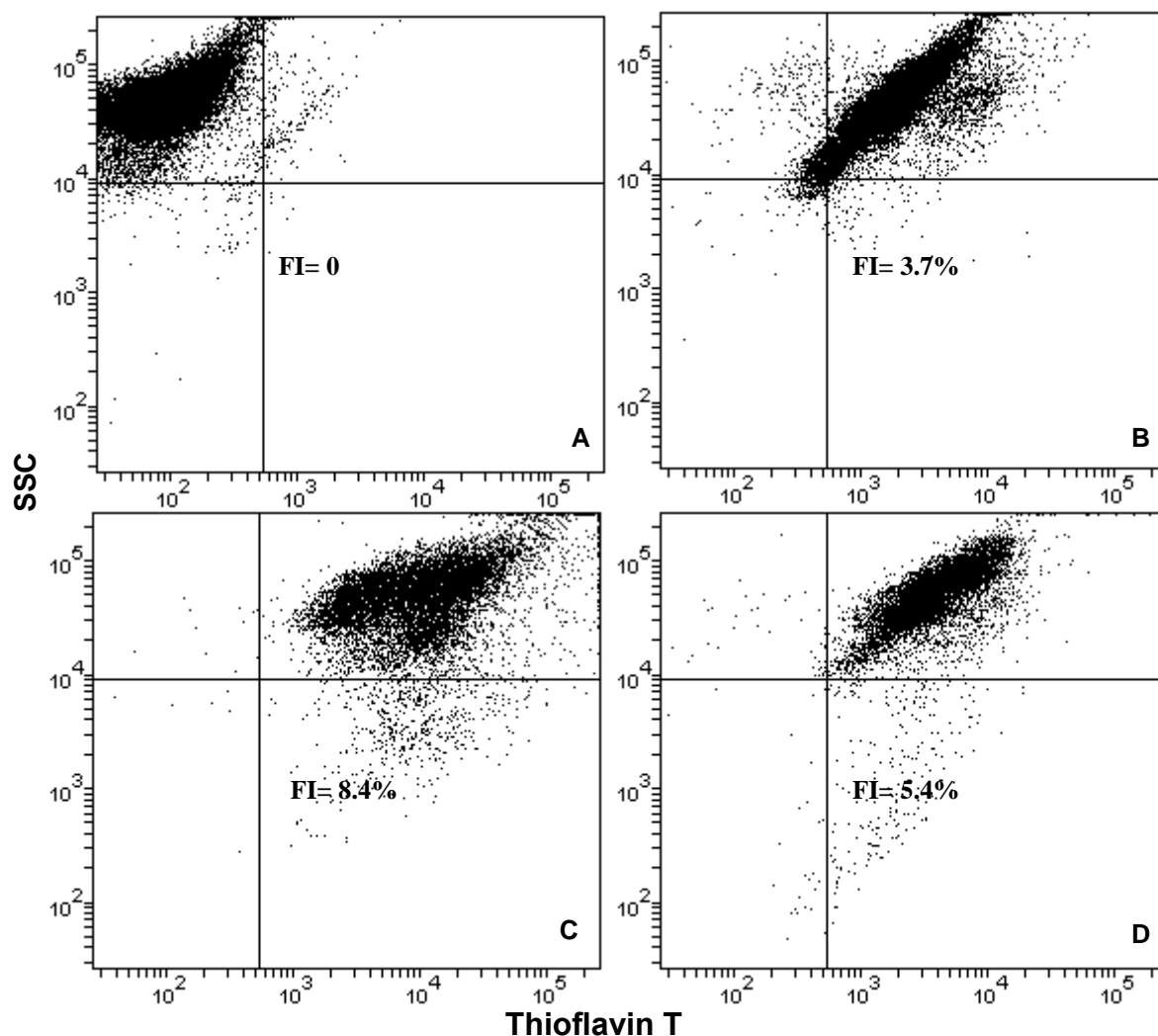


Figure 4-9 Flow cytometry analysis of *S. cerevisiae* treated with HFIP and NH_4OH prepared $\text{A}\beta_{42}$. The fluorescent intensity (FI) of ThT in the experimental samples was determined as a percentage of unstained cells. Yeast cells were grown to exponential phase and were washed and resuspended in H_2O . Cells were then treated with HFIP and NH_4OH pretreated $\text{A}\beta_{42}$ and incubated overnight along with control (untreated samples) at 30°C with shaking. The next day, cells were treated with $20\ \mu\text{M}$ ThT and were analysed by flow cytometry. A pacific blue filter was chosen to measure fluorescence. Unstained control cells (A), ThT stained control cells (B) and those treated with $5\ \mu\text{M}$ of HFIP (C), and NH_4OH pretreated $\text{A}\beta_{42}$ are shown.

4.4.10 Microscopic analysis of amyloidogenic proteins on the surface of *S. cerevisiae* and their aggregation propensity in the presence of HFIP and NH₄OH pretreated A β ₄₂

In order to examine the presence of amyloidogenic proteins on the surface of yeast cells, ThT treated cells were visualised with a confocal microscope under a DAPI filter. Untreated control samples of *S. cerevisiae* exhibited the presence of high levels of amyloid proteins on their surface visualised by ThT dye (Figure 4-10A). Treated samples with the HFIP method of A β ₄₂ on the other hand revealed more cell aggregation propensity, causing the cells to adhere and attach to each other (Figure 4-10A). This aggregation of cells was missing in those cells treated with NH₄OH pretreated A β ₄₂ (Figure 4-10A). These results indicated that peptide conformation produced by each method of preparation interacts differently with the yeast cell walls. Also, after prolonged incubation, the shape of *S. cerevisiae* cells treated with the HFIP pretreated A β ₄₂ was different to those of NH₄OH A β ₄₂ pretreated and control samples (Figure 4-10B). This demonstrated that A β ₄₂ peptide pretreated with HFIP interacts differently with the cells compared with the peptide pretreated with NH₄OH and results in loss of cell wall integrity (Figure 4-10B).

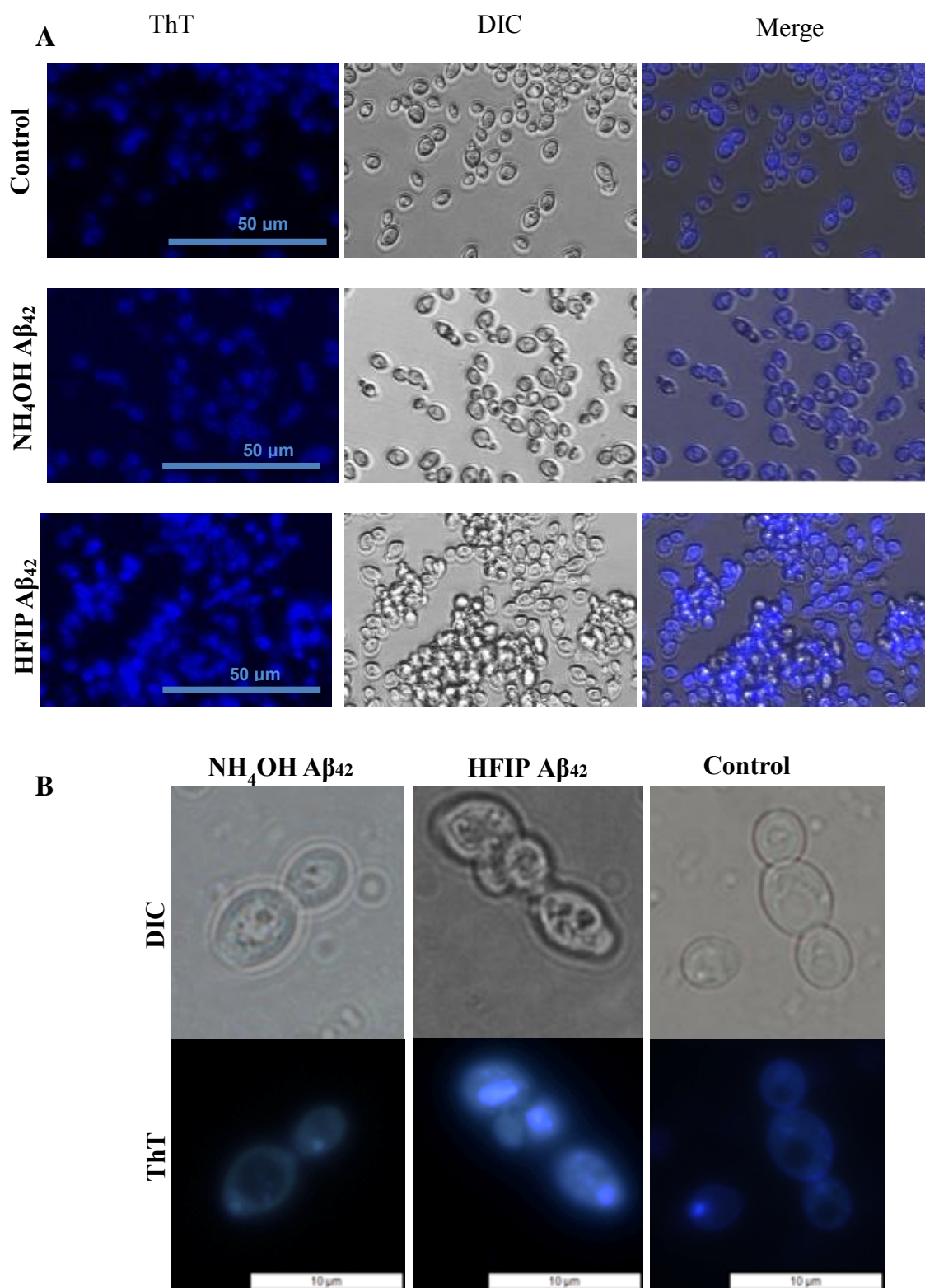
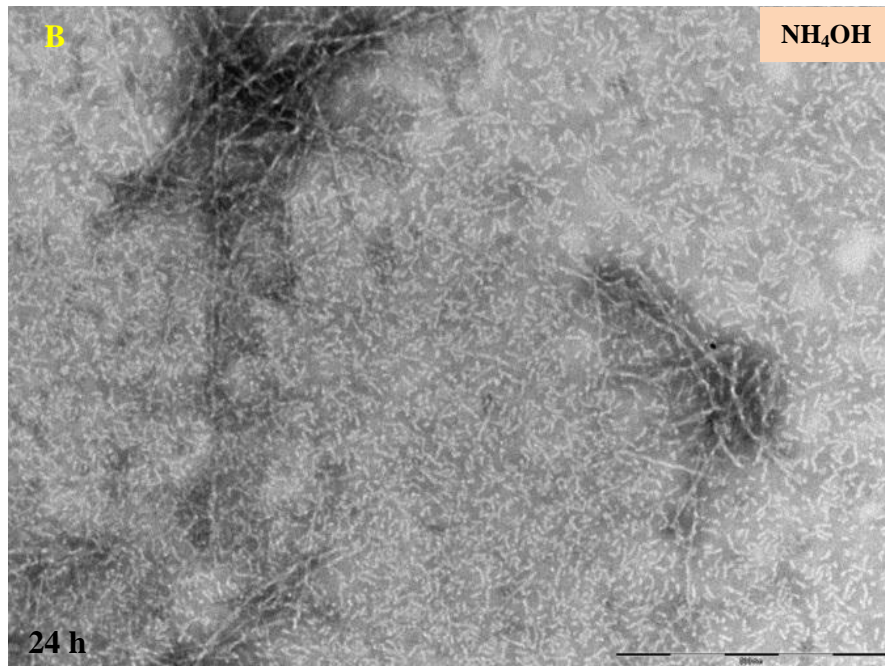
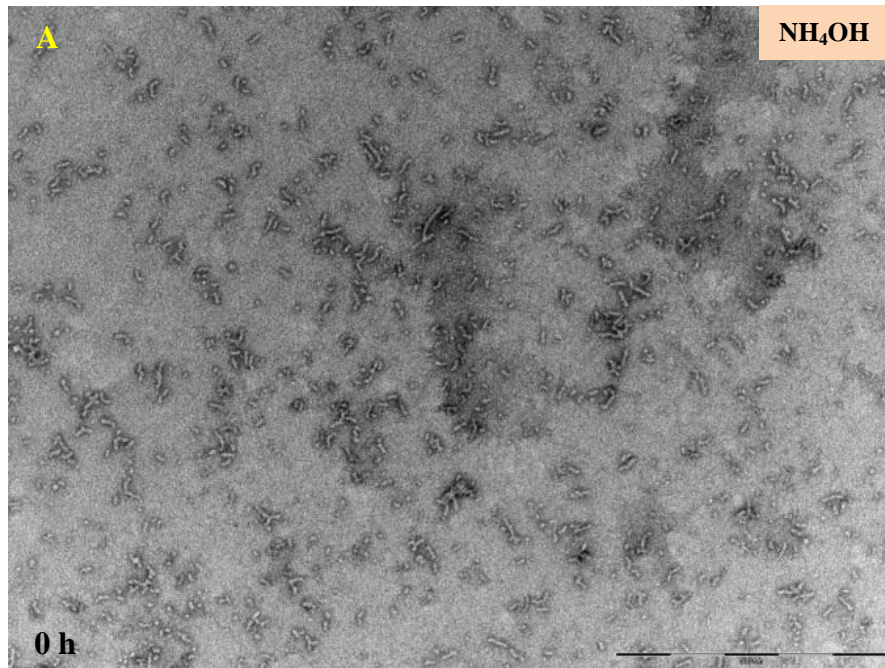


Figure 4-10 Microscopic analysis of Thioflavin T treated *S. cerevisiae*. (A) The ThT attaches to the amyloidogenic proteins that are present on the cell walls of yeast cell. First panels shows untreated *S. cerevisiae* cells in presence of ThT in comparison with cells treated with 5 μ M NH₄OH (middle panels) and HFIP (last panels) prepared A β ₄₂ for 24 h in H₂O. Scale bars indicate 50 μ m. (B) microscopic images of the *S. cerevisiae* cells treated with HFIP and NH₄OH pretreated A β ₄₂ compared with the control. Scale bars indicate 10 μ m.

4.4.11 TEM analysis of A β ₄₂ peptide conformers generated by pretreatment

The A β ₄₂ solutions that were prepared for biological assays on yeast cells were further analysed by TEM to explore their morphological characteristics. HFIP and NH₄OH pretreated A β ₄₂ dissolved in H₂O were visualised immediately after preparation (0 h) and after 24 h incubation. Extensive analysis of TEM micrographs revealed that the NH₄OH method results in more uniform solutions with undetectable fibrils (Figure 4-11A) compared with HFIP pretreated samples at 0 h (Figure 4-11C). The HFIP treated samples showed the presence of protofibrils and short and long fibrillar structures even after immediate preparation (0 h). After 24 h incubation at 37°C, morphological differences as result of peptide pretreatments became more apparent. Although peptide preparations with both methods generated fibrillar structures their morphology differed (Figure 4-11B, D). Short fibrils were observed in NH₄OH pretreated peptide (Figure 4-11B) whilst, the HFIP method (Figure 4-11D) was associated with formation of long and twisted fibrillar morphology (Figure 4-11E).



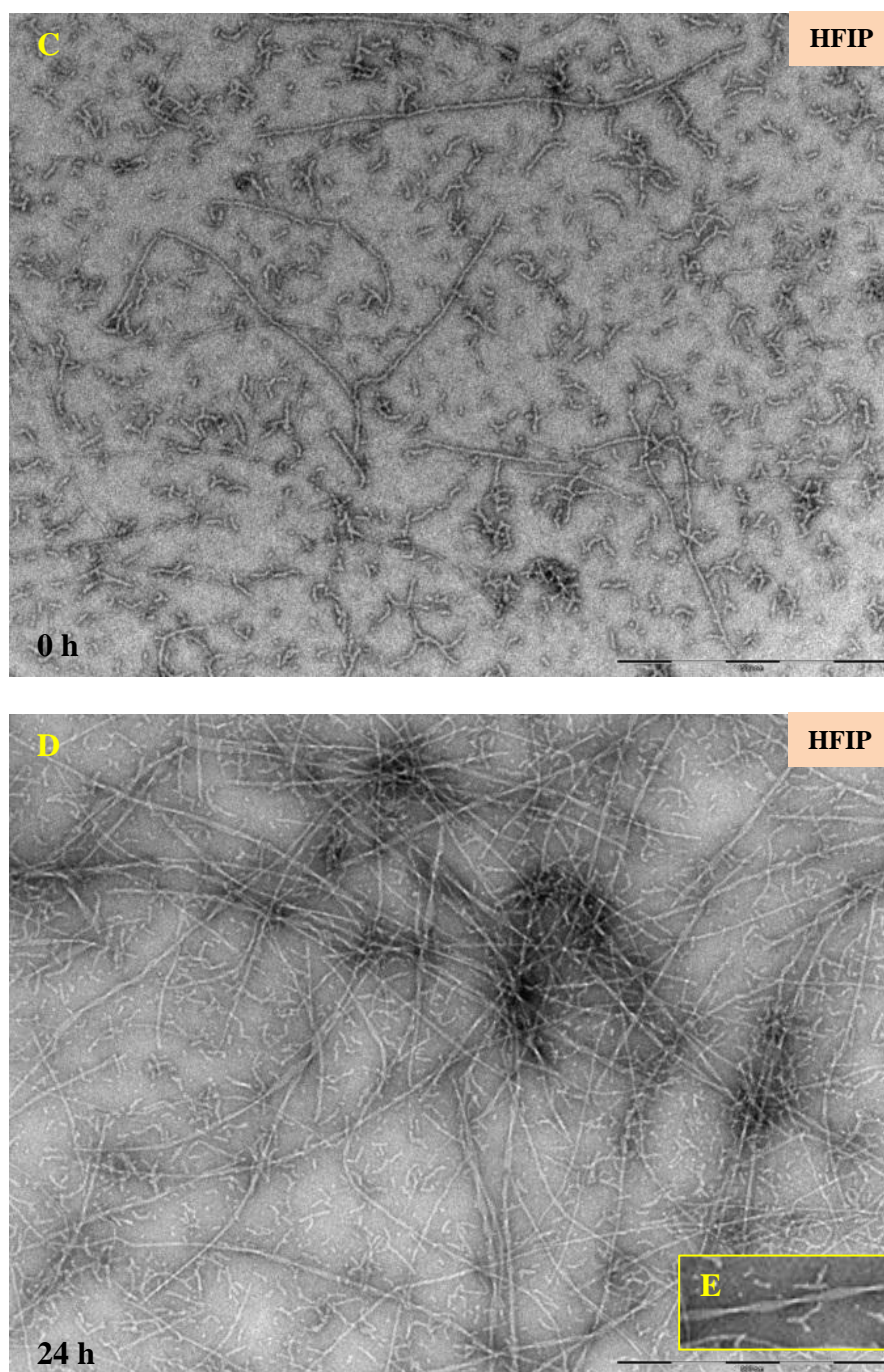


Figure 4-11 TEM micrograph of conformational changes in synthetic A β ₄₂ prepared by HFIP and NH₄OH methods. Samples of NH₄OH pretreated A β ₄₂ after preparation (0 h) (A) and after 24 h incubation (B) were compared with the HFIP pretreated A β ₄₂ (C) and 24 h after incubation (D) at 37°C with no shaking. The HFIP pretreated A β ₄₂ formed twisted fibrillar structures (E). (Scale bar = 200 nm)

4.4.12 Effect of prolonged incubation of A β ₄₂ peptide on *S. cerevisiae* cells

Analyses of cytotoxicity screening in Section 4.4.7 revealed that pretreatment of A β ₄₂ peptide is the major determinant for the extent of its toxic behaviour and its overall interaction with the yeast cells. Also, visualisation of the A β ₄₂ conformers by TEM described in 4.4.10 suggested that HFIP pretreatment accelerated self-aggregation and fibril formation compared with the NH₄OH method. Therefore, it was hypothesised that high molecular weight oligomers and fibrillar structures are more toxic to the yeast cells than low molecular weight aggregates. In order to hasten the aggregation and determine the effect of fibrils on the yeast cells, samples of peptides were incubated for 7 d prior to use.

After prolonged incubation the effect of fibrillar structures on the survival of exponential phase *S. cerevisiae* cells were examined. Interestingly, fibrils generated from both HFIP and NH₄OH pretreatment methods were cytotoxic (Figure 4-12). The cytotoxicity was significant with both pretreatment methods but the killing affect was much slower with NH₄OH pretreatment ($p < 0.05$) than HFIP ($p < 0.001$).

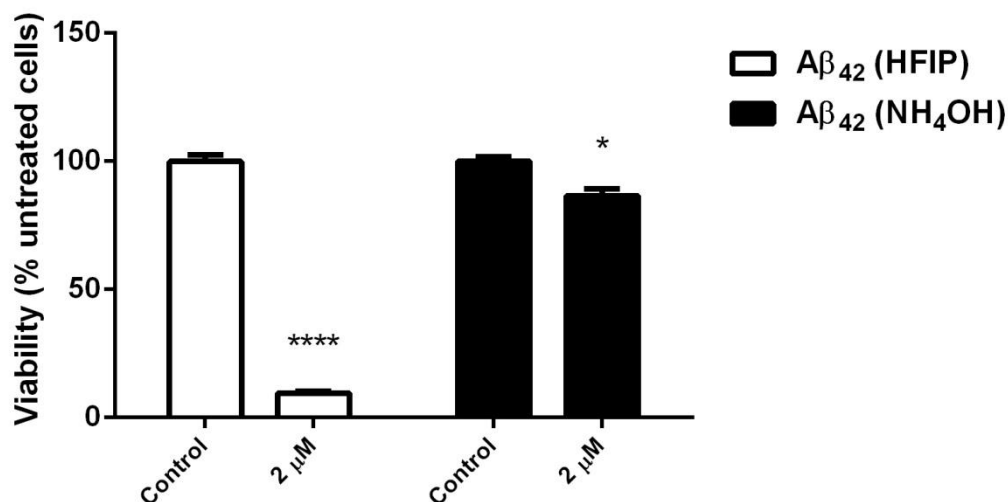


Figure 4-12 Effect of aged peptide on yeast cells. The NH₄OH and HFIP pretreated Aβ₄₂ peptide was incubated for 7 d at 37°C without shaking. Exponentially growing *S. cerevisiae* were washed and suspended in H₂O and then treated with 2 μM of these aged peptides and incubated overnight. Viability was determined the next day by transferring 100 μl of treated and untreated samples onto YEPD solid agar.

4.4.13 Western blot analysis of NH₄OH and HFIP pretreated Aβ₄₂ peptide at 0 h and after prolonged incubation

Qualitative assessment using western immunoblotting analysis (Figure 4-13) of freshly prepared Aβ₄₂ peptide solution pretreated with NH₄OH and HFIP was conducted to further detect differences between the two methods. These results were compared with the pretreated peptides that were incubated for 7 d.

Analysis of the immunoblotting indicated that oligomeric fractions generated by each method were different in size. Aβ₄₂ peptide pretreated with NH₄OH was observed without any incubation (0 h) as monomers (~4.5 kDa) and SDS stable oligomers in the 6 - 17 kDa range, indicative of low-n oligomers (dimers, trimers, and tetramers) by immunoblotting using WO2 monoclonal antibody (Figure 4-13A). However,

prolonged incubation generated a characteristic smear of high-n oligomers (> 28 kDa) indicative of protofibrils (Figure 4-13A). This result support the reports of Ryan et al. (2013) that showed that NH₄OH treatment of A β ₄₂ produces more aggregate free solutions that are suitable for kinetic studies.

The HFIP pretreated samples had very different characteristics. Similar patterns for the presence of monomers (~4.5 kDa), low-n oligomers (< 17 kDa) and high-n oligomers were observed at 0 h incubation (Figure 4-13B, lane 1) and after prolonged incubation (Figure 4-13B, lane 2). This indicated the HFIP pretreatment is not capable of eliminating aggregates and small nuclei that initiate fibrillar structure formation (Stine et al., 2003; Teplow, 2006).

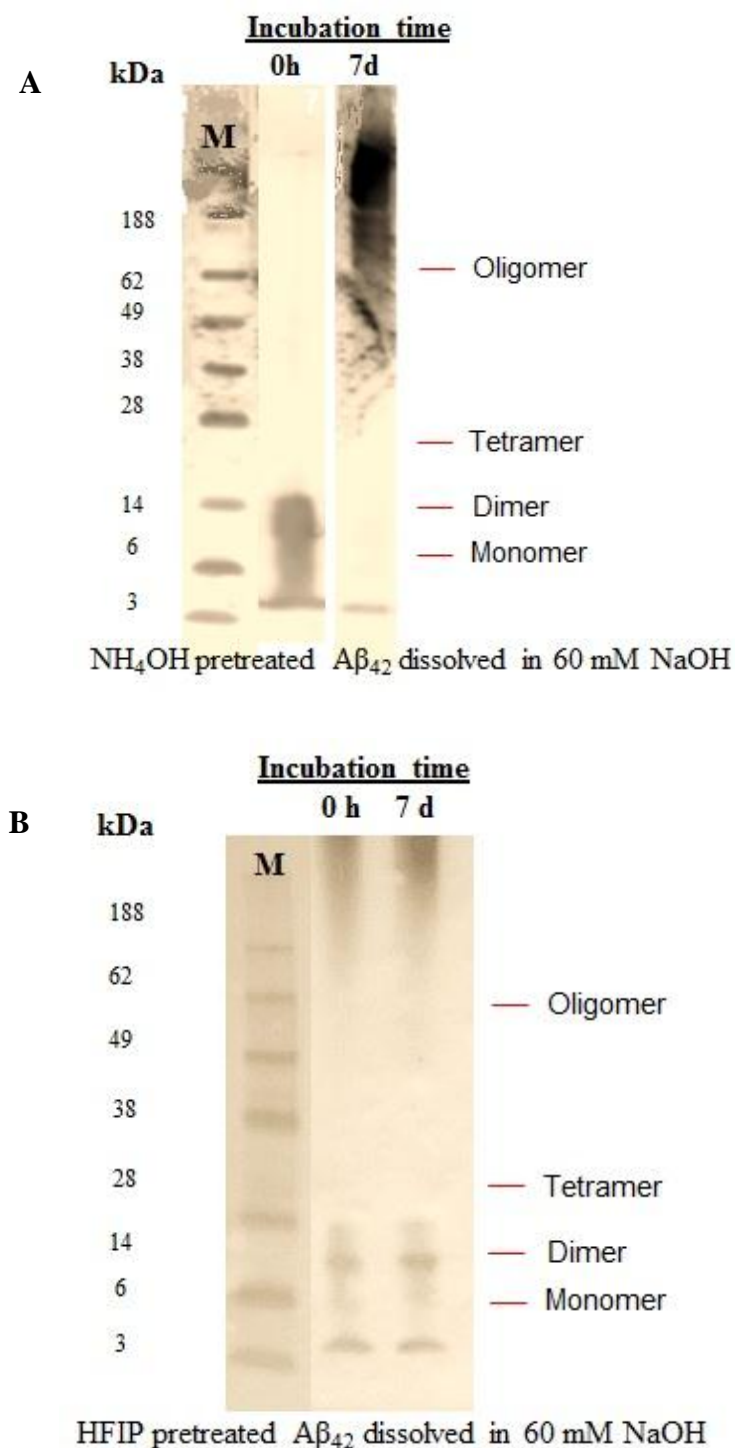


Figure 4-13 Western blot analysis of effect of pretreatment on the size of A β ₄₂. The NH₄OH pretreated samples dissolved in 60 mM NaOH (A) were examined immediately after preparation (0 h) and after prolonged incubation (7 d). Similarly HFIP pretreated A β ₄₂ samples were examined at 0 h and 7 d (B). Pretreatment with NH₄OH showed the presence of high levels of monomeric and dimeric A β ₄₂ whereas after prolonged incubation high molecular weight oligomers became apparent. The HFIP method resulted in both low and high oligomeric species both at the baseline and after prolonged incubation. The first lane in both figures shows the molecular marker. 0.5 μ g of each peptide were used for electrophoresis on SDS-PAGE.

4.4.14 Role of *AHP1* overexpression in the protection against cellular toxicity induced by HFIP pre-treated A β ₄₂

It is worth noting that the Section 4.4.9 data and in Section 4.4.10 demonstrated that the effect of A β ₄₂ on cellular killing possibly resulted from aggregation of the existing amyloidogenic proteins on the surface of yeast. Therefore, it was hypothesised that this aggregation might in turn increase the oxidative stress within the cell which contributes to the killing. Hence in the current section, the effect of HFIP pretreated A β ₄₂ has been tested on *S. cerevisiae* that overexpress *AHP1* (Ahp1p), an *ahp1* mutant and a WT strain that has been transformed with the empty vector (p416.GPD).

The *ahp1* mutant strain as shown in the previous section is very sensitive and the viability of untreated control samples declined in the absence of nutrients (Figure 4-14). Compared with the untreated control samples all three strains were sensitive to the effect of A β ₄₂ ($p < 0.001$). Analyses of data also showed a significant difference in the percentage cell survival in all three strains with pretreated HFIP compared with the NH₄OH method ($p < 0.001$). The Ahp1p overexpression did not result in the protection of cells against the effect of A β ₄₂ as expected. These results may suggest that the effect of A β ₄₂ is limited to the extracellular compartment of the yeast cells; therefore *AHP1* overexpression cannot rescue cells from exogenous toxins.

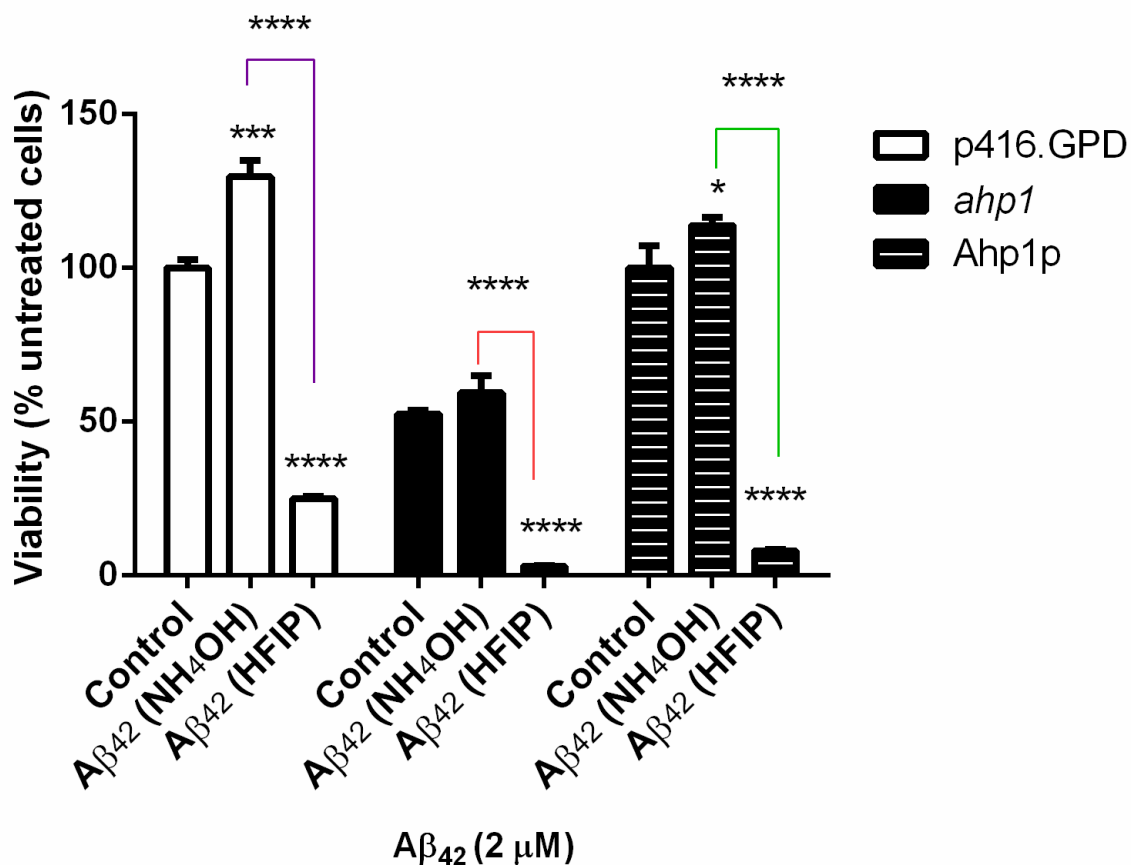


Figure 4-14 Role of AHPI in the cytotoxicity induced by Aβ₄₂. HFIP and NH₄OH pretreated Aβ₄₂ were used for the treatment of exponentially growing *S. cerevisiae* WT (BY4743) transformed with the p416.GPD empty vector, *ahp1* null mutant and BY4743 overexpressing the Ahp1p. (* $p < 0.05$, *** $p < 0.005$, **** $p < 0.001$).

4.5 DISCUSSION

The contribution of yeast to elucidating the biology of cells has been immense. Studies in yeast have deepened our knowledge of the eukaryotic cell, DNA damage and check points, autophagy and more recently as a model for the study of protein misfolding (reviewed in Khurana and Lindquist, 2010). It is well known that yeast lack the specialised processes of cell to cell communication that exists in neuronal cells. However yeast exhibit some relevant responses to A β ₄₂ peptide. For instance Park et al. (2011) and Treusch et al. (2011) found that intracellular expression of A β ₄₂ disrupts endocytosis and cause a defect in receptor protein trafficking which supports that yeast are good models for studying the effects of A β ₄₂ on neuronal cells. Another similarity is the presence of the YAP1802 yeast gene with a human homolog of phosphatidylinositol binding clathrin assembly protein (PICALM), which is considered as a risk factor for sporadic AD (Treusch et al., 2011). Limitations to this model organism are also expected since yeast lack receptors that have been proposed for A β ₄₂ binding. Putative receptors include the insulin receptor (Xie et al., 2002), the alpha7 nicotinic receptor (Wang et al., 2000), the metabotropic glutamate receptor (Renner et al., 2010) and cellular prion protein (Lauren et al., 2009).

Chemically-synthesised A β ₄₂ is also used for cytotoxicity studies in yeast (Chacińska et al., 2002; Bharadwaj et al., 2012). To understand the effect of pretreatment on the structure of A β ₄₂ and ultimately cytotoxicity responses and validate a yeast model for extracellular toxicity studies, two methods of pretreatment were used in the current chapter. The data presented elucidate the effect of pretreatment on A β ₄₂ potency and how yeast cells respond differently to the effect compared with neural cell culture.

4.5.1 Pretreatment determines the activity of A β ₄₂ peptide

Amyloid oligomers are found to be diverse both structurally and morphologically (Glabe, 2009). There are three classes of amyloid oligomers associated with neurodegenerative diseases identified by immunologically distinct type antibodies (Glabe, 2008; Kaye et al., 2009). These include “fibrillar oligomers” (Kaye et al., 2007), “annular protofibrils” (Lashuel et al., 2002; Kaye et al., 2009) and “prefibrillar oligomers” (Kaye et al., 2003; Baglioni et al., 2006).

Structural polymorphism of amyloid- β and other amyloid fibrils have been reported previously (Fandrich et al., 2009; Härd and Lendel, 2012). Many variables such as incubation temperature, pH, salt and ionic strength of the solvents can affect the structure and morphology of amyloids (Sahoo et al., 2009; Yu et al., 2009; Ahmed et al., 2010). At low temperature and low salt conditions, the oligomers were found to be more stabilised and lacked the β -sheet structure characteristic of fibrils and were more toxic to the mouse cortical neurons than protofibrils and fibrils (Ahmed et al., 2010). Pretreatment of chemically-synthesised A β ₄₂ in order to generate smaller oligomers for kinetic studies of its aggregation however is required and many methods have been developed over the years. HFIP pretreatment of A β ₄₂ is routinely used as it has been shown to induce α -helical conformations, produce monomeric solutions and remove the conformational memory from the peptide which otherwise would accelerate the fibril formation (Walsh et al., 1997; Stine et al., 2003). Nicolas and colleagues (2005a) however, reported that HFIP pretreated A β ₄₂ results in amyloid aggregates that are polymorphic and a single polypeptide can fold into multiple amyloid conformation (Nichols et al., 2005a).

The current study indicates that different preparations of A β ₄₂ peptide can lead to different biological activity towards yeast. A β ₄₂ pretreated with HFIP, was previously shown to cause toxicity to *C. glabrata* cells but only in oligomeric form with fibrils being ineffective (Bharadwaj et al., 2008). The present study however confirms significant cytotoxicity of HFIP pretreated A β ₄₂ immediately after preparation and after prolonged incubation with *C. glabrata* and to *S. cerevisiae*, with fibrillar structures being the more toxic species.

The recently introduced ammonium hydroxide (NH₄OH) pretreatment of synthetic A β ₄₂ reportedly results in formation of higher levels of monomeric peptide (Ryan et al., 2013) and has not previously been tested on yeast. In this study, soluble oligomers of the A β ₄₂ prepared by NH₄OH caused cell proliferation and increased the number of colonies in both *S. cerevisiae* and *C. glabrata*, regardless of the type of solvent (H₂O or NaOH). *C. glabrata* more than doubled in number, and *S. cerevisiae* numbers significantly increased over time. This method of pretreatment also resulted in A β ₄₂ that became toxic to the cells as it progressed to form fibrillar structures after prolonged incubation. The results presented in this chapter suggest that A β ₄₂ is more toxic to the yeast cells in fibrillar structures rather than the smaller oligomeric form despite some previous findings (Bharadwaj et al., 2008). This is in agreement with the findings of Chacińska et al. (2002) where A β ₄₂ was found to stimulate cell growth in monomeric form.

The A β ₄₂ peptide conformation appears to be the major determinant of its effect on yeast cells. This finding is contrary to the effect of extracellular A β ₄₂ to neural cells in tissue culture (Lambert et al., 2001) and animal models (Knobloch et al., 2007) in which oligomeric forms appear to be more toxic (reviewed in Benilova et al., 2012; Kaye and Lasagna-Reeves, 2013). This discrepancy can be explained by the complexity and dynamic nature of amyloid oligomers which contribute to the molecular mechanism underlying the toxicity of various forms. However the data from this chapter also identified that NH₄OH pretreated A β ₄₂ results in proliferation in yeast whereas it caused toxicity to the PC12 cells. These results indicate that A β ₄₂ peptide species with identical conformation have opposing effects on neural cells compared with yeast cells further questioning the validity of yeast as a model for determining extracellular effects of A β ₄₂.

4.5.2 Older cells are more susceptible to the effect of A β ₄₂ than younger cells

The data from this chapter indicates that oligomeric A β ₄₂ can cause cytotoxicity and proliferation in yeast regardless of growth phase. After separating the quiescent and non-quiescent fractions of stationary phase cells it became apparent that quiescent cells which represents the daughter cells (Allen et al., 2006; Aragon et al., 2008) were more resistant to cytotoxicity and proliferation induced by the A β ₄₂ peptide compared with the non-quiescent fractions which consist mainly of older mother cells (Allen et al., 2006; Aragon et al., 2008). These results are expected and can be explained by differences that have been proposed for these two cell populations by previous studies (reviewed in Smets et al., 2010). A microarray analysis of stationary phase cells from a previous publication by Aragon et al. (2008) revealed > 1300 mRNAs that

distinguished quiescent from non-quiescent fractions. Quiescent cells were found to be more associated with mRNAs that encode proteins required for membrane maintenance and signal transduction as well as the presence of more than 2000 protease-released mRNAs (Aragon et al., 2008). Quiescence is also associated with distinct physiological properties such as a thickened cell wall with enhanced integrity, resistance to heat shock and oxidative stress (Klosinska et al., 2011). These facts demonstrate that quiescent cells are physiologically poised to respond to environmental changes (Li et al., 2009). The non-quiescent mother cells on the other hand comprise mRNAs consistent with apoptosis in these cells. Allen et al. (2006) has explained this observation by indicating that non-quiescent cells are depleted in glycogen but are high in autophagic vesicles and do not compete for resources in the mixed culture but rather serve as non-fermentable storage reserves for quiescent cells.

4.5.3 Effect of chemically-synthesised A β ₄₂ is limited to the extracellular compartment of yeast

This study revealed that the A β ₄₂ peptide formed cell surface amyloid that stained intensely with ThT. Without A β ₄₂ peptide treatment, there was some ThT staining and this is attributed to binding by yeast cell wall proteins such as Flo1p, Als1p, Als5p, Muc1p and Bgl2p that are known to have amyloid like properties (Kalebina et al., 2008; Gorkovskii et al., 2009; Ramsook et al., 2010; Bezsonov et al., 2013). HFIP-pretreated A β ₄₂ resulted in peptide with long strand fibrillar morphology compared with the NH₄OH method. In yeast, this HFIP pretreatment resulted in peptide that has a high propensity to adhere to the yeast cell wall. On the other hand, A β ₄₂, freshly pretreated with NH₄OH caused cell proliferation due to the presence of monomeric and oligomeric forms (Section 4.4.12) while prolonged incubation led to

a fibrillar conformation which was toxic to *S. cerevisiae* cells. The association of HFIP pretreated A β ₄₂ with the cell wall proteins were much higher than the NH₄OH pretreated A β ₄₂ peptide. Previous studies showed that A β ₄₂ prepared using HFIP tend to be more potent in electrophysiological tests and have greater tendency to modulate biological membrane properties (Zagorski et al., 1999; Roccatano et al., 2005; Lioudyno et al., 2012). Amyloid- β peptide has been referred to as a prion due to its self-aggregation capability (White et al., 2001; Stohr et al., 2012). This might also explain its propensity for adhering to amyloidogenic cell wall proteins of yeast cell. Subsequent data also suggest that certain A β assembly might have prion-dependent toxicity (Nicoll et al., 2013).

The effect of exogenous A β ₄₂ on yeast cells is limited to the extracellular compartment. These findings further confirm those of Chacińska and colleagues (2002) which demonstrated the presence of approximately 15,000 A β ₄₂ binding sites per yeast cell. Further, Treusch et al. (2011) indicated that cell wall retains the intracellular expressed A β ₄₂ and prevents the secreted peptides from diffusion into the culture medium. *C. glabrata* cells treated with A β ₄₂ peptide labelled with fluorescein isothiocyanate (FITC) as well as immune-gold labelled A β ₄₂ peptide have also confirmed that the A β ₄₂ is associated with the cell surface and no entry of the peptide within the cells was detected (Bharadwaj, 2011). Similarly in this study it was found that the A β ₄₂ attaches to the cell surface and does not appear to enter into the cell compartment due to the cell wall acting as a barrier to this entry. Therefore, despite previous reports on the suitability of yeast as model for extracellular cytotoxicity studies using the chemically-synthesised A β ₄₂, the intracellular expression of the protein seems more relevant to the disease. The data in this current study is novel in

that it shows the interaction of extracellular A β_{42} with yeast cells is dissimilar to that of neural cells so caution should be taken when reporting their cytotoxicity effect. Overall, these findings indicate that extracellular toxicity studies of A β_{42} in yeast are not suitable because it is impossible to explore the endocytosis and vesicular trafficking which are very critical for studying the A β_{42} toxicity and allows unbiased screening of A β_{42} modifiers (Treusch et al., 2011). Further, the non-permeability of the yeast cell wall was illustrated in an elegant study by Treusch et al. (2011) in which intracellular expression of A β_{42} in *S. cerevisiae* was able to be studied as the yeast cell wall restrained secreted protein from diffusing into the culture medium and allowing its interaction with the plasma membrane and endocytosis. Also, movement and migration of the A β_{42} within the cell was described as an important factor for the study of its interaction with internal organelles and compartments (Jung and Haucke, 2007; Deane et al., 2009; Sakono and Zako, 2010; Holtzman, 2011). A β_{42} oligomers have been found to increase endocytosis in cultured cells (Minano-Molina et al., 2011) and cause defects in endocytosis in human induced neuronal cells derived from AD patients (Qiang et al., 2011).

It has been reported that exogenous amyloid protein such as those in food or cosmetics can cause cross-seeding, aggregation and propagation of A β_{42} amyloidosis (Ono et al., 2014). TEM micrographs of HFIP pretreated A β_{42} showed that this preparation contain high level of fibrils which suggests that it may act as seeding for increased amyloidogenicity and aggregation pathways. The yeast cell wall may also possesses a high level of amyloidogenic protein that could also act as cross-seeds and accelerate the amyloidosis of the exogenous A β_{42} . Although, the cytotoxicity of the A β_{42} was found to be associated with aggregation of the yeast cells, the exact

mechanism of its action remains elusive. It can be speculated that cell wall integrity (CWI) might be compromised by A β ₄₂ which is required for progression through the cell cycle (Levin, 2005, 2011). This implies that cell wall mutant strains could be even more susceptible to the effect of A β ₄₂.

4.5.4 Ahp1p overexpression cannot rescue cells from the toxicity effect of A β ₄₂

AHP1 is a member of Prx (type II) with alkyl hydroperoxide defence in yeast (Lee et al., 1999; Trivelli et al., 2003; Iwai et al., 2010). The *AHP1* null mutant yeast strain was very sensitive when suspended in water with 50% decrease in cell viability after an overnight incubation. This severe growth retardation and hypersensitivity to oxidative stress in the mutant has been reported previously (Wong et al., 2004). Although findings from this study illustrate that A β ₄₂ may be localised to the extracellular region of the yeast it still seems to generate a form of stress which became apparent in the *ahp1* null mutant strain. The *ahp1* null mutant strain was very sensitive to the effect of exogenous A β ₄₂ and this sensitivity was lower in the WT *S. cerevisiae* strain. Because *AHP1* provides protection against ROS (Nguyen-nhu and Knoops, 2002; Lian et al., 2012), it was expected that the overexpression of Ahp1p could rescue the cells from the cytotoxic effect of HFIP pretreated A β ₄₂ while surprisingly the overexpressed cells were more sensitive than the WT strain. Apart from ROS regulation *AHP1* has been shown to play a role in manganese (Mn²⁺) homeostasis and trafficking (Farcasanu et al., 1999). They have also shown that Ahp1p is involved in the regulation of cytoplasmic Mn²⁺ concentration. Overexpression of *AHP1* therefore, may cause disruption in Mn²⁺ trafficking and instead of being protective against the cytotoxic effect of A β ₄₂, it may become more prone to its effect. Interestingly, the *AHP1* gene was found to be not essential for

vegetative growth while it is required for growth under stressful conditions. Ahp1p reportedly is localised both in the cytosol and mitochondria as both organelles are associated with high level of ROS intermediates (Farcasanu et al., 1999; Park et al., 2000). Therefore, if the A β ₄₂ is localised to the cell wall of yeast according to the findings from this study it can be speculated that overexpression of the Ahp1p produced a strain in which the cellular metal trafficking was disrupted hence was more sensitive to the effect of A β ₄₂ than the wild-type.

Ahp1p has been found to be an antioxidant protein and play a role in the urmylation pathway by forming a conjugate with Urm1p during nutrient sensing and budding which ultimately induces a strong oxidative-stress response and protection (Goehring et al., 2003). *AHP1* has shown to preferentially eliminate organic peroxides rather than hydrogen peroxide (H₂O₂) and Ahp1p was found to be specific for organic peroxides (Lee et al., 1999). A study by Jeong et al. (1999) showed that overexpression of the Ahp1p in *E. coli* cells reversed the growth sensitivity induced by alkyl hydroperoxides. Consistent with these previous findings, in this chapter overexpression of *AHP1* could not rescue cells from the cytotoxic effect of A β ₄₂. Further, Ahp1p acts to protect against organic peroxides therefore, stress induced by A β ₄₂ peptide could not be overcome by this antioxidant protein. However, thioredoxin protein 1 (Tsa1), a cytosolic antioxidant protein (Garrido and Grant, 2002) have been shown to provide protection against ROS induced by protein misfolding and aggregates (Weids and Grant, 2014).

4.6 CONCLUSION

The tendency of amyloid beta ($A\beta$), in particular $A\beta_{42}$ isoform to misfold and aggregate into insoluble amyloid fibrils in the early stages of AD has been well documented. Investigations using chemically-synthesised $A\beta_{42}$ peptide for extracellular studies therefore have become a common practice, the outcome of these studies, however, have not been in agreement.

My original contribution to knowledge is showing that the pretreatment method of synthetic $A\beta_{42}$ peptide determines $A\beta_{42}$ activity and ultimately how it interacts with yeast cells. Here by manipulating the growth phase, the chronological lifespan of yeast has been studied to gain understandings into the aging process in yeast and how $A\beta_{42}$ influence survival and cell division. The effect of $A\beta_{42}$ is found to be limited to the yeast cell wall and interactions with the amyloidogenic cell wall proteins. *S. cerevisiae* were found to be more resistant than *C. glabrata* to the effect of $A\beta_{42}$ peptide. It was identified that conformational changes in the peptide due to preparation methods, determine its fate on toxicity and proliferation. The hexafluoroisopropanol pretreated $A\beta_{42}$ had a greater tendency to aggregate on yeast cells as determined by thioflavin T staining followed by flow cytometry and microscopy. Both quiescent and non-quiescent cells were analysed by these methods of peptide preparation, of which the latter is found to be more susceptible to the toxicity of $A\beta_{42}$. Also, similar peptide preparations which resulted in cytotoxicity in PC12 cells caused proliferation in yeast cells.

5 CHAPTER 5: VALIDATING THE YEAST MODEL OF ALZHEIMER'S DISEASE FOR COMPOUND LIBRARY SCREENING

5.1 INTRODUCTION

As reviewed in Chapter 1 (Section 1.1.1) deposition and aggregation of amyloid- β (A β) is believed to play a key role in the pathogenesis of Alzheimer's disease (AD) (Findeis, 2007; Bignante et al., 2013; Tay et al., 2013). The physicochemical properties of the amino acid sequence in A β peptides, particularly the central hydrophobic region (residues 16-20; KLVFF) is believed to be responsible for the initiation of amyloid formation by favouring the ordered aggregation of A β (Kim and Hecht, 2005; Mathura et al., 2005; Selkoe, 2008). Various sizes of A β species have been associated with the onset and progression of AD (Glabe, 2008; Klyubin et al., 2012). For example, dimeric forms have shown to induce synaptic dysfunction (Jin et al., 2011), SDS-stable oligomers were found to be neurotoxic (Lacor et al., 2004) whereas, A β monomers and mature fibrils are relatively inert (Lambert et al., 1998; Wu et al., 2010). Therefore, targeting the A β aggregation pathway has become a key target in an effort to discover therapeutics which may be capable of preventing or delaying the onset of AD (Matharu et al., 2010). Studies have shown that the anti-parallel β -sheet orientation of the peptide and hence the aggregation, could be blocked by compounds that can act as β -sheet breakers or ligands (Keshet and Good, 2010; Härd and Lendel, 2012).

Small molecule inhibitors have been defined by Cheng et al. (2013) as low molecular weight organic compounds with capability to form a bond with high affinity biomacromolecules. Small molecules are routinely screened for their ability to prevent aggregation or reduction of the A β -induced cytotoxicity, but their other important roles such as enhancing fibril formation is ignored. Although, the dynamic relationship between intracellular oligomers and extracellular plaques is still unknown, suggestions have been proposed that the larger fibrillar structures and plaques may make inert or even aid in preventing toxic oligomer formation (Glabe, 2005; Necula et al., 2007a; Chen et al., 2010). So, an effective small molecule may be one that prevents the formation of toxic oligomeric species by accelerating the fibril formation. Therefore, screening for fibril stabilisers is as important as those with anti-aggregation propensity since it has been reported that fibrils are not very toxic (Kayed et al., 2003). Also, many aggregate inhibitors have been identified previously but the mechanism of their action is rather complex and may be related to oxidation reactions and covalent modifications (Kim et al., 2014). These examples illustrate that targeting only a single approach for screening does not seem to be appropriate and informative but multiple analytical approaches may be required to fully investigate and identify the potential therapeutic compounds. 2,2',4'-Trihydroxychalcone (TDC), a flavonoid belonging to the chalcone family has been found to have therapeutic potential including BACE1 inhibition and showed potential in tissue culture and in an animal model of AD significant reduction was shown in BACE1-cleavage of APP and improved memory and neuro-behavioural activities (Zhu et al., 2010).

High-throughput *in vivo* screening of compounds that inhibit aggregation of A β ₄₂ using green fluorescent protein (GFP) fusion has been reported previously (Kim et al., 2006). This method has successfully been applied to identify those compounds that inhibit aggregation and enable GFP to fold into its native structure in *E. coli* transformants (Wurth et al., 2002; Kim and Hecht, 2005; Kim et al., 2006). In this chapter compounds were screened for their effect on the reduction or increase in fluorescence due to aggregation of A β ₄₂ in *AHP1* deletant strain and WT *S. cerevisiae* transformants expressing GFP-A β ₄₂. The alkyl hydroperoxide reductase protein (Ahp1p) is a thiol-specific peroxiredoxin that provide protection against reactive oxygen species (ROS) (Iwai et al., 2010; Lian et al., 2012). Using this mutant strain *ahp1* should allow identification of those compounds that can provide protection against oxidation and those capable of inhibition of amyloid aggregation in the GFP-A β ₄₂ fusion-associated fluorescence assay.

There is a growing consensus in the literature that the frequently investigated polyphenols could be key molecules for the development of therapeutics or as a part of a prevention strategy for AD (Ono et al., 2003; Harvey et al., 2011; Qin et al., 2012; Cheng et al., 2013; Pallauf and Rimbach, 2013). The chemo-protective effects of (-)-epigallocatechin-3-gallate (EGCG), a polyphenol in green tea as an anti-aging and cancer prevention has been well documented (Rezai-Zadeh et al., 2005; Mandel et al., 2006; Maurya and Rizvi, 2009; Nichols and Katiyar, 2010). EGCG has shown to provide protection against the toxicity of A β (Lee et al., 2009a; Harvey et al., 2011; Smid et al., 2012), modulate the amyloid precursor protein (APP) cleavage and reduce cerebral amyloidosis through activation of the non-amyloidogenic pathway

(Levites et al., 2003; Rezai-Zadeh et al., 2005; Avramovich-Tirosh et al., 2007) and directly bind to A β (Palhano et al., 2013). EGCG has been shown to activate cellular antioxidant defense capacity against the ROS stress induced by A β_{42} identified by an increase in mRNA expression of γ -glutamylcysteine ligase (Kim et al., 2009). Consequently, in this chapter EGCG has been included as a positive control for comparison of compound potency. Also, the compounds that were screened include both small molecule inhibitors and polyphenols.

This chapter aimed at screening a library of chemicals containing three groups of compounds (42 compounds in total) and verifying whether the outcome of an *in vivo* yeast based screening assay for potential chemo-protectors is compatible with *in vitro* conventional methods. 42 compounds were screened, these include 21 Danshen derivative and analogue chemicals (Appendix A, Table 1), and 6 Biscoumarin analogues (Figure 5-3) which have been synthesised and supplied by Assoc. Prof. Helmut H \ddot{u} gel (RMIT University, School of Applied Sciences). Another 15 proprietary compounds (Appendix A, Table 2) of unknown identity were supplied by Dr. Sylvia Urban (RMIT University, School of Applied Sciences) at 1 mM concentration dissolved in dimethyl sulfoxide (DMSO). Polyphenols were investigated for their capacity to inhibit protein aggregation and toxicity, their radical scavenging activity and their ability to stabilise oligomeric species (Ono et al., 2003; Huber et al., 2006; Mandel et al., 2006).

5.1.1 Danshen compounds

This group consists of danshen derived compounds and their analogs which were chemically-synthesised by Alford and Hugel (2013), (Appendix A, Table 1). Danshen, the dried root of *Salvia miltiorrhiza* (a type of sage), has been widely used in Chinese medicine for treatment of cardiovascular diseases (Izzat et al., 1998; Zhou et al., 2005). Danshen constituents have also been shown to possess potential therapeutic effects in the treatment of AD in both animal models by attenuating cognitive dysfunction induced by A β ₄₂ peptide (Kim et al., 2011; Feng et al., 2012; Lee et al., 2013) and in tissue culture studies (Tian et al., 2008; Zhou et al., 2011; Shi et al., 2012; Yu et al., 2014a) due to protection against toxicity of the peptide. The beneficial effect of danshen is reportedly attributed to the presence of diverse hydrophilic (caffeic acid, salvianolic acid and rosmarinic acid) and hydrophobic constituents (Tanshinones) including antioxidant properties which have been summarised in Figure 5-1.

Since the number and position of the hydroxyl moieties attached to the phenyl rings in benzoic acid and cinnamic acid analogs differ in various compounds, an investigation was performed into the role of hydroxyl groups in the inhibitory activity of these phenolic acids. Further, to be able to explore whether the hydroxyl group possess inhibitory activity in those phenolic acids, different benzoic acid and cinnamic acid derivatives having methoxy groups instead of hydroxyl moieties have been examined.

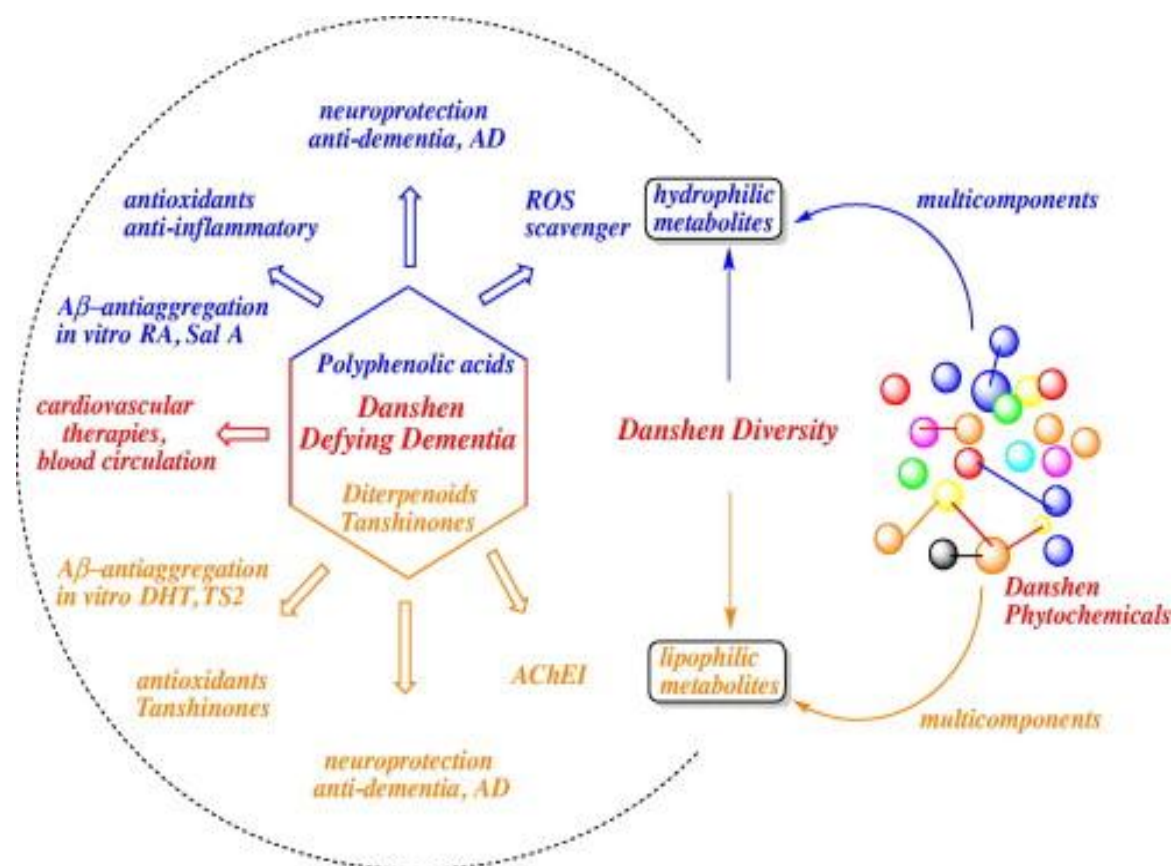


Figure 5-1 Overview of the diverse therapeutic applications of danshen constituents. AchE1: Acetylcholinesterase, ROS: Reactive oxygen species, RA: Rosmarinic acid, Sal A: Salvianolic acid A, DHT: Dihydro-tanshinone, TS2: Tanshinones IIA. From Hügel and Jackson (2014).

5.1.2 MATNAP proprietary compounds

The Marine and Terrestrial Natural Product (MATNAP) are a group of 15 naturally occurring novel compounds with undisclosed structures and were synthesised in the laboratory of Dr. Sylvia Urban (RMIT University). Due to interest in characterising their biological activities, these compounds (small molecules) have been investigated in the current chapter for their anti-aggregation propensities.

5.1.3 Biscoumarins

The early therapeutic potential of coumarins has been reported in 1936 (von Werder and Merck's, 1936). Since then coumarins have been identified for their anti-inflammatory (Hadjipavlou-Litina et al., 2007; Witaicenis et al., 2014), antibacterial (Ojala et al., 2000; de Souza et al., 2005), antitumor (Stefanova et al., 2007), anti-HIV activities (Dong et al., 2011) and their role as a stimulator of the central nervous system (CNS) (Pereira et al., 2009). The coumarins are naturally occurring in plants and consist of a large class of phenolic compounds consisting of benzo- α -pyrone (2*H*-1-benzopiran-2-one) rings (Venugopala et al., 2013). Generally coumarins are classified into five groups, namely; 1) simple coumarins, 2) Furanocoumarins, 3) Pyranocoumarins, 4) Biscoumarins and Triscoumarins and 5) Coumarinolignans (Borges et al., 2005). Structure-activity relationships for biscoumarins have been reported previously (Khan et al., 2004; Chiang et al., 2007; Kancheva et al., 2010). In the current chapter, six structurally distinct biscoumarins have been investigated for their chemoprotection against AD.

All of these compound groups were screened for identification of bioactive small molecules which may show potential anti-oligomerisation and anti-toxicity activities. This was done using *in vitro* and *in vivo* yeast based assays validated by standard conventional *in vitro* screening methods.

5.2 AIMS

- 1) Define the anti-oligomerisation property of select compounds using conventional *in vitro* methods (e.g. ThT assay)
- 2) Determine the cytotoxicity effect of various A β ₄₂ conformers produced after prolonged incubation with potential chemo-protective ligands
- 3) Verify whether the GFP-A β ₄₂ fusion in yeast can be used for high-throughput detection of anti-amyloidogenic compounds

5.3 MATERIALS AND METHODS

S. cerevisiae (BY4743) was utilised in most of the analyses but in some assays *C. glabrata* (ATCC90030) was used as it was shown to be more sensitive to the toxicity of synthetic A β ₄₂ peptide (Chapter 2). Wild-type *S. cerevisiae* strain and the *AHP1* deletant strain (*ahp1*) were transformed with plasmids encoding direct constitutive expression of GFP and GFP-A β ₄₂. Cells were then grown in the presence of 50 μ M danshen compounds and were analysed after 24 h incubation for green fluorescence levels using flow cytometry (Section 2.6.2). *AHP1* provides protection to the cells against oxidation therefore, compounds with antioxidant properties can have substantial effect on the survival of the *ahp1* strain.

The chemically-synthesised A β ₄₂ peptide solutions were prepared as described respectively in Section 2.7.1. The cytotoxicity effect of the HFIP pretreated A β ₄₂ and viability of the yeast cells after any treatment was measured as described in Section 2.3.3. Yeast cell survival in the presence of A β ₄₂ pretreated with NH₄OH and HFIP was determined as described in Section 2.7.5. The amyloidogenicity potential of the compounds was examined using thioflavin T (ThT) assay at 0, 16 and 24 h as described in Section 2.8.

Sample preparation for TEM and the micrograph imaging of A β ₄₂ conformers produced as a result of 7 d co-incubation with the compounds was done respectively according to Section 2.12.1 and Section 2.12. The TEM images revealed the presence of various A β ₄₂ peptide species, with a wide range of sizes and conformation. In order to explore whether any of the compounds partially or fully

blocked the oligomerisation process, protein analysis and cytotoxicity of the co-incubated A β ₄₂ and compounds after 7 d was performed. The A β ₄₂ peptide species generated from prolonged co-incubation with the compounds was characterised by SDS-PAGE (Section 2.10.1) followed by western blot and silver staining analysis. Immunoblotting of prolonged incubated A β ₄₂ and compound samples with WO2 anti-A β antibody was studied as described 2.10.3. Protein detection was also performed by silver staining of the gel as described in Section 2.10.2.

5.4 RESULTS

Three groups of compounds namely, danshen (Section 5.4.1), proprietary MATNAP compounds (Section 5.4.2) and biscoumarin derivatives (Section 5.4.3) were analysed. These were assayed for their ability to prevent amyloid- β oligomer or fibril formation *in vivo* and *in vitro*, or to provide protection to yeast against the cytotoxicity of the A β ₄₂.

5.4.1 DANSHEN COMPOUNDS ANALYSIS

In vivo and *in vitro* yeast based assays were used to analyse these danshen derivatives or their chemically-synthesised analogs (Appendix A, Table 1) and for comparison with the *in vitro* conventional methods of anti-oligomerisation screening. This would allow identification of bioactive molecules and functional groups as well as the selection of the positional isomer that shows the greatest therapeutic effect.

5.4.1.1 Screening of danshen compounds in an *ahp1* mutant expressing green fluorescent protein fused to A β ₄₂ (GFP-A β ₄₂)

This screening is based on the percentage of fluorescence emission from the correct folding of GFP as a reporter for A β ₄₂ aggregation in the presence of compounds. The GFP fusion system used in this study has been described previously (Caine et al., 2007a). This GFP-A β ₄₂ fusion results in the green fluorescent being visible in punctuate patches. In the GFP expression alone, the GFP is distributed uniformly throughout the cell (Figure 5-2A). The green fluorescence associated with GFP alone was very strong and present in most cells (Figure 5-3) compared with the GFP-A β ₄₂

fusion. In fact in vehicle buffer (DMSO) control samples the GFP fluorescence was observed in ~80% of cells (78.5 ± 1.4). This level did not change significantly in the presence of 50 μ M danshen compounds (Figure 5-3A).

In control *ahp1* mutant samples transformed with GFP-A β_{42} (GA), fluorescence was present in ~30% of cells. Cells incubated in the presence of BA_PG 65 and BA_PG84 exhibited a significantly higher fluorescence ($p < 0.01$ and $p < 0.05$ respectively) compared with the control (Figure 5-3B). Fourteen danshen compounds caused a significant reduction in the fluorescent level of the transformants (Figure 5-3A). Rosmarinic acid, BA_PG63, 3, 4-dihydroxybenzoic acid, salvianolic acid B, 2, 4, 5-trihydroxybenzoic acid significantly lowered the fluorescence expression level similarly to EGCG ($p < 0.001$). This effect was lower with 3, 4, 5-trihydroxybenzoic acid ($p < 0.005$), BA_PG44, BA_PG51, BA_PG87, BA_PG83 ($p < 0.01$) compared with EGCG.

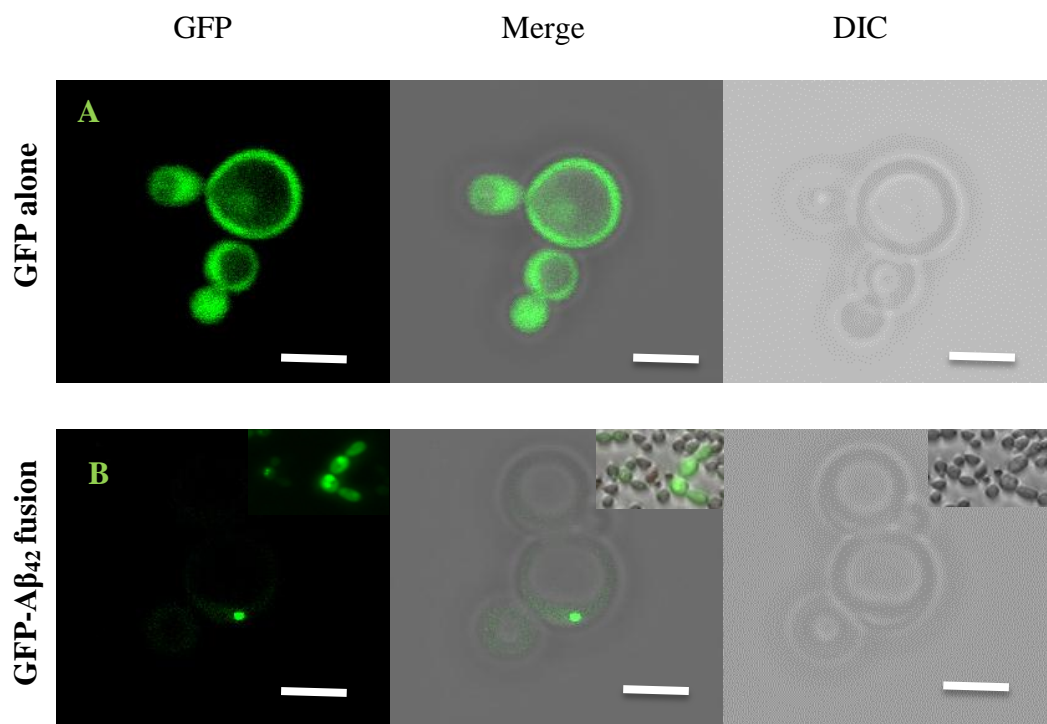


Figure 5-2 Fluorescent and light images of *S. cerevisiae* (*ahp1* mutant) transformed with GFP and GFP-A β_{42} plasmids. Green fluorescent expression pattern in the presence of GFP is well distributed (A) while; GFP-A β_{42} (B) is viewed in punctate form. Visualisation was done using a confocal microscope (Scale bar = 5 μ m).

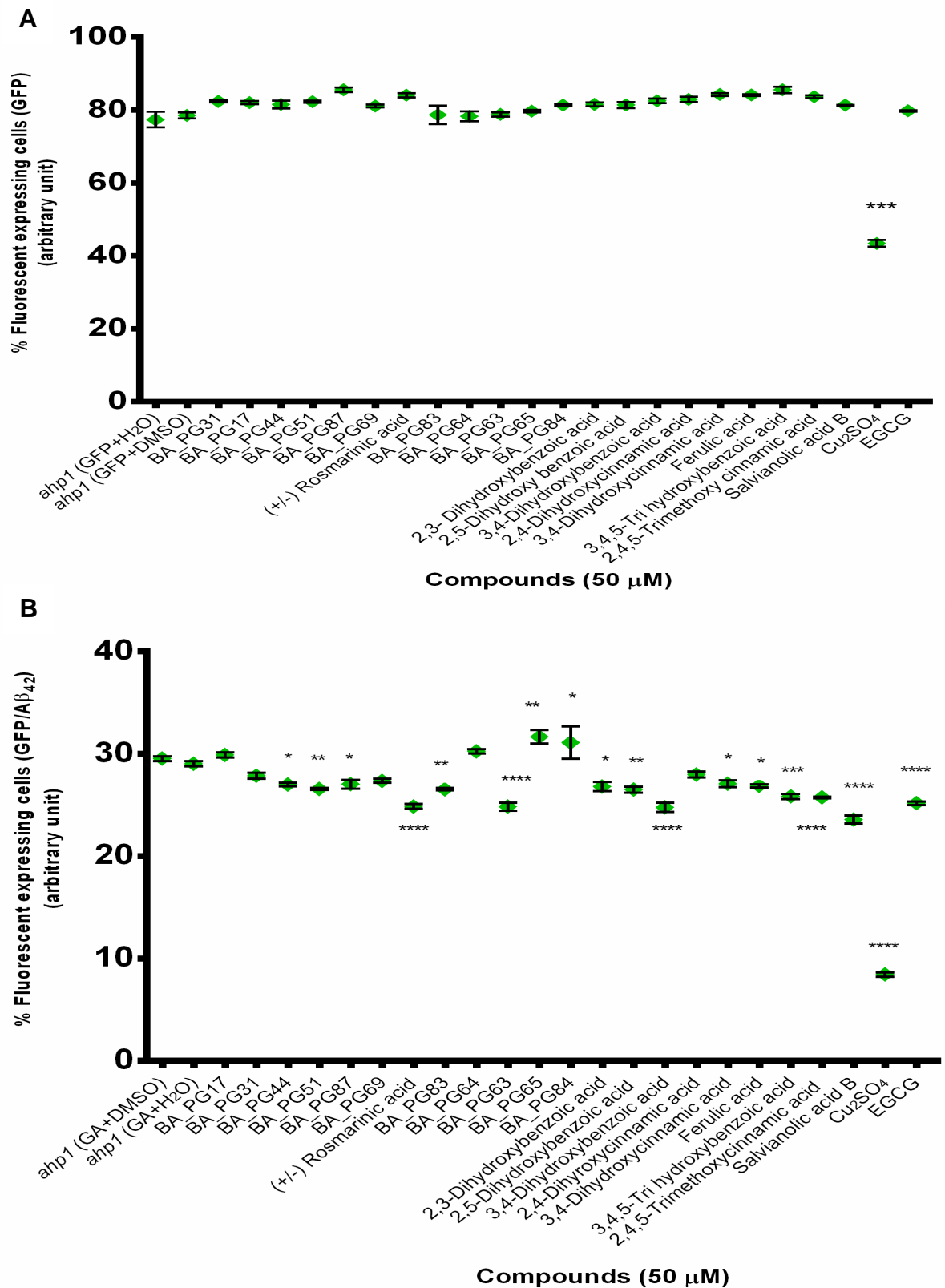


Figure 5-3 GFP and GFP-A β ₄₂ transformants of *AHP1* knock-out mutant. Fraction of fluorescent cells in *ahp1* transformed with GFP (A) and GFP-A β ₄₂ (GA)

(B) as measured by flow cytometry. A library of 21 danshen derived compounds was examined with yeast based assays to identify those with anti-misfolding capability. EGCG was used as a positive control and Cu_2SO_4 as a negative control for indication of toxicity. (**** $p < 0.001$, *** $p < 0.005$, ** $p < 0.01$, * $p < 0.05$). All data are expressed as mean \pm SEM (n = 3).

Among salvianolic acid analogs (Appendix A, Table 1), salvianolic acid B ($p < 0.001$) and BA_PG87 ($p < 0.05$) significantly decreased the fluorescence level whereas, BA_PG65 ($p < 0.01$) and BA_PG84 ($p < 0.05$) increased the fluorescence emission and BA_PG69 remained ineffective compared with control (Figure 5-3B).

Danshensu, the most potent constituent of the aqueous extract of danshen is a relatively simple polyphenol (Chan et al., 2004; Wu et al., 2007). Here three isomers of Danshensu, two of which have been methylated to resemble the by-products generated during its metabolic pathway were analysed. All three Danshensu isomers of BA_PG63 ($p < 0.001$), BA_PG51 ($p < 0.01$), and BA_PG44 ($p < 0.05$) reduced the percentage of fluorescent expressing cells significantly (Figure 5-3B). Further, the percentage of fluorescing cells decreased in the presence of all three positional isomers of dihydroxybenzoic acid (Figure 5-3B). However, 3, 4-dihydroxybenzoic acid ($p < 0.001$) was more potent compared with 2, 5-dihydroxybenzoic acid ($p < 0.01$) and 2, 3-dihydroxybenzoic acid ($p < 0.05$) respectively (Figure 5-3B). Also, the two caffeic acid monomers of 4-hydroxy-3-methoxycinnamic acid, and 3, 4-dihydroxycinnamic acid decreased the percentage of fluorescing cells significantly ($p < 0.05$). These results showed that only BA_PG84 and BA_PG65 which are salvianolic acid C analogues were able to increase the number of fluorescing cells.

This is an indication of increased levels of correctly fold GFP-A β_{42} . To further determine the effect of these compounds on the GFP-A β_{42} fusion system and role of AHP1 protein (Ahp1p) on the outcome, analysis was conducted in the WT strain.

5.4.1.2 Screening of danshen compounds in the BY4743 wild-type *S. cerevisiae* expressing green fluorescent protein associated with GFP and GFP-A β_{42}

To verify whether the effect of danshen compounds on the *ahp1* mutant strain is similar to the WT *S. cerevisiae* (BY4743), propidium iodide (PI) was used to monitor cell damage, while levels of fluorescence associated with a GFP-A β_{42} constructs were measured (Section 2.6.2).

The percentage fluorescent intensity (FI) of the green fluorescence (GFP) expression level of BY4743 cells in the presence of 50 μ M danshen compounds was analysed quantitatively. This was done by measuring the average GFP expression of each sample compared with the untreated control. The percentage of fluorescent intensity of cells only increased with the presence of ferulic acid ($p < 0.005$; Figure 5-4A).

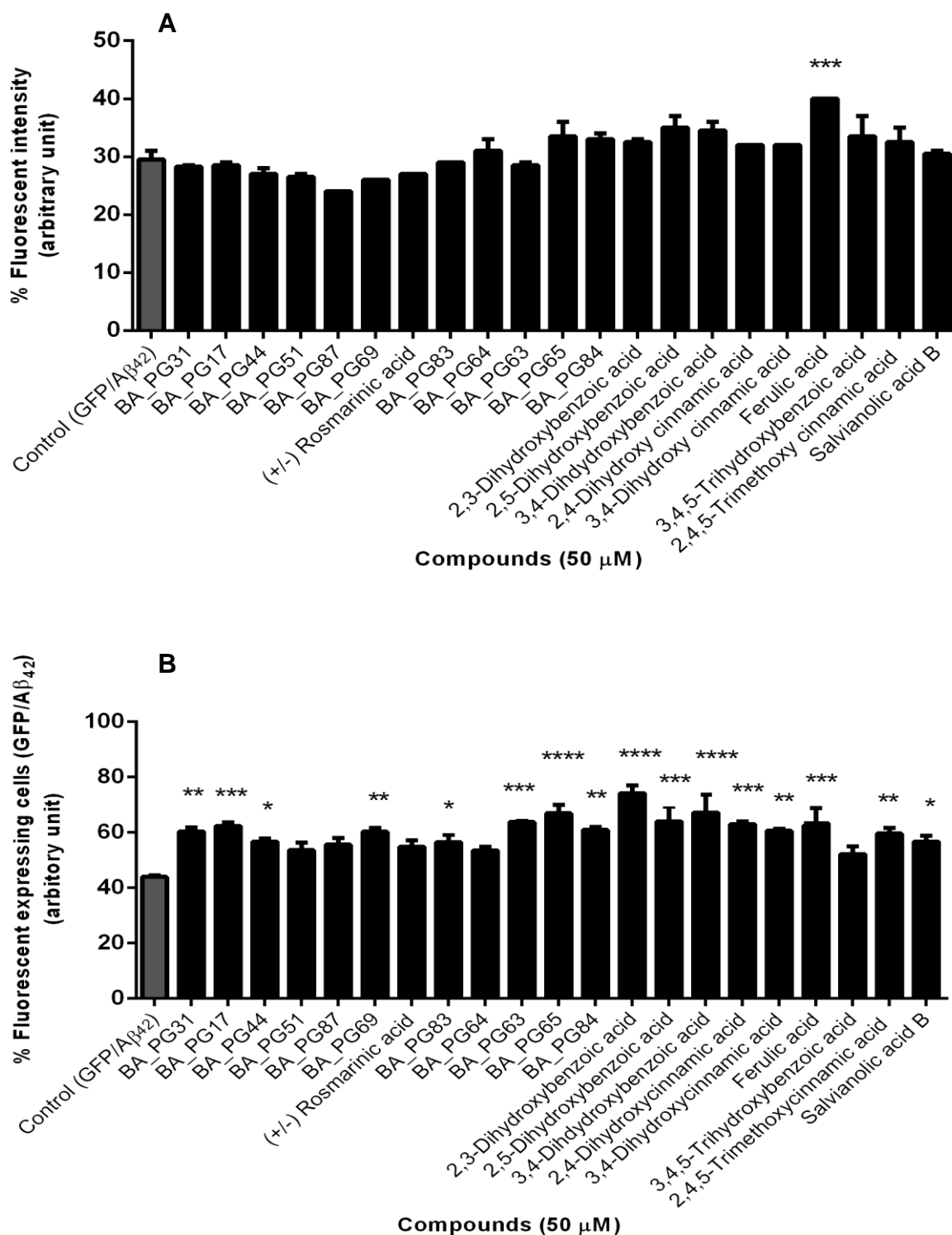
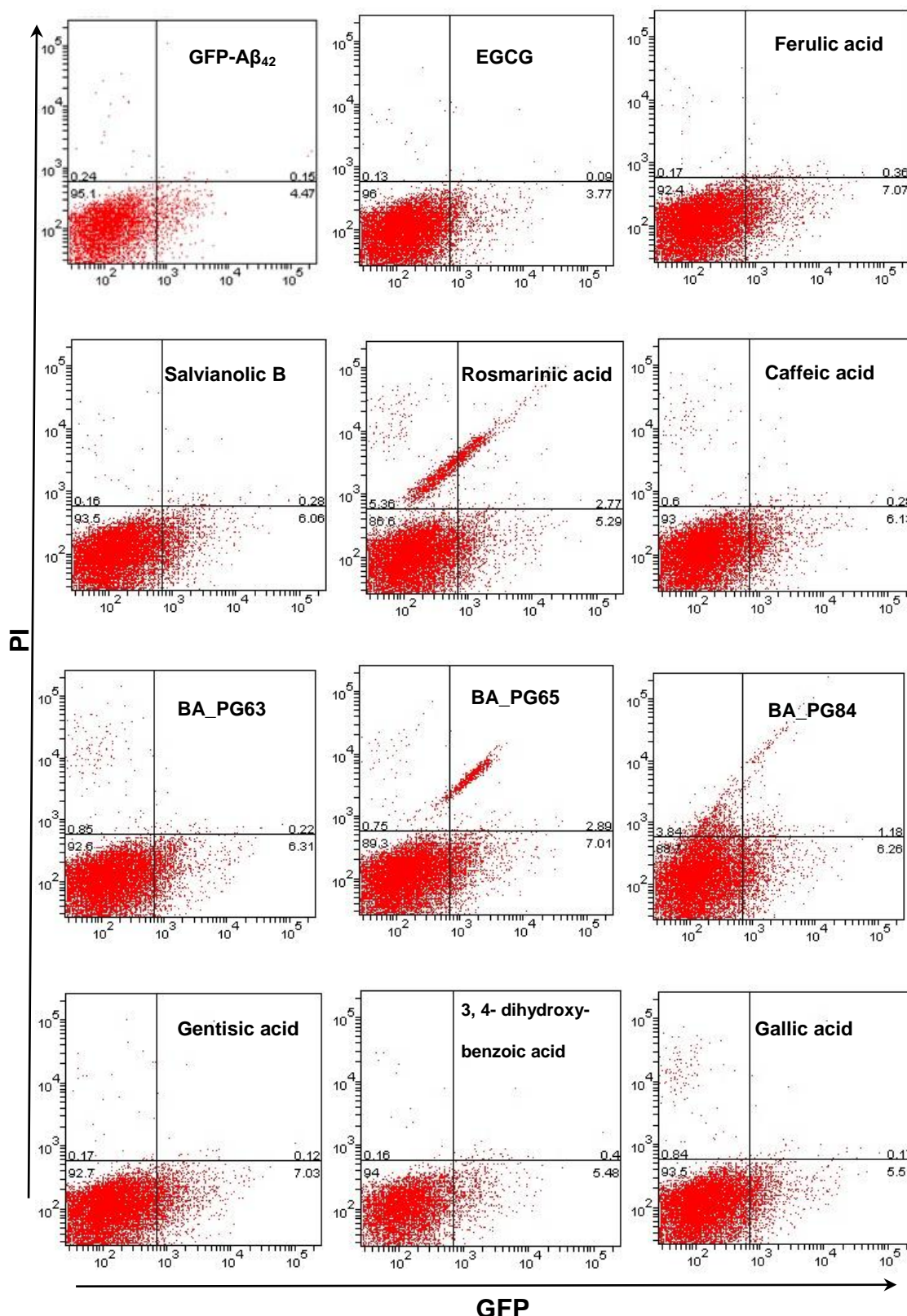


Figure 5-4 Quantitative analysis of danshen compounds on wild-type BY4743 *S. cerevisiae* expressing GFP-A β_{42} measured by flow cytometry. Percentage FI of GFP-A β_{42} expressing cells compared with untreated control sample (A). Percentage

of GFP-A β_{42} cells expressing green fluorescence (B). (**** $p < 0.001$, *** $p < 0.005$, ** $p < 0.01$, * $p < 0.05$). All data are expressed as mean \pm SEM (n = 3).

None of the compounds decreased the number of cells expressing GFP-A β_{42} while, sixteen compounds significantly increased the percentage of fluorescing cells (Figure 5-4B). This indicates a different effect in the WT compared with the *ahp1* mutant strain which resulted in enhanced fluorescence emission in the presence of the compounds. The number of cells expressing green fluorescence was significantly higher in the presence of BA-PG65, 2, 3- dihydroxybenzoic acid and 3,4-dihydroxybenzoic acid ($p < 0.001$), followed by BA_PG17, BA_PG63, ferulic acid, 2, 5-dihydroxybenzoic acid, and 2, 4-dihydroxycinnamic acid ($p < 0.005$). Further, rosmarinic acid (an ester of caffeic acid) did not have any effect on the green fluorescence expression level in WT yeast. Analysis of the data indicated that some of the compounds contributed to cell death (Figure 5-5). The effect of the compounds on the cells within the population varied. The population distribution effect was more profound in the presence of rosmarinic acid, BA_PG65 and BA_PG84 with formation of two distinct populations of cells (Figure 5-5). The level of green fluorescence expression was reduced in the presence of EGCG (3.78 +/- 0.22) as compared with control (4.39 +/- 0.08). Ferulic acid similar to EGCG is a potent antioxidant but its effect on the green fluorescence expression level was totally opposite to that of EGCG by increasing the green fluorescence expressing cells (6.33 +/- 0.95; Figure 5-5). These data might indicate that some of these compounds increase the resistance of the cells to the effect of GFP-A β_{42} by inducing autophagy. Also, at present it is unclear why there were differences in the outcome of compound treatments on the GFP-A β_{42} expression level between the two strains that were tested. Further, *in vitro* analysis was conducted to determine the effect of these compounds on the synthetic A β_{42} peptide.



5-5 Flow cytometry analysis of the apoptosis and green fluorescence expression induced by ten selected danshen compounds on WT *S. cerevisiae* expressing GFP-A β ₄₂. The exponentially growing BY4743 transformants in selective media (YNB-U) were treated with 50 μ M of danshen compounds and incubated for 6 h. Samples were then treated with PI (1 μ g/ ml) prior to analysis. The fluorescence associated with PI and GFP was then measured on a flow cytometer. Flow cytometry

of nine compounds along with GFP-A β_{42} control and EGCG has been shown. Analysis was performed using WESEAL WEHI software.

5.4.1.3 Anti-oligomerisation screening of danshen derivatives and analogues using thioflavin T analysis

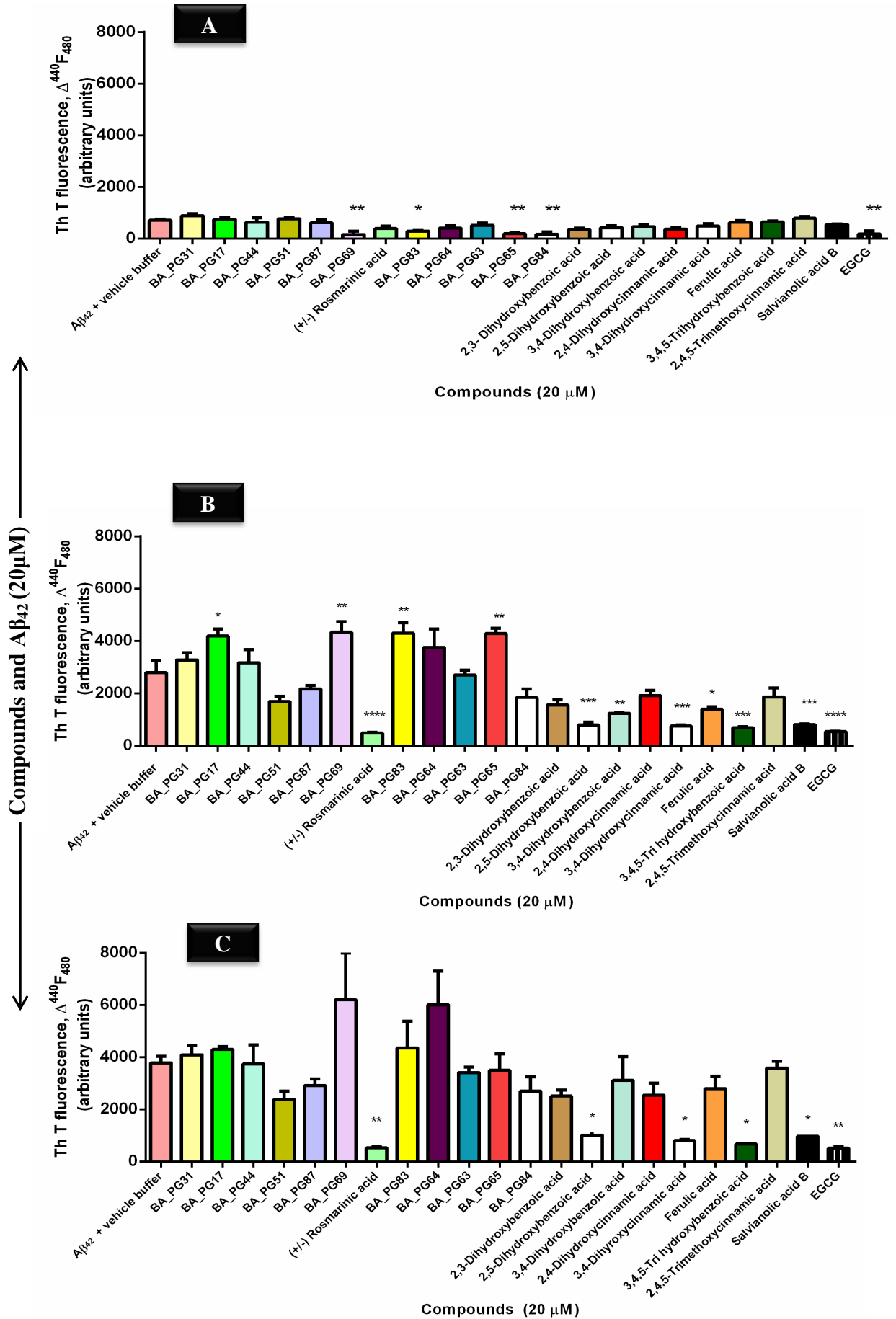
Previous research classified the aggregation inhibitors into three main classes namely those with capability of inhibiting fibril formation, those that inhibit oligomerisation and the last class consists of those that possess both activities (Necula et al., 2007b). Therefore, a ThT assay was employed for identification and classification of danshen compounds. ThT was first described in 1959 (Vassar and Culling, 1959) and is regarded as a “gold standard” due to its capability to selectively stain and identify amyloid fibrils (Naiki et al., 1989; LeVine, 1993; Freire et al., 2014). The ability of danshen compounds to inhibit the formation of A β_{42} aggregates was monitored by co-incubating freshly prepared A β_{42} with compounds and measuring the ThT-induced fluorescence intensity. The colours associated with many of these compounds might interfere with ThT, modulate the fluorescence yield of ThT and bias the results (Hudson et al., 2009). Therefore, analysis of these compounds without addition of A β_{42} peptide was also included. This allowed adjustment of the baselines and elimination of the effect of colour on the photometric readings or quenching of the ThT fluorescence in this assay.

At the baseline (0 h) the starting fluorescence intensity was significantly lower in the positive control (EGCG) compared with A β_{42} and vehicle buffer ($p < 0.01$; Figure 5-6A). A similar effect was also viewed in the presence of BA_PG65, BA_PG84,

BA_PG69, and to lesser extent in BA_PG83 ($p < 0.05$). After 16 h of co-incubation of the compounds with the A β_{42} , the fluorescence intensity in the presence of ThT was measured. Five compounds lowered the fluorescence intensity compared with control samples (ThT negative) indicating their capability to slow aggregation and fibril formation (Figure 5-6B). These were rosmarinic acid ($p < 0.01$), 2, 5-dihydroxybenzoic acid, 3, 4-dihydroxycinnamic acid (caffeic acid), 3, 4, 5-trihydroxybenzoic acid (gallic acid) and salvianolic acid B ($p < 0.05$).

After 24 h co-incubation of compounds with A β_{42} , rosmarinic acid similar to EGCG ($p < 0.001$) exerted the most potent inhibitory effect on peptide aggregate formation (Figure 5-6C). Other compounds that showed aggregation inhibition capacity were 2, 5-dihydroxybenzoic acid (gentisic acid), 3, 4-dihydroxycinnamic acid, 3, 4, 5-trihydroxybenzoic acid, and salvianolic acid B ($p < 0.005$). Also, 3, 4-dihydroxybenzoic acid significantly reduced the aggregation propensity of A β_{42} compared with the control sample ($p < 0.01$).

On the other hand BA_PG69, BA_PG83, BA_PG65 ($p < 0.01$), and BA_PG17 ($p < 0.05$) significantly contributed to an increased ThT associated fluorescence after 24 h co-incubation with chemically-synthesised A β_{42} . Further, the results suggest that these compounds accelerated the aggregation and fibril formation capacity of the peptide compared with the control sample (Figure 5-6C).



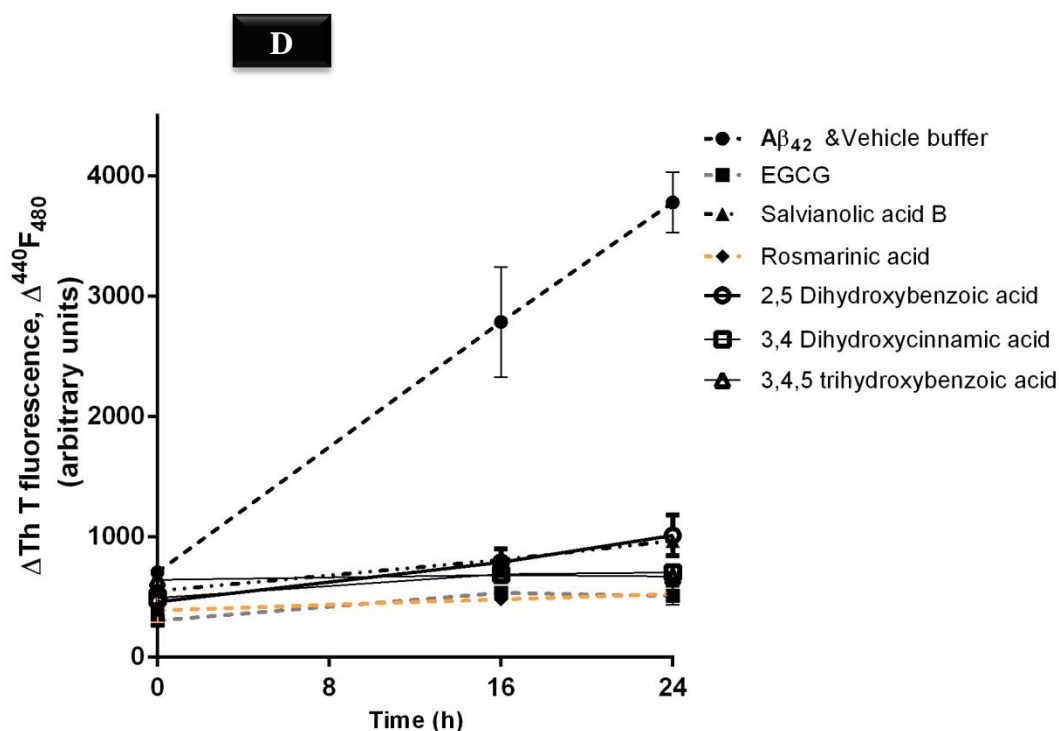


Figure 5-6 Amyloid formation assayed by thioflavin T fluorescence. Fibril formation of A β_{42} and the associated increase in *in situ* ThT fluorescence in the presence and absence of compounds were measured at 0 h (baseline) (A), 16 h (B) and after 24 h (C) incubation was calculated by subtracting the ThT blank from each sample. Significant anti-fibril propensity was determined by comparing the absorbance of compounds in comparison with the control sample. Analysis was done in triplicate. Control samples of only compounds with the ThT without the addition of the A β_{42} peptide were also included to minimise the effect of the compounds' colour on the fluorescence intensity of the ThT. Selected danshen compounds that resulted in a significant anti amyloidogenic property compared with the positive control (EGCG) and negative control (A β_{42} & vehicle buffer) determined by ThT measured at 0, 16 and 24 h after incubation with chemically-synthesised A β_{42} (D). (**** $p < 0.001$, *** $p < 0.005$, ** $p < 0.01$, * $p < 0.05$). All data are expressed as mean \pm SEM (n = 3).

5.4.1.4 Immunoblotting analysis of chemically-synthesised A β_{42} co-incubated with selected danshen compounds

When studying the A β aggregation, although larger fibrillar aggregates remain important (Echeverria et al., 2005; Robinson et al., 2011), small oligomeric aggregates which are reportedly toxic and contribute to the progression of the disease continue to be of interest (Carvalho et al., 2014). Nevertheless, ordered self-

association of A β molecule was identified to be essential for toxicity (Pike et al., 1991). This aggregation pathway however, is reversible such that fibrils can dismantle and give rise to intermediate protofibrils and soluble oligomers (Pryor et al., 2012). In this experiment the selected danshen compounds were investigated for their capacity to prevent oligomeric A β_{42} formation after prolonged incubation. SDS-PAGE of the A β_{42} conformers that formed over 7 days incubation in the presence of ThT negative compounds were analysed by silver staining and Western blot using WO2 monoclonal antibody against the A β peptide.

Silver staining confirmed the presence of A β_{42} peptide in all of the samples but despite being a sensitive technique it did not show differences between treatment and control samples (Figure 5-7A). A β_{42} peptide was detected for all experimental samples (Figure 5-7A; lane 2-6) and control samples (Figure 5-7A; lane 1 & 7). The band intensity for monomer, dimer and tetramer were similar in both silver staining and immunoblot analysis. However, the resolution of oligomeric species was very low, possibly due to gel smearing which prevented quantification of individual sizes of oligomers within this range (Figure 5-7).

The immunoblotting assay revealed that all of the compounds (Figure 5-7B; lanes 1-5) seem to be hindering fibrillogenesis when compared with the untreated control (Figure 5-7B; lane 6). Freshly prepared A β_{42} only formed monomeric and dimeric structures (<14 kDa) with no aggregation detected (Figure 5-7B; lane 7). In monomeric form (4.5 kDa) A β_{42} peptide is said to be harmless (Giuffrida et al., 2010). However, nucleation can trigger self-assembly of these monomeric species of

A β_{42} into oligomers, large intermediate aggregates and eventually fibrillar aggregates (Teplow, 1998, Morris et al., 2009).

Low molecular weight (LMW) oligomer species are distinguished by their solubility and size (>14 kDa) which appear between monomeric and insoluble fibrils (Walsh and Selkoe, 2007). The level of oligomeric peptide was very high in the presence of salvianolic acid B (Figure 5-7B; lane 1). These results indicate the presence of high molecular weight (HMW) species of oligomers and protofibrils especially at > 70 kDa (Figure 5-7B; lane 1). The oligomeric detection in the untreated control on the other hand was very low demonstrating acceleration in formation of insoluble fibrils (Figure 5-7B; lane 6). All of the compounds that lowered the ThT associated fluorescence (ThT negative) apparently were capable of hindering the fibril formation but were not able to prevent oligomerisation altogether. Longer incubation resulted in slower aggregation propensity of the A β_{42} peptide in the presence of these selected ThT negative compounds. These results suggest that selected compounds might act as a ligand for the β -sheet regions on the A β_{42} , hence delaying the association of these regions for aggregation and therefore interfering with the oligomerisation and fibril formation process.

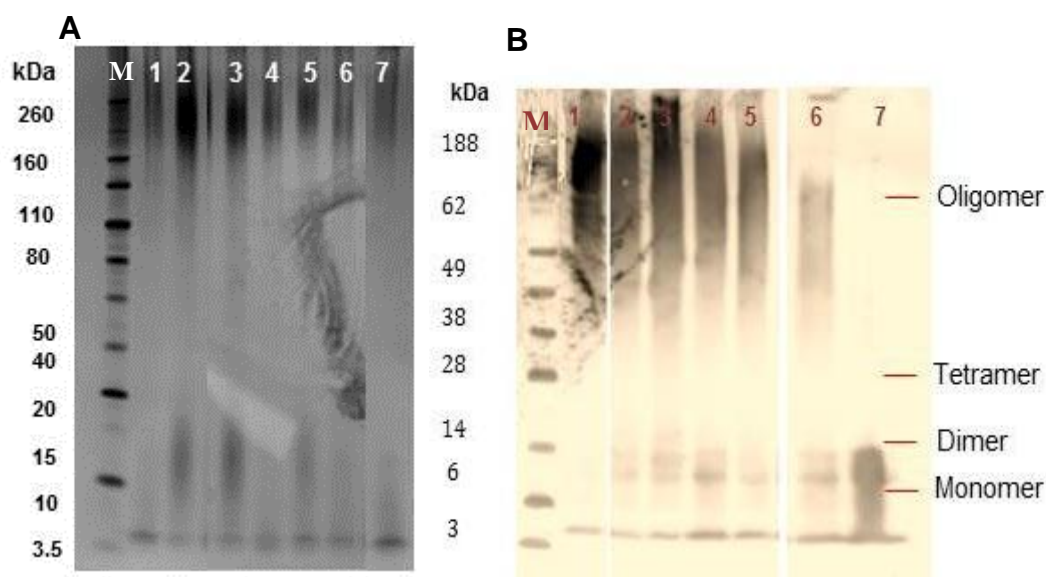


Figure 5-7 SDS-PAGE analyses of A β ₄₂ conformers in the presence and absence of compounds. Peptide solutions co-incubated with the selected danshen compounds were fractionated by SDS-PAGE electrophoresis (4-12% Bis-Tris gel) (Section 2.10.1). 100 ng of each A β ₄₂ sample was analysed by silver staining (A) (Section 2.10.2). Samples are vehicle buffer control & A β ₄₂ (lane 1), salvianolic acid B (lane 2), rosmarinic acid (lane 3), 2, 5-dihydroxybenzoic acid (lane 4), 3, 4-dihydroxycinnamic acid (lane 5), 3, 4, 5-trihydroxybenzoic acid (lane 6), and freshly prepared A β ₄₂ (lane 7). Lane M contains molecular weight marker. 0.5 μ g of each A β ₄₂ sample (from TEM experiment) was also analysed by immunoblotting (Section 2.10.3) using anti-A β WO2 antibody; (B). Samples are salvianolic acid B (lane 1), rosmarinic acid (lane 2), 2, 5-dihydroxybenzoic acid (lane 3), 3, 4-dihydroxycinnamic acid (lane 4), 3, 4, 5-trihydroxybenzoic acid (lane 5), vehicle buffer control & A β ₄₂ (lane 6), and freshly prepared A β ₄₂ (lane 7). Molecular weight markers are shown in lane M.

5.4.1.5 TEM analysis of A β ₄₂ species formed in the presence of selected potent danshen compounds

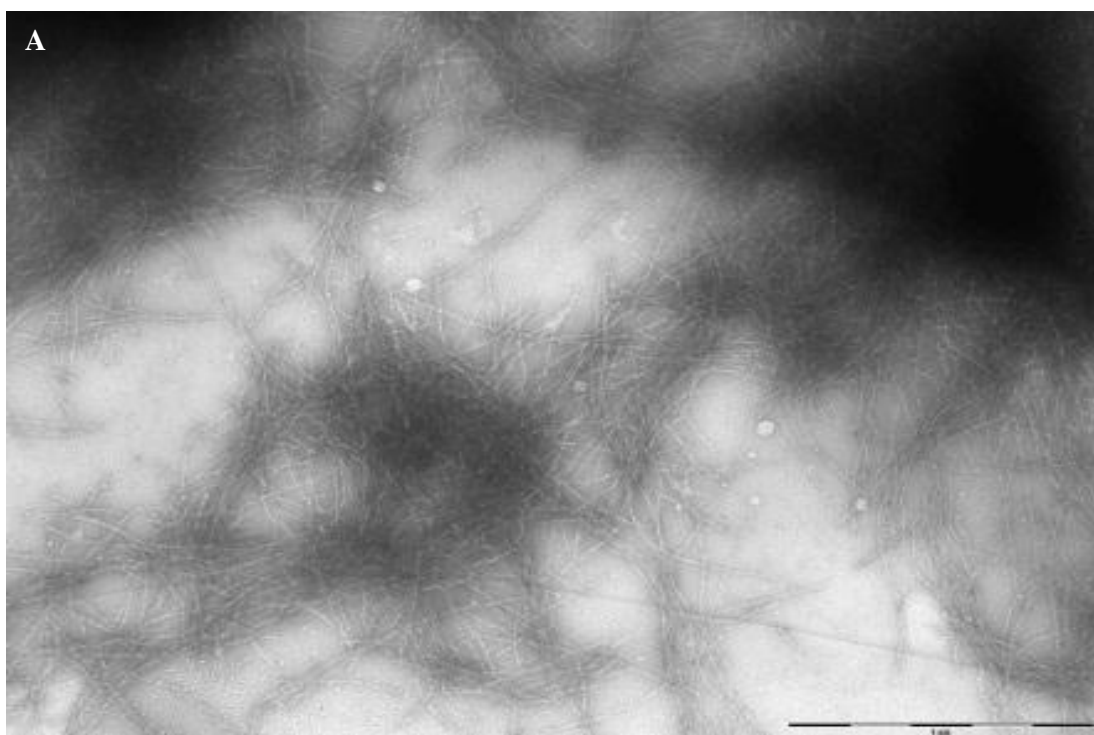
To further explore the effects of the selected ThT negative danshen compounds (Figure 5-5D) on amyloid aggregation and fibril formation, morphological changes during 7 d incubation of A β ₄₂ peptide in the presence of these five selected compounds were examined by TEM. A control sample of chemically-synthesised

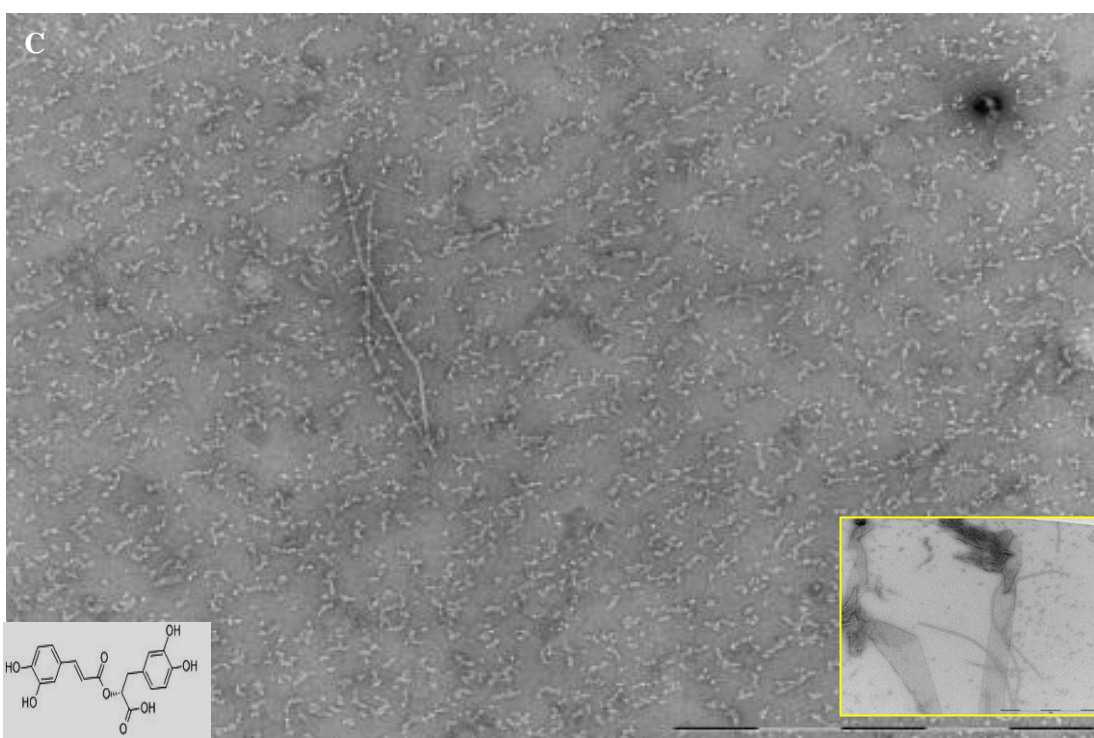
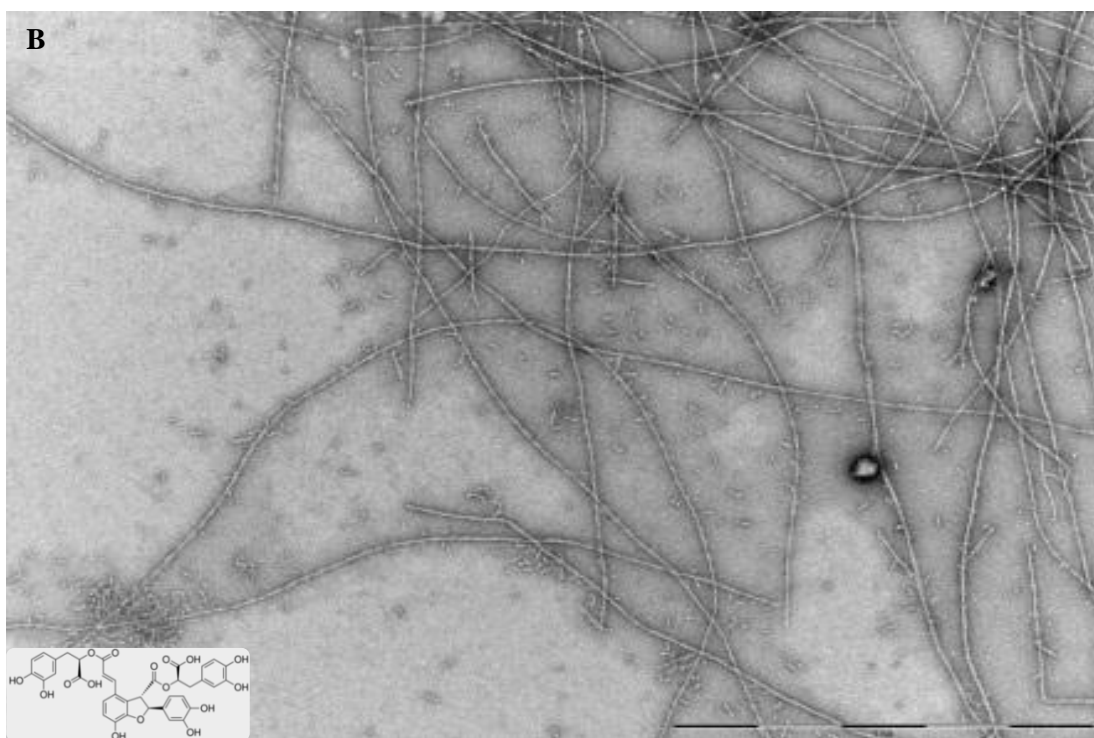
A β ₄₂ peptide with only addition of vehicle buffer was analysed for morphological comparison.

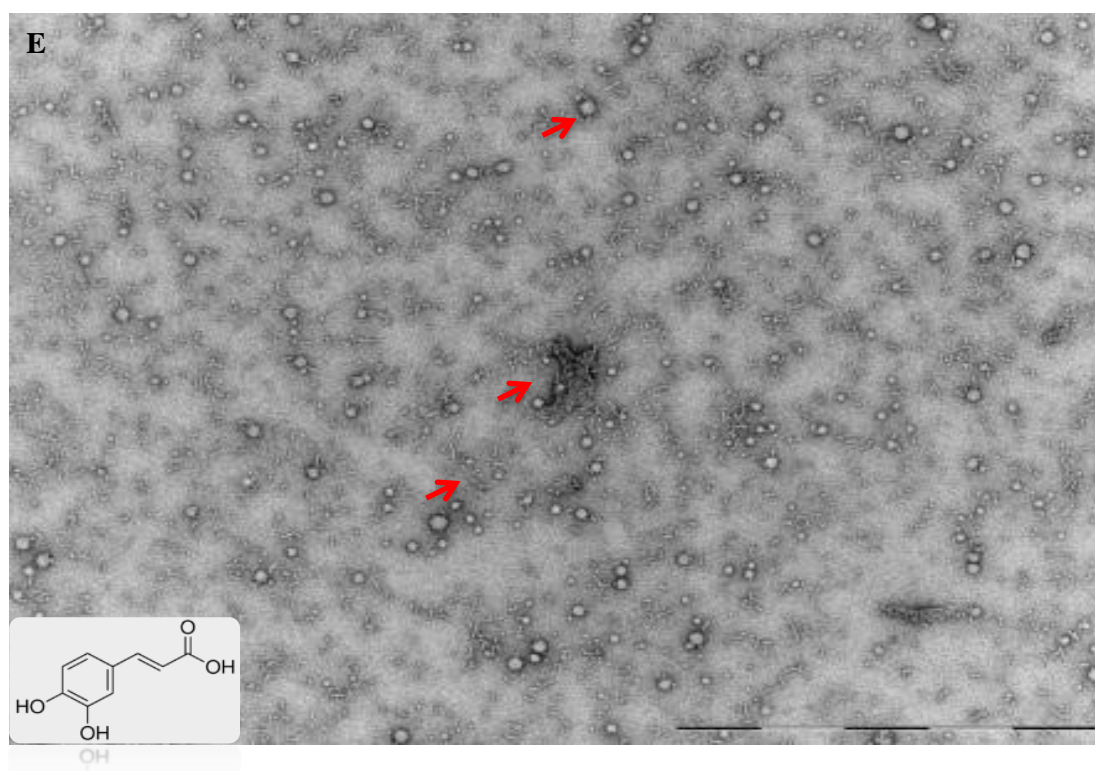
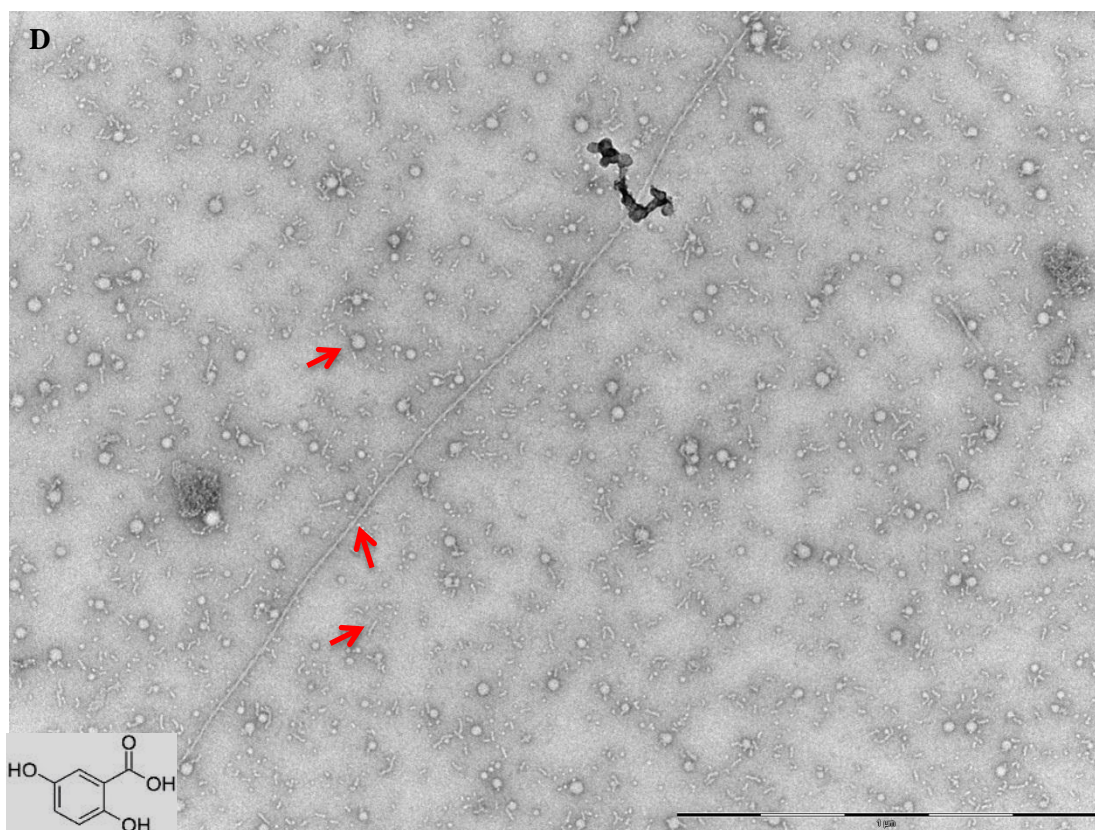
The control A β ₄₂ sample resulted in highly ordered fibrillar structures (Figure 5-8A). Although none of the compounds prevented the aggregation altogether, the extent of protofibrils and fibril formation varied in the presence of different compounds. Structures like sheets, globular and short or long fibrils were formed as a result of the effect of the compounds on the A β ₄₂ conformation.

Salvianolic acid B resulted in formation of HMW species including protofibrils and mature amyloid fibrils. The fibrils were well separated and dispersed compared with the control sample (Figure 5-8B). Rosmarinic acid on the other hand resulted in formation of oligomers, protofibrils, long fibrils, as well as clusters of short fibrillar structures which were merged into sheet-like structures (Figure 5-8C). In the presence of 2, 5-dihydroxybenzoic acid (gentisic acid) (Figure 5-8D) micelle like structures (Vitalis and Caflisch, 2010) along with many protofibrils became visible. However, very few fibrillar structures were detected which were very long in length. Caffeic acid also formed spherical globular micelle-like species (Figure 5-8E). The globule structures presumably represented caffeic acid microdroplets in which A β ₄₂ had deposited and begun to aggregate. After 7 d co-incubation, caffeic acid proved to be a good ligand for the A β ₄₂ peptide, preventing extensive aggregation and fibril formation. 3, 4, 5-trihydroxybenzoic acid (gallic acid; Figure 5-8F) resulted in formation of only a few very long, twisted fibrils.

One possible explanation for detection of high levels of fibrillar structures in the presence of salvianolic acid B and rosmarinic is that these two compounds are capable of accelerating fibril formation after prolonged incubation resulting in a less toxic form of oligomer compared with the soluble toxic form. Another possible explanation would be that these selected ThT negative compounds competitively binds to the β -sheet site of the amyloid fibrils. This result in, inhibition or minimising the ThT interactions with these active sites along the length of the fibrils causing a lower fluorescence emission associated with ThT. These findings have also been previously reported (Hudson et al., 2009) and it could be that similarity in the aromatic structure of ThT and polyphenols contributes to differing results generated by the ThT method compared with TEM.







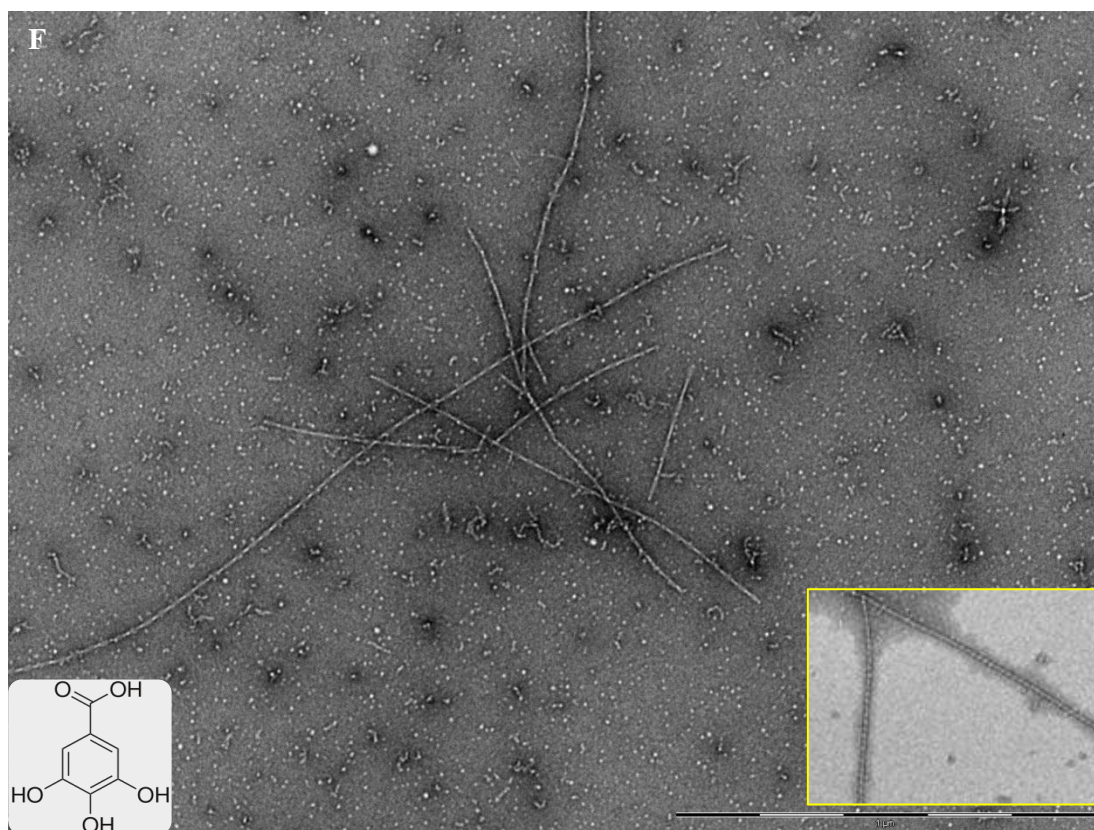


Figure 5-8 TEM micrographs of $A\beta_{42}$ co-incubated with selected compounds. Morphological effects of selected compounds on chemically-synthesised $A\beta_{42}$ aggregation was investigated and compared with control samples. Micrograph of $A\beta_{42}$ sample without addition of compounds (control) (A). Micrograph of chemically-synthesised $A\beta_{42}$ in presence of salvianolic acid B (B), rosmarinic acid (C), 2, 5-dihydroxybenzoic acid (gentisic acid) (D), 3, 4-dihydroxycinnamic acid (caffeic acid; E), and 3, 4, 5-trihydroxybenzoic acid (gallic acid; F). Arrows show micelle (globular) structures, protofibrils and fibrillar species of $A\beta_{42}$. Micrographs showing other conformational species of peptide formed by the compound is highlighted in yellow box. Structure of each compound is also shown on the micrograph. Scale bars = 200 nm

5.4.1.6 Effect of selected danshen compounds on the toxicity of $A\beta_{42}$

The cytotoxicity effect of HFIP pretreated $A\beta_{42}$ (5 μM) and the protection of the five selected danshen compounds (50 μM) were tested on *C. glabrata* cells. It should be noted that at 50 μM concentration none of these selected compounds are toxic or inhibitory to yeast cells.

The percentage survival of yeast cells in the presence of A β ₄₂ was only ~10% of the untreated control sample (Figure 5-9). All of the selected danshen compounds were capable of inhibiting toxicity to the *C. glabrata* cells when compared with the control. Salvianolic acid B ($p < 0.001$) followed by gentisic acid gallic acid, and Caffeic acid ($p < 0.005$) were the most effective (Figure 5-9).

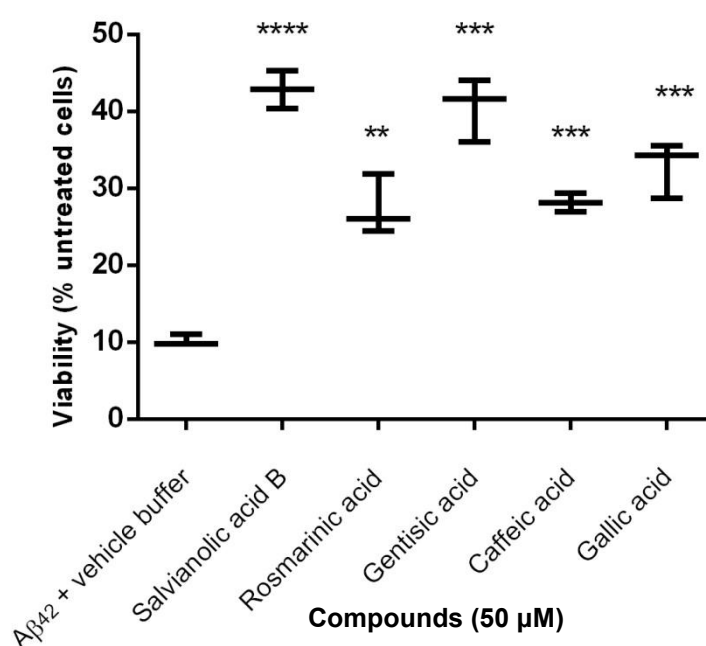


Figure 5-9 Cytotoxicity effect of freshly prepared A β ₄₂ on *C. glabrata* cells. *C. glabrata* was grown into exponential phase according to section 2.3.1. Cells were then treated with selected danshen compounds and incubated for minimum of 6 h. Then HFIP pre-treated A β ₄₂ (5 μ M) was prepared and then added to each sample, including control and incubated overnight. Untreated samples were also included. Viability was determined by transferring 100 μ l of cell suspension the next day on YEPD solid media and reporting it as a percentage of untreated cells. (**** $p < 0.001$, *** $p < 0.005$, ** $p < 0.01$). All data are expressed as mean \pm SEM ($n = 4$).

5.4.1.7 Cytotoxicity of the A β ₄₂ species generated in the presence of the selected five danshen compounds

In order to elucidate the modulation in the structural conformation of A β ₄₂ upon treatments with compounds for 7 d (Section 2.12.1), the cytotoxicity of these conformers were tested on yeast cells. In order to achieve similar A β ₄₂ species in the presence of the compounds, samples were prepared in a similar manner to that for TEM. The conformation produced by the aged A β ₄₂ control solution is not toxic. The toxic effect is very similar and probably as a result of the vehicle control buffer (Figure 5-10A, B). The vehicle control buffer contains 10 x PBS with a high level of phosphate and is seemingly toxic to yeast cells. This toxicity is more profound in *C. glabrata* than *S. cerevisiae* with almost double cell survival with the latter (< 60%) compared with former (< 30%). While identical aliquots of each sample of A β ₄₂ co-incubated with compound were used for treatment of *C. glabrata* and *S. cerevisiae*, the effect is vastly different (Figure 5-10A, B). Further, significant cytoprotective activity in *C. glabrata* (Figure 5-10A) was observed with gallic acid ($p < 0.005$) whereas in *S. cerevisiae* (Figure 5-10B), rosmarinic acid ($p < 0.001$) was the most protective followed by gentisic and caffeic acid ($p < 0.005$). Interestingly, gallic acid was the only compound that caused significant toxicity to the *S. cerevisiae* cells ($p < 0.005$). It is important to note that the fibrillar species formed by gallic acid were more twisted compared with rosmarinic and salvianolic acid. These differences in the fibrillar conformation might be a major contributing factor for their interaction with the yeast cell wall.

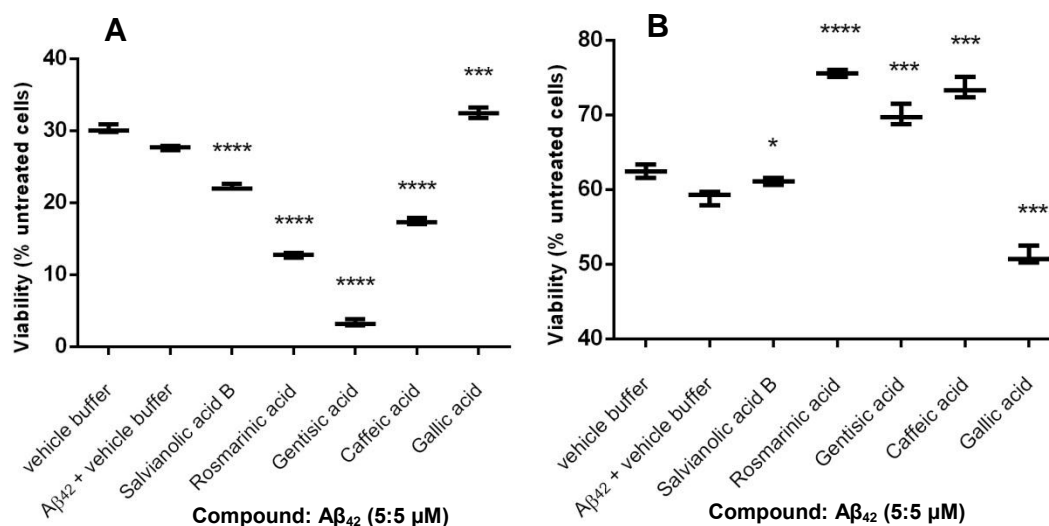


Figure 5-10 Effect of conformational changes of synthetic Aβ₄₂ produced in the presence of danshen compounds on the survival of yeast cells. *C. glabrata* (ATCC90030) (A) and *S. cerevisiae* (BY4743) (B) were grown to exponential phase. Aβ₄₂ conformers were generated according to Section 2.12.1. Cells were then incubated with the Aβ₄₂ conformers developed by incubation for 7 d with compounds. Survival was determined by colony forming units on YEPD complete media plate. (**** $p < 0.001$, *** $p < 0.005$, ** $p < 0.01$). All data are expressed as mean \pm SEM (n = 3).

5.4.2 MATNAP PROPRIETARY COMPOUNDS ANALYSIS- Minimum inhibitory concentration determination

The following compound group consists of 15 chemicals that were dissolved in DMSO to the final concentration of 1 mM (Appendix A, Table 2). As the toxicity of these compounds is not known, the MIC 90 was determined on *C. albicans* to determine their effect on the survival of yeast (Figure 5-11). The DMSO level was kept to < 0.1% in all of the following experiments.

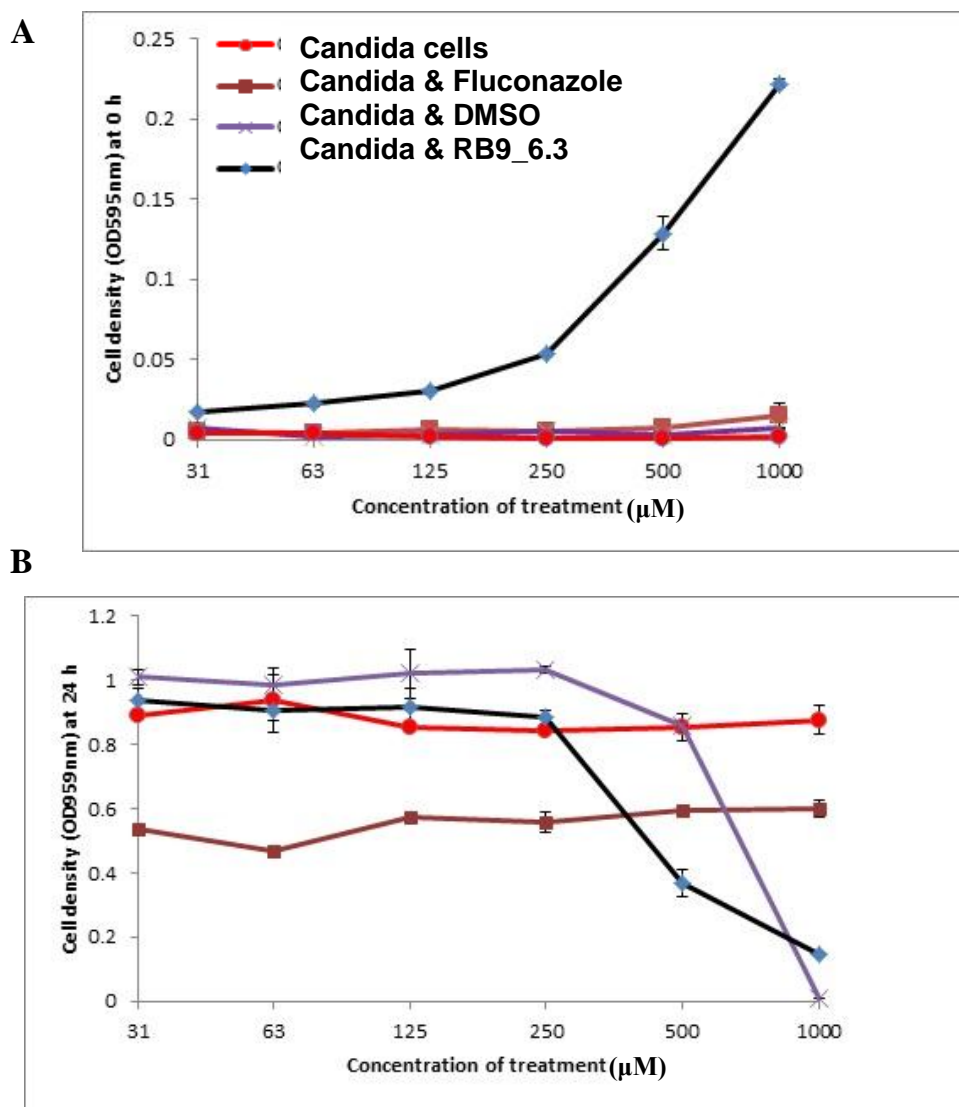


Figure 5-11 An example of MIC 90 determination for RB9_6.3 on *C. albicans* WM1172. Positive control of untreated *C. albicans* cells and negative controls containing Fluconazole were also included (Section 2.3.5). Growths of the cells were monitored by measuring optical density at 595 nm at the baseline (0 h) (A) and after 24 h of incubation (B). All compounds were tested using a broth micro-dilution method. In order to avoid bias in the MIC determination due to colour associated with each compound, the differences between treated and untreated samples at the baseline was subtracted from the final values for the compounds. The approximate MICs for 90% were determined as the lowest concentration that suppressed any visible growth.

5.4.2.1 Fluorescence produced in associated with an *AHP1* deletant mutant expressing green fluorescent protein fused to A β ₄₂ (GFP-A β ₄₂) in the presence of MATNAP compounds

The *S. cerevisiae*, *ahp1* mutant transformed with GFP and GFP-A β ₄₂ were used to analyse the effect of these compounds (50 μ M) on the fluorescent protein expression level. None of the compounds affected the fluorescent expression of GFP transformant (Figure 5-12A) whereas, RB9_6.3 significantly reduced ($p < 0.01$) the number cells capable of expressing green fluorescent in GFP-A β ₄₂ transformants (Figure 5-12B).

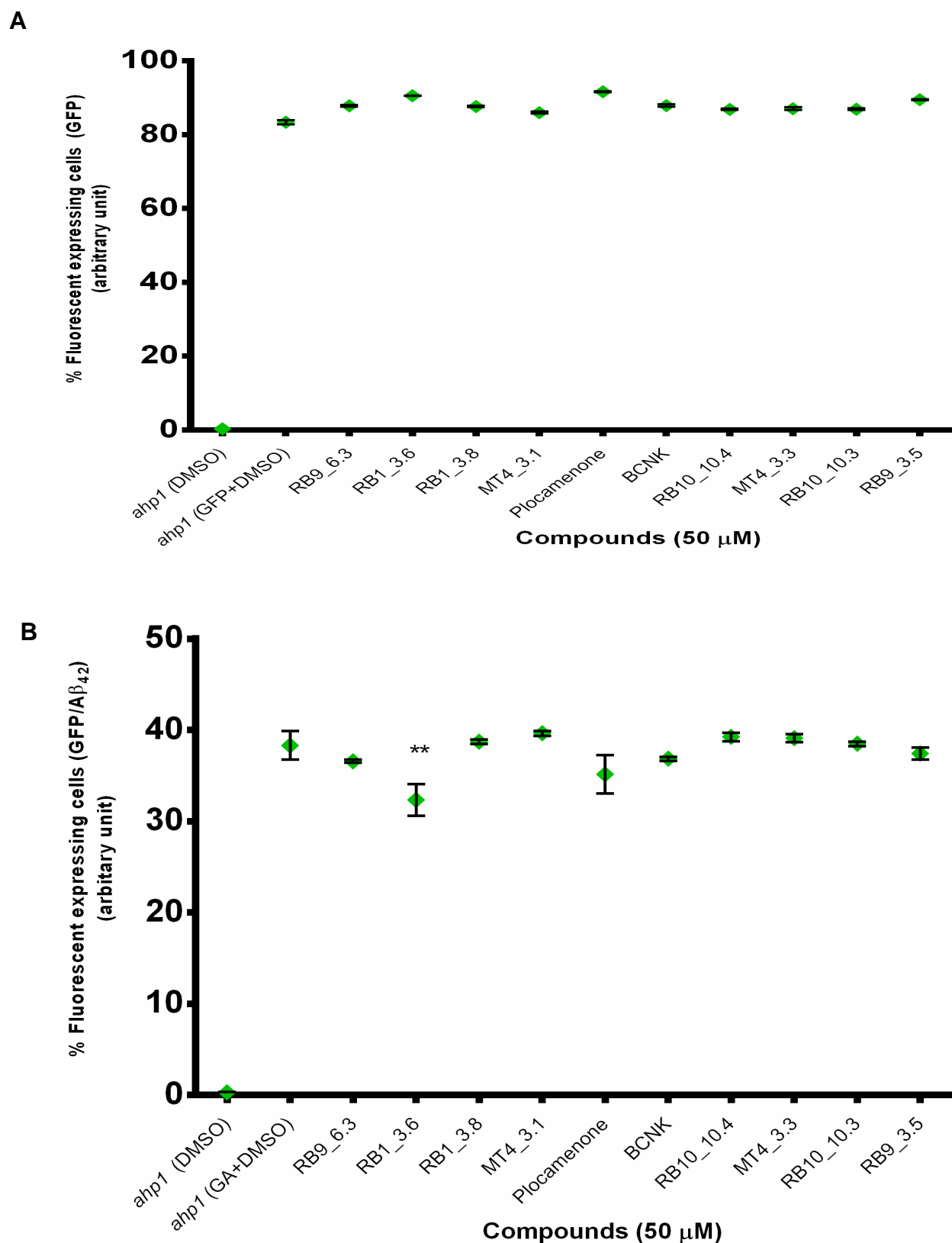
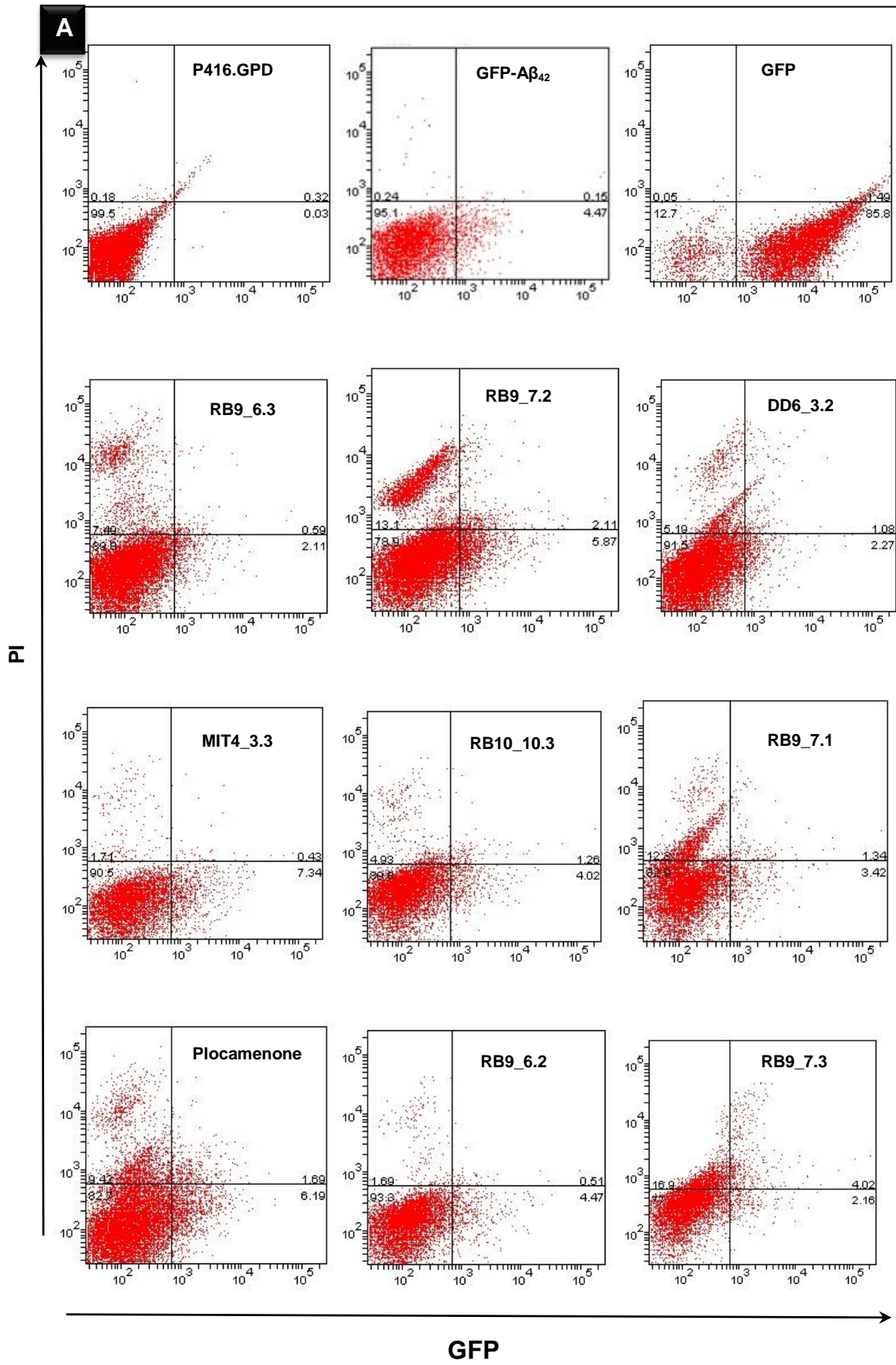


Figure 5-12 Intensity of fluorescence expression in *ahp1* transformed with GFP (A) and GFP-A β_{42} (GA) (B) as measured by flow cytometry. A library of 15 compounds (50 μ M) dissolved in DMSO was examined with *in vivo* yeast based assays to identify those with capability of enhancing autophagy or anti-misfolding characteristics. Exponentially growing yeast cells transformed with GFP and GA

plasmids were incubated with 50 μ M compounds in selective media and grown for further 6 h at 30°C with shaking. Samples were taken and analysed by flow cytometry. None of the compounds affected the green fluorescence level in the GFP transformants (A). Only RB9_6.3 significantly decreased the fluorescence level of the GA transformants compared with GA/DMSO control sample ($p < 0.01$). All data are expressed as mean \pm SEM ($n = 6$).

5.4.2.2 Fluorescence based screening of the wild-type *S. cerevisiae* (BY4743) transformed with GFP-A β ₄₂ plasmid in the presence of MATNAP compounds

Green fluorescence in BY4743 cells transformed with GFP- A β ₄₂ plasmid in the presence of these compounds (50 μ M) was analysed using a flow cytometer (Section 2.6.2). The fluorescent intensity (FI) of each compound was then determined as a percentage of average fluorescence of samples compared with control samples transformed with an empty vector (p416.GPD). The scatter graph of the flow cytometer showed the presence of two distinct cell populations in the presence of RB9_6.3, Plocamenone, and RB9_7.2 (Figure 5-13A). The effect of the compounds on the green fluorescence expression in WT transformants was different to the mutant (5.2.2.2). Analysis of data showed a significant decrease in FI in the presence of RB1_3.6 ($p < 0.05$) whilst, nine compounds increased the FI (Figure 5-13B). Also, the level of GFP-A β ₄₂ expression was affected by these compounds with five chemicals namely, RB9_6.3, RB1_3.6, DD6_3.2, RB10_10.4 and RB9_7.3 and was observed as a significant reduction of fluorescing cells ($p < 0.001$). Another five chemicals remained ineffective while, the last five compounds enhanced the number of fluorescing cells (Figure 5-13C).



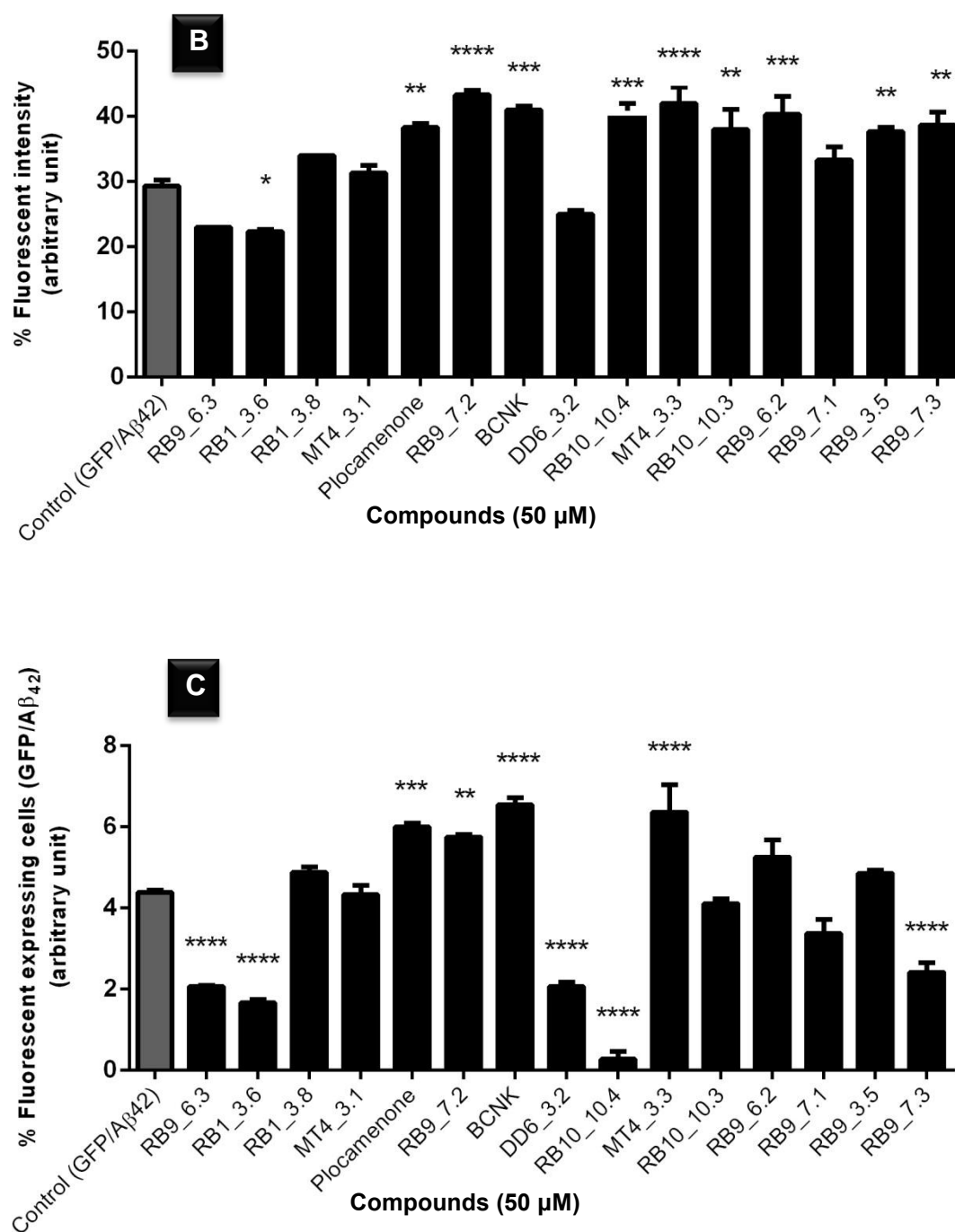
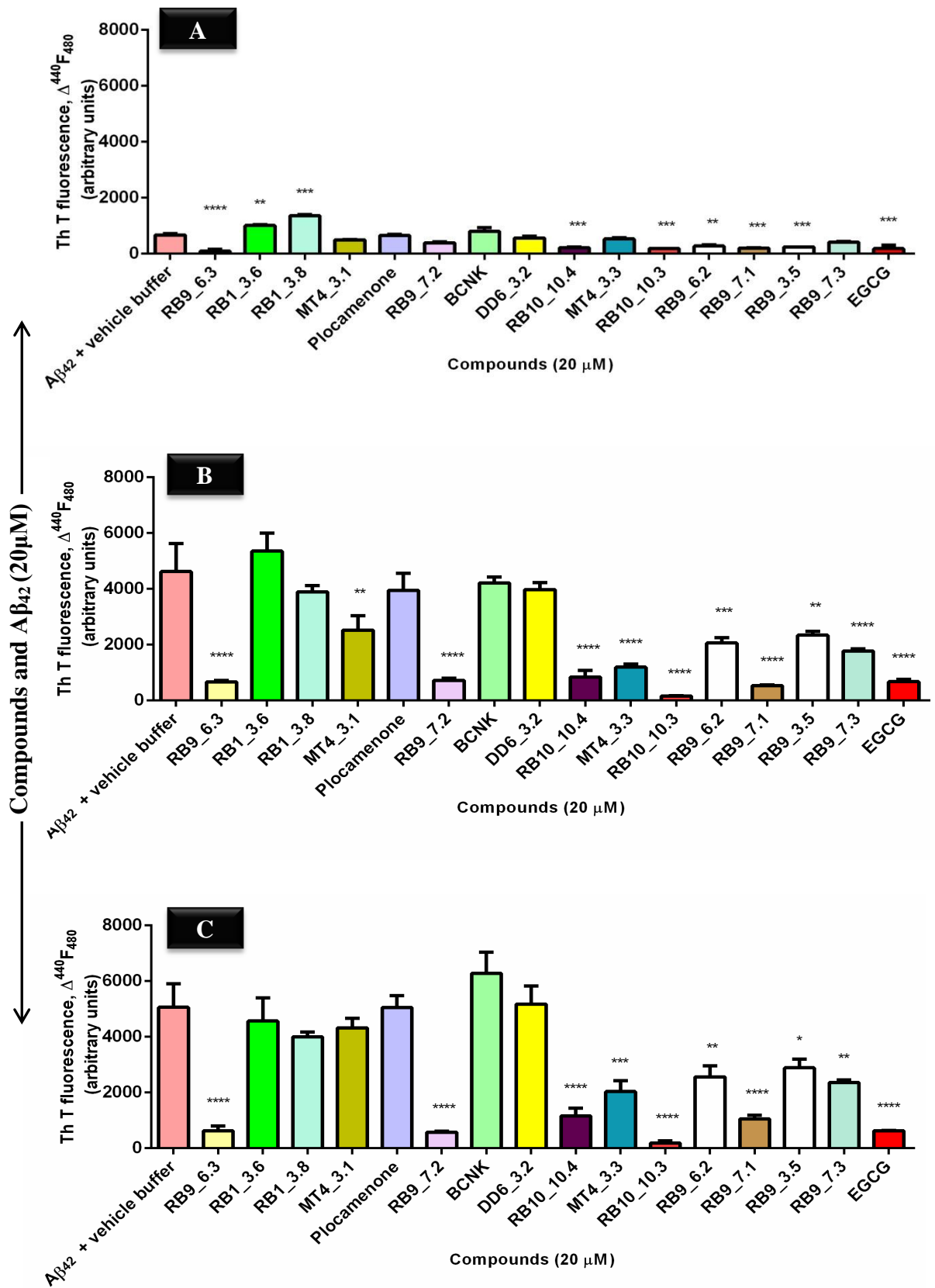


Figure 5-13 Anti aggregation propensity of MATNAP compounds (50 μM) using GFP-Aβ₄₂ WT *S. cerevisiae* transformants. Flow cytometry graphs displaying the effect of selected compounds on the survival of cells (measured by propidium iodide) and green fluorescence expression level are shown (A). The percentage FI of transformants in the presence of compounds compared with control (B). Exponentially growing cells were treated with treated with the compounds and incubated for at least 6 h prior to flow cytometry analysis. (*** $p < 0.005$, ** $p < 0.01$, * $p < 0.05$). All data are expressed as mean \pm SEM (n = 6).

5.4.2.3 Anti-oligomerisation analysis of structurally designed, MATNAP molecules by thioflavin T assay

In order to determine the anti-amyloidogenicity of this class of compounds, ThT analysis was performed at 0, 16 and 24 h of co-incubation of (20 μ M) compounds with A β ₄₂. Most of these compounds have associated colours which might interfere with the ThT fluorescence. Despite adjusting the effect of associated colours by including samples without addition of A β ₄₂, many samples revealed their capability to quench or interfere with the ThT fluorescence significantly at 0 h (Figure 5-5A). After 16 h incubation ten compounds showed significant lower ThT associated fluorescence compared with the control sample (Figure 5-14B). Overnight co-incubation however resulted in identifying eight compounds with ability to reduce fluorescence associated with ThT. Among those, only four compounds were selected as ThT negative, due to their similarities in oligomerisation kinetics to EGCG (Figure 5-14D).



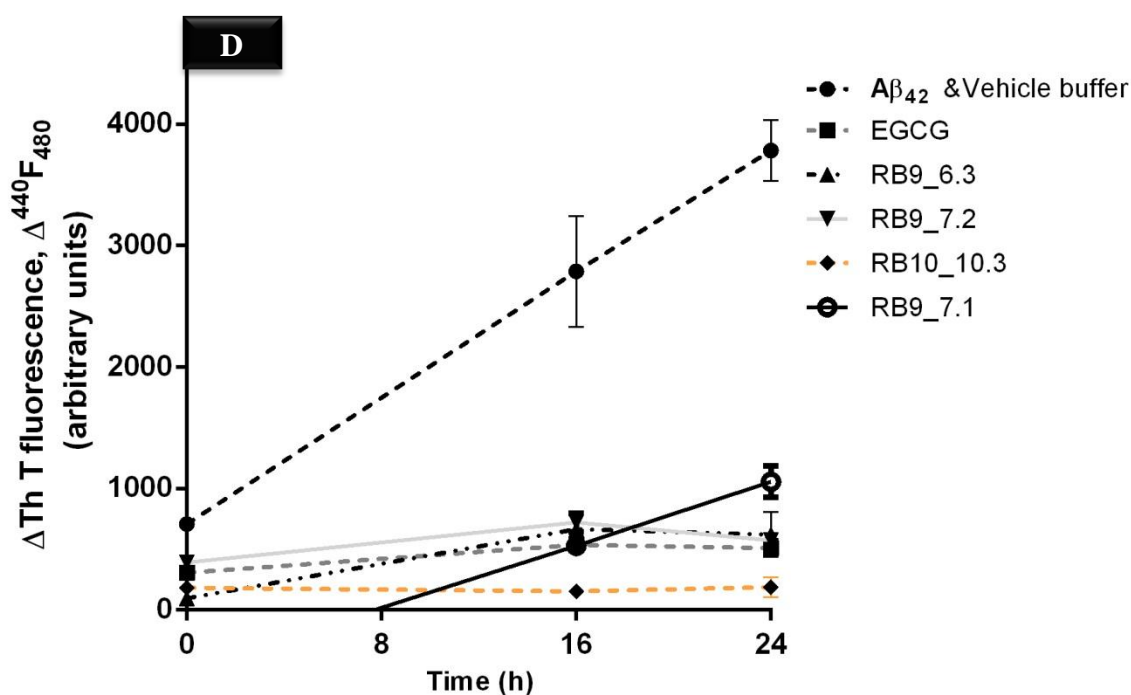
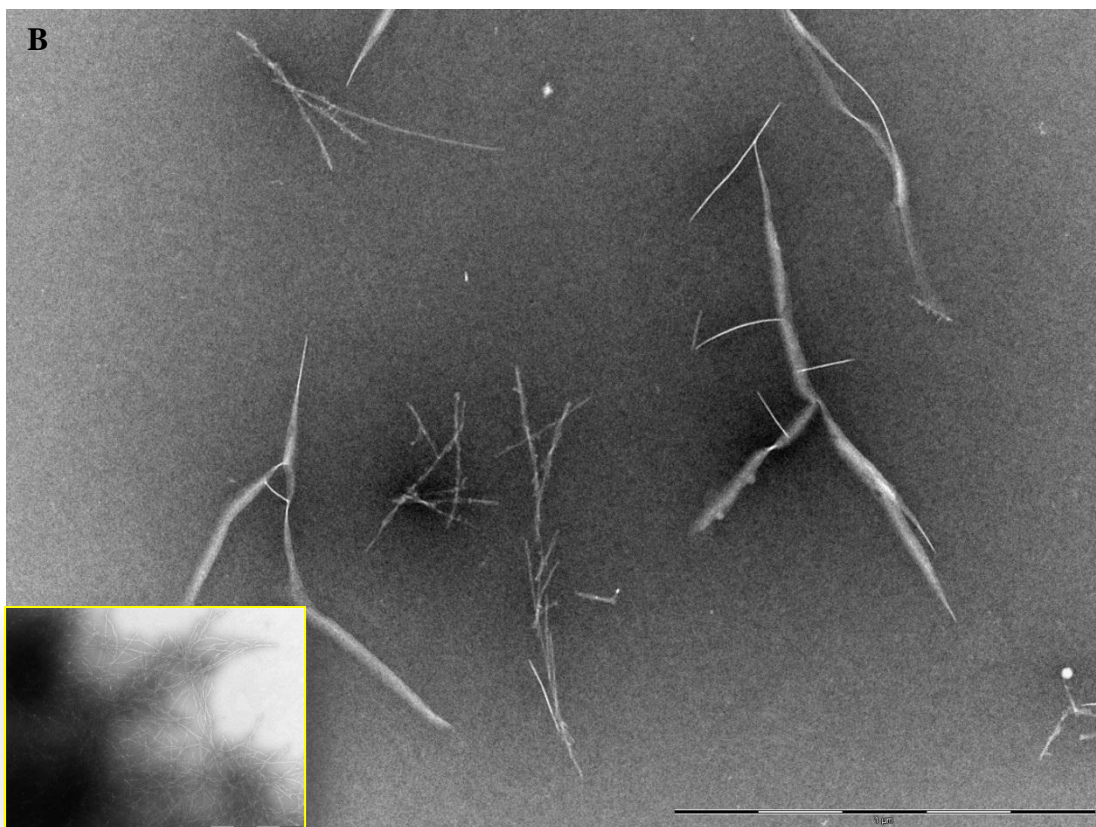
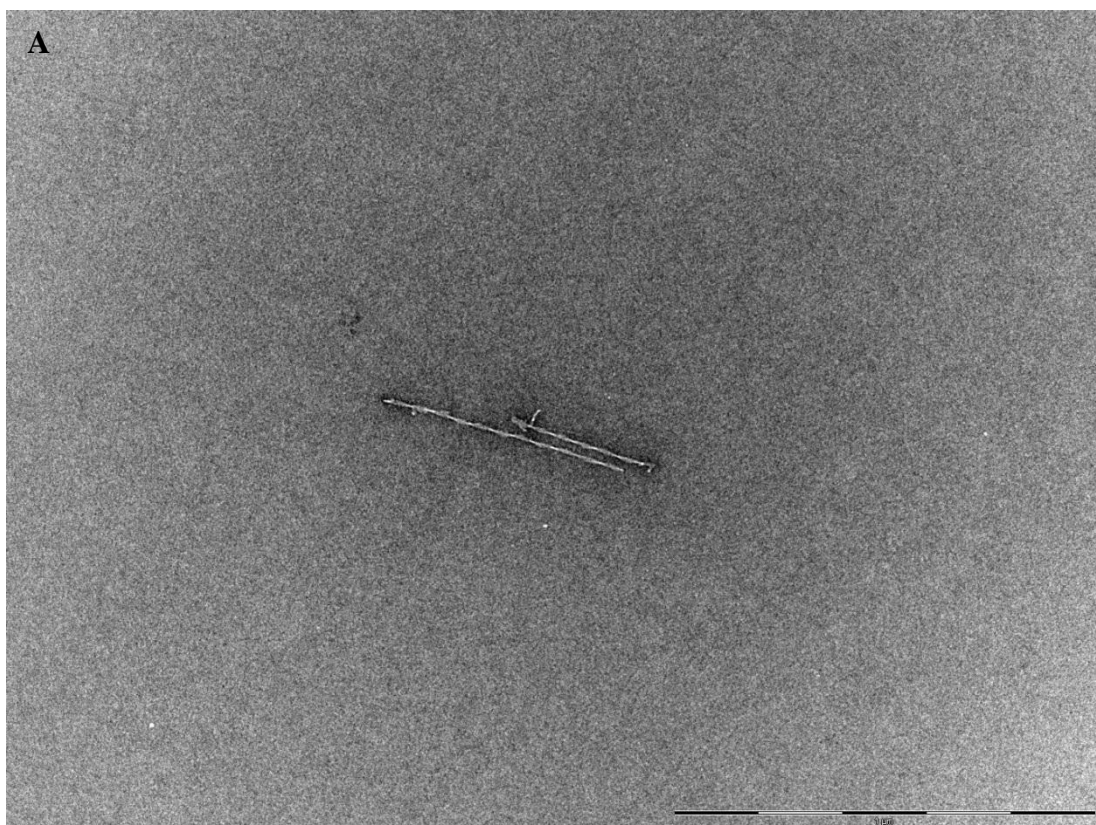


Figure 5-14 Amyloid formation assayed by thioflavin T fluorescence after incubation with MATNAP compounds. Fibril formation of Aβ₄₂ and the associated increase in *in situ* ThT fluorescence in presence and absence of compounds were measured at 0 h (baseline) (A), 16 h (B) and after 24 h (C) incubation. Kinetics of fibril formation of selected compounds monitored by ThT fluorescence compared with the positive control (EGCG) and negative control (Aβ₄₂ & vehicle buffer) measured at 0, 16 and 24 h after incubation with chemically-synthesised Aβ₄₂ (D). (**** $p < 0.001$, *** $p < 0.005$, ** $p < 0.01$, * $p < 0.05$). All data are expressed as mean \pm SEM (n = 3).

5.4.2.4 TEM analysis of Aβ₄₂ species formed in the presence of selected MATNAP compounds

Morphological changes to the Aβ₄₂ incubated for 7 d in the presence and absence of the compounds was investigated by TEM imaging. RB9_6.3 was associated with formation of very few fibrils which were very short in length but branched (Figure 5-15A). RB9_7.2 resulted in clusters of highly branched amyloid fibrils as well as long ribbon like species (Figure 5-15B). RB9_7.1 also did not show any anti-

aggregation propensity as clusters of fibrils similar in morphology to the control sample were visible in some of the micrographs (Figure 5-15C). This indicated the colour associated with these compounds was perhaps quenching the ThT fluorescence and as a result displayed false ThT effects. Only RB10_10.3 showed signs of hindering oligomerisation and fibril formation as only few short fibrillar species were detected (Figure 5-15D).



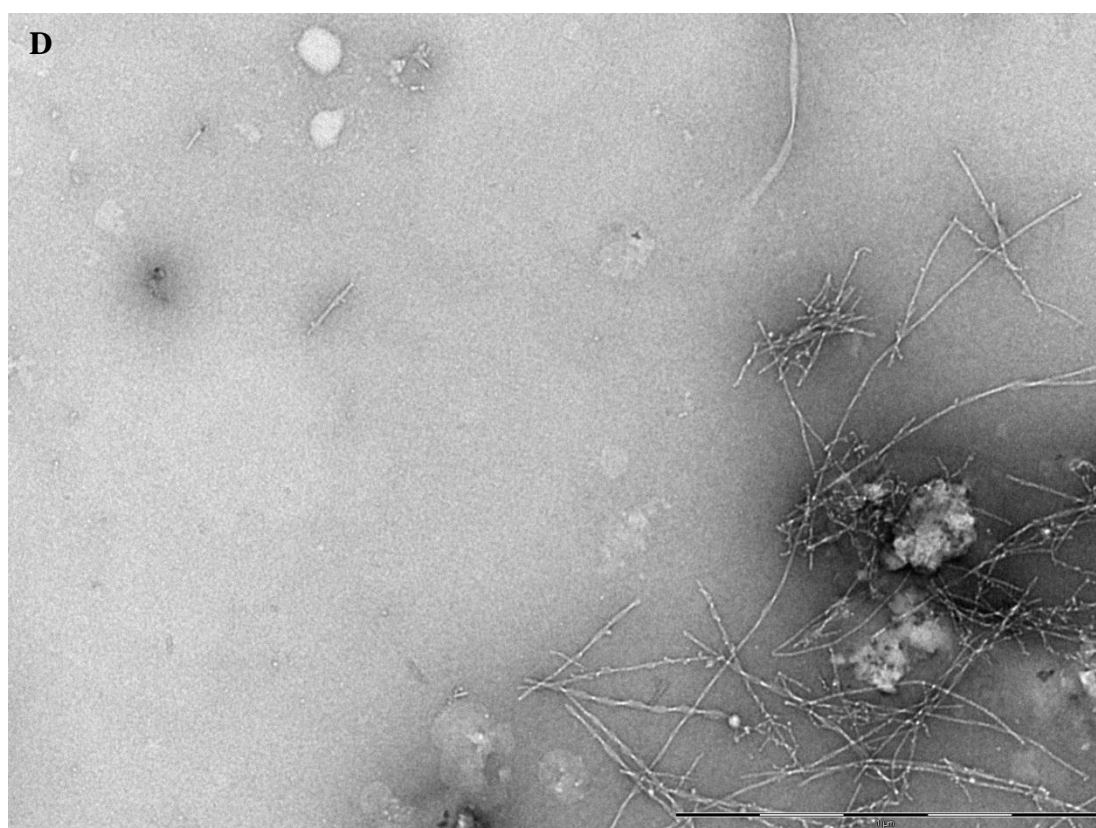
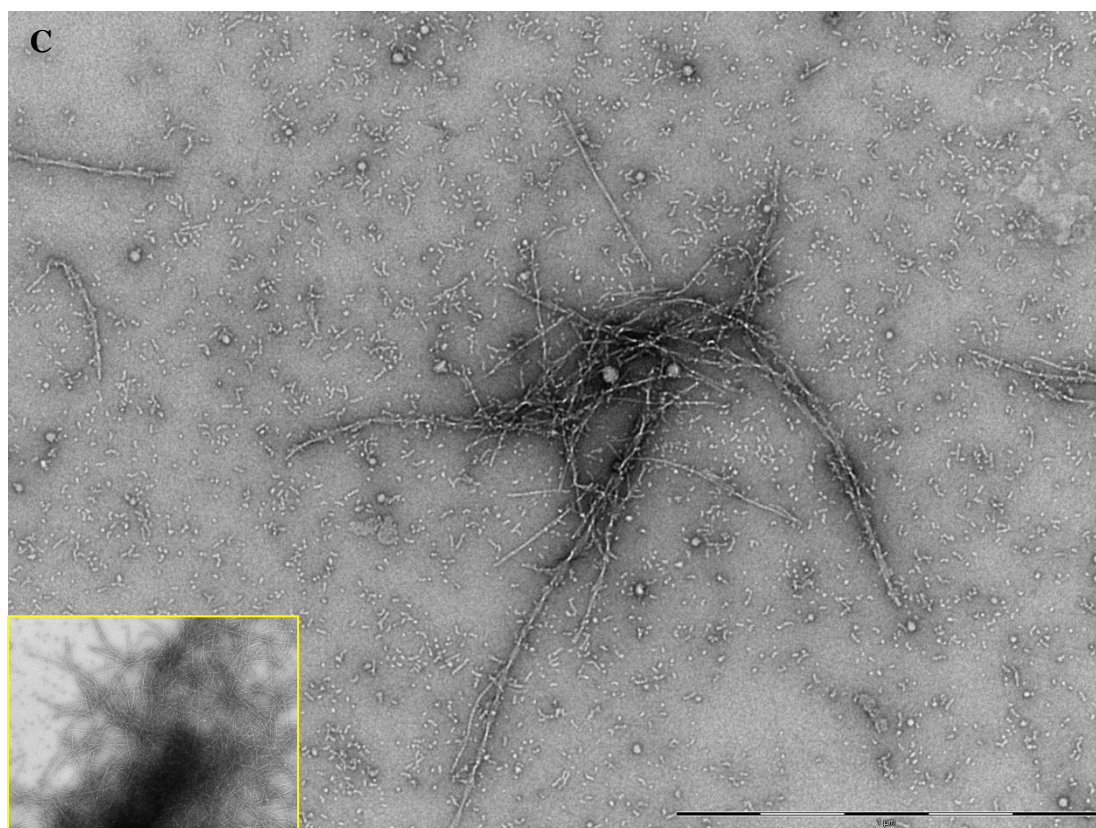


Figure 5-15 TEM micrographs of $A\beta_{42}$ co-incubated with selected ThT negative compounds. Morphological differences of the peptide formed in the presence of 20 μM of RB9_6.3 (A) RB9_7.2 (B) RB9_7.1(C) RB10_10.3 (D) after 7 d incubation has been shown. Only RB9_6.3 and RB10_10.3 reduced the formation of fibrillar

structures compared with an untreated control sample. Micrograph showing other conformational species of peptide formed by the compound is highlighted in the yellow box. Scale bars = 200 nm

5.4.2.5 Silver staining and western blot analysis of the anti-amyloidogenic candidates

SDS-PAGE, the most common electrophoretic technique for A β oligomer size determination, was applied in conjunction with silver staining and immunoblot with monoclonal WO2 antibody. This allowed analysis of the anti-aggregation propensity of these selected compounds. A β ₄₂ peptide was co-incubated with the selected ThT negative compounds for 7 d. Then 0.5 μ g was analysed for detection of low and high molecular weight oligomers. Based on these ThT results it was expected to identify high levels of monomeric species of A β ₄₂ peptide associated with co-incubation with selected compounds.

Freshly dissolved A β ₄₂ peptide exhibited a range of monomeric species from 5-15 kDa. The resolution of these species was low with silver staining due to gel smearing, although the band intensity for monomer, trimer, and tetramer bands were similar in both methods as reported previously (Moore et al., 2009). It appears that 40 to 60 kDa intermediate sized oligomers were more apparent in the immunoblot analysis (Figure 5-16).

Sample RB9_7.2 (Figure 5-16B; lane 3) and RB9_7.1 (Figure 5-16B; lane 4) demonstrated the presence of HMW oligomers which was consistent with the TEM

images where fibrillar and oligomer intermediates were detected (Figure 5-16B, C). Although, freshly prepared peptide exhibited a range of LMW species <14 kDa (Figure 5-16B; lane 6), the aged peptide contained only high molecular weight oligomers from 49 to 200 kDa, illustrating that the peptide had formed into insoluble fibrils. The other two samples of RB9_6.3 (lane 1) and RB10_10.3 (lane 2) exhibited the presence of dimeric species, HMW oligomers were still visible (> 38 kDa; Figure 5-16B). This indicates that the effect of many of these compounds is time dependant and they lose their potency over the time.

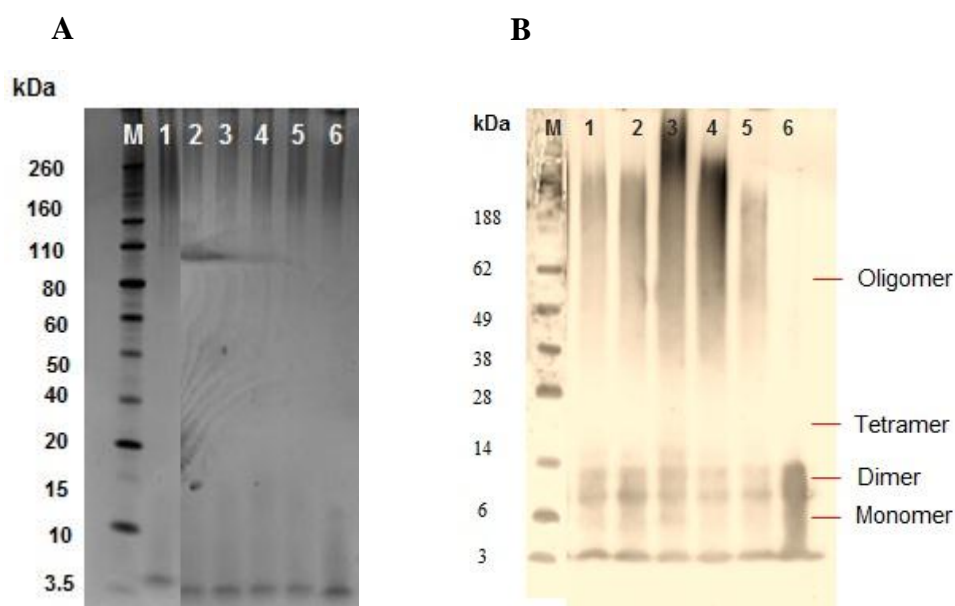


Figure 5-16 SDS-PAGE analysis of the aggregation states of Aβ₄₂ peptides. Freshly dissolved Aβ₄₂ (20 μM) was incubated with selected compounds (20 μM) at 37°C for 7 d. Peptide solutions were fractionated by SDS-PAGE electrophoresis (4-12% Bis-Tris gel) (section 2.10.1). 100 ng of peptide from each sample was analysed by silver staining (A) and 0.5 μg for immunoblot using monoclonal WO2 antibody (B). Lanes 1 to 6 in silver staining are vehicle buffer control & Aβ₄₂ (lane 1), RB9_6.3 (lane 2), RB9_7.2 (lane 3), RB9_7.1 (lane 4), RB10_10.3 (lane 5), and freshly prepared Aβ₄₂ (lane 6). Molecular weight markers are shown in lane M. The samples on western blot gel are; RB9_6.3 (lane 1), RB10_10.3 (lane 2), RB9_7.2 (lane 3), RB9_7.1 (lane 4), vehicle control and Aβ₄₂ sample (lane 5), freshly prepared Aβ₄₂ (lane 6). As a chemifluorescent substrate was used, the fluorescence selected for imaging the western blot was based on sensitivity and ability to provide better visualisation of the protein sizes formed in each sample.

5.4.2.6 Cytotoxicity of the A β ₄₂ species formed as a result of co-incubation with selected compounds on yeast

Prolonged co-incubation of A β ₄₂ with selected compounds resulted in formation of various oligomeric species (Section 5.4.2.4). To further identify whether any of these A β ₄₂ species can influence the survival of yeast, exponentially growing *C. glabrata* and *S. cerevisiae* were used to examine their effect on viability. Data analysis revealed that only the A β ₄₂ conformation made in the presence of RB9_7.2 which displayed high level of ribbon like species was toxic to both *S. cerevisiae* (Figure 5-17A) and *C. glabrata* (Figure 5-17B) cells ($p < 0.001$). It should be noted that the toxicity of RB9_7.2 co-incubated with A β ₄₂ is due to the conformational structure of the peptide as the compound in the tested concentration is not toxic to yeast cells (Appendix A, Table 2).

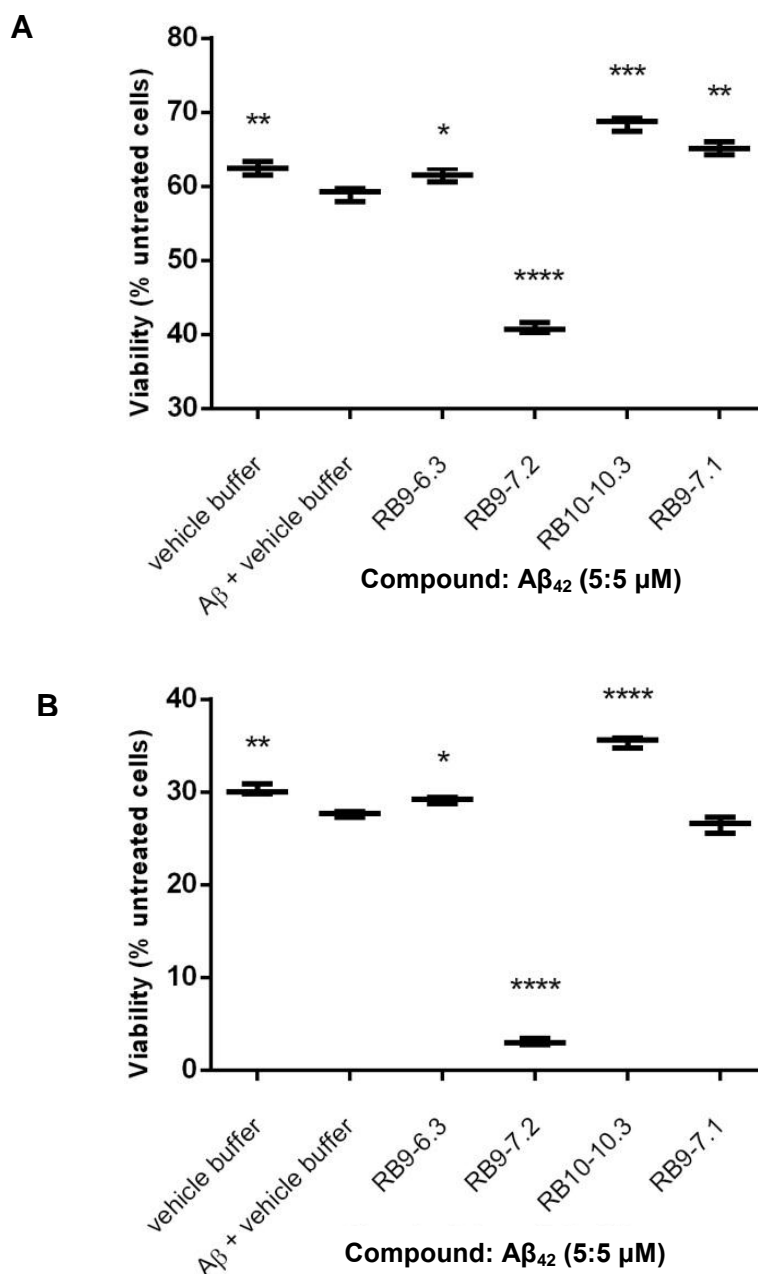


Figure 5-17 Toxicity effect of synthetic Aβ₄₂ species produced in the presence of selected ThT negative compounds on the survival of yeast cells. (A) *S. cerevisiae* (BY4743) (B) *C. glabrata* (ATCC90030) were grown to exponential phase. Conformers were generated according to section 2.12. Cells were then incubated with the Aβ₄₂ conformers developed by incubation for 7 d with compounds. Survival was determined by colony forming units on YEPD media. (** $p < 0.001$, *** $p < 0.005$, ** $p < 0.01$). All data are expressed as mean \pm SEM (n = 3).**

5.4.3 ANTI-OLIGOMERISATION ACTIVITIES OF BISCOUMARIN ANALOGS

Coumarins (1,2-benzopyrone or 2*H*-1-benzopyran-2-one) are widely distributed in nature (Benci et al., 2012). A set of six synthesised biscoumarins were analysed in this section. These biscoumarins have different chemical compositions, due to the presence of various types of substitutions in their basic structure, which might influence their biological activity (Figure 5-18). Four of the biscoumarins share the same basic molecular structure, 3-((aryl) (4-hydroxy-2-oxo-2*H*-chromen-3-yl) methyl)-4-hydroxyl-2*H*-chromen-2-one with different substitutes; R= *H* (MW= 412.29), R= 4-*Cl* (MW= 446.74), R= 4-*OMe* (MW= 442.75), or R= 2-*Cl* (MW= 446.74). The other two biscoumarins are 2, 3-bis (4-hydroxy-2-oxo-2*H*-chromen-3-yl) 1, 4-benzoquinone (MW= 428.29), and 2, 3-bis (4-hydroxy-2-oxo-2*H*-chromen-3-yl) 1, 4-naphthoquinone (MW= 478.43). In this study an investigation of the structure-activity relationship of each of the biscoumarins with respect to their anti oligomerisation and aggregation propensity was performed. Difficulty in dissolving these compounds in biological buffers and H₂O was a main constraint in their analysis in the yeast model.

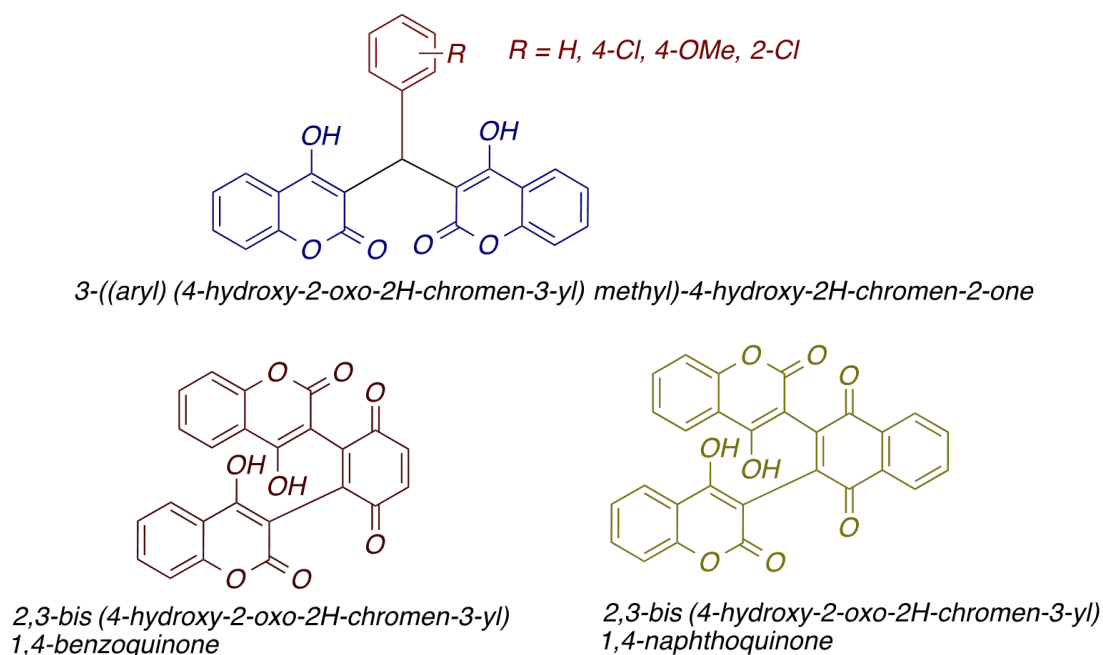
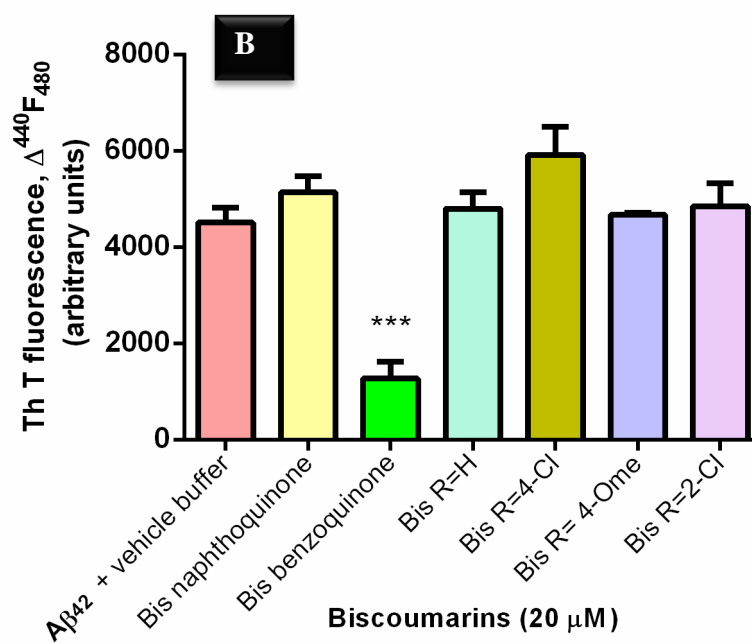
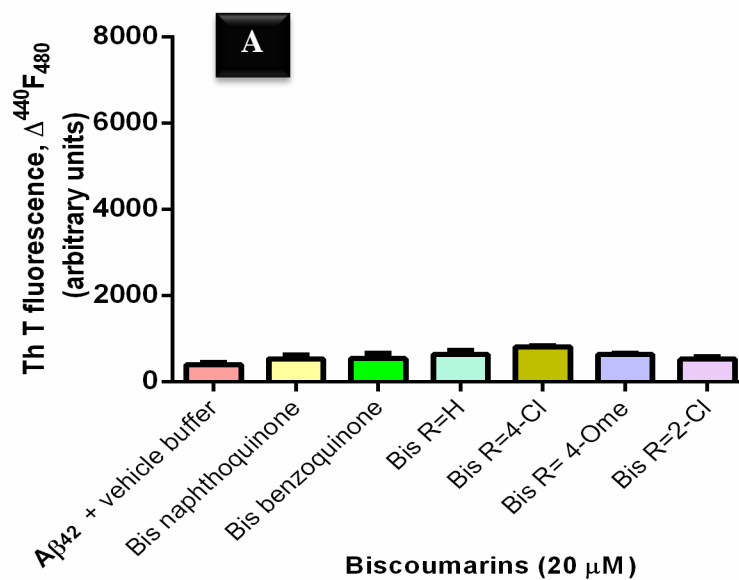


Figure 5-18 Structure of six Biscoumarin analogs investigated in this study (source: supplied by Helmut Hugel, RMIT University, 2013).

5.4.3.1 Anti-oligomerisation activity of biscoumarins measured by ThT assay

ThT assays were performed to identify biscoumarins that can hinder oligomerisation and fibril formation. The effect of colour associated with these compounds were minimised by setting up ThT control samples for the compound without addition of the peptide. Treatments were done by co-incubating an equal volume of $A\beta_{42}$ with the compounds for 24 h. Analysis of the results showed a greater level of fluorescence emission at the baseline (0 h) for all biscoumarin analogues compared with the $A\beta_{42}$ alone (Figure 5-19A) due to colours associated with these compounds. However, as the co-incubation with the $A\beta_{42}$ continued for 16 h, only 2, 3-bis-benzoquinone derivatives showed ThT negative response ($p < 0.05$; Figure 5-19B). After 24 h of co-incubation with the $A\beta_{42}$ again only 2, 3-bis-benzoquinone showed anti-fibril propensity and decreased the fluorescence intensity associated with ThT

significantly ($p < 0.005$; Figure 5-19C). The results indicated that bis-benzoquinone might have the ability to reduce β -sheet associated with amyloid aggregation.



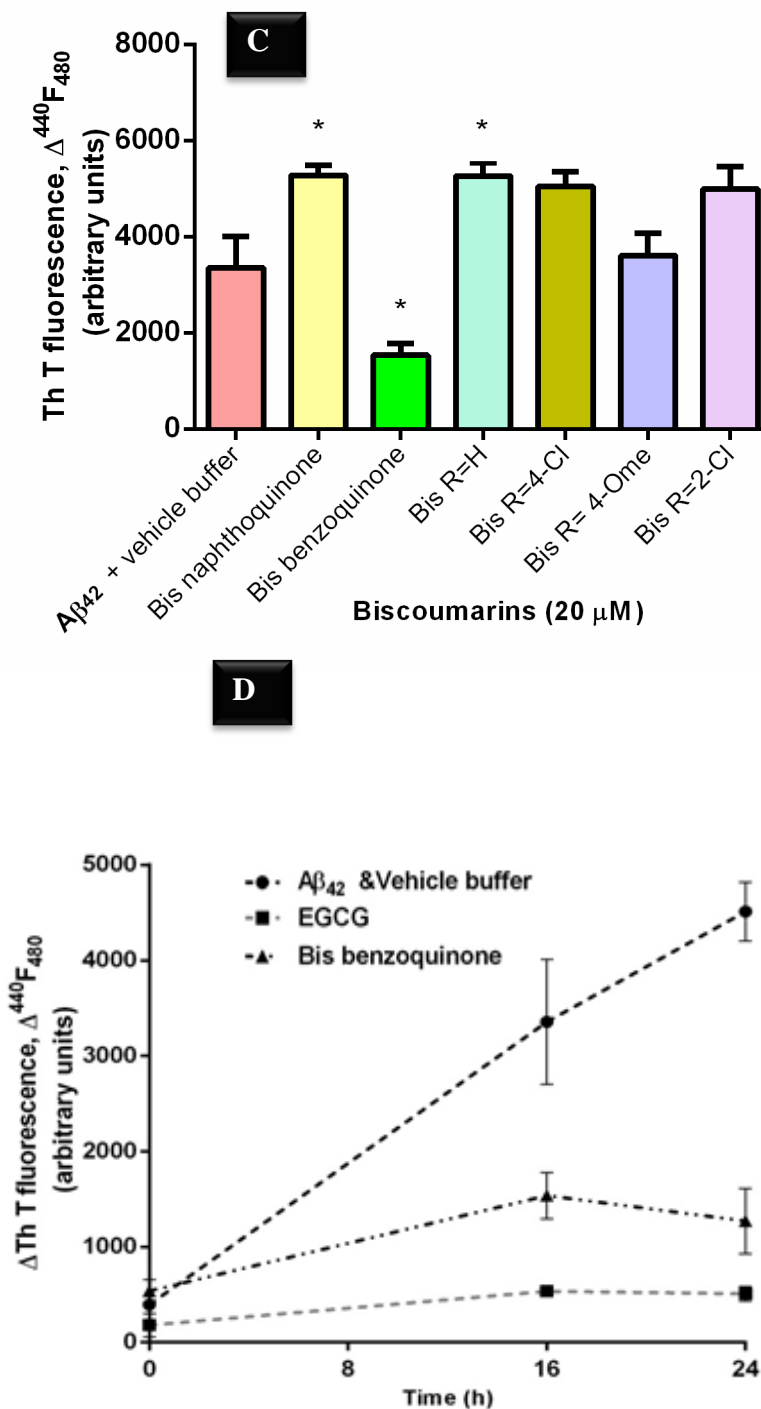


Figure 5-19 Amyloid formation assayed by thioflavin T fluorescence after incubation with biscoumarin analogs. Freshly prepared A β_{42} was added to each compound with final concentration of both being 20 μ M. Aggregation propensity of the peptide was monitored at 0 h (A), 16 h (B), and 24 h (C) after incubation. Kinetic anti-fibril progression of bis-benzoquinone compared with vehicle control buffer and EGCG measured by ThT fluorescence (D).

5.4.3.2 Cytotoxicity effect of A β ₄₂ co-incubated with biscoumarin on *C. glabrata*

Cellular protection capability of biscoumarins was evaluated by incubating exponentially growing *C. glabrata* cells in the presence of 50 μ M of each biscoumarin analogs for 6 h. After this time, HFIP pretreated A β ₄₂ was added to each sample to the final concentration of 5 μ M (Section 2.7.5). All of the biscoumarin analogs showed the capability to block cellular toxicity mediated by extracellular A β ₄₂ (Figure 5-20; $p < 0.001$). This might be due to their attachment to the cell wall of the yeast, and preventing the attachment and aggregation of the A β ₄₂ to the amyloidogenic proteins on the surface of *C. glabrata*, hence preventing the cytotoxicity (Chapter 4).

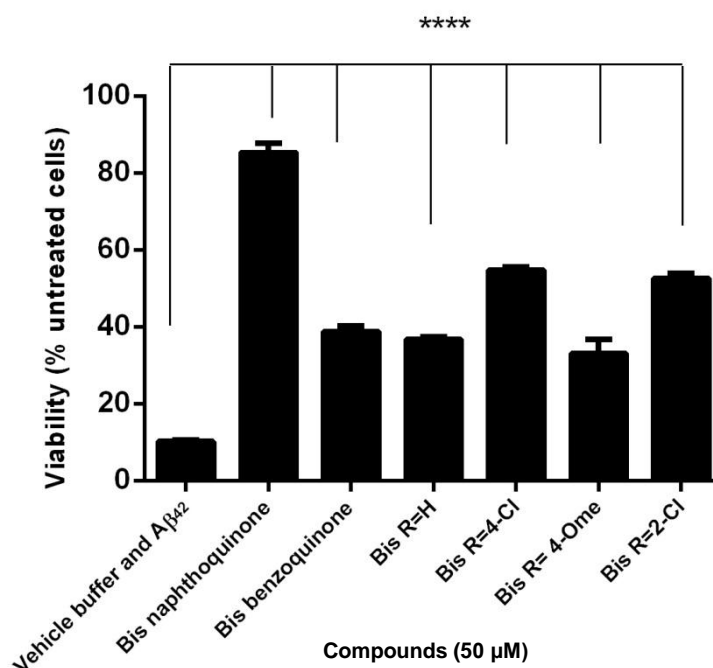


Figure 5-20 Cellular protections from A β ₄₂ toxicity mediated by Biscoumarin samples. *C. glabrata* cells were grown to exponential phase. Triplicate samples were incubated with each of six biscoumarin (50 μ M) analogs for 6 h prior to addition of HFIP pretreated A β ₄₂ (5 μ M). The survival rate has been calculated as a percentage of untreated control cells ($n = 3$; **** $p < 0.001$).

5.4.3.3 TEM analysis of A β ₄₂ co-incubated with bis-benzoquinone

The bis-benzoquinone displayed some anti-oligomeric activity by inhibiting the ThT associated fluorescence. However, its prolonged co-incubation with A β ₄₂ did not reveal any inhibitory activities against aggregation and oligomerisation (Figure 5-21). Two micrograph panels have been shown (Figure 5-21) to illustrate the extent of oligomerisation and fibril formation.

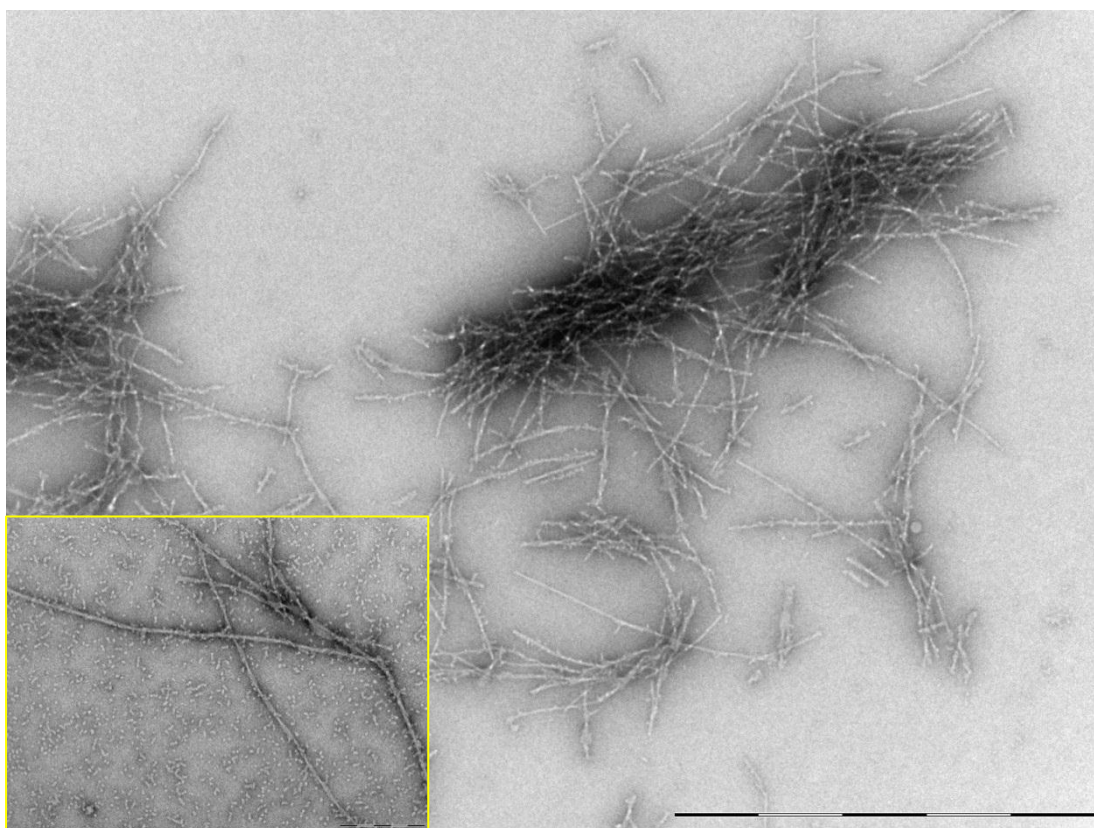


Figure 5-21 Transmission EM micrograph of A β ₄₂ co-incubated with 2, 3-bis-benzoquinone. Samples were incubated at 37°C for 7 d prior to analysis. A high level of oligomeric and fibrillar structures became obvious. The fibrils were highly twisted and long (micrograph in yellow box). Scale bar = 200 nm

5.5 DISCUSSION

Alzheimer's disease (AD) is the most common cause of dementia and is the most prevalent neurodegenerative disorder (Wang and Ding, 2008; Herskovits and Guarente, 2013). Amyloid beta ($A\beta$) protein, which was first identified by Masters et al. (1985) has been hypothesised as the major cause of neurodegenerative effects seen in AD. $A\beta$ has the ability to form aggregates and misfold which ultimately deposit as plaques identified in the brain of AD sufferers. This protein has been shown to be harmless in its monomeric form (Giuffrida et al., 2010). Its self-assembly, however, can result in the formation of various species including oligomers, intermediate aggregates and eventually the fibrillar aggregates that deposit in the brain (Teplow, 1998; Stefani and Dobson, 2003; Walsh and Selkoe, 2007; Sperling et al., 2011). This self-assembly of the $A\beta_{42}$ peptide is reversible and can also be inhibited. Candidate drugs were examined in this chapter for their ability to slow or prevent the aggregation and misfolding of $A\beta_{42}$ peptide.

A majority of tested phenolic compounds have shown a reduction of amyloid toxicity and inhibition of fibril formation (Smid et al., 2012). Any potential $A\beta$ aggregation agent should not only exhibit direct interference with $A\beta$ but also cross the blood-brain barrier (BBB). All of the identified efficient polyphenol inhibitors to date are composed of at least two phenolic rings with a minimum of two hydroxyl groups on the aromatic rings which enables them to form strong bonds with β -sheet regions of oligomers (Porat et al., 2006). The role of polyphenols in alleviating AD can be either direct or indirect. Their direct effect has been reported to be due to the interactions between $A\beta_{42}$ and aromatic residues (Levites et al., 2003; Wang et al.,

2006; Karuppagounder et al., 2009). Many polyphenols are thought to exhibit an indirect effect on alleviating AD by reducing oxidative stress due to accumulation of ROS and inflammation induced by A β (reviewed in Shi et al., 2013). This chapter details the effect of forty two candidate compounds on A β ₄₂ aggregation and their antioxidant potential for prevention of cytotoxicity in a yeast model. All of their activities have been characterised with respect to their structure, number of hydroxyl groups and identification of the position of OH-group on the aromatic ring for maximum potency and activity. *S. cerevisiae* (S288c) WT and *AHP1* deletant mutant expressing GFP-A β ₄₂ were utilised as models for high-throughput screening of anti-amyloidogenic compounds. The efficacy of this screening method was then compared to those generated from the conventional *in vitro* assays such as the ThT assay.

Screening compounds and small molecules for their chemo-protection against dementia and AD for human use must be approached from diverse angles as many aspects should be considered, not just the target region. Some inhibitors might display benefit in *in vitro* assays or in a simpler organism, but when introduced into more complex biological systems they may generate differing results. The *in vivo* safety of the chemo-protector, its bioavailability, absorption, metabolism and excretion must be considered. Natural products therefore appear to be attractive candidates due to their assumed safety profiles as they have been consumed as food or medicine for a long time (Ji and Zhang, 2008; Williams et al., 2011; Zhang, 2012). Although the results of most clinical trials of polyphenols and natural products

remain inconclusive, they are used as chemical scaffolds for the development of new bio-inspired compounds for the prevention of AD.

Polyphenolic compounds could protect against the toxic effects of ROS either by preventing A β from forming toxic oligomers (Mazza et al., 2006; Zhang et al., 2006; Yang et al., 2010) or by having inherent antioxidant activity (Avramovich-Tirosh et al., 2007; Belinha et al., 2007; Shaykhalishahi et al., 2009; Awaad et al., 2013). The cytotoxicity results in this chapter demonstrated that different species of yeast show dissimilar susceptibility to the effect of exogenous A β_{42} , with *C. glabrata* being more susceptible to the toxicity effect of A β_{42} than *S. cerevisiae*. This finding highlights the choice of using *S. cerevisiae* when studying human related diseases since it is the model eukaryotic organism (Foury, 1997; Gorkovskii et al., 2009; Braun et al., 2010; D'Angelo et al., 2013). *S. cerevisiae* has provided insights into the molecular mechanisms of many diseases (Table 1.1) including neurodegenerative disease (Table 1.2). The use of *S. cerevisiae* cells however, have some disadvantages due to the presence of the cell wall (Klis et al., 2002; Levin, 2005, 2011), which protects cells during environmental stress and may limit the permeability of some compounds. The outer membrane of the cell wall is composed of proteins which reportedly limit this permeability (Klis et al., 2002). The *SSDI* locus is known to be involved in cell wall integrity (CWI) and the S288c strain of *S. cerevisiae* which was used in this chapter, is known to have a functional, full-length allele (*ssd1-v*) (Kaeberlein and Guarente, 2002). Misfolded proteins have been identified to be toxic to the cells and expression of misfolded proteins has been found to induce CWI stress pathways and cause its defect (Spear and Ng, 2001; Sayeed and Ng, 2005; Ron

and Walter, 2007; Scrimale et al., 2009). In addition, many chemical agents including caffeine have been found to activate CWI signalling (Lum et al., 2004; Kuranda et al., 2006).

5.5.1 The position rather than the number of -OH groups are more important determinants of anti-oligomerisation activity

The ThT results showed that five danshen compounds had the ability to inhibit amyloid fibril formation. In order to prevent bias in the ThT assay, control samples without addition of the A β ₄₂ were also tested as identified by Hudson et al. (2009). The selected ThT negative compounds were; rosmarinic acid, salvianolic acid B, gallic acid, gentisic acid and caffeic acid. The therapeutic effect of many polyphenols has been attributed to the presence of aromatic rings namely; benzene rings and hydroxyl groups, which result in decreased fibril formation (Levy-Sakin et al., 2009). The effect of these aromatic residues reportedly is due to their binding mode which disrupt the π -stacking interaction occurring with aromatic amino acids in the amyloid, hence halting of the self-assembly process that leads to oligomerisation (Gazit, 2002; Tartaglia et al., 2004). Ono et al. (2006) have indicated that the more hydroxyl groups present in the molecule, the higher the anti-amyloidogenic activity. In contrast, the results in this chapter indicate that the number of hydroxyl moieties attached to the phenyl ring is not the major determinant. After analysing the positional isomers it became clear that position of the hydroxyl moieties on the aromatic ring is the major determinant of their potency. Overall, the effect of these aromatic residues in polyphenols is due to their ability to prevent transition of α -helix conformation to β -sheet and therefore fibril formation (Jayamani and Shanmugam, 2014). Also, it became apparent that the positions of the

hydroxyl groups may be more important rather than the numbers in the structure for their optimum biological activity. For instance, the position of hydroxyl groups on 2, 5-dihydroxybenzoic acid was found to result in a more potent compound with anti-oligomerisation activity compared with other positions (Figure 5-22).

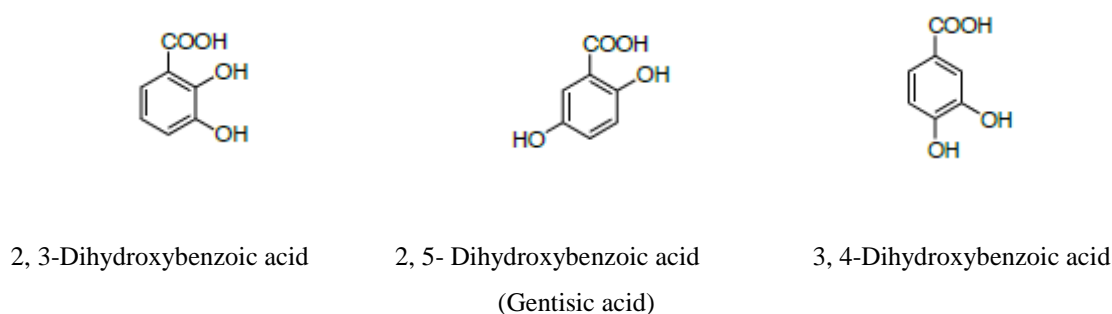


Figure 5-22 Chemical structure of dihydroxybenzoic acid isomers.

5.5.2 Conformational changes and toxicity associated with co-incubation of A β ₄₂ with compounds

Several pathogenic species of A β in AD affected patients that proceed to form neuritic plaques have been described previously (Deshpande et al., 2006; Fandrich et al., 2009; Ahmed et al., 2010; Butterfield et al., 2012). These consist of both LMW oligomers (dimers to dodecamers) and HMW oligomers with globular, circular protofibrils and fibrils structure (McKoy et al., 2012). Some examples of the polymorphism of soluble A β ₄₂ aggregates has become apparent in this chapter similar to the previous findings by Fandrich (2012), with some fibrils exhibiting strong toxicity effects while other fibrils were found to be non-toxic. Most of the aggregates exhibited some of the classic features of β -sheet-rich structures, including binding to

ThT and enhancing its fluorescence. However, they differed in morphology and capacity to seed A β ₄₂ monomer deposition.

It should be noted that a synthetic A β ₄₂ peptide was utilised in this current chapter and according to previous reports, the oligomers formed by these synthetic A β ₄₂ are less stable than naturally occurring oligomers (Walsh et al., 2005). Natural cell-derived A β has also been shown to be more potent than synthetic A β ₄₂ (Wang et al., 2004). Despite these dissimilarities, synthetic A β ₄₂ peptide is used widely for identification of anti-amyloidogenic compounds (Esler et al., 1997; Nakagami et al., 2002; Blanchard et al., 2004; De Felice et al., 2004). It should therefore be expected that the biological potency of selected chemicals on inhibiting the aggregation of A β ₄₂ oligomers may not be similar under different conditions. The mechanism by which the selected chemicals however rescued the cells from the toxicity of A β ₄₂ oligomers in this chapter could be explained by two distinct pathways. The first is that these compounds may not be cell-permeable and are attaching to the cell wall and forming a bond with the surface of the yeast hence, limiting A β ₄₂ contact and association. The second is that the compounds generate A β ₄₂ conformations that are not toxic to the cells. Further, the results confirm the findings in Chapter 4 in which the effect of HFIP-pretreated A β ₄₂ was shown to be limited to the cell wall due to presence of amyloidogenic surface proteins in yeast and preventing the endocytosis which is essential for the initiation of cell damage and toxicity.

Coumarins in general have been shown to be effective ROS scavengers with strong antitumor and anti-inflammatory activity (Kancheva et al., 2010; Benci et al., 2012; Bansal et al., 2013) as well as being a potential acetylcholinesterase inhibitor (Anand et al., 2012). A study of 1,4-benzoquinone and 1,4-naphthoquinone on insulin degradation revealed that these compounds are capable of attenuating the oligomerisation significantly (Gong et al., 2014). The biological evaluation of these six novel biscoumarin derivatives screened in the current chapter revealed a generally weak anti-oligomeric effect, but very good cytotoxic protection of the cells was observed. Only benzoquinone however exerted a strong effect when tested with the ThT assay. The EM micrographs revealed that after prolonged incubation, this effect become minimal with no potential anti-aggregation activity. These findings raise two possible explanations. One is that benzoquinone may compete with the A β in binding to the β -sheet region of the structure at the start of incubation, while after prolonged incubation, they become outcompeted by the presence of excess oligomers. Therefore, benzoquinone may generate less fluorescence associated with ThT (ThT negative) but has limited anti-fibril and anti-aggregation propensity when incubation is continued. The second possible explanation could be that benzoquinone and other biscoumarins tested in this chapter, may have significant potential by accelerating the fibril formation or contributing to formation of oligomeric conformations that are not toxic. Their potential should be characterised in tissue culture as they were not found to be toxic and their co-incubation with the A β ₄₂ resulted in non-toxic peptide species.

Rosmarinic acid has been identified as an attractive candidate for prevention of AD due to its biological activities (Hamaguchi et al., 2009). Rosmarinic acid, an ester of caffeic acid (3, 4-dihydroxyphenyllactic acid), possesses several biological activities, including antioxidant, anti-inflammatory, antibacterial and antiviral (Petersen and Simmonds, 2003). Animal model experiments have shown that rosmarinic acid can reduce A β -induced neurotoxicity (Alkam et al., 2007) and can provide protection against ROS in tissue culture (Iuvone et al., 2006). The results from this chapter have also identified the oligomerisation inhibition property of rosmarinic acid along with formation of A β ₄₂ species that are non-toxic to yeast cells.

5.5.3 Fluorescence associated with GFP-A β ₄₂ for screening of anti-oligomers is not identical to the ThT assay

The flow cytometry analysis of GFP-A β ₄₂ expressing WT *S. cerevisiae* cells co-incubated with the compounds, were inconclusive as the strain seemed to be hardly affected by the fusion. Further, none of the compounds were able to change the green fluorescence associated with the fusion protein in these WT cells. In contrast, the green fluorescence expression in the *AHP1* deletant mutant expressing GFP-A β ₄₂ was affected in the presence of some compounds. This was more profound with the danshen class of compounds, as all five ThT negative compounds in this class along with the EGCG which had anti-oligomeric property also reduced the fluorescence associated with the GFP-A β ₄₂ fusion, indicating their anti-aggregation potential (Figure 5-23- clustered in a red circle). However, this mutant strain was not suitable for identifying compounds with antioxidant property as expected. Also, some of ThT negative selected compounds in the MATNAP with the exception of RB9_6.3

showed different effect in the *in vivo* GFP-A β_{42} screening (Figure 5-23). This might indicate that the mechanism of action for the selected potent compounds on the aggregation and oligomerisation of A β_{42} is different, therefore not classified in one cluster.

Despite these findings, *in vivo* methods developed by Lee et al. (2009b) utilising an *E. coli* Tat protein export system with A β_{42} fusion, allowed high-throughput screening of a hundred chemicals and identified four that were cell-permeable and prevented the aggregation of the A β_{42} peptide. A previous study by Kim and colleagues (2006) also successfully employed the expression of A β_{42} -GFP fusion in *E. coli* as a method for high-throughput screening of anti-amyloidogenic compounds. Surprisingly, their subsequent analysis was only focused on one chemical that showed similar potency in both an *in vivo* A β_{42} -GFP fusion assay and the ThT and EM methods of screening for fibrillogenesis. Therefore, it is not clear whether this method can provide valid results for high-throughput screening. Also, Park and colleagues (2011) developed a fusion system based on A β_{42} fused to functional release factor (Sup35p) which was capable of identifying small molecules with anti-oligomeric activity. Differences in findings however, may be related to the use of a different GFP fusion construct. The fusion that was utilised in this study resulted in a cytosolic punctate appearance of GFP whereas in the studies by Kim et al. (Kim and Hecht, 2005; Kim et al., 2006) the fusion inhibited the GFP-associated fluorescence but inhibitors of A β_{42} aggregation enabled GFP to fold into its native structure and produce green fluorescence signals. D'Angelo et al. (2013) have shown that an

intracellular trafficking pathway is necessary for the generation of toxic species of A β peptide, further indicating the differences in the results.

The N-terminal tagging with GFP has been shown to adversely affect the protein localisation compared with C-terminal fusion (Palmer and Freeman, 2004). Further, tagging with GFP at the C-terminal is found to result in greater subcellular localisation of the native protein (Palmer and Freeman, 2004). The A β ₄₂ in this chapter was fused to the N-terminus of the GFP which resulted in punctate fluorescent signalling of GFP rather than total misfolding and inhibition of the fluorescence associated with aggregation and misfolding of A β ₄₂ peptide.

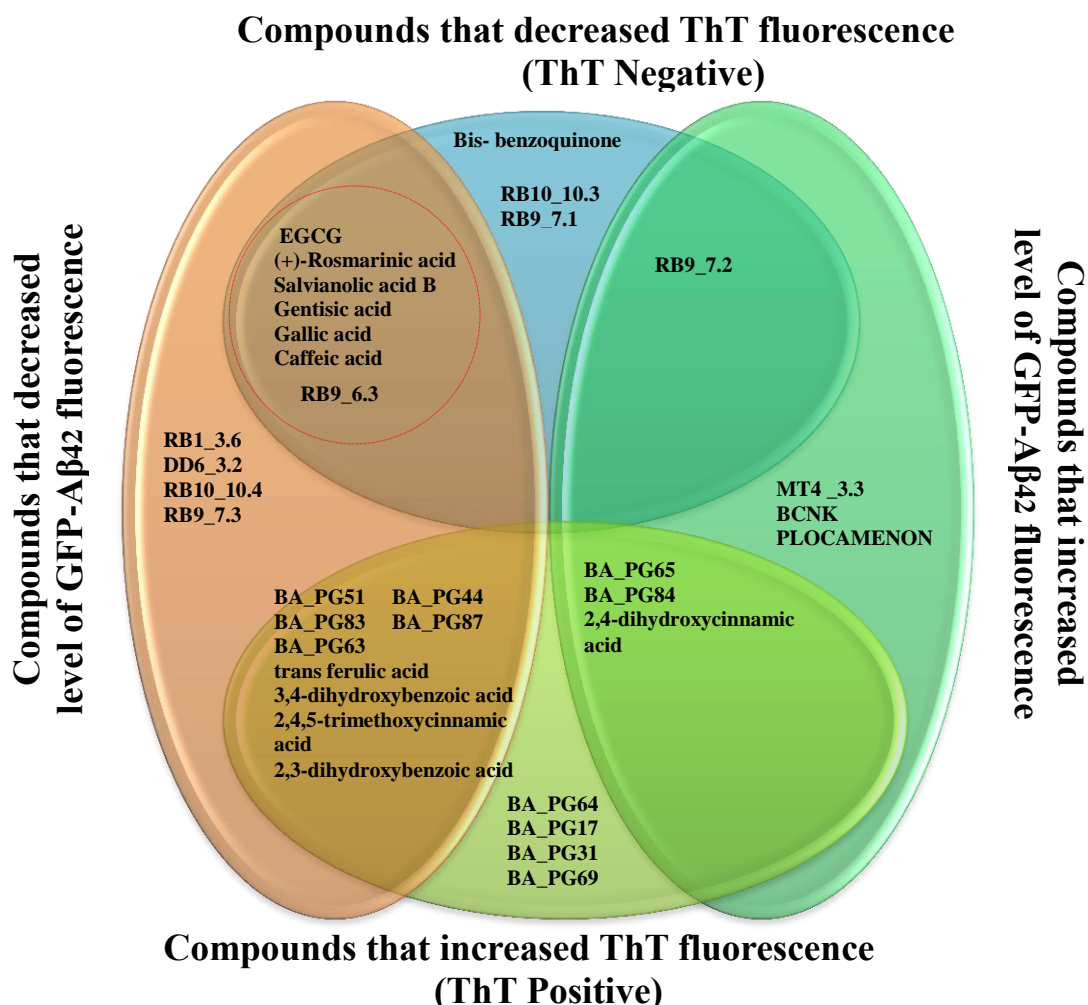


Figure 5-23 Schematic overview of compounds identified that enhanced or decreased fluorescence associated with GFP-A β ₄₂ or Thioflavin T or both. EGCG, rosmarinic acid, salvianolic acid B, gentisic acid, gallic acid, caffeic acid, and RB9_6.3 were able to reduce fluorescent associated with ThT (anti-oligomerisation activity) and fluorescent associated with GFP-A β ₄₂ (Clustered in red circle).

Although, the GFP-A β ₄₂ screening system did not enable the classification of these compounds, the *in vitro* results of biological activities of the compounds were similar to previous findings. Similar to previous reports on the anti-oligomerisation effect of polyphenols, rosmarinic acid and salvianolic acid B were found to inhibit cytotoxicity (Feng et al., 2009; Zhou et al., 2009; Lee et al., 2013) but were not able to prevent A β ₄₂ oligomer formation. It is also known that the therapeutic effect of

these chemicals is similar to other polyphenols and not just limited to their direct interaction with the A β . For instance, salvianolic acid B demonstrated antidepressant-like effects (Feng et al., 2012) and an ability to ameliorate spatial memory impairment in animal models (Teng et al., 2014) possibly due to its anti-inflammatory activities. Some other therapeutic effects attributed to danshen are the ability to reduce ROS and prevent DNA fragmentation (Iuvone et al., 2006), anti-tumour and antioxidant activity (Jiang et al., 2005).

All of the potential chemicals identified with anti-oligomerisation property in this study showed reduced fluorescence associated with GFP-A β_{42} fusion in an *ahp1* mutant strain. These chemicals were also found to reduce the fluorescence associated with the ThT assay, however, proposing this method for identification of potential inhibitors is not possible. This is mainly due to the presence of many other chemicals which caused a similar reduction in fluorescence associated with the GFP-A β_{42} fusion but failed to prevent oligomerisation hence reduction of ThT associated fluorescence. Similar to findings in this chapter, Jimenez et al. (2010) reported that hypersensitivity of *ahp1* was not reversed in the presence of the polyphenols. This further indicates that interaction of small molecules with the intracellular expressed amyloid aggregates is limited to the ability of the compounds to enter the cell.

5.6 CONCLUSION

Improvements and validation of the yeast screening model and assays are necessary in order to generate a suitable disease model that can be used successfully for designing therapeutic strategies and interventions which correlates with *in vitro* and mammalian testing systems. An improvement found in this study was the use of yeast lacking Ahp1p for screening of compounds.

A novel outcome of this study was identifying most suitable isomers of bio-inspired compounds with anti-amyloidogenic properties using both *in vivo* assays and *in vitro* assays. Also, the positions of the hydroxyl moieties on the aromatic rings were found to be the major determinant of their potency rather than number of hydroxyl group. These results indicate that any yeast screening assays should be complemented with conventional *in vitro* assays to ensure its validity prior to high-throughput analysis.

6 CHAPTER 6: FINAL CONCLUSIONS AND FUTURE DIRECTIONS

At present, the precise changes in the brain that cause the development of AD are unknown. Various biological model systems of Alzheimer's disease (AD) have been developed to investigate cascades of events that occur in the brain of AD patients. One of the major focus is on the intracellular A β peptide, and finding ways to block or prevent its production, toxicity or aggregation. Currently, both prevention and cure to alleviate the symptoms associated with AD are proving difficult to achieve. One reason for this could be the lack of a simple model system which could be used as a "gold standard" for high-throughput screening of AD modifiers. Yeast as a simple model to study AD and to screen potential A β ₄₂ inhibitors has in the present study enabled relatively inexpensive high-throughput screening. It also allowed the immediate elimination of cytotoxic compounds. However, the yeast model has drawbacks as some potentially useful compounds might not pass the cell wall of the yeast or their interaction might be different to what occurs in a multi-cellular organism. Further, interaction of compounds might become obscured due to the presence of the yeast cell wall glycoproteins, resulting in a different outcome to those of neuronal cells.

Cell cycle reactivation and expression of cell cycle proteins which leads to neurodegeneration in the brain of AD patients has been reported by many investigators. In order to replicate the cell cycle reactivation event of senescent cells, in yeast cells and find ways to block its progression, folate was used as an external stimulator to trigger aberrant cell division (Chapter 3). Aberrant proliferation of

stationary phase *Candida glabrata* in the presence of folate was identified. Formation of multiple buds in the presence of folate was a novel finding. Although, these findings are not closely related to AD, their investigation is important for better understanding of yeast cell biology. Multiple bud formation also requires further investigations into how the bud selection occurs during nutrient depletion and folic acid treatment. At this point it is unclear whether all of the multiple buds emerge spontaneously or whether after each bud, cytokinesis fails. Analysis of spindle pole bodies in *C. glabrata* might unravel the pattern of multiple bud emergences.

This study further examined the cellular uptake of folate by utilising a putative folate transporter (YJL163C) of *Saccharomyces cerevisiae*. Overexpression of the YJL163C gene did not alter the susceptibility or resistance of the cells to the toxicity induced by chemically-synthesised A β ₄₂ peptide. Aberrant sporulation of *S. cerevisiae* however, with overexpression of this putative transporter gene was detected which resulted in formation of a triad of spores within asci. It should be noted that sporulation itself is different to mitotic divisions in that not all of the cellular contents are packaged into the progeny cells. In vegetative growth, the cytoplasm and its contents are divided between mother and daughter cells whereas in sporulation, the contents are divided between the spores in the ascus. Dissection of the ascus and analysis of each spore is therefore recommended. This may provide additional information on gene regulation of each individual spore and whether the starvation or folic acid has caused any changes to cellular function. Folic acid was observed to stain various organelles of *S. cerevisiae* during incubation. It would

therefore be important to demonstrate the entry of folate into the cells using an electron microscope and directly labelled either folate or receptor.

Methotrexate (MTX), an antifolate was utilised in an attempt to investigate its effect on yeast cells in the presence and absence of folate source. MTX was not found to be inhibitory on the growth of wild-type *S. cerevisiae* strain but, it did not support the growth of EHY1 strain which relies on an exogenous source of folate. In the presence of MTX, the EHY1 strain could only grow when folinic acid was also present simultaneously whilst, folic acid addition did not contribute to cell growth. The cellular uptake of exogenous folic acid was found to be similar to MTX, whilst folinic acid mechanism of entry was different and unrelated to MTX uptake. MTX effect on yeast cells was found to be dissimilar to that seen in humans. This contributed to a limitation of this model system and caused a barrier for further investigation.

The tendency of amyloid beta ($A\beta$), in particular $A\beta_{42}$ isoform to misfold and aggregate into insoluble amyloid fibrils in the early stages of AD has been well documented. Investigations using chemically-synthesised $A\beta_{42}$ peptide for extracellular kinetic studies of fibril assembly therefore have become a common practice. The outcomes of these studies in yeast, however, have not been in agreement. Chapter 4 set out to explore the suitability of yeast as a model organism for simple high-throughput screening of compounds using exogenous chemically-synthesised $A\beta_{42}$ peptide and evaluate the discrepancy in the previous findings which has not been resolved. My study shows for the first time that the pretreatment method

of synthetic A β ₄₂ peptide determines its activity and ultimately how it interacts with the yeast cells. Here by manipulating growth phase, the chronological lifespan of yeast was studied to gain understandings into the aging process in yeast and how A β ₄₂ influence survival and cell division. The effect of A β ₄₂ was found to be limited to the yeast cell wall and interactions with the amyloidogenic cell wall proteins. *S. cerevisiae* was found to be more resistant than *C. glabrata* to the effect of A β ₄₂ peptide. These might be due to differences in the level of outer cell membrane proteins which are found to be around 50% higher in *C. glabrata* than *S. cerevisiae* (de Groot et al., 2008). It was identified that conformational changes in the peptide due to preparation methods, determine its fate on toxicity and proliferation. The hexafluoroisopropanol pretreated A β ₄₂ had a greater tendency to aggregate on yeast cells as determined by thioflavin t (ThT) staining followed by flow cytometry and microscopy. Both quiescent and non-quiescent cells were analysed by these methods of peptide preparation, of which the latter was found to be more susceptible to the toxicity of A β ₄₂. Also, similar peptide preparation which resulted in cytotoxicity in PC12 neuronal cell culture caused proliferation in yeast cells. This study highlighted many important issues that need to be considered when using the chemically-synthesised A β ₄₂ peptide for screening. Firstly, the pretreatment method was found to be the major determinant of the fate of chemically-synthesised A β ₄₂ peptide on the yeast cells. This limited synthetic A β ₄₂ peptide application in yeast and the interpretation of the results, particularly when utilised for screening of compounds. Secondly, solvents that were used for dissolution of synthetic A β ₄₂ peptide were found to affect the outcome of the analysis therefore suitable vehicle buffer control should be included in all experiments despite what was reported previously (Bharadwaj et al., 2008). Further, Dubey et al. (2009) found that 20 mM NaOH

partially rescued yeast cells from the toxicity induced by chemically-synthesised A β ₄₂ peptide while, in the study by Bharadwaj et al. (2008), 20 mM NaOH was utilised however no vehicle buffer control was included in the experiments. Interestingly, in this current study, the NH₄OH pretreated peptide dissolved in NaOH resulted in proliferation in yeast while the vehicle buffer itself was toxic. This further indicates the importance of the vehicle buffer inclusion when reporting the outcome of cytotoxicity investigations. Finally, findings by these investigators also showed that the effect of chemically-synthesised A β ₄₂ peptide in yeast was similar to neuronal cells with the oligomeric form causing cytotoxicity to *C. glabrata* cells while fibrillar structures were found to be inert. The current study however, showed that biological activity of chemically-synthesised A β ₄₂ peptide is different to that seen in neuronal cells and that the pretreatment will determine how the peptide interacts with the yeast cells. Fibrillar structures formed by prolonged incubation of both HFIP and NH₄OH pretreated A β ₄₂ peptide caused toxicity to *C. glabrata*. Extracellular kinetic studies of chemically-synthesised A β ₄₂ peptide and cytotoxicity assays in yeast is prone to various limitations as mentioned earlier. In order therefore to validate yeast based assays for future studies it is imperative to examine the effect of brain homogenates from AD affected individuals on the survival of yeast cells and investigate the molecular mechanism underlying any effect. It is also critical to determine whether A β ₄₂ causes pore formation and abnormal flow of ions as seen in neural cells and how various conformations can affect the outcome.

Polyphenolic compounds have been found to have effects on the assembly of A β ₄₂ fibrils and oligomers. Although, many polyphenols have been identified as potential

chemo-protectors, their therapeutic effects have not been well established. This is partly due to the inherent limitations in screening methods. Screening natural compounds for their chemo-protection ability does not take into account their digestion and metabolism in the human body which ultimately leads to formation of new structures and molecules. It is also unknown whether the absorbed substances will remain biologically active and able to cross the blood brain barrier. Therefore, it is important to design bio-inspired compounds and their metabolites which could be tested using cell based assays in order to ascertain their potency and therapeutic potential. A yeast model was used in Chapter 5 to screen small molecules and identify those with potential anti-oligomeric and anti-aggregation properties. However, limitations exist with this yeast model when screening for potential therapeutic compounds. For instance, some beneficial polyphenols such as caffeic acid and rosmarinic acid have been found to possess antimicrobial properties which limit their testing in the yeast model. Also, some other compounds do not enter yeast cells due to the presence of the cell wall which could act as a barrier to cellular entry.

Expression of GFP-A β ₄₂ fusion in yeast was utilised in the current study to identify compounds with potential anti-aggregation properties. However, when *S. cerevisiae* BY4743 wild-type was utilised for expression of this fusion protein, no significant effect on fluorescent level in the presence of any of the compounds was identified. Expression of GFP-A β ₄₂ in an alkyl hydroperoxide reductase (*AHP1*) deletant strain however, allowed identification and classification of compounds into three groups. These were compounds that caused an increase in the green fluorescence intensity compared with the control samples, those that decreased fluorescence intensity and

finally those without any effect. Despite these classifications the method did not identify potential compounds with chemo-protection activities. Further, it was expected to see that those compounds that reduced the ThT associated fluorescence, also reduced the green fluorescence associated with GFP-A β_{42} fusion. Screening of compounds using GFP-A β_{42} fusion in the *AHPI* deletant strain showed 20 compounds with an ability to lower the level of green fluorescence associated with fusion. Further screening for anti-oligomers using this ThT assays only identified seven of those twenty that had shown potential anti-oligomeric properties. Four other compounds also were found to have anti-oligomeric potential using the ThT assay but were not identified in the GFP-A β_{42} fusion system. For efficient high-throughput screening, it will be necessary to develop a GFP-A β_{42} expression model in yeast that can successfully identify the potential anti-oligomerisation or anti-aggregation compounds. This could be achieved by utilising autophagic-mutant strains transformed with GFP-A β_{42} fusion. Comparisons of the autophagic mutant to WT can identify the mechanism underlying the GFP-A β_{42} fusion transport and degradation. In order to validate such a system, potential therapeutic compounds such as EGCG, salvianolic acid B and caffeic acid should be screened and their effect on cell survival, vacuole morphology, and fluorescence-associated with the fusion, monitored. Such a strain would also need to be screened in the presence of the compounds only, prior to transformation with the fusion protein, to check the phenotype and to eliminate any altered expression or changes in cell growth due to the compound itself. The experimental design should include various concentrations of the compounds to determine correct dosage of the compound in order to capture optimum fluorescence production or elimination associated with the fusion in the presence of the compound.

Further analyses of the compounds using ThT and TEM in Chapter 5, however, allowed identification of the most suitable isomers of bio-inspired compounds with anti-amyloidogenic properties. The positions of the hydroxyl moieties on the aromatic rings were found to be the major determinant of their potency rather than number of hydroxyl groups. These results indicate that any yeast screening assays should be complemented with conventional *in vitro* assays (e.g. ThT) to ensure its validity prior to high-throughput analysis. The data presented on activities of phenolic compounds may also represent the starting point for designing new molecules that could be used for the treatment of AD and related neurological disorders.

There is still potential to further develop yeast as a model organism for neurodegeneration studies despite the current lack of a standard system. Future focus hence should be on developing standardised methods and protocols that could be utilised successfully by any investigator, (similar to other cell culture models) and thus enable the generation of comparable results. Further improvements and validation of the yeast screening model and assays would be necessary but may lead to a cost-effective and simple disease model that could be used successfully for designing therapeutic strategies and interventions with better correlation with *in vitro* and mammalian testing systems.

REFERENCES

- Ahmed, M., Davis, J., Aucoin, D., Sato, T., Ahuja, S., Aimoto, S., Elliott, J. I., Van Nostrand, W. E., and Smith, S. O. 2010. Structural conversion of neurotoxic amyloid- β (1-42) oligomers to fibrils. *Nat Struct Mol Biol*, 17, 561-7.
- Aich, P., Patra, M., Chatterjee, A.K., Roy, S.S., and Basu, T. 2012. Calcium chloride made *E. coli* competent for uptake of extraneous DNA through overproduction of OmpC protein. *Protein J*, 31, 366-73.
- Airoldi, C., Colombo, L., Manzoni, C., Sironi, E., Natalello, A., Doglia, S.M., Forloni, G., Tagliavini, F., Del Favero, E., Cantù, L., Nicotra, F., and Salmona, M. 2011. Tetracycline prevents A β oligomer toxicity through an atypical supramolecular interaction. *Org Biomol Chem*, 21, 463-72.
- Alarco, A.M., Balan, I., Talibi, D., Mainville, N., and Raymond, M. 1997. AP1-mediated multidrug resistance in *Saccharomyces cerevisiae* requires *FLR1* encoding a transporter of the major facilitator superfamily. *J Biol Chem*, 272, 19304-13.
- Alford, B.L., and Hügel, H.M. 2013. Total synthesis of (+)-pentamethylsalvianolic acid C. *Orga Biomol Chem*, 11, 2724-7.
- Alkam, T., Nitta, A., Mizoguchi, H., Itoh, A., and Nabeshima, T. 2007. A natural scavenger of peroxynitrites, rosmarinic acid, protects against impairment of memory induced by A β (25-35). *Behav Brain Res*, 180, 139-45.
- Allen, C., Buttner, S., Aragon, A.D., Thomas, J.A., Meirelles, O., Jaetao, J.E., Benn, D., Ruby, S.W., Veenhuis, M., Madeo, F., and Werner-Washburne, M. 2006. Isolation of quiescent and nonquiescent cells from yeast stationary-phase cultures. *J Cell Biol*, 174, 89-100.
- Altschul, S.F., Gish, W., Miller, W., Myers, E.W., and Lipman, D.J. 1990. Basic local alignment search tool. *J Mol Biol*, 215, 403-10.
- Alzheimer, A. 1906. Über einen eigenartigen schweren Erkrankungsprozeß der Hirnrinde. *Neurol Central*, 25.
- Alzheimer, A. 1907. Über eine eigenartige Erkrankung der Hirnrinde [Concerning a novel disease of the cortex]. *Allgemeine Zeitschrift für Psychiatrie und Psychisch-gerichtliche Medizin*, 64, 146-148.
- Anand, P., Singh, B., and Singh, N. 2012. A review on coumarins as acetylcholinesterase inhibitors for Alzheimer's disease. *Bioorg Med Chem*, 20, 1175-1180.

-
- Anekonda, T.S., and Quinn, J.F. 2011. Calcium channel blocking as a therapeutic strategy for Alzheimer's disease: The case for isradipine. *Biochim Biophys Acta*, 1812, 1584-1590.
- Antony, A.C. 1992. The biological chemistry of folate receptors. *Blood*, 79, 2807-20.
- Antony, A.C. 1996. Folate receptors. *Annu Rev Nutr*, 16, 501-21.
- Aragon, A.D., Rodriguez, A.L., Meirelles, O., Roy, S., Davidson, G.S., Tapia, P.H., Allen, C., Joe, R., Benn, D., and Werner-Washburne, M. 2008. Characterization of differentiated quiescent and nonquiescent cells in yeast stationary-phase cultures. *Mol Biol Cell*, 19, 1271-80.
- Armstrong, R.A., Cairns, N.J., Patel, R., Lantos, P.L., and Rossor, M.N. 1996. Relationships between β -amyloid (A β) deposits and blood vessels in patients with sporadic and familial Alzheimer's disease. *Neurosci Lett*, 207, 171-174.
- Avila-Muñoz, E., and Arias, C. 2014. When astrocytes become harmful: Functional and inflammatory responses that contribute to Alzheimer's disease. *Aging Res Rev*, 18, 29-40.
- Avramovich-Tirosh, Y., Reznichenko, L., Mit, T., Zheng, H., Fridkin, M., Weinreb, O., Mandel, S., and Youdim, M.B. 2007. Neurorescue activity, APP regulation and A β peptide reduction by novel multi-functional brain permeable iron-chelating-antioxidants, M-30 and green tea polyphenol, EGCG. *Curr Alzheimer Res*, 4, 403-11.
- Awaad, A.S., Al-Jaber, N.A., Moses, J.E., El-Meligy, R.M., and Zain, M.E. 2013. Antiulcerogenic activities of the extracts and isolated flavonoids of *Euphorbia cuneata Vahl*. *Phytothe Res : PTR*, 27, 126-30.
- Bacalini, M.G., Friso, S., Olivieri, F., Pirazzini, C., Giuliani, C., Capri, M., Santoro, A., Franceschi, C., and Garagnani, P. 2014. Present and future of anti-ageing epigenetic diets. *Mech Ageing Dev*, 136-137, 101-115.
- Bach, S., Talarek, N., Andrieu, T, Vierfond, J-M, Mettey, Y, Galons, H, Dormont, D, Meijer, L, Cullin, C., and Blondel, M 2003. Isolation of drugs active against mammalian prions using a yeast-based screening assay. *Nat Biotech*, 1075-1081.
- Baglioni, S., Casamenti, F., Bucciantini, M., Luheshi, L. M., Taddei, N., Chiti, F., Dobson, C. M., and Stefani, M. 2006. Prefibrillar amyloid aggregates could be generic toxins in higher organisms. *J Neurosci*, 26, 8160-7.
- Bagriantsev, S., and Liebman, S. 2006. Modulation of A β 42 low-n oligomerization using a novel yeast reporter system. *BMC Biol*, 4, 32.
- Bailey, L.B., and Gregory, J.F. 1999. Folate metabolism and requirements. *J Nutr*, 129, 779-82.
-

-
- Ballard, C., Gauthier, S., Corbett, A., Brayne, C., Aarsland, D., and Jones, E. 2011. Alzheimer's disease. *Lancet*, 377, 1019-1031.
- Ban, T., and Goto, Y. 2006. Direct observation of amyloid growth monitored by total internal reflection fluorescence microscopy. *Methods Enzymol*, 413, 91-102.
- Bansal, Y., Sethi, P., and Bansal, G. 2013. Coumarin: a potential nucleus for anti-inflammatory molecules. *Med Chem Res*, 22, 3049-3060.
- Barchiesi, F., Tortorano, A.M., Di Francesco, L.F., Cogliati, M., Scalise, G., and Viviani, M.A. 1999. *In-vitro* activity of five antifungal agents against uncommon clinical isolates of *Candida spp.* *J Antimicrob Chemother*, 43, 295-9.
- Bayly, A.M., and Macreadie, I.G. 2002. Folic acid antagonism of sulfa drug treatments. *Trends Parasitol*, 18, 49-50.
- Belinha, I., Amorim, M.A., Rodrigues, P., de Freitas, V., Moradas-Ferreira, P., Mateus, N., and Costa, V. 2007. Quercetin increases oxidative stress resistance and longevity in *Saccharomyces cerevisiae*. *J Agric Food Chem*, 55, 2446-51.
- Benci, K., Mandic, L., Suhina, T., Sedic, M., Klobucar, M., Kraljevic Pavelic, S., Pavelic, K., Wittine, K., and Mintas, M. 2012. Novel coumarin derivatives containing 1,2,4-triazole, 4,5-dicyanoimidazole and purine moieties: synthesis and evaluation of their cytostatic activity. *Molecules*, 17, 11010-25.
- Benilova, I., Karran, E., and De Strooper, B. 2012. The toxic A β oligomer and Alzheimer's disease: an emperor in need of clothes. *Nat Neurosci*, 15, 349-57.
- Berhanu, W.M., and Masunov, A.E. 2010. Natural polyphenols as inhibitors of amyloid aggregation. Molecular dynamics study of GNNQQNY heptapeptide decamer. *Biophys Chem*, 149, 12-21.
- Bezsonov, E.E., Groenning, M., Galzitskaya, O.V., Gorkovskii, A.A., Semisotnov, G.V., Selyakh, I.O., Ziganshin, R.H., Rekestina, V.V., Kudryashova, I.B., Kuznetsov, S.A., Kulaev, I.S., and Kalebina, T.S. 2013. Amyloidogenic peptides of yeast cell wall glucantransferase Bgl2p as a model for the investigation of its pH-dependent fibril formation. *Prion*, 7, 175-84.
- Bharadwaj, P. 2011. *Studying A β aggregation, toxicity and clearance*. Ph. D thesis, Edith Cowan University.
- Bharadwaj, P.R., Verdile, G., Barr, R.K., Gupta, V., Steele, J.W., Lachenmayer, M. L., Yue, Z., Ehrlich, M.E., Petsko, G., Ju, S., Ringe, D., Sankovich, S.E., Caine, J.M., Macreadie, I.G., Gandy, S., and Martins, R.N. 2012. Latrepirdine (Dimebon) enhances autophagy and reduces intracellular GFP-A β ₄₂ levels in yeast. *J Alzheimers Dis*, 32, 949-967.
-

-
- Bharadwaj, P., Waddington, L., Varghese, J., and Macreadie, I.G. 2008. A new method to measure cellular toxicity of non-fibrillar and fibrillar Alzheimer's A β using yeast. *J Alzheimers Dis*, 13, 147-50.
- Bharadwaj, P., Martins, R., and Macreadie, I. 2010. Yeast as a model for studying Alzheimer's disease. *FEMS Yeast Res*, 10, 961-969.
- Bignante, E.A., Heredia, F., Morfini, G., and Lorenzo, A. 2013. Amyloid β precursor protein as a molecular target for A β -induced neuronal degeneration in Alzheimer's disease. *Neurobiol Aging*, 34, 2525-2537.
- Bird, T.D. 2008. Genetic aspects of Alzheimer disease. *Genet Med*, 10, 231-9.
- Bishop, G.M., and Robinson, S.R. 2002. The amyloid hypothesis: let sleeping dogmas lie? *Neurobiol Aging*, 23, 1101-1105.
- Blagosklonny, M.V. 2007. An anti-aging drug today: from senescence-promoting genes to anti-aging pill. *Drug Discov Today*, 12, 218-224.
- Blanchard, B.J., Chen, A., Rozeboom, L.M., Stafford, K.A., Weigele, P., and Ingram, V.M. 2004. Efficient reversal of Alzheimer's disease fibril formation and elimination of neurotoxicity by a small molecule. *Proc Natl Acad Sci U S A*, 101, 14326-32.
- Blum, H., Beier, H., and Gross, H. J. 1987. Improved silver staining of plant proteins, RNA and DNA in polyacrylamide gels. *Electrophoresis*, 8, 93-99.
- Bonda, D.J., Lee, H.P., Kudo, W., Zhu, X., Smith, M.A., and Lee, H.G. 2010. Pathological implications of cell cycle re-entry in Alzheimer disease. *Expert Rev Mol Med*, 12, e19.
- Boot, M. J., Steegers-Theunissen, R.P., Poelmann, R. E., Van Iperen, L., Lindemans, J., and Gittenberger-de Groot, A.C. 2003. Folic acid and homocysteine affect neural crest and neuroepithelial cell outgrowth and differentiation *in vitro*. *Dev Dyn*, 227, 301-8.
- Borges, F., Roleira, F., Milhazes, N., Santana, L., and Uriarte, E. 2005. Simple coumarins and analogues in medicinal chemistry: occurrence, synthesis and biological activity. *Curr Med Chem*, 12, 887-916.
- Braak, H., and Del Tredici, K. 2012. Where, when, and in what form does sporadic Alzheimer's disease begin? *Curr Opin Neurol*, 25, 708-14.
- Braun, R. J., Büttner, S., Ring, J., Kroemer, G., and Madeo, F. 2010. Nervous yeast: modeling neurotoxic cell death. *Trends Biochem Sci*, 35, 135-144.
- Bregues, M., and Parker, R. 2007. Accumulation of polyadenylated mRNA, Pab1p, eIF4E, and eIF4G with P-bodies in *Saccharomyces cerevisiae*. *Mol Biol Cell*, 18, 2592-602.
-

-
- Bregues, M., Teixeira, D., and Parker, R. 2005. Movement of eukaryotic mRNAs between polysomes and cytoplasmic processing bodies. *Science*, 310, 486-9.
- Bretteville, A., and Planel, E. 2008. Tau aggregates: toxic, inert, or protective species? *J Alzheimers Dis*, 14, 431-6.
- Broco, N., Tenreiro, S., Viegas, C. A., and Sa-Correia, I. 1999. *FLR1* gene (ORF YBR008c) is required for benomyl and methotrexate resistance in *Saccharomyces cerevisiae* and its benomyl-induced expression is dependent on *pdr3* transcriptional regulator. *Yeast*, 15, 1595-608.
- Burdon, R.H. 1995. Superoxide and hydrogen peroxide in relation to mammalian cell proliferation. *Free Radic Biol Med*, 18, 775-94.
- Burdon, R.H., Gill, V., and Alliangana, D. 1996. Hydrogen peroxide in relation to proliferation and apoptosis in BHK-21 hamster fibroblasts. *Free Radic Res*, 24, 81-93.
- Bush, A.I. 2013. The metal theory of Alzheimer's disease. *J Alzheimers Dis*, 33 Suppl 1, S277-81.
- Busser, J., Geldmacher, D. S., and Herrup, K. 1998. Ectopic cell cycle proteins predict the sites of neuronal cell death in Alzheimer's disease brain. *J Neurosci*, 18, 2801-7.
- Butterfield, S., Hejjaoui, M., Fauvet, B., Awad, L., and Lashuel, H.A. 2012. Chemical strategies for controlling protein folding and elucidating the molecular mechanisms of amyloid formation and toxicity. *J Mol Biol*, 421, 204-236.
- Buttner, S., Bitto, A., Ring, J., Augsten, M., Zabrocki, P., Eisenberg, T., Jungwirth, H., Hutter, S., Carmona-Gutierrez, D., Kroemer, G., Winderickx, J., and Madeo, F. 2008. Functional mitochondria are required for α -synuclein toxicity in aging yeast. *J Biol Chem*, 283, 7554-60.
- Cacabelos, R. 2004. Genomic characterization of Alzheimer's disease and genotype-related phenotypic analysis of biological markers in dementia. *Pharmacogen*, 5, 1049-105.
- Cacabelos, R., and Torrellas, C. 2014. Epigenetic drug discovery for Alzheimer's disease. *Expert Opin Drug Discov*, 9, 1059-86.
- Cai, J., Qi, X., Kociok, N., Skosyrski, S., Emilio, A., Ruan, Q., Han, S., Liu, L., Chen, Z., Bowes Rickman, C., Golde, T., Grant, M. B., Saftig, P., Serneels, L., de Strooper, B., Jousen, A. M., and Boulton, M. E. 2012. β -Secretase (BACE1) inhibition causes retinal pathology by vascular dysregulation and accumulation of age pigment. *EMBO Mol Med*, 4, 980-91.
-

-
- Caine, J., Sankovich, S., Antony, H., Waddington, L., Macreadie, P., Varghese, J., and Macreadie, I. 2007a. Alzheimer's A β fused to green fluorescent protein induces growth stress and a heat shock response. *FEMS Yeast Res*, 7, 1230-6.
- Caine, J., Volitakis, I., Cherny, R., Varghese, J., and Macreadie, I. 2007b. A β produced as a fusion to maltose binding protein can be readily purified and stably associates with copper and zinc. *Protein Pept Lett*, 14, 83-6.
- Cali, T., Ottolini, D., and Brini, M. 2011. Mitochondria, calcium, and endoplasmic reticulum stress in Parkinson's disease. *Biofactors*, 37, 228-40.
- Campbell, A. 2006. The role of aluminum and copper on neuroinflammation and Alzheimer's disease. *J Alzheimers Dis*, 10, 165-72.
- Carvalho, C., Katz, P. S., Dutta, S., Katakam, P. V., Moreira, P. I., and Busija, D. W. 2014. Increased susceptibility to amyloid- β toxicity in rat brain microvascular endothelial cells under hyperglycemic conditions. *J Alzheimers Dis*, 38, 75-83.
- Castelli, L.M., Lui, J., Campbell, S.G., Rowe, W., Zeef, L.A., Holmes, L.E., Hoyle, N.P., Bone, J., Selley, J.N., Sims, P.F., and Ashe, M.P. 2011. Glucose depletion inhibits translation initiation via eIF4A loss and subsequent 48S preinitiation complex accumulation, while the pentose phosphate pathway is coordinately up-regulated. *Mol Biol Cell*, 22, 3379-93.
- Chacińska, A., Woźny, W., Boguta, M., Misicka, A., Brzyska, M., and Elbaum, D. 2002. Effects of β -amyloid on proliferation and morphology of yeast *Saccharomyces cerevisiae*. *Lett Pept Sci*, 9, 197-201.
- Chan, K., Chui, S.H., Wong, D.Y.L., Ha, W.Y., Chan, C.L., and Wong, R.N.S. 2004. Protective effects of Danshensu from the aqueous extract of *Salvia miltiorrhiza* (Danshen) against homocysteine-induced endothelial dysfunction. *Life Sci*, 75, 3157-3171.
- Chartier-Harlin, M.C., Parfitt, M., Legrain, S., Perez-Tur, J., Brousseau, T., Evans, A., Berr, C., Vidal, O., Roques, P., and Gourlet, V. 1994. Apolipoprotein E, ϵ 4 allele as a major risk factor for sporadic early and late-onset forms of Alzheimer's disease: analysis of the 19q13.2 chromosomal region. *Human Mol Gen*, 3, 569-74.
- Chazotte, B. 2011. Labeling Nuclear DNA Using DAPI. *Cold Spring Harbor Protocols*, 2011. NY, USA, pdb.prot5556.
- Chen, J., Armstrong, A.H., Koehler, A.N., and Hecht, M.H. 2010. Small molecule microarrays enable the discovery of compounds that bind the Alzheimer's A β peptide and reduce its cytotoxicity. *J Am Chem Soc*, 132, 17015-17022.
- Chenal, A., Vendrely, C., Vitrac, H., Karst, J.C., Gonneaud, A., Blanchet, C.E., Pichard, S., Garcia, E., Salin, B., Catty, P., Gillet, D., Hussy, N., Marquette,

-
- C., Almunia, C., and Forge, V. 2012. Amyloid fibrils formed by the programmed cell death regulator Bcl-xL. *J Mol Biol*, 415, 584-599.
- Cheng, B., Gong, H., Xiao, H., Petersen, R.B., Zheng, L., and Huang, K. 2013. Inhibiting toxic aggregation of amyloidogenic proteins: A therapeutic strategy for protein misfolding diseases. *Biochim Biophys Acta*, 1830, 4860-4871.
- Cherry, J.M., Hong, E.L., Amundsen, C., Balakrishnan, R., Binkley, G., Chan, E.T., Christie, K.R., Costanzo, M.C., Dwight, S.S., Engel, S.R., Fisk, D.G., Hirschman, J.E., Hitz, B.C., Karra, K., Krieger, C. J., Miyasato, S. R., Nash, R.S., Park, J., Skrzypek, M.S., Simison, M., Weng, S., and Wong, E.D. 2012. *Saccharomyces* Genome Database: the genomics resource of budding yeast. *Nucleic Acids Res*, 40, D700-5.
- Chiang, C.C., Mouscadet, J.F., Tsai, H.J., Liu, C.T., and Hsu, L.Y. 2007. Synthesis and HIV-1 integrase inhibition of novel bis- or tetra-coumarin analogues. *Chem Pharm Bull*, 55, 1740-3.
- Choo, X.Y., Alukaidey, L., White, A.R., and Grubman, A. 2013. Neuroinflammation and copper in Alzheimer's disease. *Int J Alzheimers Dis*, 2013, 12.
- Churcher, C., Bowman, S., Badcock, K., Bankier, A., Brown, D., Chillingworth, T., Connor, R., Devlin, K., Gentles, S., Hamlin, N., Harris, D., Horsnell, T., Hunt, S., Jagels, K., Jones, M., Lye, G., Moule, S., Odell, C., Pearson, D., Rajandream, M., Rice, P., Rowley, N., Skelton, J., Smith, V., Barrell, B., and Davis, R.W. 1997. The nucleotide sequence of *Saccharomyces cerevisiae* chromosome IX. *Nature*, 387, 84-7.
- Cohen, F.E., and Kelly, J.W. 2003. Therapeutic approaches to protein-misfolding diseases. *Nature*, 426, 905-9.
- Cohen, S.N., Chang, A.C., and Hsu, L. 1972. Nonchromosomal antibiotic resistance in bacteria: genetic transformation of *Escherichia coli* by R-factor DNA. *Proc Natl Acad Sci U S A*, 69, 2110-4.
- Copani, A., Guccione, S., Giurato, L., Caraci, F., Calafiore, M., Sortino, M. A., and Nicoletti, F. 2008. The cell cycle molecules behind neurodegeneration in Alzheimer's disease: perspectives for drug development. *Curr Med Chem*, 15, 2420-32.
- Costanzo, M., Baryshnikova, A., Bellay, J., Kim, Y., Spear, E.D., Sevier, C.S., Ding, H., Koh, J.L., Toufighi, K., Mostafavi, S., Prinz, J., St Onge, R.P., VanderSluis, B., Makhnevych, T., Vizeacoumar, F.J., Alizadeh, S., Bahr, S., Brost, R.L., Chen, Y., Cokol, M., Deshpande, R., Li, Z., Lin, Z.Y., Liang, W., Marback, M., Paw, J., San Luis, B. J., Shuteriqi, E., Tong, A.H., van Dyk, N., Wallace, I.M., Whitney, J.A., Weirauch, M.T., Zhong, G., Zhu, H., Houry, W. A., Brudno, M., Ragibizadeh, S., Papp, B., Pal, C., Roth, F.P., Giaever, G., Nislow, C., Troyanskaya, O. G., Bussey, H., Bader, G. D., Gingras, A.C.,
-

-
- Morris, Q.D., Kim, P.M., Kaiser, C. A., Myers, C.L., Andrews, B.J., and Boone, C. 2010. The genetic landscape of a cell. *Science*, 327, 425-31.
- Crescenzi, O., Tomaselli, S., Guerrini, R., Salvadori, S., D'Ursi, A.M., Temussi, P. A., and Picone, D. 2002. Solution structure of the Alzheimer amyloid β -peptide (1–42) in an apolar microenvironment. *Eur J Biochem*, 269, 5642-48.
- Crider, K.S., Yang, T.P., Berry, R.J., and Bailey, L.B. 2012. Folate and DNA methylation: A review of molecular mechanisms and the evidence for folate's role. *Adv Nutr*, 3, 21-38.
- Cullen, P.J., and Sprague, G.F. 2002. The roles of bud-site-selection proteins during haploid invasive growth in yeast. *Mol Biol Cell*, 13, 2990-3004.
- Culotti, J., and Hartwell, L.H. 1971. Genetic control of the cell division cycle in yeast: III. Seven genes controlling nuclear division. *Exp Cell Res*, 67, 389-401.
- D'Angelo, F., Vignaud, H., Di Martino, J., Salin, B., Devin, A., Cullin, C., and Marchal, C. 2013. A yeast model for amyloid- β aggregation exemplifies the role of membrane trafficking and PICALM in cytotoxicity. *Dis Model Mech*, 6, 206-16.
- D'Souza, R.J., Phillips, H.M., Jones, P.W., Strange, R.C., and Aber, G.M. 1993. Interactions of hydrogen peroxide with interleukin-6 and platelet-derived growth factor in determining mesangial cell growth: effect of repeated oxidant stress. *Clin Sci*, 85, 747-51.
- David, D.C., Layfield, R., Serpell, L., Narain, Y., Goedert, M., and Spillantini, M.G. 2002. Proteasomal degradation of tau protein. *J Neurochem*, 83, 176-85.
- Davidow, L. S., Goetsch, L., and Byers, B. 1980. Preferential occurrence of non-sister spores in two-spored asci of *Saccharomyces cerevisiae*: evidence for regulation of spore-wall formation by the spindle pole body. *Genetics*, 94, 581-595.
- Day, R. M., and Suzuki, Y.J. 2005. Cell proliferation, reactive oxygen and cellular glutathione. *Dose-response : Int Hormesis Soc*, 3, 425-42.
- de Groot, P. W., Kraneveld, E.A., Yin, Q.Y., Dekker, H.L., Gross, U., Crielaard, W., de Koster, C.G., Bader, O., Klis, F.M., and Weig, M. 2008. The cell wall of the human pathogen *Candida glabrata*: differential incorporation of novel adhesion-like wall proteins. *Eukaryot Cell*, 7, 1951-64.
- De Felice, F.G., Vieira, M.N., Saraiva, L.M., Figueroa-Villar, J.D., Garcia-Abreu, J., Liu, R., Chang, L., Klein, W.L., and Ferreira, S.T. 2004. Targeting the neurotoxic species in Alzheimer's disease: inhibitors of A β oligomerization. *FASEB J*, 18, 1366-72.
-

-
- De Ferrari, G.V., Mallender, W. D., Inestrosa, N.C., and Rosenberry, T.L. 2001. Thioflavin T is a fluorescent probe of the acetylcholinesterase peripheral site that reveals conformational interactions between the peripheral and acylation sites. *J Biol Chem*, 276, 23282-87.
- de Souza, S.M., Delle Monache, F., and Smania, A. 2005. Antibacterial activity of coumarins. *Zeitschrift fur Naturforschung. J Biosci*, 60, 693-700.
- De Virgilio, C. 2012. The essence of yeast quiescence. *FEMS Microbiol Rev*, 36, 306-39.
- De Vos, A., Anandhakumar, J., Van den Brande, J., Verduyck, M., Franssens, V., Winderickx, J., and Swinnen, E. 2011. Yeast as a model system to study tau biology. *Int J Alzheimer's Dis*, 2011, e428970, doi:10.4061/2011/428970
- Deane, R., Bell, R.D., Sagare, A., and Zlokovic, B.V. 2009. Clearance of amyloid- β peptide across the blood-brain barrier: implication for therapies in Alzheimer's disease. *CNS Neurol Disord Drug Targets*, 8, 16-30.
- Delitheos, A., Karavokyros, I., and Tiligada, E. 1995. Response of *Saccharomyces cerevisiae* strains to antineoplastic agents. *J App Bacteriol*, 79, 379-83.
- Deshpande, A., Mina, E., Glabe, C., and Busciglio, J. 2006. Different conformations of amyloid beta induce neurotoxicity by distinct mechanisms in human cortical neurons. *J Neurosci*, 26, 6011-8.
- Ding, X.L., Husseman, J., Tomashevski, A., Nochlin, D, Jin, L.W., and Vincent, I. 2000. The cell cycle Cdc25A tyrosine phosphatase is activated in degenerating postmitotic neurons in Alzheimer's disease. *Am J Pathol*, 157, 1983-1990.
- Dong, B., Ma, T., Zhang, T., Zhou, C.M., Liu, G., Wang, L., Tao, P.Z., and Zhang, X.Q. 2011. Anti-HIV-1 activity and structure-activity relationship of pyranocoumarin analogs. *Acta pharmaceutica Sinica*, 46, 35-8.
- Douaud, G., Refsum, H., de Jager, C.A., Jacoby, R., E. Nichols, T., Smith, S. M., and Smith, A.D. 2013. Preventing Alzheimer's disease-related gray matter atrophy by B-vitamin treatment. *Proc Natl Acad Sci U S A*, 110, 9523-8.
- Du, H., and Yan, S.S. 2010. Mitochondrial permeability transition pore in Alzheimer's disease: Cyclophilin D and amyloid beta. *Biochim Biophys Acta*, 1802, 198-204.
- Dubey, A.K., Bharadwaj, P.R., Varghese, J.N. and Macreadie, I.G. 2009. Alzheimer's A β rescues yeast from hydroxide toxicity. *J Alzheimers Dis*, 18, 31-3.
- Echeverria, V., Ducatenzeiler, A., Chen, C.H., and Cuello, A.C. 2005. Endogenous β -amyloid peptide synthesis modulates cAMP response element-regulated gene expression in PC12 cells. *Neurosci*, 135, 1193-1202.
-

-
- Eckert, A., Hauptmann, S., Scherping, I., Meinhardt, J., Rhein, V., Drose, S., Brandt, U., Fandrich, M., Muller, W.E., and Gotz, J. 2008. Oligomeric and fibrillar species of β -amyloid (A β 42) both impair mitochondrial function in P301L tau transgenic mice. *J Mol Med*, 86, 1255-67.
- Edbauer, D., Winkler, E., Regula, J.T., Pesold, B., Steiner, H., and Haass, C. 2003. Reconstitution of γ -secretase activity. *Nat Cell Biol*, 5, 486-8.
- Emili, A., Schieltz, D.M., Yates Iii, J.R., and Hartwell, L.H. 2001. Dynamic interaction of DNA damage checkpoint protein Rad53 with chromatin assembly factor Asf1. *Mol Cell*, 7, 13-20.
- Enyenihi, A.H., and Saunders, W.S. 2003. Large-scale functional genomic analysis of sporulation and meiosis in *Saccharomyces cerevisiae*. *Genetics*, 163, 47-54.
- Erickson, K.I., Suever, B.L., Prakash, R.S., Colcombe, S.J., McAuley, E., and Kramer, A.F. 2008. Greater intake of vitamins B6 and B12 spares gray matter in healthy elderly: A voxel-based morphometry study. *Brain Res*, 1199, 20-26.
- Esler, W.P., Stimson, E.R., Ghilardi, J.R., Felix, A.M., Lu, Y.A., Vinters, H.V., Mantyh, P.W., and Maggio, J.E. 1997. A β deposition inhibitor screen using synthetic amyloid. *Nat Biotech*, 15, 258-63.
- Esteban, J.A. 2004. Living with the enemy: a physiological role for the β -amyloid peptide. *Trends Neurosci*, 27, 1-3.
- Evangelisti, E., Wright, D., Zampagni, M., Cascella, R., Fiorillo, C., Bagnoli, S., Relini, A., Nichino, D., Scartabelli, T., Nacmias, B., Sorbi, S., and Cecchi, C. 2013. Lipid rafts mediate amyloid-induced calcium dyshomeostasis and oxidative stress in Alzheimer's disease. *Curr Alzheimer Res*, 10, 143-53.
- Evans, T., Rosenthal, E.T., Youngblom, J., Distel, D., and Hunt, T. 1983. Cyclin: a protein specified by maternal mRNA in sea urchin eggs that is destroyed at each cleavage division. *Cell*, 33, 389-96.
- Evin, G., Sernee, M.F., and Masters, C.L. 2006. Inhibition of γ -secretase as a therapeutic intervention for Alzheimer's disease: prospects, limitations and strategies. *CNS Drugs*, 20, 351-72.
- Fabrizio, P., and Longo, V.D. 2003. The chronological life span of *Saccharomyces cerevisiae*. *Aging cell*, 2, 73-81.
- Fabrizio, P., and Longo, V.D. 2008. Chronological aging-induced apoptosis in yeast. *Biochim Biophys Acta*, 1783, 1280-5.
- Fabrizio, P., Pozza, F., Pletcher, S.D., Gendron, C.M., and Longo, V.D. 2001. Regulation of longevity and stress resistance by Sch9 in yeast. *Science*, 292, 288-90.
-

-
- Fandrich, M. 2012. Oligomeric intermediates in amyloid formation: structure determination and mechanisms of toxicity. *J Mol Biol*, 421, 427-40.
- Fandrich, M., Meinhardt, J., and Grigorieff, N. 2009. Structural polymorphism of Alzheimer A β and other amyloid fibrils. *Prion*, 3, 89-93.
- Farcasanu, I.C., Hirata, D., Tsuchiya, E., Mizuta, K., and Miyakawa, T. 1999. Involvement of thioredoxin peroxidase type II (Ahp1p) of *Saccharomyces cerevisiae* in Mn²⁺ homeostasis. *Biosci Biotech Biochem*, 63, 1871-81.
- Farioli-Vecchioli, S., Mattera, A., Micheli, L., Ceccarelli, M., Leonardi, L., Sarauli, D., Costanzi, M., Cestari, V., Rouault, J.P., and Tirone, F. 2014. Running rescues defective adult neurogenesis by shortening the length of the cell cycle of neural stem and progenitor cells. *Stem Cells*, 32, 1968-82.
- Faux, N.G., Ellis, K.A., Porter, L., Fowler, C.J., Laws, S.M., Martins, R.N., Pertile, K.K., Rembach, A., Rowe, C. C., Rumble, R. L., Szoeki, C., Taddei, K., Taddei, T., Trounson, B.O., Villemagne, V.L., Ward, V., Ames, D., Masters, C.L., and Bush, A.I. 2011. Homocysteine, vitamin B12, and folic acid levels in Alzheimer's disease, mild cognitive impairment, and healthy elderly: baseline characteristics in subjects of the Australian Imaging Biomarker Lifestyle study. *J Alzheimers Dis*, 27, 909-22.
- Feng, Y., You, Z., Yan, S., He, G., Chen, Y., Gou, X., and Peng, C. 2012. Antidepressant-like effects of salvianolic acid B in the mouse forced swim and tail suspension tests. *Life Sci*, 90, 1010-4.
- Feng, Y., Wang, X., Yang, S., Wang, Y., Zhang, X., Du, X., Sun, X., Zhao, M., Huang, L., and Liu, R. 2009. Resveratrol inhibits β -amyloid oligomeric cytotoxicity but does not prevent oligomer formation. *Neuro Toxicol*, 30, 986-995.
- Ferreiro, E., Baldeiras, I., Ferreira, I.L., Costa, R. O., Rego, A.C., Pereira, C.F., and Oliveira, C. R. 2012. Mitochondrial and endoplasmic reticulum-associated oxidative stress in Alzheimer's disease: from pathogenesis to biomarkers. *Int J Cell Biol*, 2012, 1-23.
- Fidel Jr, P. L., Vazquez, J. A., and Sobel, J.D. 1999. *Candida glabrata*: Review of Epidemiology, Pathogenesis, and Clinical Disease with Comparison to *C. albicans*. *Clin Microbiol Rev*, 12, 80-96.
- Fields, S., and Song, O. 1989. A novel genetic system to detect protein-protein interactions. *Nature*, 340, 245-46.
- Findeis, M.A. 2007. The role of amyloid- β peptide 42 in Alzheimer's disease. *Pharmacol Therap*, 116, 266-86.
- Flicker, L. 2010. Modifiable lifestyle risk factors for Alzheimer's disease. *J Alzheimers Dis*, 20, 803-11.
-

-
- Foury, F. 1997. Human genetic diseases: a cross-talk between man and yeast. *Gen*, 195, 1-10.
- Fowler, B. 2001. The folate cycle and disease in humans. *Kidney Int Supp*, 78, S221-9.
- Freire, S., de Araujo, M.H., Al-Soufi, W., and Novo, M. 2014. Photophysical study of Thioflavin T as fluorescence marker of amyloid fibrils. *Dyes Pigm*, 110, 97-105.
- Frits A.M. 2005. The importance of (early) folate status to primary and secondary coronary artery disease prevention. *Reprod Toxicol*, 20, 403-410.
- Galas, M. C., Dourlen, P., Begard, S., Ando, K., Blum, D., Hamdane, M., and Buee, L. 2006. The peptidylprolyl cis/trans-isomerase Pin1 modulates stress-induced dephosphorylation of tau in neurons. Implication in a pathological mechanism related to Alzheimer disease. *J Biol Chem*, 281, 19296-304.
- Games, D., Adams, D., Alessandrini, R., Barbour, R., Borthellette, P., Blackwell, C., Carr, T., Clemens, J., Donaldson, T., Gillespie, F., Guido, T., Hagopian, S., Johnson-Wood, K., Khan, K., Lee, M., Leibowitz, P., Lieberburg, I., Little, S., Masliah, E., McConlogue, L., Montoya-Zavala, M., Mucke, L., Paganini, L., Penniman, E., Power, M., Schenk, D., Seubert, P., Snyder, B., Soriano, F., Tan, H., Vitale, J., Wadsworth, S., Wolozin, B., and Zhao, J. 1995. Alzheimer-type neuropathology in transgenic mice overexpressing V717F β -amyloid precursor protein. *Nature*, 373, 523-27.
- Garrido, E.O., and Grant, C.M. 2002. Role of thioredoxins in the response of *Saccharomyces cerevisiae* to oxidative stress induced by hydroperoxides. *Mol Microbiol*, 43, 993-1003.
- Gaur, M., Puri, N., Manoharlal, R., Rai, V., Mukhopadhyay, G., Choudhury, D., and Prasad, R. 2008. MFS transportome of the human pathogenic yeast *Candida albicans*. *BMC Genomics*, 9, 579.
- Gazit, E. 2002. A possible role for π -stacking in the self-assembly of amyloid fibrils. *FASEB J*, 16, 77-83.
- Gella, A., and Durany, N. 2009. Oxidative stress in Alzheimer disease. *Cell Adhes Migrat*, 3, 88-93.
- Ghannoum, M. A., Motawy, M. S., AbuHatab, M. A., and AbuElteen, K.A. 1989. Interactive effect of antifungal and antineoplastic agents on yeasts commonly prevalent in cancer patients. *Antimicrob Agents Chemother*, 33, 726-30.
- Ghannoum, M. A., AbuElteen, K. A., Motawy, M. S., AbuHatab, M. A., Ibrahim, A.S., and Criddle, R.S. 1990. Combinations of antifungal and antineoplastic drugs with interactive effects on inhibition of yeast growth. *Chemother*, 36, 308-20.
-

-
- Giuffrida, M.L., Caraci, F., De Bona, P., Pappalardo, G., Nicoletti, F., Rizzarelli, E., and Copani, A. 2010. The monomer state of β -amyloid: where the Alzheimer's disease protein meets physiology. *Rev Neurosci*, 21, 83-93.
- Glabe, C. 2009. Amyloid oligomer structures and toxicity. *The Open Biol J*, 2, 222-227.
- Glabe, C.C. 2005. Amyloid accumulation and pathogenesis of Alzheimer's disease: significance of monomeric, oligomeric and fibrillar A β . *Subcell Biochem*, 38, 167-77.
- Glabe, C.G. 2008. Structural classification of toxic amyloid oligomers. *J Biol Chem*, 283, 29639-43.
- Goate, A., Chartier-Harlin, M.C., Mullan, M., Brown, J., Crawford, F., Fidani, L., Giuffra, L., Haynes, A., Irving, N., James, L., Mant, R., Newton, P., Rooke, K., Roques, P., Talbot, C., Pericak-Vance, M., Roses, A., Williamson, R., Rossor, M., Owen, M., and Hardy, J. 1991. Segregation of a missense mutation in the amyloid precursor protein gene with familial Alzheimer's disease. *Nature*, 349, 704-706.
- Goedert, M. 2009. Oskar Fischer and the study of dementia. *Brain*, 132, 1102-11.
- Goehring, A.S., Rivers, D.M., and Sprague, G.F. 2003. Attachment of the ubiquitin-related protein Urm1p to the antioxidant protein Ahp1p. *Eukar Cell*, 2, 930-6.
- Goffeau, A., Barrell, B.G., Bussey, H., Davis, R.W., Dujon, B., Feldmann, H., Galibert, F., Hoheisel, J.D., Jacq, C., Johnston, M., Louis, E. J., Mewes, H. W., Murakami, Y., Philippsen, P., Tettelin, H., and Oliver, S.G. 1996. Life with 6000 genes. *Science*, 274, 563-7.
- Goldbaum, O., Oppermann, M., Handschuh, M., Dabir, D., Zhang, B., Forman, M. S., Trojanowski, J.Q., Lee, V.M., and Richter-Landsberg, C. 2003. Proteasome inhibition stabilizes tau inclusions in oligodendroglial cells that occur after treatment with okadaic acid. *J Neurosci*, 23, 8872-80.
- Gong, H., He, Z., Peng, A., Zhang, X., Cheng, B., Sun, Y., Zheng, L., and Huang, K. 2014. Effects of several quinones on insulin aggregation. *Sci Rep*, 4, 5648.
- Gorkovskii, A.A., Bezsonov, E.E., Plotnikova, T.A., Kalebina, T.S., and Kulaev, I.S. 2009. Revealing of *Saccharomyces cerevisiae* yeast cell wall proteins capable of binding thioflavin T, a fluorescent dye specifically interacting with amyloid fibrils. *Biochem (Mosc)*, 74, 1219-24.
- Grabowski, T.J., Cho, H.S., Vonsattel, J.P., Rebeck, G.W., and Greenberg, S.M. 2001. Novel amyloid precursor protein mutation in an Iowa family with dementia and severe cerebral amyloid angiopathy. *Annals Neurol*, 49, 697-705.
-

-
- Granot, D., and Snyder, M. 1993. Carbon source induces growth of stationary phase yeast cells, independent of carbon source metabolism. *Yeast*, 9, 465-79.
- Gray, J.V., Petsko, G.A., Johnston, G. C., Ringe, D., Singer, R.A., and Werner-Washburne, M. 2004. "Sleeping beauty": quiescence in *Saccharomyces cerevisiae*. *Microbiol Mol Biol Rev*, 68, 187-206.
- Gunuzlu, P.L., White, W.H., Davis, G.L., Hollis, G.F., and Toyn, J.H. 2000. A yeast genetic assay for caspase cleavage of the A β precursor protein. *Mol Biotech*, 15, 29-37.
- Hadjipavlou-Litina, D., Kontogiorgis, C., Pontiki, E., Dakanali, M., Akoumianaki, A., and Katerinopoulos, H.E. 2007. Anti-inflammatory and antioxidant activity of coumarins designed as potential fluorescent zinc sensors. *J Enzyme Inhibit Med Chem*, 22, 287-92.
- Halsted, C.H. 1991. Jejunal brush-border folate hydrolase. A novel enzyme. *West J Med*, 155, 605-9.
- Hamaguchi, T., Ono, K., Murase, A., and Yamada, M. 2009. Phenolic compounds prevent Alzheimer's pathology through different effects on the amyloid- β aggregation pathway. *Am J Pathol*, 175, 2557-65.
- Hanahan, D., Jessee, J., and Bloom, F. R. 1991. Plasmid transformation of *Escherichia coli* and other bacteria. *Method Enzymol*, 204, 63-113.
- Haque, R., and Nazir, A. 2014. Insulin-degrading enzyme: a link between Alzheimer's and type 2 diabetes mellitus. *CNS Neurol Disord Drug Targets*, 13, 259-64.
- Härd, T., and Lendel, C. 2012. Inhibition of amyloid formation. *J Mol Biol*, 421, 441-465.
- Hardy, J. A., and Higgins, G.A. 1992. Alzheimer's disease: the amyloid cascade hypothesis. *Science*, 256, 184-5.
- Hardy, J., and Allsop, D. 1991. Amyloid deposition as the central event in the aetiology of Alzheimer's disease. *Trends Pharmacol Sci.*, 12, 383-8.
- Hardy, J., and Selkoe, D.J. 2002. The amyloid hypothesis of Alzheimer's disease: progress and problems on the road to therapeutics. *Science*, 297, 353-6.
- Hardy, J. 2006. A hundred years of Alzheimer's disease research. *Neuron*, 52, 3-13.
- Harris-White, M. E., and Frautschy, S.A. 2005. Low density lipoprotein receptor-related proteins (LRPs), Alzheimer's and cognition. *Curr Drug Targets CNS Neurol Disord*, 4, 469-80.

-
- Harris, J.R., and Milton, N.G. 2010. Cholesterol in Alzheimer's disease and other amyloidogenic disorders. *Subcell Biochem*, 51, 47-75.
- Hartwell, L.H. 1971. Genetic control of the cell division cycle in yeast: IV. Genes controlling bud emergence and cytokinesis. *Exp Cell Res*, 69, 265-276.
- Hartwell, L.H. 1992. Defects in a cell cycle checkpoint may be responsible for the genomic instability of cancer cells. *Cell*, 71, 543-546.
- Hartwell, L.H., Culotti, J., and Reid, B. 1970. Genetic control of the cell-division cycle in yeast, I. Detection of Mutants. *Proc Natl Acad Sci U S A*, 66, 352-359.
- Harvey, B.S., Musgrave, I.F., Ohlsson, K.S., Fransson, Å., and Smid, S.D. 2011. The green tea polyphenol (-)-epigallocatechin-3-gallate inhibits amyloid- β evoked fibril formation and neuronal cell death *in vitro*. *Food Chem*, 129, 1729-1736.
- Hendriks, L., van Duijn, C.M., Cras, P., Cruts, M., Van Hul, W., van Harskamp, F., Warren, A., McInnis, M.G., Antonarakis, S.E., Martin, J.J., Hofman, A., and Broeckhoven, C.V. 1992. Presenile dementia and cerebral haemorrhage linked to a mutation at codon 692 of the β -amyloid precursor protein gene. *Nat Genet*, 1, 218-21.
- Heo, C., Chang, K.A., Choi, H.S., Kim, H.S., Kim, S., Liew, H., Kim, J.A., Yu, E., Ma, J., and Suh, Y.H. 2007. Effects of the monomeric, oligomeric, and fibrillar A β ₄₂ peptides on the proliferation and differentiation of adult neural stem cells from subventricular zone. *J Neurochem*, 102, 493-500.
- Herrup, K., and Busser, J.C. 1995. The induction of multiple cell cycle events precedes target-related neuronal death. *Development*, 121, 2385-95.
- Herrup, K., Neve, R., Ackerman, S. L., and Copani, A. 2004. Divide and die: cell cycle events as triggers of nerve cell death. *J Neurosci*, 24, 9232-9.
- Herskovits, A.Z., and Guarente, L. 2013. Sirtuin deacetylases in neurodegenerative diseases of aging. *Cell Res*, 23, 746-758.
- Hjortmo, S., Patring, J., and Andlid, T. 2008. Growth rate and medium composition strongly affect folate content in *Saccharomyces cerevisiae*. *Int J Food Microbiol*, 123, 93-100.
- Hoepfner, D., Helliwell, S. B., Sadlish, H., Schuierer, S., Filipuzzi, I., Brachat, S., Bhullar, B., Plikat, U., Abraham, Y., Altorfer, M., Aust, T., Baeriswyl, L., Cerino, R., Chang, L., Estoppey, D., Eichenberger, J., Frederiksen, M., Hartmann, N., Hohendahl, A., Knapp, B., Krastel, P., Melin, N., Nigsch, F., Oakeley, E.J., Petitjean, V., Petersen, F., Riedl, R., Schmitt, E. K., Staedtler, F., Studer, C., Tallarico, J.A., Wetzler, S., Fishman, M.C., Porter, J. A., and Movva, N.R. 2014. High-resolution chemical dissection of a model eukaryote reveals targets, pathways and gene functions. *Microbiol Res*, 169, 107-20.
-

-
- Holtzman, D.M. 2011. CSF biomarkers for Alzheimer's disease: current utility and potential future use. *Neurobiol Aging*, 32 Suppl 1, S4-9.
- Honjo, K., van Reekum, R., and Verhoeff, N. P. L. G. 2009. Alzheimer's disease and infection: Do infectious agents contribute to progression of Alzheimer's disease? *Alzheimers Dement*, 5, 348-360.
- Howitz, K.T., Bitterman, K.J., Cohen, H.Y., Lamming, D.W., Lavu, S., Wood, J.G., Zipkin, R.E., Chung, P., Kisielewski, A., Zhang, L.L., Scherer, B., and Sinclair, D.A. 2003. Small molecule activators of sirtuins extend *Saccharomyces cerevisiae* lifespan. *Nature*, 425, 191-6.
- Hu, X., Hicks, C.W., He, W., Wong, P., Macklin, W.B., Trapp, B.D., and Yan, R. 2006. Bace1 modulates myelination in the central and peripheral nervous system. *Nat Neurosci*, 9, 1520-5.
- Huang, C. J., Haataja, L., Gurlo, T., Butler, A. E., Wu, X., Soeller, W.C., and Butler, P.C. 2007. Induction of endoplasmic reticulum stress-induced β -cell apoptosis and accumulation of polyubiquitinated proteins by human islet amyloid polypeptide. *Am J Physiol Endocrin Metabol*, 293, E1656-62.
- Huang, H.C., Chang, P., Dai, X.L., and Jiang, Z.F. 2012. Protective effects of curcumin on amyloid- β -induced neuronal oxidative damage. *Neurochem Res*, 37, 1584-97.
- Huber, A., Stuchbury, G., Burkle, A., Burnell, J., and Munch, G. 2006. Neuroprotective therapies for Alzheimer's disease. *J Curr Pharm Des*, 12, 705-717.
- Hudson, S.A., Ecroyd, H., Kee, T.W., and Carver, J.A. 2009. The thioflavin T fluorescence assay for amyloid fibril detection can be biased by the presence of exogenous compounds. *FEBS J*, 276, 5960-72.
- Hügel, H.M., and Jackson, N. 2014. Danshen diversity defeating dementia. *Bioorg Medicin Chem Lett*, 24, 708-716.
- Hughes, S.R., Goyal, S., Sun, J.E., Gonzalez-DeWhitt, P., Fortes, M.A., Riedel, N. G., and Sahasrabudhe, S.R. 1996. Two-hybrid system as a model to study the interaction of β -amyloid peptide monomers. *Proc Natl Acad Sci U S A*, 93, 2065-2070.
- Ida, N., Hartmann, T., Pantel, J., Schroder, J., Zerfass, R., Forstl, H., Sandbrink, R., Masters, C.L., and Beyreuther, K. 1996. Analysis of heterogeneous β A4 peptides in human cerebrospinal fluid and blood by a newly developed sensitive Western blot assay. *J Biol Chem*, 271, 22908-14.
- Irie, K., Murakami, K., Masuda, Y., Morimoto, A., Ohigashi, H., Ohashi, R., Takegoshi, K., Nagao, M., Shimizu, T., and Shirasawa, T. 2005. Structure of β -amyloid fibrils and its relevance to their neurotoxicity: Implications for the pathogenesis of Alzheimer's disease. *J Biosci Bioeng*, 99, 437-447.
-

-
- Iuvone, T., De Filippis, D., Esposito, G., D'Amico, A., and Izzo, A.A. 2006. The spice sage and its active ingredient rosmarinic acid protect PC12 cells from amyloid- β peptide-induced neurotoxicity. *J Pharmacol Expl Ther*, 317, 1143-9.
- Iwai, K., Naganuma, A., and Kuge, S. 2010. Peroxiredoxin Ahp1 acts as a receptor for alkylhydroperoxides to induce disulfide bond formation in the Cad1 transcription factor. *J Biol Chem*, 285, 10597-604.
- Izzat, M.B., Yim, A.P. C., and El-Zufari, M. H. 1998. A taste of Chinese medicine! *An Thora Surg*, 66, 941-942.
- Jayamani, J., and Shanmugam, G. 2014. Gallic acid, one of the components in many plant tissues, is a potential inhibitor for insulin amyloid fibril formation. *Eur J Med Chem*, 85, 352-358.
- Jeong, J.S., Kwon, S.J., Kang, S.W., Rhee, S.G., and Kim, K. 1999. Purification and characterization of a second type thioredoxin peroxidase (type II TPx) from *Saccharomyces cerevisiae*. *Biochem*, 38, 776-83.
- Ji, H.F., and Zhang, H.Y. 2008. Multipotent natural agents to combat Alzheimer's disease. Functional spectrum and structural features. *Acta Pharmacologica Sinica*, 29, 143-51.
- Jiang, R.W., Lau, K.M., Hon, P.M., Mak, T.C.W., Woo, K.S., and Fung, K.P. 2005. Chemistry and biological activities of caffeic acid derivatives from *Salvia miltiorrhiza*. *Curr Med Chem*, 12, 237-246.
- Jimenez, A., Lisa-Santamaria, P., Garcia-Marino, M., Escribano-Bailon, M.T., Rivas-Gonzalo, J.C., and Revuelta, J.L. 2010. The biological activity of the wine anthocyanins delphinidin and petunidin is mediated through Msn2 and Msn4 in *Saccharomyces cerevisiae*. *FEMS Yeast Res*, 10, 858-69.
- Jin, M., Shepardson, N., Yang, T., Chen, G., Walsh, D., and Selkoe, D.J. 2011. Soluble amyloid- β protein dimers isolated from Alzheimer cortex directly induce Tau hyperphosphorylation and neuritic degeneration. *Proc Natl Acad Sci U S A*, 108, 5819-24.
- Jones, E.L., Mok, K., Hanney, M., Harold, D., Sims, R., Williams, J., and Ballard, C. 2013. Evidence that PICALM affects age at onset of Alzheimer's dementia in Down syndrome. *Neurobiol Aging*, 34, 2441.e1-2441.e5.
- Jung, N., and Haucke, V. 2007. Clathrin-mediated endocytosis at synapses. *Traffic*, 8, 1129-36.
- Kaeberlein, M., and Guarente, L. 2002. *Saccharomyces cerevisiae* MPT5 and SSD1 function in parallel pathways to promote cell wall integrity. *Genetics*, 160, 83-95.
-

-
- Kalebina, T.S., Plotnikova, T.A., Gorkovskii, A.A., Selyakh, I.O., Galzitskaya, O. V., Bezsonov, E.E., Gellissen, G., and Kulaev, I.S. 2008. Amyloid-like properties of *Saccharomyces cerevisiae* cell wall glucantransferase Bgl2p: prediction and experimental evidences. *Prion*, 2, 91-6.
- Kamboh, M.I. 2004. Molecular genetics of late-onset Alzheimer's disease. *Annals Human Gen*, 68, 381-404.
- Kamenetz, F., Tomita, T., Hsieh, H., Seabrook, G., Borchelt, D., Iwatsubo, T., Sisodia, S., and Malinow, R. 2003. APP processing and synaptic function. *Neuron*, 37, 925-37.
- Kanatsu, K., Morohashi, Y., Suzuki, M., Kuroda, H., Watanabe, T., Tomita, T., and Iwatsubo, T. 2014. Decreased CALM expression reduces A β ₄₂ to total A β ratio through clathrin-mediated endocytosis of γ -secretase. *Nat Commun*, 5.
- Kancheva, V.D., Boranova, P.V., Nechev, J. T., and Manolov, I.I. 2010. Structure–activity relationships of new 4-hydroxy bis-coumarins as radical scavengers and chain-breaking antioxidants. *Biochimie*, 92, 1138-46.
- Kane, M.D., Lipinski, W.J., Callahan, M.J., Bian, F., Durham, R.A., Schwarz, R.D., Roher, A.E., and Walker, L.C. 2000. Evidence for seeding of β -amyloid by intracerebral infusion of Alzheimer brain extracts in β -amyloid precursor protein-transgenic mice. *J Neurosci*, 20, 3606-11.
- Karuppagounder, S.S., Pinto, J.T., Xu, H., Chen, H. L., Beal, M.F., and Gibson, G.E. 2009. Dietary supplementation with resveratrol reduces plaque pathology in a transgenic model of Alzheimer's disease. *Neurochem Int*, 54, 111-8.
- Kayed, R., Head, E., Sarsoza, F., Saing, T., Cotman, C. W., Necula, M., Margol, L., Wu, J., Breydo, L., Thompson, J.L., Rasool, S., Gurlo, T., Butler, P., and Glabe, C.G. 2007. Fibril specific, conformation dependent antibodies recognize a generic epitope common to amyloid fibrils and fibrillar oligomers that is absent in prefibrillar oligomers. *Mol Neurodegen*, 2, 1-11.
- Kayed, R., and Lasagna-Reeves, C.A. 2013. Molecular mechanisms of amyloid oligomers toxicity. *J Alzheimers Dis*, 33 Suppl 1, S67-78.
- Kayed, R., Pensalfini, A., Margol, L., Sokolov, Y., Sarsoza, F., Head, E., Hall, J., and Glabe, C. 2009. Annular protofibrils are a structurally and functionally distinct type of amyloid oligomer. *J Biol Chem*, 284, 4230-37.
- Kayed, R., Head, E., Thompson, J.L., McIntire, T.M., Milton, S.C., Cotman, C.W., and Glabe, C.G. 2003. Common structure of soluble amyloid oligomers implies common mechanism of pathogenesis. *Science*, 300, 486-89.
- Keshet, B., and Good, T. 2010. A β toxicity inhibitors as probes of A β “active-site”. *Alzheimers Dement*, 6, S247.
-

-
- Khan, K.M., Iqbal, S., Lodhi, M.A., Maharvi, G.M., Ullah, Z., Choudhary, M.I., Rahman, A., and Perveen, S. 2004. Biscoumarin: new class of urease inhibitors; economical synthesis and activity. *Bioorg Med Chem*, 12, 1963-68.
- Khurana, V., and Lindquist, S. 2010. Modelling neurodegeneration in *Saccharomyces cerevisiae*: why cook with baker's yeast? *Nat Rev Neurosci*, 11, 436-49.
- Kim, C.Y., Lee, C., Park, G.H., and Jang, J.H. 2009. Neuroprotective effect of epigallocatechin-3-gallate against β -amyloid-induced oxidative and nitrosative cell death via augmentation of antioxidant defense capacity. *Arch Pharma Res*, 32, 869-81.
- Kim, D.H., Park, S.J., Kim, J.M., Jeon, S.J., Kim, D.H., Cho, Y.W., Son, K.H., Lee, H.J., Moon, J.H., Cheong, J.H., Ko, K.H., and Ryu, J.H. 2011. Cognitive dysfunctions induced by a cholinergic blockade and A β 25-35 peptide are attenuated by salvianolic acid B. *Neuropharmacol*, 61, 1432-40.
- Kim, H.S., Quon, M.J., and Kim, J.A. 2014. New insights into the mechanisms of polyphenols beyond antioxidant properties; lessons from the green tea polyphenol, epigallocatechin 3-gallate. *Redox Biol*, 2, 187-195.
- Kim, J.M., Stewart, R., Kim, S.W., Shin, I.S., Yang, S.J., Shin, H.Y., and Yoon, J.S. 2008. Changes in folate, vitamin B12 and homocysteine associated with incident dementia. *J Neurol Neurosurg Psychiatry*, 79, 864-8.
- Kim, W., and Hecht, M.H. 2005. Sequence determinants of enhanced amyloidogenicity of Alzheimer A β ₄₂ peptide relative to A β ₄₀. *J Biol Chem*, 280, 35069-76.
- Kim, W., Kim, Y., Min, J., Kim, D.J., Chang, Y.T., and Hecht, M.H. 2006. A high-throughput screen for compounds that inhibit aggregation of the Alzheimer's peptide. *ACS Chem Biol*, 1, 461-9.
- Kim, Y.I. 2003. Role of folate in colon cancer development and progression. *J Nut*, 133, 3731s-3739s.
- Klein, W.L., Stine, W.B., and Teplow, D.B. 2004. Small assemblies of unmodified amyloid- β protein are the proximate neurotoxin in Alzheimer's disease. *Neurobiol Aging*, 25, 569-80.
- Klis, F.M., Mol, P., Hellingwerf, K., and Brul, S. 2002. Dynamics of cell wall structure in *Saccharomyces cerevisiae*. *FEMS Microbiol Rev*, 26, 239-56.
- Klosinska, M.M., Crutchfield, C.A., Bradley, P.H., Rabinowitz, J.D., and Broach, J.R. 2011. Yeast cells can access distinct quiescent states. *Genes Develop*, 25, 336-49.
-

-
- Klyubin, I., Cullen, W.K., Hu, N.W., and Rowan, M.J. 2012. Alzheimer's disease A β assemblies mediating rapid disruption of synaptic plasticity and memory. *Mol Brain*, 5, e25, doi: 10.1186/1756-6606-5-25.
- Knobloch, M., Konietzko, U., Krebs, D.C., and Nitsch, R.M. 2007. Intracellular A β and cognitive deficits precede β -amyloid deposition in transgenic arcA β mice. *Neurobiol Aging*, 28, 1297-306.
- Kruman, I.I., Kumaravel, T.S., Lohani, A., Pedersen, W.A., Cutler, R.G., Kruman, Y., Haughey, N., Lee, J., Evans, M., and Mattson, M.P. 2002. Folic acid deficiency and homocysteine impair DNA repair in hippocampal neurons and sensitize them to amyloid toxicity in experimental models of Alzheimer's disease. *J Neurosci*, 22, 1752-62.
- Kumar, S., and Walter, J. 2011. Phosphorylation of amyloid beta (A β) peptides - a trigger for formation of toxic aggregates in Alzheimer's disease. *Aging*, 3, 803-12.
- Kuranda, K., Leberre, V., Sokol, S., Palamarczyk, G., and Francois, J. 2006. Investigating the caffeine effects in the yeast *Saccharomyces cerevisiae* brings new insights into the connection between TOR, PKC and Ras/cAMP signalling pathways. *Mol Microbiol*, 61, 1147-66.
- Lacor, P.N., Buniel, M. C., Chang, L., Fernandez, S.J., Gong, Y., Viola, K.L., Lambert, M.P., Velasco, P.T., Bigio, E.H., Finch, C.E., Krafft, G.A., and Klein, W.L. 2004. Synaptic targeting by Alzheimer's-related amyloid- β oligomers. *J Neurosci*, 24, 10191-200.
- Ladiwala, A.R., Litt, J., Kane, R. S., Aucoin, D.S., Smith, S.O., Ranjan, S., Davis, J., Van Nostrand, W.E., and Tessier, P.M. 2012. Conformational differences between two amyloid- β oligomers of similar size and dissimilar toxicity. *J Biol Chem*, 287, 24765-73.
- LaFerla, F.M., Green, K.N., and Oddo, S. 2007. Intracellular A β in Alzheimer's disease. *Nat Rev Neurosci*, 8, 499-509.
- Lambert, M.P., Barlow, A.K., Chromy, B.A., Edwards, C., Freed, R., Liosatos, M., Morgan, T.E., Rozovsky, I., Trommer, B., Viola, K.L., Wals, P., Zhang, C., Finch, C.E., Krafft, G.A., and Klein, W.L. 1998. Diffusible, nonfibrillar ligands derived from A β ₁₋₄₂ are potent central nervous system neurotoxins. *Proc Natl Acad Sci U S A*, 95, 6448-53.
- Lambert, M.P., Viola, K.L., Chromy, B.A., Chang, L., Morgan, T.E., Yu, J., Venton, D.L., Krafft, G.A., Finch, C.E., and Klein, W.L. 2001. Vaccination with soluble A β oligomers generates toxicity-neutralizing antibodies. *J Neurochem*, 79, 595-605.
- Laque-Ruperez, E., Ruiz-Gomez, M. J., de la Pena, L., Gil, L., and Martinez-Morillo, M. 2003. Methotrexate cytotoxicity on MCF-7 breast cancer cells is not
-

- altered by exposure to 25 Hz, 1.5 mT magnetic field and iron (III) chloride hexahydrate. *Bioelectrochemistry*, 60, 81-6.
- Lashuel, H.A., Hartley, D., Petre, B.M., Walz, T., and Lansbury, P.T. 2002. Neurodegenerative disease: amyloid pores from pathogenic mutations. *Nature*, 418, 291.
- Lauren, J., Gimbel, D.A., Nygaard, H.B., Gilbert, J.W., and Strittmatter, S.M. 2009. Cellular prion protein mediates impairment of synaptic plasticity by amyloid- β oligomers. *Nature*, 457, 1128-32.
- Le Brocq, D., Henry, A., Cappai, R., Li, Q.X., Tanner, J. E., Galatis, D., Gray, C., Holmes, S., Underwood, J.R., Beyreuther, K., Masters, C.L. and Evin, G. 1998. Processing of the Alzheimer's disease amyloid precursor protein in *Pichia pastoris*: immunodetection of α -, β -, γ -secretase products. *Biochem*, 37, 14958-65.
- Le Corre, S., Klafki, H.W., Plesnila, N., Hubinger, G., Obermeier, A., Sahagun, H., Monse, B., Seneci, P., Lewis, J., Eriksen, J., Zehr, C., Yue, M., McGowan, E., Dickson, D.W., Hutton, M., and Roder, H.M. 2006. An inhibitor of tau hyperphosphorylation prevents severe motor impairments in tau transgenic mice. *Proc Natl Acad Sci U S A*, 103, 9673-78.
- Ledesma, M.D., and Dotti, C.G. 2005. The conflicting role of brain cholesterol in Alzheimer's disease: lessons from the brain plasminogen system. *Biochem Soc Symp*, 72, 129-38.
- Ledesma, M.D., and Dotti, C.G. 2006. Amyloid excess in Alzheimer's disease: what is cholesterol to be blamed for? *FEBS Lett*, 580, 5525-32.
- Lee, A.Y., St Onge, R.P., Proctor, M.J., Wallace, I.M., Nile, A.H., Spagnuolo, P.A., Jitkova, Y., Gronda, M., Wu, Y., Kim, M.K., Cheung-Ong, K., Torres, N.P., Spear, E.D., Han, M.K., Schlecht, U., Suresh, S., Duby, G., Heisler, L.E., Surendra, A., Fung, E., Urbanus, M. L., Gebbia, M., Lissina, E., Miranda, M., Chiang, J.H., Aparicio, A.M., Zeghouf, M., Davis, R.W., Cherfils, J., Boutry, M., Kaiser, C.A., Cummins, C.L., Trimble, W. S., Brown, G.W., Schimmer, A.D., Bankaitis, V.A., Nislow, C., Bader, G.D., and Giaever, G. 2014. Mapping the cellular response to small molecules using chemogenomic fitness signatures. *Science*, 344, 208-11.
- Lee, J., Spector, D., Godon, C., Labarre, J., and Toledano, M.B. 1999. A new antioxidant with alkyl hydroperoxide defense properties in yeast. *J Biol Chem*, 274, 4537-44.
- Lee, J., Lee, Y.K., Ban, J. O., Ha, T.Y., Yun, Y.P., Han, S.B., Oh, K.W., and Hong, J.T. 2009a. Green tea (-)-epigallocatechin-3-gallate inhibits β -amyloid-induced cognitive dysfunction through modification of secretase activity via inhibition of ERK and NF- κ B pathways in mice. *J Nutr*, 139, 1987-93.

-
- Lee, L.L., Ha, H., Chang, Y.T., and DeLisa, M.P. 2009b. Discovery of amyloid- β aggregation inhibitors using an engineered assay for intracellular protein folding and solubility. *Protein Sci*, 18, 277-86.
- Lee, Y.W., Kim, D.H., Jeon, S.J., Park, S.J., Kim, J.M., Jung, J.M., Lee, H.E., Bae, S.G., Oh, H.K., Son, K.H., and Ryu, J.H. 2013. Neuroprotective effects of salvianolic acid B on an A β_{25-35} peptide-induced mouse model of Alzheimer's disease. *Eur J Pharmacol*, 704, 70-7.
- Levin, D.E. 2005. Cell wall integrity signaling in *Saccharomyces cerevisiae*. *Microbiol Mol Biol Rev*, 69, 262-91.
- Levin, D.E. 2011. Regulation of cell wall biogenesis in *Saccharomyces cerevisiae*: the cell wall integrity signaling pathway. *Genetics*, 189, 1145-75.
- LeVine, H., 3rd. 1993. Thioflavine T interaction with synthetic Alzheimer's disease beta-amyloid peptides: detection of amyloid aggregation in solution. *Protein Sci*, 2, 404-10.
- Levites, Y., Amit, T., Mandel, S., and Youdim, M.B. 2003. Neuroprotection and neurorescue against A β toxicity and PKC-dependent release of nonamyloidogenic soluble precursor protein by green tea polyphenol (-)-epigallocatechin-3-gallate. *FASEB J*, 17, 952-4.
- Levy-Sakin, M., Shreberk, M., Daniel, Y., and Gazit, E. 2009. Targeting insulin amyloid assembly by small aromatic molecules: toward rational design of aggregation inhibitors. *Islets*, 1, 210-5.
- Levy, E., Carman, M. D., Fernandez-Madrid, I. J., Power, M. D., Lieberburg, I., van Duinen, S. G., Bots, G. T., Luyendijk, W., and Frangione, B. 1990. Mutation of the Alzheimer's disease amyloid gene in hereditary cerebral hemorrhage, Dutch type. *Science*, 248, 1124-1126.
- Li, C., Wang, J., and Zhou, B. 2010. The metal chelating and chaperoning effects of clioquinol: insights from yeast studies. *J Alzheimers Dis*, 21, 1249-62.
- Li, L., Lu, Y., Qin, L.X., Bar-Joseph, Z., Werner-Washburne, M., and Breeden, L.L. 2009. Budding yeast *SSD1-V* regulates transcript levels of many longevity genes and extends chronological life span in purified quiescent cells. *Mol Biol Cell*, 20, 3851-64.
- Li, L., Miles, S., Melville, Z., Prasad, A., Bradley, G., and Breeden, L.L. 2013. Key events during the transition from rapid growth to quiescence in budding yeast require posttranscriptional regulators. *Mol Biol Cell*, 24, 3697-709.
- Lian, F.M., Yu, J., Ma, X.X., Yu, X.J., Chen, Y., and Zhou, C.Z. 2012. Structural snapshots of yeast alkyl hydroperoxide reductase Ahp1 peroxiredoxin reveal a novel two-cysteine mechanism of electron transfer to eliminate reactive oxygen species. *J Biol Chem*, 287, 17077-87.
-

-
- Lioudyno, M.I., Broccio, M., Sokolov, Y., Rasool, S., Wu, J., Alkire, M.T., Liu, V., Kozak, J.A., Dennison, P.R., Glabe, C.G., Lösche, M., and Hall, J. E. 2012. Effect of synthetic A β peptide oligomers and fluorinated solvents on Kv1.3 channel properties and membrane conductance. *PLoS One*, 7, e35090.
- Looke, M., Kristjuhan, K., and Kristjuhan, A. 2011. Extraction of genomic DNA from yeasts for PCR-based applications. *Bio Techniq*, 50, 325-8.
- Lopez, L.C., Dos-Reis, S., Espargaro, A., Carrodegua, J.A., Maddelein, M.L., Ventura, S., and Sancho, J. 2012. Discovery of novel inhibitors of amyloid β -peptide 1-42 aggregation. *J Med Chem*, 55, 9521-30.
- LoPresti, P., and Konat, G.W. 2001. Hydrogen peroxide induces transient dephosphorylation of tau protein in cultured rat oligodendrocytes. *Neurosci Lett*, 311, 142-4.
- Luchsinger, J.A., Tang, M.X., Shea, S., and Mayeux, R. 2002. Caloric intake and the risk of Alzheimer disease. *Arch Neurol*, 59, 1258-63.
- Lum, P.Y., Armour, C.D., Stepaniants, S. B., Cavet, G., Wolf, M.K., Butler, J.S., Hinshaw, J.C., Garnier, P., Prestwich, G.D., Leonardson, A., Garrett-Engele, P., Rush, C.M., Bard, M., Schimmack, G., Phillips, J.W., Roberts, C.J., and Shoemaker, D.D. 2004. Discovering modes of action for therapeutic compounds using a genome-wide screen of yeast heterozygotes. *Cell*, 116, 121-37.
- Luo, Y., Bolon, B., Damore, M. A., Fitzpatrick, D., Liu, H., Zhang, J., Yan, Q., Vassar, R., and Citron, M. 2003. BACE1 (β -secretase) knockout mice do not acquire compensatory gene expression changes or develop neural lesions over time. *Neurobiol Dis*, 14, 81-8.
- Luo, Y., Bolon, B., Kahn, S., Bennett, B.D., Babu-Khan, S., Denis, P., Fan, W., Kha, H., Zhang, J., Gong, Y., Martin, L., Louis, J.C., Yan, Q., Richards, W.G., Citron, M., and Vassar, R. 2001. Mice deficient in BACE1, the Alzheimer's β -secretase, have normal phenotype and abolished β -amyloid generation. *Nat Neurosci*, 4, 231-32.
- Luo, Y., Hawver, D.B., Iwasaki, K., Sunderland, T., Roth, G.S., and Wolozin, B. 1997. Physiological levels of β -amyloid peptide stimulate protein kinase C in PC12 cells. *Brain Res*, 769, 287-95.
- Luo, Y., Sunderland, T., Roth, G.S., and Wolozin, B. 1996. Physiological levels of β -amyloid peptide promote PC12 cell proliferation. *Neurosci Lett*, 217, 125-28.
- Lüthi, U., Schaerer-Brodbeck, C., Tanner, S., Middendorp, O., Edler, K., and Barberis, A. 2003. Human β -secretase activity in yeast detected by a novel cellular growth selection system. *Biochim Biophys Acta*, 1620, 167-78.
-

-
- Macreadie, I., Lotfi-Miri, M., Mohotti, S., Shapira, D., Bennett, L., and Varghese, J. 2008. Validation of folate in a convenient yeast assay suited for identification of inhibitors of Alzheimer's A β aggregation. *J Alzheimers Dis*, 15, 391-6.
- Maetzawa, I., Hong, H.S., Liu, R., Wu, C.Y., Cheng, R. H., Kung, M.P., Kung, H.F., Lam, K.S., Oddo, S., LaFerla, F.M., and Jin, L.W. 2008. Congo red and thioflavin-T analogs detect A β oligomers. *J Neurochem*, 104, 457-68.
- Mager, W.H., and Winderickx, J. 2005. Yeast as a model for medical and medicinal research. *Trends Pharmacol Sci*, 26, 265-73.
- Malaguarnera, M., Bella, R., Alagona, G., Ferri, R., Carnemolla, A., and Pennisi, G. 2004. *Helicobacter pylori* and Alzheimer's disease: a possible link. *Eur J Int Med*, 15, 381-86.
- Mandel, S., Amit, T., Reznichenko, L., Weinreb, O., and Youdim, M. B. 2006. Green tea catechins as brain-permeable, natural iron chelators-antioxidants for the treatment of neurodegenerative disorders. *Mol Nutr Food Res*, 50, 229-34.
- Mason, J.B., and Kim, S.J. 2010. Revisiting the goldilocks phenomenon: folate and colorectal cancer risk. *Am J Gastro*, 105, 1914-16.
- Mason, J.M., Kokkoni, N., Stott, K., and Doig, A.J. 2003. Design strategies for anti-amyloid agents. *Curr Opin Struct Biol*, 13, 526-32.
- Masters, C.L., Simms, G., Weinman, N.A., Multhaup, G., McDonald, B.L., and Beyreuther, K. 1985. Amyloid plaque core protein in Alzheimer disease and Down syndrome. *Proc Natl Acad Sci U S A*, 82, 4245-49.
- Matharu, B., El-Agnaf, O., Razvi, A., and Austen, B.M. 2010. Development of retro-inverso peptides as anti-aggregation drugs for β -amyloid in Alzheimer's disease. *Peptides*, 31, 1866-72.
- Mathura, V.S., Paris, D., Ait-Ghezala, G., Quadros, A., Patel, N.S., Kolippakkam, D. N., Volmar, C.H., and Mullan, M.J. 2005. Model of Alzheimer's disease amyloid- β peptide based on a RNA binding protein. *Biochem Biophys Res Commun*, 332, 585-92.
- Matlack, K.E., Tardiff, D.F., Narayan, P., Hamamichi, S., Caldwell, K.A., Caldwell, G.A., and Lindquist, S. 2014. Clioquinol promotes the degradation of metal-dependent amyloid-beta (A β) oligomers to restore endocytosis and ameliorate A β toxicity. *Proc Natl Acad Sci U S A*, 111, 4013-8.
- Mattson, M.P., and Goodman, Y. 1995. Different amyloidogenic peptides share a similar mechanism of neurotoxicity involving reactive oxygen species and calcium. *Brain Res*, 676, 219-24.
- Mattson, M.P., and Shea, T.B. 2003. Folate and homocysteine metabolism in neural plasticity and neurodegenerative disorders. *Trends Neurosci*, 26, 137-46.
-

-
- Maurya, P.K., and Rizvi, S.I. 2009. Protective role of tea catechins on erythrocytes subjected to oxidative stress during human aging. *Nat Product Res*, 23, 1072-79.
- Mawuenyega, K.G., Sigurdson, W., Ovod, V., Munsell, L., Kasten, T., Morris, J.C., Yarasheski, K.E., and Bateman, R.J. 2010. Decreased clearance of CNS β -amyloid in Alzheimer's disease. *Science*, 330, 1-4.
- May, P.C., Dean, R.A., Lowe, S.L., Martenyi, F., Sheehan, S.M., Boggs, L.N., Monk, S.A., Mathes, B.M., Mergott, D.J., Watson, B.M., Stout, S.L., Timm, D.E., Smith Labell, E., Gonzales, C.R., Nakano, M., Jhee, S.S., Yen, M., Ereshefsky, L., Lindstrom, T.D., Calligaro, D.O., Cocke, P.J., Greg Hall, D., Friedrich, S., Citron, M., and Audia, J.E. 2011. Robust central reduction of amyloid- β in humans with an orally available, non-peptidic β -secretase inhibitor. *J Neurosci*, 31, 16507-16.
- Mayanil, C.S., Ichi, S., Farnell, B.M., Boshnjaku, V., Tomita, T., and McLone, D.G. 2011. Maternal intake of folic acid and neural crest stem cells. *Vit Hormon*, 87, 143-73.
- Mazza, M., Capuano, A., Bria, P., and Mazza, S. 2006. Ginkgo biloba and donepezil: a comparison in the treatment of Alzheimer's dementia in a randomized placebo-controlled double-blind study. *Eur J Neurol*, 13, 981-85.
- McFaline-Figueroa, J.R., Vevea, J., Swayne, T.C., Zhou, C., Liu, C., Leung, G., Boldogh, I.R., and Pon, L.A. 2011. Mitochondrial quality control during inheritance is associated with lifespan and mother-daughter age asymmetry in budding yeast. *Aging Cell*, 10, 885-95.
- McGowan, E., Pickford, F., Kim, J., Onstead, L., Eriksen, J., Yu, C., Skipper, L., Murphy, M.P., Beard, J., Das, P., Jansen, K., DeLucia, M.I., Lin, W.L., Dolios, Georgia, Wang, Rong, Eckman, Christopher B., Dickson, Dennis W., Hutton, M., Hardy, J., and Golde, T. 2005. $A\beta_{42}$ is essential for parenchymal and vascular amyloid deposition in mice. *Neuron*, 47, 191-99.
- McKoy, A.F., Chen, J., Schupbach, T., and Hecht, M.H. 2012. A novel inhibitor of amyloid beta ($A\beta$) peptide aggregation: from high-throughput screening to efficacy in an animal model of Alzheimer disease. *J Biol Chem*, 287, 38992-9000.
- McMurray, M. A., and Gottschling, D. E. 2004. Aging and genetic instability in yeast. *Curr Opin Microbiol*, 7, 673-679.
- McShea, A., Lee, H.G., Petersen, R.B., Casadesus, G., Vincent, I., Linford, N.J., Funk, J.O., Shapiro, R.A., and Smith, M.A. 2007. Neuronal cell cycle re-entry mediates Alzheimer disease-type changes. *Biochim Biophys Acta*, 1772, 467-72.
-

-
- Mendenhall, M.D. 1998. Cyclin-dependent kinase inhibitors of *Saccharomyces cerevisiae* and *Schizosaccharomyces pombe*. *Curr Topic Microbiol Immun*, 227, 1-24.
- Meaneau, I., Sanglard, D., Bille, J., and Hauser, P.M. 2004. *Pneumocystis jiroveci* dihydropteroate synthase polymorphisms confer resistance to sulfadoxine and sulfanilamide in *Saccharomyces cerevisiae*. *Antimicrob Agents Chemother*, 48, 2610-16.
- Middendorp, O., Luthi, U., Hausch, F., and Barberis, A. 2004a. Searching for the most effective screening system to identify cell-active inhibitors of β -secretase. *Biol Chem*, 385, 481-85.
- Middendorp, O., Ortler, C., Neumann, U., Paganetti, P., Luthi, U., and Barberis, A. 2004b. Yeast growth selection system for the identification of cell-active inhibitors of β -secretase. *Biochim Biophys Acta*, 1674, 29-39.
- Miles, L.A., Wun, K.S., Crespi, G.A., Fodero-Tavoletti, M.T., Galatis, D., Bagley, C.J., Beyreuther, K., Masters, C.L., Cappai, R., McKinstry, W.J., Barnham, K.J., and Parker, M.W. 2008. Amyloid- β -anti-amyloid- β complex structure reveals an extended conformation in the immunodominant B-cell epitope. *J Mol Biol*, 377, 181-92.
- Miller, J.P., Lo, R.S., Ben-Hur, A., Desmarais, C., Stagljar, I., Noble, W. S., and Fields, S. 2005. Large-scale identification of yeast integral membrane protein interactions. *Proc Natl Aca Sci U S A*, 102, 12123-8.
- Minano-Molina, A. J., Espana, J., Martin, E., Barneda-Zahonero, B., Fado, R., Sole, M., Trullas, R., Saura, C.A., and Rodriguez-Alvarez, J. 2011. Soluble oligomers of amyloid- β peptide disrupt membrane trafficking of α -amino-3-hydroxy-5-methylisoxazole-4-propionic acid receptor contributing to early synapse dysfunction. *J Biol Chem*, 286, 27311-21.
- Minear, S., O'Donnell, A.F., Ballew, A., Giaever, G., Nislow, C., Stearns, T., and Cyert, M.S. 2011. Curcumin inhibits growth of *Saccharomyces cerevisiae* through iron chelation. *Eukar Cell*, 10, 1574-81.
- Miners, J.S., Baig, S., Tayler, H., Kehoe, P.G., and Love, S. 2009. Neprilysin and insulin-degrading enzyme levels are increased in Alzheimer disease in relation to disease severity. *J Neuropathol Exper Neurol*, 68, 902-14.
- Minois, N., Lagona, F., Frajnt, M., and Vaupel, J.W. 2009. Plasticity of death rates in stationary phase in *Saccharomyces cerevisiae*. *Aging Cell*, 8, 36-44.
- Misiti, F., Sampaiolese, B., Mezzogori, D., Orsini, F., Pezzotti, M., Giardina, B., and Clementi, M. E. 2006. Protective effect of rhubarb derivatives on amyloid- β (1-42) peptide-induced apoptosis in IMR-32 cells: A case of nutrigenomic. *Brain Res Bull*, 71, 29-36.
-

-
- Mitra, J., Guerrero, E.N., Hegde, P.M., Wang, H., Boldogh, I., Rao, K. S., Mitra, S., and Hegde, M.L. 2014. New perspectives on oxidized genome damage and repair inhibition by pro-oxidant metals in neurological diseases. *Biomolecules*, 4, 678-703.
- Mitrica, R., Dumitru, I., Ruta, L.L., Ofiteru, A.M., and Farcasanu, I.C. 2012. The dual action of epigallocatechin gallate (EGCG), the main constituent of green tea, against the deleterious effects of visible light and singlet oxygen-generating conditions as seen in yeast cells. *Molecules*, 17, 10355-69.
- Moore, B.D., Rangachari, V., Tay, W.M., Milkovic, N.M., and Rosenberry, T.L. 2009. Biophysical analyses of synthetic amyloid- β (1-42) aggregates before and after covalent cross-linking. implications for deducing the structure of endogenous amyloid- β oligomers. *Biochem*, 48, 11796-806.
- Moreno-Treviño, M.G., Castillo-López, J., and Meester, I. 2015. Moving away from amyloid β in Alzheimer research. *Front Aging Neurosci*, 7, 2.
- Morgan, C., Colombres, M., Nuñez, M.T., and Inestrosa, N.C. 2004. Structure and function of amyloid in Alzheimer's disease. *Prog Neurobiol*, 74, 323-49.
- Morris, A.M., Watzky, M.A., and Finke, R.G. 2009. Protein aggregation kinetics, mechanism, and curve-fitting: a review of the literature. *Biochim Biophys Acta*, 1794, 375-97.
- Morris, M.S. 2003. Homocysteine and Alzheimer's disease. *Lancet Neurol*, 2, 425-8.
- Mosch, B., Morawski, M., Mittag, A., Lenz, D., Tarnok, A., and Arendt, T. 2007. Aneuploidy and DNA replication in the normal human brain and Alzheimer's disease. *J Neurosci*, 27, 6859-67.
- Motter, R., Vigo-Pelfrey, C., Kholodenko, D., Barbour, R., Johnson-Wood, K., Galasko, D., Chang, L., Miller, B., Clark, C., Green, R., Olson, D., Southwick, P., Wolfert, R., Lieberburg, I., Seubert, P., Schenk, D., Müller, B., and Grossniklaus, U. 1995. Reduction of β -amyloid peptide 42 in the cerebrospinal fluid of patients with Alzheimer's disease. *Anal Neurol*, 38, 643-48.
- Muller, C., and Schibli, R. 2013. Prospects in folate receptor-targeted radionuclide therapy. *Front Onco*, 3, e249, doi: 10.3389/fonc.2013.00249.
- Mumberg, D., Muller, R., and Funk, M. 1995. Yeast vectors for the controlled expression of heterologous proteins in different genetic backgrounds. *Gene*, 156, 119-22.
- Nagy, Z. 2007. The dysregulation of the cell cycle and the diagnosis of Alzheimer's disease. *Biochim Biophys Acta*, 1772, 402-08.
- Nagy, Z., Esiri, M.M., and Smith, A.D. 1998. The cell division cycle and the pathophysiology of Alzheimer's disease. *Neuroscience*, 87, 731-39.
-

-
- Naiki, H., Higuchi, K., Hosokawa, M., and Takeda, T. 1989. Fluorometric determination of amyloid fibrils *in vitro* using the fluorescent dye, thioflavin T. *Anal Biochem*, 177, 244-49.
- Nakagami, Y., Nishimura, S., Murasugi, T., Kaneko, I., Meguro, M., Marumoto, S., Kogen, H., Koyama, K., and Oda, T. 2002. A novel β -sheet breaker, RS-0406, reverses amyloid β -induced cytotoxicity and impairment of long-term potentiation *in vitro*. *Brit J Pharmacol*, 137, 676-82.
- Nakamura, M., Shishido, N., Nunomura, A., Smith, M. A., Perry, G., Hayashi, Y., Nakayama, K., and Hayashi, T. 2007. Three histidine residues of amyloid-beta peptide control the redox activity of copper and iron. *Biochem*, 46, 12737-43.
- Nakdook, W., Khongsombat, O., Taepavarapruk, P., Taepavarapruk, N., and Ingkaninan, K. 2010. The effects of *Tabernaemontana divaricata* root extract on amyloid β -peptide 25–35 peptides induced cognitive deficits in mice. *J Ethnopharmacol*, 130, 122-26.
- Necula, M., Breydo, L., Milton, S., Kaye, R., van der Veer, W.E., Tone, P., and Glabe, C.G. 2007a. Methylene blue inhibits amyloid- β oligomerization by promoting fibrillization. *Biochem*, 46, 8850-60.
- Necula, M., Kaye, R., Milton, S., and Glabe, C.G. 2007b. Small molecule inhibitors of aggregation indicate that amyloid β oligomerization and fibrillization pathways are independent and distinct. *J Biol Chem*, 282, 10311-24.
- Neiman, A.M. 2011. Sporulation in the budding yeast *Saccharomyces cerevisiae*. *Genetics*, 189, 737-65.
- Nemavarkar, P., Chourasia, B. K., and Pasupathy, K. 2004a. Evaluation of radioprotective action of compounds using *Saccharomyces cerevisiae*. *J Environ Pathol Toxicol Oncol*, 23, 145-51.
- Nemavarkar, P.S., Chourasia, B.K., and Pasupathy, K. 2004b. Detection of γ -irradiation induced DNA damage and radioprotection of compounds in yeast using comet assay. *J Radi Res*, 45, 169-74.
- Nguyen-nhu, N.T., and Knoops, B. 2002. Alkyl hydroperoxide reductase 1 protects *Saccharomyces cerevisiae* against metal ion toxicity and glutathione depletion. *Toxicol Lett*, 135, 219-28.
- Nichols, J.A., and Katiyar, S.K. 2010. Skin photoprotection by natural polyphenols: anti-inflammatory, antioxidant and DNA repair mechanisms. *Arch Dermatol Res*, 302, 71-83.
- Nichols, M.R., Moss, M.A., Reed, D.K., Cratic-McDaniel, S., Hoh, J.H., and Rosenberry, T.L. 2005a. Amyloid- β protofibrils differ from amyloid- β aggregates induced in dilute hexafluoroisopropanol in stability and morphology. *J Biol Chem*, 280, 2471-80.
-

-
- Nichols, M.R., Moss, M.A., Reed, D.K., Hoh, J.H., and Rosenberry, T.L. 2005b. Amyloid- β aggregates formed at polar-nonpolar interfaces differ from amyloid- β protofibrils produced in aqueous buffers. *Microscop Res Tech*, 67, 164-74.
- Nickerson, W.J., and Webb, M. 1956. Effect of folic acid analogues on growth and cell division of nonexacting microorganisms. *J Bacteriol*, 71, 129-39.
- Nicoll, A.J., Panico, S., Freir, D.B., Wright, D., Terry, C., Risse, E., Herron, C.E., O'Malley, T., Wadsworth, J.D.F., Farrow, M.A., Walsh, D.M., Saibil, H.R., and Collinge, J. 2013. Amyloid- β nanotubes are associated with prion protein-dependent synaptotoxicity. *Nat Commun*, 4, e2416, doi: 10.1038/ncomms3416.
- Nilsberth, C., Westlind-Danielsson, A., Eckman, C. B., Condron, M. M., Axelman, K., Forsell, C., Stenh, C., Luthman, J., Teplow, D.B., Younkin, S.G., Naslund, J., and Lannfelt, L. 2001. The 'Arctic' APP mutation (E693G) causes Alzheimer's disease by enhanced A β protofibril formation. *Nat Neurosci*, 4, 887-93.
- Nurse, P., Thuriaux, P., and Nasmyth, K. 1976. Genetic control of the cell division cycle in the fission yeast *Schizosaccharomyces pombe*. *Mol General Genetic*, 146, 167-78.
- Oddo, S., Billings, L., Kesslak, J.P., Cribbs, D.H., and LaFerla, F.M. 2004. A β immunotherapy leads to clearance of early, but not late, hyperphosphorylated tau aggregates via the proteasome. *Neuron*, 43, 321-32.
- Ojala, T., Remes, S., Haansuu, P., Vuorela, H., Hiltunen, R., Haahtela, K., and Vuorela, P. 2000. Antimicrobial activity of some coumarin containing herbal plants growing in Finland. *J Ethnopharmacol*, 73, 299-305.
- Okamoto, S., and Iino, T. 1981. Selective abortion of two nonsister nuclei in a developing ascus of the hfd-1 mutant in *Saccharomyces cerevisiae*. *Genetics*, 99, 197-209.
- Ono, K., Hamaguchi, T., Naiki, H., and Yamada, M. 2006. Anti-amyloidogenic effects of antioxidants: implications for the prevention and therapeutics of Alzheimer's disease. *Biochim Biophys Acta*, 1762, 575-86.
- Ono, K., Takahashi, R., Ikeda, T., Mizuguchi, M., Hamaguchi, T., and Yamada, M. 2014. Exogenous amyloidogenic proteins function as seeds in amyloid β -protein aggregation. *Biochim Biophys Acta*, 1842, 646-53.
- Ono, K., Yoshiike, Y., Takashima, A., Hasegawa, K., Naiki, H., and Yamada, M. 2003. Potent anti-amyloidogenic and fibril-destabilizing effects of polyphenols *in vitro*: implications for the prevention and therapeutics of Alzheimer's disease. *J Neurochem*, 87, 172-81.
-

-
- Owen, S.A., Hider, S.L., Martin, P., Bruce, I.N., Barton, A., and Thomson, W. 2013. Genetic polymorphisms in key methotrexate pathway genes are associated with response to treatment in rheumatoid arthritis patients. *Pharmacogen J*, 13, 227-34.
- Pagani, L., and Eckert, A. 2011. Amyloid- β interaction with mitochondria. *Int J Alzheimers Dis*, 2011, e925050, doi: 10.4061/2011/925050.
- Palhano, F.L., Lee, J., Grimster, N.P., and Kelly, J.W. 2013. Toward the molecular mechanism(s) by which EGCG treatment remodels mature amyloid fibrils. *J Am Chem Soc*, 2013, 135, 7503-10.
- Pallauf, K., and Rimbach, G. 2013. Autophagy, polyphenols and healthy ageing. *Ageing Res Rev*, 12, 237-52.
- Palmer, E., and Freeman, T. 2004. Investigation into the use of C- and N-terminal GFP fusion proteins for subcellular localization studies using reverse transfection microarrays. *Comparative Function Genom*, 5, 342-53.
- Park, S.G., Cha, M.K., Jeong, W., and Kim, I.H. 2000. Distinct physiological functions of thiol peroxidase isoenzymes in *Saccharomyces cerevisiae*. *J Biol Chem*, 275, 5723-32.
- Park, S.K., Pegan, S.D., Mesecar, A.D., Jungbauer, L.M., LaDu, M.J., and Liebman, S.W. 2011. Development and validation of a yeast high-throughput screen for inhibitors of A β ₄₂ oligomerization. *Dis Model Mech*, 4, 822-31.
- Pasinetti, G.M., Zhao, Z., Qin, W., Ho, L., Shrishailam, Y., Macgrogan, D., Ressmann, W., Humala, N., Liu, X., Romero, C., Stetka, B., Chen, L., Ksiezak-Reding, H., and Wang, J. 2007. Caloric intake and Alzheimer's disease. Experimental approaches and therapeutic implications. *Interdisciplin Topic Gerontol*, 35, 159-75.
- Paulovich, A.G., Toczyski, D.P., and Hartwell, L.H. 1997. When checkpoints fail. *Cell*, 88, 315-21.
- Paz, I., and Choder, M. 2001. Eukaryotic translation initiation factor 4E-dependent translation is not essential for survival of starved yeast cells. *J Bacteriol*, 183, 4477-83.
- Pearson, H.A., and Peers, C. 2006. Physiological roles for amyloid β peptides. *J Physiol*, 575, 5-10.
- Pereira, C., Bessa, C., Soares, J., Leao, M., and Saraiva, L. 2012. Contribution of yeast models to neurodegeneration research. *J Biomed Biotech*, 2012, e941232, doi: 10.1155/2012/941232.
- Pereira, E.C., Lucetti, D.L., Barbosa-Filho, J.M., de Brito, E.M., Monteiro, V.S., Patrocinio, M.C., de Moura, R.R., Leal, L.K., Macedo, D.S., de Sousa, F.C., de Barros Viana, G.S., and Vasconcelos, S.M. 2009. Coumarin effects on
-

-
- amino acid levels in mice prefrontal cortex and hippocampus. *Neurosci Lett*, 454, 139-42.
- Petersen, M., and Simmonds, M.S. 2003. Rosmarinic acid. *Phytochemistry*, 62, 121-5.
- Pike, C.J., Walencewicz, A.J., Glabe, C.G., and Cotman, C.W. 1991. *In vitro* aging of β -amyloid protein causes peptide aggregation and neurotoxicity. *Brain Res*, 563, 311-14.
- Pimentel, C., Batista-Nascimento, L., Rodrigues-Pousada, C., and Menezes, R.A. 2012. Oxidative stress in Alzheimer's and Parkinson's diseases: insights from the yeast *Saccharomyces cerevisiae*. *Oxid Med Cell Longev*, 2012, e132146, doi: 10.1155/2012/132146.
- Plant, L.D., Boyle, J.P., Smith, I.F., Peers, C., and Pearson, H.A. 2003. The production of amyloid- β peptide is a critical requirement for the viability of central neurons. *J Neurosci.* , 23, 5531-35.
- Plant, L.D., Webster, N.J., Boyle, J.P., Ramsden, M., Freir, D.B., Peers, C., and Pearson, H.A. 2006. Amyloid β peptide as a physiological modulator of neuronal 'A'-type K^+ current. *Neurobiol Aging*, 27, 1673-83.
- Poojari, C., Kukol, A., and Strodel, B. 2013. How the amyloid- β peptide and membranes affect each other: An extensive simulation study. *Biochim Biophys Acta*, 1828, 327-39.
- Poppek, D., Keck, S., Ermak, G., Jung, T., Stolzing, A., Ullrich, O., Davies, K J., and Grune, T. 2006. Phosphorylation inhibits turnover of the tau protein by the proteasome: influence of RCAN1 and oxidative stress. *Biochemical J*, 400, 511-20.
- Porat, Y., Abramowitz, A., and Gazit, E. 2006. Inhibition of amyloid fibril formation by polyphenols: structural similarity and aromatic interactions as a common inhibition mechanism. *Chem Biol Drug Des*, 67, 27-37.
- Porzoor, A., and Macreadie, I.G. 2013. Application of yeast to study the Tau and Amyloid- β abnormalities of Alzheimer's disease. *J Alzheimers Dis*, 35, 217-225.
- Prasad, P.D., Ramamoorthy, S., Moe, A.J., Smith, C.H., Leibach, F.H., and Ganapathy, V. 1994. Selective expression of the high-affinity isoform of the folate receptor (FR-alpha) in the human placental syncytiotrophoblast and choriocarcinoma cells. *Biochim Biophys Acta*, 1223, 71-5.
- Pruyne, D., and Bretscher, A. 2000. Polarization of cell growth in yeast. I. Establishment and maintenance of polarity states. *J Cell Sci*, 113 (Pt 3), 365-75.
-

-
- Pryor, N.E., Moss, M.A., and Hestekin, C.N. 2012. Unraveling the early events of Amyloid- β protein (A β) aggregation: techniques for the determination of A β aggregate size. *Int J Mol Sci*, 13, 3038-72.
- Puglielli, L., Tanzi, R.E., and Kovacs, D.M. 2003. Alzheimer's disease: the cholesterol connection. *Nat Neurosci*, 6, 345-51.
- Qiang, L., Fujita, R., Yamashita, T., Angulo, S., Rhinn, H., Rhee, D., Doege, C., Chau, L., Aubry, L., Vanti, W. B., Moreno, H., and Abeliovich, A. 2011. Directed conversion of Alzheimer's disease patient skin fibroblasts into functional neurons. *Cell*, 146, 359-71.
- Qin, X.Y., Cheng, Y., and Yu, L.C. 2012. Potential protection of green tea polyphenols against intracellular amyloid β -induced toxicity on primary cultured prefrontal cortical neurons of rats. *Neurosci Lett*, 513, 170-73.
- Qu, B., Boyer, P.J., Johnston, S.A., Hynan, L.S, and Rosenberg, R.N. 2006. A β ₄₂ gene vaccination reduces brain amyloid plaque burden in transgenic mice. *J Neuro Sci*, 244, 151-158.
- Quadri, P., Fragiaco, C., Pezzati, R., Zanda, E., Forloni, G., Tettamanti, M., and Lucca, U. 2004. Homocysteine, folate, and vitamin B-12 in mild cognitive impairment, Alzheimer disease, and vascular dementia. *Am J Clin Nutr*, 80, 114-22.
- Rabilloud, T., Vuillard, L., Gilly, C., and Lawrence, J.J. 2009. Silver-staining of proteins in polyacrylamide gels: A general overview. *Cell Mol Biol*, 40, 57-75.
- Ramsook, C.B., Tan, C., Garcia, M.C., Fung, R., Soybelman, G., Henry, R., Litewka, A., O'Meally, S., Otoo, H.N., Khalaf, R.A., Dranginis, A.M., Gaur, N.K., Klotz, S.A., Rauceo, J.M., Jue, C.K., and Lipke, P.N. 2010. Yeast cell adhesion molecules have functional amyloid-forming sequences. *Eukar Cell*, 9, 393-404.
- Rapoport, M., Dawson, H.N., Binder, L.I., Vitek, M.P., and Ferreira, A. 2002. Tau is essential to β -amyloid-induced neurotoxicity. *Proc Natl Acad Sci U S A*, 99, 6364-69.
- Ravaglia, G., Forti, P., Maioli, F., Martelli, M., Servadei, L., Brunetti, N., Porcellini, E. and Licastro, F. 2005. Homocysteine and folate as risk factors for dementia and Alzheimer disease. *Amer J Clin Nutr*, 82, 636-43.
- Redlich, E. 1898. Ueber miliare sklerose der Hirnrinde bei seniler Atrophie *Jahrbücher Psychiat Neurol* 17, 208-16.
- Renner, M., Lacor, P.N., Velasco, P.T., Xu, J., Contractor, A., Klein, W. L., and Triller, A. 2010. Deleterious effects of amyloid- β oligomers acting as an extracellular scaffold for mGluR5. *Neuron*, 66, 739-54.
-

-
- Rezai-Zadeh, K., Shytle, D., Sun, N., Mori, T., Hou, H., Jeanniton, D., Ehrhart, J., Townsend, K., Zeng, J., Morgan, D., Hardy, J., Town, T., and Tan, J. 2005. Green tea epigallocatechin-3-gallate (EGCG) modulates amyloid precursor protein cleavage and reduces cerebral amyloidosis in Alzheimer transgenic mice. *J Neurosci*, 25, 8807-14.
- Robinson, J.L., Geser, F., Corrada, M.M., Berlau, D.J., Arnold, S.E., Lee, V.M., Kawas, C.H., and Trojanowski, J.Q. 2011. Neocortical and hippocampal amyloid-beta and tau measures associate with dementia in the oldest-old. *Brain*, 134, 3708-15.
- Robinson, S.R., and Bishop, G.M. 2002. A β as a bioflocculant: implications for the amyloid hypothesis of Alzheimer's disease. *Neurobiol Aging*, 23, 1051-72.
- Roccatano, D., Fioroni, M., Zacharias, M., and Colombo, G. 2005. Effect of hexafluoroisopropanol alcohol on the structure of melittin: A molecular dynamics simulation study. *Protein Sci*, 14, 2582-89.
- Rochet, J. C., and Lansbury, P. T. 2000. Amyloid fibrillogenesis: themes and variations. *Curr Opin Struct Biol*, 10, 60-8.
- Ron, D., and Walter, P. 2007. Signal integration in the endoplasmic reticulum unfolded protein response. *Nat Rev. Mol Cell Biol*, 8, 519-29.
- Rots, M.G., Pieters, R., Peters, G.J., Noordhuis, P., van Zantwijk, C. H., Kaspers, G. J., Hahlen, K., Creutzig, U., Veerman, A.J., and Jansen, G. 1999. Role of foylpolylglutamate synthetase and foylpolylglutamate hydrolase in methotrexate accumulation and polyglutamylolation in childhood leukemia. *Blood*, 93, 1677-83.
- Ruiz-Gomez, M. J., and Martinez-Morillo, M. 2006. Iron(III) chloride hexahydrate does not enhance methotrexate cytotoxicity on *Saccharomyces cerevisiae*. *Chemotherapy*, 52, 226-30.
- Ryan, T.M., Caine, J., Mertens, H.D., Kirby, N., Nigro, J., Breheney, K., Waddington, L.J., Streltsov, V.A., Curtain, C., Masters, C.L., and Roberts, B. R. 2013. Ammonium hydroxide treatment of A β produces an aggregate free solution suitable for biophysical and cell culture characterization. *Peer J*, 1, e73.
- Ryan, T.M., Friedhuber, A., Lind, M., Howlett, G.J., Masters, C., and Roberts, B. R. 2012. Small amphipathic molecules modulate secondary structure and amyloid fibril-forming kinetics of Alzheimer disease peptide A β (1-42). *J Biol Chem*, 287, 16947-54.
- Sabate, R., and Saupe, S.J. 2007. Thioflavin T fluorescence anisotropy: an alternative technique for the study of amyloid aggregation. *Biochem Biophys Res Commun*, 360, 135-38.
-

-
- Sahanawaz A.S.K., and Panigrahi, A.K. 2012. Transformation efficiency on *E. coli* in response to different bivalent salts. *J Res Biol*, 2, 704-10.
- Sahoo, B., Nag, S., Sengupta, P., and Maiti, S. 2009. On the stability of the soluble amyloid aggregates. *Biophys J*, 97, 1454-60.
- Saito, T., Suemoto, T., Brouwers, N., Slegers, K., Funamoto, S., Mihira, N., Matsuba, Y., Yamada, K., Nilsson, P., Takano, J., Nishimura, M., Iwata, N., Van Broeckhoven, C., Ihara, Y., and Saido, T.C. 2011. Potent amyloidogenicity and pathogenicity of A β ₄₃. *Nat Neurosci*, 14, 1023-32.
- Saitoh, S., Takahashi, K., Nabeshima, K., Yamashita, Y., Nakaseko, Y., Hirata, A., and Yanagida, M. 1996. Aberrant mitosis in fission yeast mutants defective in fatty acid synthetase and acetyl CoA carboxylase. *J Cell Biol*, 134, 949-61.
- Sakono, M., and Zako, T. 2010. Amyloid oligomers: formation and toxicity of A β oligomers. *FEBS J*, 277, 1348-58.
- Samaranayake, Y.H., Cheung, B.P., Wang, Y., Yau, J.Y., Yeung, K.W., and Samaranayake, L.P. 2013. Fluconazole resistance in *Candida glabrata* is associated with increased bud formation and metallothionein production. *J Med Microbiol*, 62, 303-18.
- Sambrook, J., and Russell, D.W. 2001. *Molecular cloning: a laboratory manual*, Cold Spring Harbor Laboratory, Cold Spring Harbor, N. Y.
- Samonis, G., and Bafaloukos, D. 1992. Fungal infections in cancer patients: an escalating problem. *J In Vivo*, 6, 183-93.
- Saunders, A.M., Strittmatter, W.J., Schmechel, D., George-Hyslop, P.H., Pericak-Vance, M.A., Joo, S.H., Rosi, B.L., Gusella, J.F., Crapper-MacLachlan, D.R., Alberts, M.J., Hulette, C., Crain, B., Goldgaber, D., and Roses, A.D. 1993. Association of apolipoprotein E allele ϵ 4 with late-onset familial and sporadic Alzheimer's disease. *Neurol*, 43, 1467-72.
- Sayeed, A., and Ng, D.T. 2005. Search and destroy: ER quality control and ER-associated protein degradation. *Critic Rev Biochem Mol Biol*, 40, 75-91.
- Schekman, R., 2010. Charting the secretory pathway in a simple eukaryote. *Mol Biol Cell*, 21, 3781-84.
- Schellenberg, G.D., Bird, T.D., Wijsman, E. M., Moore, D.K., and Martin, G.M. 1989. The genetics of Alzheimer's disease. *Biomed Pharmacother*, 43, 463-68.
- Scrimale, T., Didone, L., de Mesy Bentley, K.L., and Krysan, D.J. 2009. The unfolded protein response is induced by the cell wall integrity mitogen-activated protein kinase signaling cascade and is required for cell wall integrity in *Saccharomyces cerevisiae*. *Mol Biol Cell*, 20, 164-75.

-
- Selfridge, J.E., Lezi, E., Lu, J., and Swerdlow, R.H. 2013. Role of mitochondrial homeostasis and dynamics in Alzheimer's disease. *Neurobiol Disease*, 51, 3-12.
- Selkoe, D.J. 2008. Soluble oligomers of the amyloid β -protein impair synaptic plasticity and behavior. *Behav Brain Res.*, 192, 106-13.
- Selkoe, D.J., and Schenk, D. 2003. Alzheimer's disease: molecular understanding predicts amyloid-based therapeutics. *Annu Rev Pharmacol Toxicol*, 43, 545-84.
- Selkoe, D.J. 2002. Alzheimer's Disease is a synaptic failure. *Science*, 298, 789-91.
- SenGupta, D.J., Zhang, B., Kraemer, B., Pochart, P., Fields, S., and Wickens, M. 1996. A three-hybrid system to detect RNA-protein interactions *in vivo*. *Proc Natl Acad Sci U S A*, 93, 8496-501.
- Sezgin, Z., and Dincer, Y. 2014. Alzheimer's disease and epigenetic diet. *Neurochem Int*, 78C, 105-16.
- Sharifpoor, S., van Dyk, D., Costanzo, M., Baryshnikova, A., Friesen, H., Douglas, A.C., Youn, J.Y., VanderSluis, B., Myers, C.L., Papp, B., Boone, C., and Andrews, B.J. 2012. Functional wiring of the yeast kinome revealed by global analysis of genetic network motifs. *Genome Res*, 22, 791-801.
- Shaykhalishahi, H., Yazdanparast, R., Ha, H.H., and Chang, Y.T. 2009. Inhibition of H₂O₂-induced neuroblastoma cell cytotoxicity by a triazine derivative, AA3E2. *Eur J Pharmacol*, 622, 1-6.
- Shi, L.L., Yang, W.N., Chen, X.L., Zhang, J.S., Yang, P.B., Hu, X.D., Han, H., Qian, Y.H., and Liu, Y. 2012. The protective effects of tanshinone IIA on neurotoxicity induced by β -amyloid protein through calpain and the p35/Cdk5 pathway in primary cortical neurons. *Neurochem Int*, 61, 227-35.
- Shi, S., Wang, Z., and Qiao, Z. 2013. The multifunctional anti-inflammatory drugs used in the therapy of Alzheimer's disease. *Curr Med Chem*, 20, 2583-8.
- Shibata, M. Shinya, Y., Kumar, R.S., Calero, M., Bading, J., Fragione, B., Holtzman, D. M., Miller., C.A., Strickland, D.K., Ghiso, J., and Zlokovic, B.V. 2000. Clearance of Alzheimer's amyloid β_{1-40} peptide from brain by LDL receptor-related protein-1 at the blood-brain barrier. *J Clin Invest*, 106, 1489-99.
- Shin, D.S., Zhao, R., Yap, E.H., Fiser, A., and Goldman, I.D. 2012. A P425R mutation of the proton-coupled folate transporter causing hereditary folate malabsorption produces a highly selective alteration in folate binding. *Amer J Physiol.: Cell Physiol*, 302, C1405-12.
- Sikora, E., Arendt, T., Bennett, M., and Narita, M. 2011. Impact of cellular senescence signature on ageing research. *Ageing Res Rev*, 10, 146-52.
-

-
- Simon, J. A., and Bedalov, A. 2004. Yeast as a model system for anticancer drug discovery. *Nat Rev Cancer*, 4, 481-487.
- Sinnott, J.T., Cullison, J.P., and Sweeney, M.P. 1987. *Candida (Torulopsis) glabrata*. *Infect Control*, 8, 334-36.
- Slaughter, J.C., and Nomura, T. 1992. Intracellular glycogen and trehalose contents as predictors of yeast viability. *Enzyme Microb Techno*, 14, 64-67.
- Smets, B., Ghillebert, R., De Snijder, P., Binda, M., Swinnen, E., De Virgilio, C., and Winderickx, J. 2010. Life in the midst of scarcity: adaptations to nutrient availability in *Saccharomyces cerevisiae*. *Curr Gen*, 56, 1-32.
- Smid, S.D., Maag, J.L., and Musgrave, I.F. 2012. Dietary polyphenol-derived protection against neurotoxic β -amyloid protein: from molecular to clinical. *Food Function*, 3, 1242-50.
- Smith, M. Z., Nagy, Z., and Esiri, M.M. 1999. Cell cycle-related protein expression in vascular dementia and Alzheimer's disease. *Neuroscience letters*, 271, 45-8.
- Solomon, B., and Frenkel, D. 2010. Immunotherapy for Alzheimer's disease. *Neuropharmacol*, 59, 303-09.
- Spear, E., and Ng, D.T. 2001. The unfolded protein response: No longer just a special teams player. *Traffic*, 2, 515-23.
- Sperling, R.A., Aisen, P.S., Beckett, L.A., Bennett, D.A., Craft, S., Fagan, A.M., Iwatsubo, T., Jack Jr, C.R., Kaye, J., Montine, T.J., Park, D.C., Reiman, E.M., Rowe, C.C., Siemers, E., Stern, Y., Yaffe, K., Carrillo, M.C., Thies, B., Morrison-Bogorad, M., Wagster, M.V., and Phelps, C.H. 2011. Toward defining the preclinical stages of Alzheimer's disease: Recommendations from the National Institute on Aging-Alzheimer's Association workgroups on diagnostic guidelines for Alzheimer's disease. *Alzheimers Dement*, 7, 280-92.
- Srikanth, V., Maczurek, A., Phan, T., Steele, M., Westcott, B., Juskiw, D., and Munch, G. 2011. Advanced glycation endproducts and their receptor RAGE in Alzheimer's disease. *Neurobiol Aging*, 32, 763-77.
- Steckmann, T., Awan, Z., Gerstman, B.S., and Chapagain, P.P. 2012. Kinetics of peptide secondary structure conversion during amyloid β -protein fibrillogenesis. *J Theor Biol*, 301, 95-102.
- Stefani, M., and Dobson, C.M. 2003. Protein aggregation and aggregate toxicity: new insights into protein folding, misfolding diseases and biological evolution. *J Mol Med*, 81, 678-99.
- Stefanova, T.H., Nikolova, N.J., Toshkova, R.A., and Neychev, H.O. 2007. Antitumor and immunomodulatory effect of coumarin and 7-

-
- hydroxycoumarin against Sarcoma 180 in mice. *J Experimen Therapeutic Oncolog*, 6, 107-15.
- Stine, W. B., Dahlgren, K.N., Krafft, G.A., and LaDu, M.J. 2003. *In vitro* characterization of conditions for amyloid- β peptide oligomerization and fibrillogenesis. *J Biol Chem*, 278, 11612-22.
- Stohr, J., Watts, J.C., Mensinger, Z.L., Oehler, A., Grillo, S.K., DeArmond, S. J., Prusiner, S.B., and Giles, K. 2012. Purified and synthetic Alzheimer's amyloid beta (A β) prions. *Proc Natl Acad Sci U S A*, 109, 11025-30.
- Swarbrick, J. D., Iliades, P., Simpson, J.S., and Macreadie, I. 2008. Folate biosynthesis- Reappraisal of old and novel targets in the search for new antimicrobials. *Open Enzym Inhib J*, 1, 12-33.
- Tartaglia, G. G., Cavalli, A., Pellarin, R., and Caflisch, A. 2004. The role of aromaticity, exposed surface, and dipole moment in determining protein aggregation rates. *Protein sci*, 13, 1939-41.
- Taxis, C., Keller, P., Kavagiou, Z., Jensen, L.J., Colombelli, J., Bork, P., Stelzer, E.H., and Knop, M. 2005. Spore number control and breeding in *Saccharomyces cerevisiae*: a key role for a self-organizing system. *J Cell Biol*, 171, 627-40.
- Tay, W.M., Huang, D., Rosenberry, T.L., and Paravastu, A.K. 2013. The Alzheimer's amyloid- β (1-42) peptide forms off-pathway oligomers and fibrils that are distinguished structurally by intermolecular organization. *J Mol Biol*, 425, 2494-2508.
- Teng, Y., Zhang, M. Q., Wang, W. L., L.T., Zhou, L.M., Miao, S. K., and Wan, L.H. 2014. Compound danshen tablet ameliorated A β ₂₅₋₃₅-induced spatial memory impairment in mice via rescuing imbalance between cytokines and neurotrophins. *BMC Compl Alt Med*, 14, 1-10.
- Tenreiro, S., Fernandes, A.R., and Sa-Correia, I. 2001. Transcriptional activation of *FLR1* gene during *Saccharomyces cerevisiae* adaptation to growth with benomyl: role of Yap1p and Pdr3p. *Biochem Biophys Res commun*, 280, 16-22.
- Teplov, D.B. 1998. Structural and kinetic features of amyloid β -protein fibrillogenesis. *Amyloid*, 5, 121-42.
- Teplov, D.B. 2006. Preparation of amyloid β -protein for structural and functional studies. In: Indu, K. & Ronald, W. (eds.) *Methods Enzymol*. Academic Press.
- Terry, R. 2002. Biofloculant hypothesis: a partial endorsement. *Neurobiol Aging*, 23, e1075.
- Thirumalai, D., Reddy, G., and Straub, J.E. 2012. Role of water in protein aggregation and amyloid polymorphism. *Account Chem Res*, 45, 83-92.
-

-
- Thorin, E. 2014. Hypertension and Alzheimer's disease: Another brick in the wall of awareness. *Hypertension*, 114, 04257.
- Tian, L.L., Wang, X.J., Sun, Y.N., Li, C. R., Xing, Y.L., Zhao, H.B., Duan, M., Zhou, Z., and Wang, S.Q. 2008. Salvianolic acid B, an antioxidant from *Salvia miltiorrhiza*, prevents 6-hydroxydopamine induced apoptosis in SH-SY5Y cells. *Int J Biochem Cell Biol*, 40, 409-22.
- Tilley, L., Morgan, K., and Kalsheker, N. 1998. Genetic risk factors in Alzheimer's disease. *Mol Pathol : MP*, 51, 293-304.
- Timmers, A.C., Niebel, A., Balague, C., and Dagkesamanskaya, A. 2002. Differential localisation of GFP fusions to cytoskeleton-binding proteins in animal, plant, and yeast cells. *Protoplasma*, 220, 69-78.
- Tong, A.H., Evangelista, M., Parsons, A.B., Xu, H., Bader, G.D., Page, N., Robinson, M., Raghibizadeh, S., Hogue, C.W., Bussey, H., Andrews, B., Tyers, M., and Boone, C. 2001. Systematic genetic analysis with ordered arrays of yeast deletion mutants. *Science*, 294, 2364-68.
- Treusch, S., Hamamichi, S., Goodman, J. L., Matlack, K.E., Chung, C.Y., Baru, V., Shulman, J.M., Parrado, A., Bevis, B.J., Valastyan, J.S., Han, H., Lindhagen-Persson, M., Reiman, E.M., Evans, D.A., Bennett, D.A., Olofsson, A., DeJager, P.L., Tanzi, R.E., Caldwell, K.A., Caldwell, G.A., and Lindquist, S. 2011. Functional links between A β toxicity, endocytic trafficking, and Alzheimer's disease risk factors in yeast. *Science*, 334, 1241-45.
- Trivelli, X., Krimm, I., Ebel, C., Verdoucq, L., Prouzet-Mauleon, V., Chartier, Y., Tsan, P., Lauquin, G., Meyer, Y., and Lancelin, J.M. 2003. Characterization of the yeast peroxiredoxin Ahp1 in its reduced active and overoxidized inactive forms using NMR. *Biochemistry*, 42, 14139-49.
- Umeda, T., Tomiyama, T., Sakama, N., Tanaka, S., Lambert, M.P., Klein, W.L., and Mori, H. 2011. Intraneuronal A β oligomers cause cell death via endoplasmic reticulum stress, endosomal/lysosomal leakage, and mitochondrial dysfunction *in vivo*. *J Neurosci Res*, 89, 1031-42.
- Ueta, E., Tanida, T., Yoneda, K., Yamamoto, T., and Osaki, T. 2001. Increase of *Candida* cell virulence by anticancer drugs and irradiation. *J Oral Microbiol Immunol*, 16, 243-49.
- Vandebroek, T., Terwel, D., Vanhelmont, T., Winderickx, J., and Van Leuven, F. Phosphorylation and aggregation of protein tau in humanized yeast cells and in transgenic mouse brain. New trends in Alzheimer and Parkinson related disorders: ADPD 2005a. Medimond, 15-19.
- Vandebroek, T., Terwel, D., Vanhelmont, T., Gysemans, M., Van Haesendonck, C., Engelborghs, Y., Winderickx, J., and Van Leuven, F. 2006. Microtubule binding and clustering of human Tau-4R and Tau-P301L proteins isolated
-

-
- from yeast deficient in orthologues of glycogen synthase kinase-3 β or cdk5. *J Biol Chem*, 281, 25388-97.
- Vandebroek, T., Vanhelmont, T., Terwel, D., Borghgraef, P., Lemaire, K., Snauwaert, J., Wera, S., Van Leuven, F., and Winderickx, J. 2005b. Identification and isolation of a hyperphosphorylated, conformationally changed intermediate of human protein tau expressed in yeast. *Biochem*, 44, 11466-75.
- Vanhelmont, T., Vandebroek, T., De Vos, A., Terwel, D., Lemaire, K., Anandhakumar, J., Franssens, V., Swinnen, E., Van Leuven, F., and Winderickx, J. 2010. Serine-409 phosphorylation and oxidative damage define aggregation of human protein tau in yeast. *FEMS Yeast Res*, 10, 992-1005.
- Vassar, P.S., and Culling, C.F. 1959. Fluorescent stains, with special reference to amyloid and connective tissues. *Arch Pathol*, 68, 487-98.
- Vassar, R., Kovacs, D. M., Yan, R., and Wong, P.C. 2009. The beta-secretase enzyme BACE in health and Alzheimer's disease: regulation, cell biology, function, and therapeutic potential. *J Neurosci*, 29, 12787-94.
- Vega, I.E., Traverso, E.E., Ferrer-Acosta, Y., Matos, E., Colon, M., Gonzalez, J., Dickson, D., Hutton, M., Lewis, J., and Yen, S.H. 2008. A novel calcium-binding protein is associated with tau proteins in tauopathy. *J Neurochem*, 106, 96-106.
- Venugopala, K.N., Rashmi, V., and Odhav, B. 2013. Review on natural coumarin lead compounds for their pharmacological activity. *BioMed Res Int*, 2013, e963248.
- Vickers, P.J., Di Cecco, R., Pristupa, Z.B., and Scrimgeour, K.G. 1985. Activation of folypolyglutamate synthetase by pteric acid. *Can J Biochem Cell Biol*, 63, 777-79.
- Vidan, S., and Snyder, M. 2001. Large-scale mutagenesis: yeast genetics in the genome era. *Curr Opin Biotechnol*, 12, 28-34.
- Vishnevskaja, A.B., Kushnirov, V.V., and Ter-Avanesian, M.D. 2007. Neurodegenerative amyloidoses: the yeast model. *Mol Biol*, 41, 346-54.
- Vitalis, A., and Caflich, A. 2010. Micelle-like architecture of the monomer ensemble of Alzheimer's amyloid- β peptide in aqueous solution and its implications for A β aggregation. *J Mol Biol*, 403, 148-165.
- Von der Haar, T., Josse, L., Wright, P., Zenthon, J., and Tuite, M.F. 2007. Development of a novel yeast cell-based system for studying the aggregation of Alzheimer's disease-associated A β peptides *in vivo*. *Neurodegener Dis*, 4, 136-47.
-

-
- von Werder, F., and Merck's, J. 1936. Derivatives of 3-coumarincarboxylic acid, a new class of synthetic medicinal. *In: Atta-Ur-Rahman, Reitz, A. B. & Choudhary, M. I. (eds.) Fron Medic Chem.* Benthan Science publishers Ltd.
- Walsh, D.M., and Selkoe, D.J. 2007. A β oligomers-a decade of discovery. *J Neurochem*, 101, 1172-84.
- Walsh, D.M., Townsend, M., Podlisny, M.B., Shankar, G. M., Fadeeva, J.V., El Agnaf, O., Hartley, D.M., and Selkoe, D.J. 2005. Certain inhibitors of synthetic amyloid β -peptide (A β) fibrillogenesis block oligomerization of natural A β and thereby rescue long-term potentiation. *J Neurosci*, 25, 2455-62.
- Walsh, D.M., Lomakin, A., Benedek, G.B., Condron, M.M., and Teplow, D.B. 1997. Amyloid β -Protein Fibrillogenesis: Detection of a protofibrillar intermediate. *J Biol Chem*, 272, 22364-72.
- Wang, H.Y., Lee, D.H., Davis, C.B., and Shank, R.P. 2000. Amyloid peptide A β ₍₁₋₄₂₎ binds selectively and with picomolar affinity to α 7 nicotinic acetylcholine receptors. *J Neurochem*, 75, 1155-61.
- Wang, H.Q., Sun, X.B., Xu, Y.X., Zhao, H., Zhu, Q.Y., and Zhu, C.Q. 2010. Astaxanthin upregulates heme oxygenase-1 expression through ERK1/2 pathway and its protective effect against β -amyloid-induced cytotoxicity in SH-SY5Y cells. *Brain Res*, 1360, 159-167.
- Wang, J., Ho, L., Zhao, Z., Seror, I., Humala, N., Dickstein, D.L., Thiyagarajan, M., Percival, S.S., Talcott, S.T., and Pasinetti, G. M. 2006. Moderate consumption of Cabernet Sauvignon attenuates A β neuropathology in a mouse model of Alzheimer's disease. *FASEB J*, 20, 2313-20.
- Wang, Q. , Walsh, D.M., Rowan, M.J. , Selkoe, D.J., and Anwyl, I.R. 2004. Block of long-term potentiation by naturally secreted and synthetic amyloid β -peptide in hippocampal slices is mediated via activation of the kinases c-Jun N-terminal kinase, cyclin-dependent kinase 5, and p38 mitogen-activated protein kinase as well as metabotropic glutamate receptor type 5. *J Neurosci*, 24, 3370-78.
- Wang, X.P., and Ding, H.L. 2008. Alzheimer's disease: epidemiology, genetics, and beyond. *Neurosci Bull*, 24, 105-9.
- Wang, Z.M., Zhou, B., Nie, Z.L., Gao, W., Wang, Y.S., Zhao, H., Zhu, J., Yan, J. J., Yang, Z.J., and Wang, L.S. 2011. Folate and risk of coronary heart disease: A meta-analysis of prospective studies. *Nutr Metab Cardiovasc Dis*, 22, 890-99.
- Webb, M., and Nickerson, W.J. 1955. Differential reversal of inhibitory effect of folic acid analogues on growth, division, and deoxyribonucleic acid synthesis of microorganisms. *J Bacteriol*, 71, 140-48.
-

-
- Weids, A.J., and Grant, C.M. 2014. The yeast peroxiredoxin Tsa1 protects against protein-aggregate-induced oxidative stress. *J Cell Sci*, 127, 1327-35.
- Weingarten, M.D., Lockwood, A.H., Hwo, S.Y., and Kirschner, M.W. 1975. A protein factor essential for microtubule assembly. *Proc Natl Acad Sci U S A*, 72, 1858-62.
- Wen, Y., Planel, E., Herman, M., Figueroa, H.Y., Wang, L., Liu, L., Lau, L.F., Yu, W.H., and Duff, K.E. 2008. Interplay between cyclin-dependent kinase 5 and glycogen synthase kinase 3 β mediated by neuregulin signaling leads to differential effects on tau phosphorylation and amyloid precursor protein processing. *J Neurosci*, 28, 2624-32.
- Werner-Washburne, M., Braun, E., Johnston, G.C., and Singer, R.A. 1993. Stationary phase in the yeast *Saccharomyces cerevisiae*. *Microbiol Rev*, 57, 383-401.
- White, A.R., Guirguis, R., Brazier, M.W., Jobling, M.F., Hill, A.F., Beyreuther, K., Barrow, C.J., Masters, C.L., Collins, S.J., and Cappai, R. 2001. Sublethal concentrations of prion peptide PrP106–126 or the amyloid- β peptide of Alzheimer's disease activates expression of proapoptotic markers in primary cortical neurons. *Neurobiol Dis*, 8, 299-316.
- Whitehead, V.M. 2006. Acquired and inherited disorders of cobalamin and folate in children. *Brit J Haematol*, 134, 125-36.
- Wiegand, I., Hilpert, K., and Hancock, R.E. 2008. Agar and broth dilution methods to determine the minimal inhibitory concentration (MIC) of antimicrobial substances. *Nat Protoc*, 3, 163-75.
- Willem, M., Garratt, A.N., Novak, B., Citron, M., Kaufmann, S., Rittger, A., DeStrooper, B., Saftig, P., Birchmeier, C., and Haass, C. 2006. Control of peripheral nerve myelination by the β -secretase BACE1. *Science*, 314, 664-6.
- Williams, P., Sorribas, A., and Howes, M.J. 2011. Natural products as a source of Alzheimer's drug leads. *Nat Prod Rep*, 28, 48-77.
- Winzeler, E.A., Shoemaker, D.D., Astromoff, A., Liang, H., Anderson, K., Andre, B., Bangham, R., Benito, R., Boeke, J.D., Bussey, H., Chu, A.M., Connelly, C., Davis, K., Dietrich, F., Dow, S.W., El Bakkoury, M., Foury, F., Friend, S.H., Gentalen, E., Giaever, G., Hegemann, J.H., Jones, T., Laub, M., Liao, H., Liebundguth, N., Lockhart, D.J., Lucau-Danila, A., Lussier, M., M'Rabet, N., Menard, P., Mittmann, M., Pai, C., Rebischung, C., Revuelta, J.L., Riles, L., Roberts, C.J., Ross-MacDonald, P., Scherens, B., Snyder, M., Sookhai-Mahadeo, S., Storms, R.K., Veronneau, S., Voet, M., Volckaert, G., Ward, T.R., Wysocki, R., Yen, G.S., Yu, K., Zimmermann, K., Philippsen, P., Johnston, M., and Davis, R.W. 1999. Functional characterization of the *S. cerevisiae* genome by gene deletion and parallel analysis. *Science*, 285, 901-6.
-

-
- Wirth, K.G., Ricci, R., Gimenez-Abian, J. F., Taghybeeglu, S., Kudo, N. R., Jochum, W., Vasseur-Cognet, M., and Nasmyth, K. 2004. Loss of the anaphase-promoting complex in quiescent cells causes unscheduled hepatocyte proliferation. *Gen Develop*, 18, 88-98.
- Witaicenis, A., Seito, L.N., da Silveira Chagas, A., de Almeida, L.D., Jr., Luchini, A. C., Rodrigues-Orsi, P., Cestari, S.H., and Di Stasi, L. C. 2014. Antioxidant and intestinal anti-inflammatory effects of plant-derived coumarin derivatives. *Phytomedicine*, 21, 240-6.
- Wittenberg, C., and Reed, S.I. 2005. Cell cycle-dependent transcription in yeast: promoters, transcription factors, and transcriptomes. *J Oncogene*, 24, 2746-55.
- Wolfe, M.S. 2008. γ -secretase inhibition and modulation for Alzheimer's disease. *Curr Alzheimer Res*, 5, 158-64.
- Wong, C.M., Siu, K.L., and Jin, D.Y. 2004. Peroxiredoxin-null yeast cells are hypersensitive to oxidative stress and are genomically unstable. *J Biol Chem*, 279, 23207-13.
- Woo, H.N., Baik, S.H., Park, J.S., Gwon, A. R., Yang, S., Yun, Y.K., and Jo, D.G. 2011. Secretases as therapeutic targets for Alzheimer's disease. *Biochem Biophys Res Commun*, 404, 10-15.
- Woods, J., Snape, M., and Smith, M.A. 2007. The cell cycle hypothesis of Alzheimer's disease: suggestions for drug development. *Biochim Biophys Acta*, 1772, 503-8.
- World Health Organisation. 2012. Dementia cases set to triple by 2050 but still largely ignored. *News Release*. Geneva WHO.
- Wright, A.J., Dainty, J.R., and Finglas, P.M. 2007. Folic acid metabolism in human subjects revisited: potential implications for proposed mandatory folic acid fortification in the UK. *Brit J Nutr*, 98, 667-75.
- Wu, H.Y., Hudry, E., Hashimoto, T., Kuchibhotla, K., Rozkalne, A., Fan, Z., Spires-Jones, T., Xie, H., Arbel-Ornath, M., Grosskreutz, C.L., Bacskai, B.J., and Hyman, B.T. 2010. Amyloid β induces the morphological neurodegenerative triad of spine loss, dendritic simplification, and neuritic dystrophies through calcineurin activation. *J Neurosci*, 30, 2636-49.
- Wu, L., Qiao, H., Li, Y., and Li, L. 2007. Cardioprotective effects of the combined use of puerarin and Danshensu on acute ischemic myocardial injury in rats. *Phytother Res*, 21, 751-56.
- Wullschleger, S., Loewith, R., and Hall, M.N. 2006. TOR signaling in growth and metabolism. *Cell*, 124, 471-84.
-

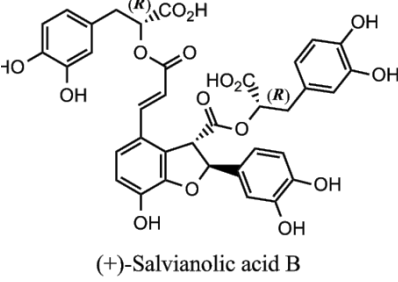
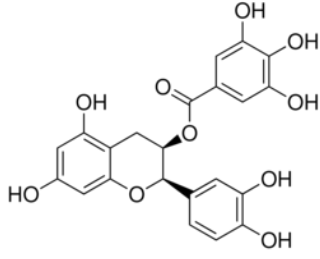
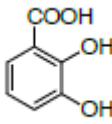
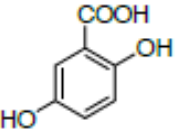
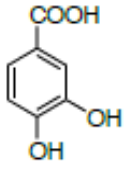
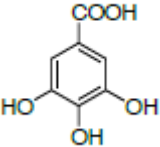
-
- Wurth, C., Guimard, N.K., and Hecht, M.H. 2002. Mutations that reduce aggregation of the Alzheimer's A β ₄₂ peptide: an unbiased search for the sequence determinants of A β amyloidogenesis. *J Mol Biol*, 319, 1279-90.
- Xie, L., Helmerhorst, E., Taddei, K., Plewright, B., Van Bronswijk, W., and Martins, R. 2002. Alzheimer's β -amyloid peptides compete for insulin binding to the insulin receptor. *J Neurosci*, 22, RC221.
- Yan, S.D., Chen, X., Fu, J., Chen, M., Zhu, H., Roher, A., Slattery, T., Zhao, L., Nagashima, M., Morser, J., Migheli, A., Nawroth, P., Stern, D., and Schmidt, A. M. 1996. RAGE and amyloid- β peptide neurotoxicity in Alzheimer's disease. *Nature*, 382, 685-91.
- Yanagimachi, M., Naruto, T., Hara, T., Kikuchi, M., Hara, R., Miyamae, T., Imagawa, T., Mori, M., Kaneko, T., Morita, S., Goto, H., and Yokota, S. 2011. Influence of polymorphisms within the methotrexate pathway genes on the toxicity and efficacy of methotrexate in patients with juvenile idiopathic arthritis. *Brit J Clin Pharmacol*, 71, 237-43.
- Yang, S., Wang, W., Ling, T., Feng, Y., Du, X., Zhang, X., Sun, X., Zhao, M., Xue, D., Yang, Y., and Liu, R. 2010. α -tocopherol quinone inhibits beta-amyloid aggregation and cytotoxicity, disaggregates preformed fibrils and decreases the production of reactive oxygen species, NO and inflammatory cytokines. *Neurochem Int*, 57, 914-22.
- Yang, Y., Geldmacher, D.S., and Herrup, K. 2001. DNA replication precedes neuronal cell death in Alzheimer's disease. *J Neurosci*, 21, 2661-68.
- Yang, Y., Varvel, N.H., Lamb, B.T., and Herrup, K. 2006. Ectopic cell cycle events link human Alzheimer's disease and amyloid precursor protein transgenic mouse models. *J Neurosci*, 26, 775-84.
- Yankner, B.A., and Mesulam, M.M. 1991. β -Amyloid and the Pathogenesis of Alzheimer's Disease. *NEJM*, 325, 1849-1857.
- Yao, R., Schneider, E., Ryan, T.J., and Galivan, J. 1996. Human γ -glutamyl hydrolase: cloning and characterization of the enzyme expressed *in vitro*. *Proc Natl Acad Sci U S A*, 93, 10134-38.
- Yoshiike, Y., Minai, R., Matsuo, Y., Chen, Y.R., Kimura, T., and Takashima, A. 2008. Amyloid oligomer conformation in a group of natively folded proteins. *PloS One*, 3, e3235.
- Yu, H., Yao, L., Zhou, H., Qu, S., Zeng, X., Zhou, D., Zhou, Y., Li, X., and Liu, Z. 2014a. Neuroprotection against A β ₂₅₋₃₅-induced apoptosis by *Salvia miltiorrhiza* extract in SH-SY5Y cells. *Neurochem Int*, 75, 89-95.
- Yu, L., Edalji, R., Harlan, J. E., Holzman, T. F., Lopez, A. P., Labkovsky, B., Hillen, H., Barghorn, S., Ebert, U., Richardson, P. L., Miesbauer, L., Solomon, L., Bartley, D., Walter, K., Johnson, R.W., Hajduk, P.J., and Olejniczak, E.T.
-

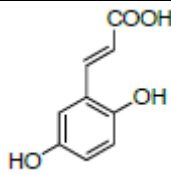
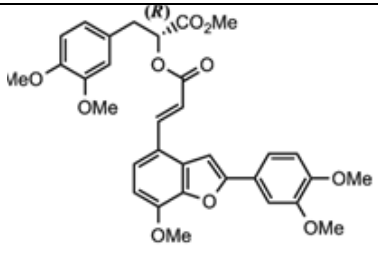
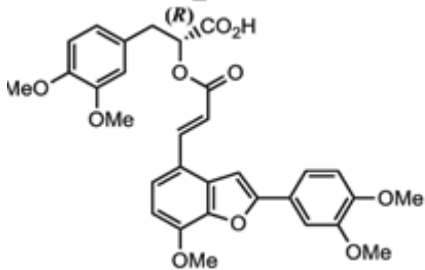
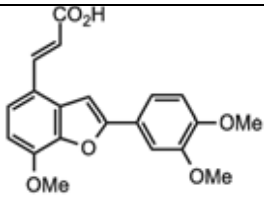
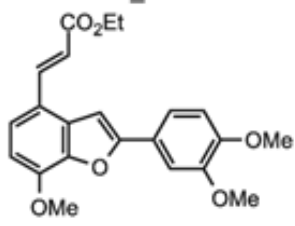
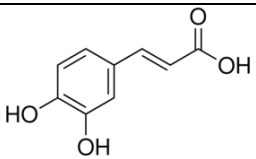
-
2009. Structural characterization of a soluble amyloid- β peptide oligomer. *Biochem*, 48, 1870-77.
- Yu, M., Li, W., Luo, S., Zhang, Y., Liu, H., Gao, Y., Wang, X., Wilson, J. X., and Huang, G. 2014b. Folic acid stimulation of neural stem cell proliferation is associated with altered methylation profile of PI3K/Akt/CREB. *J Nutr Biochem*, 25, 496-502.
- Zabrocki, P., Pellens, K., Vanhelmont, T., Vandebroek, T., Griffioen, G., Wera, S., Van Leuven, F., and Winderickx, J. 2005. Characterization of α -synuclein aggregation and synergistic toxicity with protein tau in yeast. *FEBS J*, 272, 1386-400.
- Zagorski, M.G., Yang, J., Shao, H., Ma, K., Zeng, H., and Hong, A. 1999. Methodological and chemical factors affecting amyloid- β peptide amyloidogenicity. *Methods Enzymol*, 309, 189-204.
- Zambrano, C.A., Egana, J.T., Nunez, M.T., Maccioni, R.B., and Gonzalez-Billault, C. 2004. Oxidative stress promotes tau dephosphorylation in neuronal cells: the roles of cdk5 and PP1. *Free Radical Biol Med*, 36, 1393-402.
- Zhang, C. 2012. Natural compounds that modulate BACE1-processing of amyloid- β precursor protein in Alzheimer's disease. *Discover Med*, 14, 189-97.
- Zhang, J., Mori, A., Chen, Q., and Zhao, B. 2006. Fermented papaya preparation attenuates β -amyloid precursor protein: β -amyloid-mediated copper neurotoxicity in β -amyloid precursor protein and β -amyloid precursor protein Swedish mutation overexpressing SH-SY5Y cells. *Neurosci*, 143, 63-72.
- Zhang, W., Espinoza, D., Hines, V., Innis, M., Mehta, P., and Miller, D.L. 1997. Characterization of β -amyloid peptide precursor processing by the yeast Yap3 and Mkc7 proteases. *Biochim Biophys Acta*, 1359, 110-22.
- Zhao, R., Min, S.H., Wang, Y., Campanella, E., Low, P.S., and Goldman, I.D. 2009. A role for the proton-coupled folate transporter (PCFT-SLC46A1) in folate receptor-mediated endocytosis. *J Biol Chem*, 284, 4267-74.
- Zhou, L., Zuo, Z., and Chow, M.S.S. 2005. Danshen: An overview of its chemistry, pharmacology, pharmacokinetics, and clinical use. *J Clin Pharmacol*, 45, 1345-59.
- Zhou, Y., Li, W., Xu, L., and Chen, L. 2011. In *Salvia miltiorrhiza*, phenolic acids possess protective properties against amyloid β -induced cytotoxicity, and tanshinones act as acetylcholinesterase inhibitors. *Environ Toxicol Phar*, 31, 443-52.
- Zhou, Y., Liang, M., Li, W., Li, K., Li, P., Hu, Y., and Yang, Z. 2009. Protective effects of *Eucommia ulmoides* Oliv. bark and leaf on amyloid β -induced cytotoxicity. *Environ Toxicol Phar*, 28, 342-49.
-

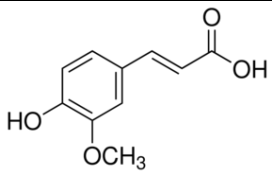
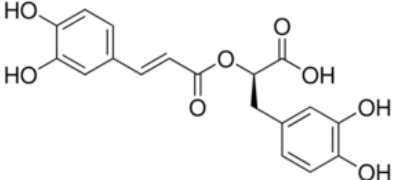
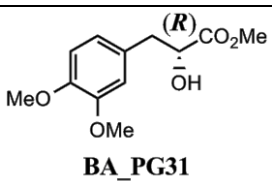
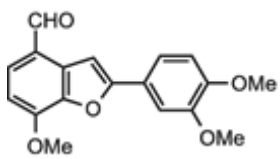
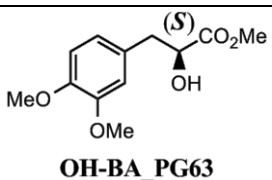
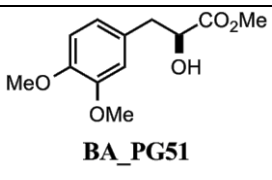
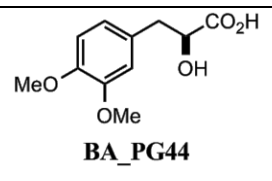
- Zhu, Z., Li, C., Wang, X., Yang, Z., Chen, J., Hu, L., Jiang, H., and Shen, X. 2010. 2,2',4'-trihydroxychalcone from *Glycyrrhiza glabra* as a new specific BACE1 inhibitor efficiently ameliorates memory impairment in mice. *J Neurochem*, 114, 374-85.

APPENDIX

Table A-1 Chemical structure of Danshen derived and synthesised analogs with their molecular weight and physical properties.

Name	Physical property	Molecular Structure	Solubility	MW
Salvianolic acid B Caffeic acid tetramer	White to tan powder	 <p>(+)-Salvianolic acid B</p>	H ₂ O: ≥ 5 mg/ml DMSO, Acetone, MeOH	718.61
Epigallocatechin gallate (EGCG)	White powder		DMSO, EtOH, DMF	442.37
2,3-Dihydroxybenzoic acid	White powder		H ₂ O, DMSO, MeOH	154.12
2,5- Dihydroxybenzoic acid (Gentisic acid)	White powder		H ₂ O, DMSO, MeOH	154.12
3,4- Dihydroxybenzoic acid (Protocatechuic acid, vanillin)	White powder		H ₂ O, DMSO, MeOH	154.12
3,4,5- Trihydroxybenzoic acid (Gallic acid)	White powder		EtOH, DMSO, DMF	238.24

2,4-Dihydroxycinnamic acid	Cream to white powder		H ₂ O, DMSO, EtOH	180.16
BA_PG65 Sal. C analogue (±)-heptamethyl lithospermate Caffeic acid trimer	Red to orange		EtOAc, CH ₂ Cl ₂ , Acetone, DMSO	576.59
BA_PG69 (+)-Salvianolic acid C hybrid Caffeic acid trimer	Yellow to green solid		EtOAc, CH ₂ Cl ₂ , Acetone, DMSO	562.56
BA_PG64 (+)-Lithospermic acid	Yellow solid		DMSO	354.35
BA_PG17 Benzo [b] furan	Cream, solid		Warm EtOAc, CH ₂ Cl ₂ , CHCl ₃ , Acetone, DMSO	382.41
Caffeic acid 3,4-Dihydroxycinnamic acid Caffeic acid monomer	Yellow to tan powder		H ₂ O, EtOAc, DMSO	180.16

4-hydroxy-3-methoxycinnamic acid (trans-ferulic acid) Caffeic acid monomer	White powder		H ₂ O, EtOH, DMSO	194.18
(+)-Rosmarinic acid Caffeic acid dimer	Light brown powder		H ₂ O, DMSO, Acetone, MeOH	360.31
BA_PG31 Danshensu	White solid	 BA_PG31	EtOAc, CH ₂ Cl ₂ , CHCl ₃ , Acetone, DMSO	240.25
BA_PG83 Benzo [b] furan	Orange to golden solid		EtOAc, CH ₂ Cl ₂ , CHCl ₃ , Acetone, DMSO	312.32
BA_PG63 Danshensu	White solid	 OH-BA_PG63	EtOAc, CH ₂ Cl ₂ , CHCl ₃ , Acetone, DMSO	240.25
BA_PG51 Danshensu	White solid	 BA_PG51	EtOAc, CH ₂ Cl ₂ , CHCl ₃ , Acetone, DMSO	240.25
BA_PG44 Danshensu	White solid	 BA_PG44	Acetone, DMSO	226.23

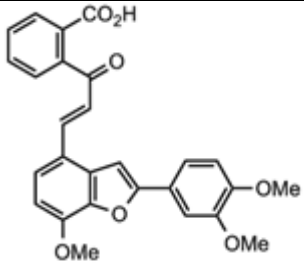
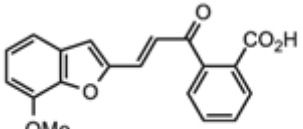
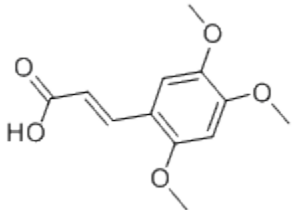
BA_PG84 Chalcone-Salvianolic acid C hybrids	Yellow, tan solid	 BA_PG84	H ₂ O, DMSO	458.46
BA_PG87 Chalcone-Salvianolic acid C hybrids	Yellow, tan solid	 BA_PG87	H ₂ O, DMSO	458.46
2,4,5- trimethoxycinnamic acid				

Table A-2 List of proprietary MATNAP compounds along with their colour and calculated minimum inhibitory concentration (MIC). MIC 90 of the compounds on *C. albicans* WM1172 compared with the positive control (*C. albicans* cells) and negative control (*C. albicans* and Fluconazole) were determined.

NAME	MIC90 (μM)	COLOUR
RB9_6.3	>250	Orange
RB1_3.6	300	White
RB1_3.8	300	White
MT4_3.1	500	Yellow
PLOCAMENONE	200	White
RB9_7.2	500	Dark pink/ peach
BCNK	500	White
DD6_3.2	300	White
RB10_10.4	300	Rose pink
MT4_3.3	400	Light yellow
RB10_10.3	400	Purple
RB9_6.2	500	Dark Yellow
RB9_7.1	300	Dark purple
RB9_3.5	350	Bright yellow
RB9_7.3	>125	Violet